2015

Modelling vertical drains with vacuum preloading considering the soil structure characteristics

Matharage Darshana Anuradha Perera
University of Wollongong

UNIVERSITY OF WOLLONGONG

School of Civil, Mining and Environmental Engineering

MODELLING VERTICAL DRAINS WITH VACUUM PRELOADING CONSIDERING THE SOIL STRUCTURE CHARACTERISTICS

Matharage Darshana Anuradha Perera

BSc. Eng. (Hons)

This thesis is presented as part of the requirements for the Award of the Degree of Doctor of Philosophy of the University of Wollongong

June 2015

THESIS CLARIFICATION

I, Matharage Darshana Anuradha Perera, declare that this thesis, submitted in fulfilment of the requirements for the award of Doctor of Philosophy, in the School of Civil, Mining & Environmental Engineering, Faculty of Engineering and Information Sciences, University of Wollongong, is wholly my own work unless otherwise referenced or acknowledged. The document has not been submitted for qualification at any other academic institution.

…….

Matharage Darshana Anuradha Perera

23rd June 2015

ABSTRACT

Vertical drains accelerate consolidation and as such they are a very effective and popular ground improvement method. When vacuum preloading is applied with vertical drains, consolidation increases even more and the stability of an embankment is enhanced due to the inward lateral movement exerted by vacuum preloading. Previous analytical models developed to predict consolidation when vacuum preloading is used with vertical drains assumed average compressibility and permeability values within the applied stress range. Even though the smear effects were incorporated into the solution by considering a reduced but constant permeability inside the smear zone, the actual variation of permeability was ignored in the vacuum preloading models developed. More importantly, compressibility of the in-situ clay structure due to the installation of a mandrel driven drain was often ignored as well. The aim of this study is to develop an analytical solution for vacuum preloading which accurately represents the variations in compressibility and permeability in actual ground conditions as a result of drain installations.

The disturbed zone created by drain installation can be characterised by using the extent of the smear zone and the ratio of the horizontal coefficient of permeability in the undisturbed zone and in the smear zone. These parameters were obtained using laboratory experiments performed on large-scale tests of samples of remoulded clay. Laboratory tests performed on samples extracted around an actual drain installed in field conditions indicated that soil was subjected to more smear under field conditions than was previously anticipated. Furthermore, this study revealed that the compressibility of soil was also adversely affected by the changes to

the soil structure, and therefore it was deemed imperative to capture these changes in the analytical models developed for radial consolidation with vacuum pressure.

A novel mathematical model was developed to incorporate soil destructuring due to drain installation and the associated changes in compressibility as the soil is improved using vertical drains and vacuum preloading. A more realistic distribution of permeability was assumed within the smear zone and the variation in permeability with the void ratio was also considered in the analysis. The predictions of average excess pore water pressure, degree of consolidation and resultant settlement, and the consolidation responses obtained using this analytical model were compared with other existing models. The importance of this model is illustrated via the case study simulations of two embankments in Australia and China that were stabilised with vertical drains; the proposed model gave more accurate predictions than the previous models. To model more realistic soil behaviour, variations in soil compressibility and permeability were incorporated into the latest edition of the PLAXIS finite element package which enabled the application of vacuum pressure, and very good agreement was observed between simulated results and the field data.

Laboratory tests were conducted on reconstituted and in-situ soil samples obtained from a soft clay site at Ballina, using the newly designed consolidation apparatus that can enable radial consolidation with vacuum pressure. These experiment results enabled the empirical relationship between the vacuum surcharge ratio and lateral strain to be postulated, and they can also be used as a design tool in initial embankment planning.

ACKNOWLEDGEMENTS

I would like to express my sincere gratitude to my supervisor Prof. Buddhima Indraratna for his enthusiastic support, patient guidance, and continuous encouragement during my PhD studies. From the first day that I sent him an email requesting the opportunity for a PhD until now, he has been extremely helpful in shaping my professional career. I would also like to acknowledge my co supervisor A/Prof. Cholachat Rujikiatkamjorn for all the help he has provided during my stay here.

I am grateful for the Endeavour Postgraduate Award programme that provided financial assistance for my PhD work. I also wish to acknowledge the contributions made by the technical officers during my laboratory experiments and field works, especially lab manager Alan Grant, and Ritchie McLean and Cameron Neilson. I would also like to acknowledge the contributions from Dr. Richard Kelly from Coffey Geotechnics during field work in Ballina and inputs for technical publications. I extend my sincere thanks to all my friends and colleagues at University of Wollongong, including Kumara, Muditha, Thiru, Udeshini, Wuditha, Nayoma, Nadeesha, Nava, Krish, Ana, Sanjay, Rui, Made, Chamindi, Rasika, Shiran, Pankaj, Firman and Keerti. They made my stay here much more enjoyable and I am grateful to them.

Last but not least I would like to extend my sincere gratitude to my parents Upathissa Perera and Mallika Perera for everything they have done in my life, and also to my sister Anuththara and my fiancée Chethani for their continuous support during my stay here.

LIST OF PUBLICATIONS

Indraratna, B., D. Perera, C. Rujikiatkamjorn and R. Kelly (2015). Soil disturbance analysis due to vertical drain installation Proceedings of the ICE- Geotechnical Engineering. (DOI: 10.1680/geng.14.00052)

Indraratna B., K. Kianfar , C. Rujikiatkamjorn amd D. Perera (2014). Soft soil properties for non-Darcian radial drainage with vacuum preloading, based on Rowe cell testing. Australian Geomechanics Journal, 49 (4), 183-190

Perera D., B. Indraratna and C. Rujikiatkamjorn (2015). Analytical modelling of vertical drains with vacuum preloading considering soil structure characteristics. (In Preperation)

Perera D., B. Indraratna and C. Rujikiatkamjorn (2014). Soil disturbance associated with mandrel-driven prefabricated vertical drains: field experience, Proceedings of soft soil engineering and ground improvement, Bundung, Indonesia, Vol 2, 1-6

TABLE OF CONTENTS

LIST OF FIGURES

LIST OF TABLES

LIST OF SYMBOLS

d_e diameter of influenced zone

b parameter representing the rate of destructuring

c_c^* gradient of compression line of reconstituted soil

$\overline{c_c}$ average compression index

c_c coefficient of consolidation for horizontal drainage

c_v coefficient of consolidation for vertical drainage

c_{hi} coefficient of radial consolidation at effective pre-consolidation pressure

c_{ho} initial coefficient of radial consolidation

c_k permeability index

c_s^* gradient of compression line in recompression region

$\overline{c_s}$ average recompression index

e void ratio of soil

e_0 initial void ratio soile^* void ratio of reconstituted soil

e_{ic}^* void ratio of reconstituted soil when σ'_v = 1 kPa

$e_{i,D}$ initial void ratio at yield stress of partially disturbed soil

$e_{i,u}$ in situ void ratio at yield stress of undisturbed soil

$e_{o,u}$ initial void ratio of soil in undisturbed zone

$e_{o(r_w)}$ initial void ratio of soil in disturbed zone next to the drain

$\bar{e}$ average void ratio at a given depth

$\overline{e_o}$ average initial void ratio

$e_{i(r_w)}$ void ratio at initial yield stress of soil in disturbed zone next to the drain

$\overline{e_i}$ average void ratio at yield stress

$\overline{e_f}$ average final void ratio

$e_{f,U}$ final void ratio of soil in undisturbed zone

$e_{f(r_w)}$ final void ratio of soil in disturbed zone close to the drain

H Thickness of clay

$k_{h(r)}$ horizontal permeability along the radius

$k_{(r_w)0}$ initial horizontal permeability of soil in disturbed zone next to the drain

k_{0u} initial horizontal permeability of soil in undisturbed zone

$k_{s(r)}$ horizontal permeability of soil in disturbed zone

$k_{i(r_w)}$ horizontal permeability at yield stress of soil in disturbed zone next to the drain

k_i average horizontal permeability at yield stress of soil

k_{iu} horizontal permeability at yield stress of soil in undisturbed zone

k_{ho} average initial horizontal permeability of soil

k_{hi} average horizontal permeability at yield stress of soil

m_v coefficient of volume compressibility

m_{vo} coefficient of volume compressibility at $\sigma_v' = \overline{\sigma_o'}$

m_{vi} coefficient of volume compressibility at $\sigma_v' = \overline{\sigma_{vi}'}$

P_0 Vacuum pressure applied

r distance from the centre of the drain

r_e radius of influenced zone

r_s radius of smear zone

r_w radius of drain well

t time

t_i time when $\sigma_v' = \overline{\sigma_{vi}'}$

T_h dimensionless time factor

T_h^* modified dimensionless time factor

u excess pore-water pressure

$\overline{u_t}$ average excess pore pressure of the smear and undisturbed zones

u_s excess pore pressure of the disturbed zone

z depth

$\bar{\sigma}'_{\mathrm{v}}$ average vertical effective stress

$\sigma'_{\mathrm{v}_{y,u}}$ initial yield stress of structured soil

$\sigma'_{\mathrm{v}_{y,D}}$ initial yield stress of the partially disturbed soil

$\bar{\sigma}'_{\mathrm{v}i}$ average yield stress

$\sigma'_{\mathrm{v}0}$ initial vertical effective stress of average curve

ε volumetric strain

γ_w unit weight of water

ρ settlement at a given time

$\Delta\sigma'$ applied preloading pressure

Chapter 1 Introduction

1.1 Ground improvement

Ground settlement in cohesive soils due to the application of external loads has been a major problem in the development of infrastructure. However, considering that the Sumerians who lived around 6000 years BC used embankments to support their temples built in soft soils, these are not new problems; indeed, a temple in Europa valley known as the White temple of Eridou has now settled 12m below street level (Leroueil, 1988).

Since then, numerous structures have suffered from the effects of ground settlement, but with an ever increasing demand for land human habitats have now been built on marshy lands that had previously been avoided. Moreover, the need for new transport infrastructure facilities has resulted in new highways being constructed over soft soil regions in order to avoid those areas occupied by humans. These soft soils have inherent properties such as high compressibility, low permeability and low

bearing capacity, which often leads to a challenging geotechnical environment, one of which being the eastern coastal area of Australia.

When an external load is applied to saturated clay the pore water pressure suddenly increases, but over time the water pressure reaches its state of static equilibrium as water is expelled from the soil strata during consolidation. However, the rapid growth in population and concentration of people in major cities has led to a significant increase in the demand for water which, in some cases has been met by extracting groundwater from deep sub soil layers, a practice that has caused the ground settlement of large areas. Cities close to the sea may face the danger of inundation by sea water and there are reports indicating that many agricultural lands have already been destroyed by the intrusion of salt water due to ground subsidence (Leroueil, 1988)

It is very clear that the adverse effects of long term deformation of any infrastructures should be avoided at all costs, which is why preloading the subsoil has been used as ground improvement method to reduce post construction settlement. This method is very simple, relatively inexpensive, and it is environmentally friendly because no chemical substances are added to the ground. Preloading is often considered as a preferred solution to improve soft marshy soil terrains to support transportation infrastructure such as roads and bridge abutments rather than expensive pile foundations.

In preloading methods, a temporary surcharge load that should be equal to or preferably slightly higher than the total load applied to the subsoil by the permanent structure is applied to consolidate the ground. This temporary surcharge, also known as pre-compression, has the following major advantages: it increases the shear

strength and reduces post construction settlement. Theoretically it should eliminate all the primary consolidation settlements and some amount of secondary compression. (Johnson, 1970a)

Even though the preloading method is simple and straight forward, a considerable amount of prior design and analysis work is required to accurately predict the rate of consolidation due to surcharge loading, dissipation of excess pore water pressures, as well as the magnitude of final settlement. Stability of the surcharge embankment and the associated lateral strains induced also need to be carefully estimated. Comprehensive subsoil analysis, accurate laboratory testing representing the true ground conditions, and continuous field monitoring is essential for all quality ground improvement works. (Johnson, 1970b)

1.2 Use of vertical drains

Most of the marshy areas encountered are very thick, sometimes more than 10m, and the permeability of the clay is very low, so it would take a long time to complete primary consolidation if the classical preloading method was used. With the current tight construction schedules it would be uneconomical to use preloading alone, while vertical drains can reduce the drainage path (Figure 1.1) and accelerate the consolidation process. Lau & Cowland (2000) presented the use of vertical drains and the effects of drain spacing to accelerate consolidation using sensitivity analysis for embankments constructed in 12m thick Hong Kong clay (Figure 1.2).

The concept of using vertical drains as alternate drainage paths was first proposed by Daniel E. Morgan in 1925, for which he obtained a patent in the following year. Inspired by this division of California highways, performed laboratory experiments and field trials and ultimately the first set of sand drains were

installed in 1934. The first comprehensive analytical solution for radial consolidation using sand drains was developed by Barron (1948), and later Richart (1959) introduced numerical techniques suitable for vertical drain analysis.

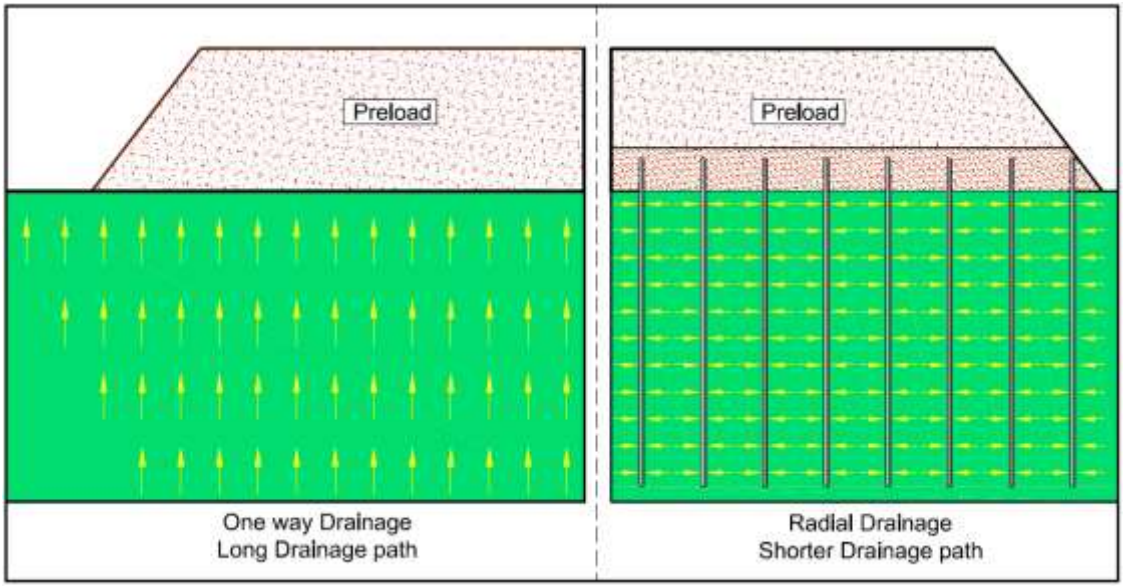

Figure 1.1 : Benefits of using vertical drains

Displaced and non-displaced types of sand drains were gradually replaced by synthetic prefabricated vertical drains. These types of drains were very popular in the early 1980's in geotechnical projects in South East Asia. The subsequently large production of drains and the development of associated techniques and materials used have significantly reduced the unit cost of PVDs. Indeed, with the latest installation rigs, even a 20m drain can be installed in less than 30 seconds, which enables contractors to installs thousands of drains within days.

1.3 Vacuum preloading as a ground improvement technique

In highly congested cities there may not be any room to expand vital infrastructures such as the airports and harbours that need large areas of land; a need

that has led to the reclamation of land using soils dredged from the bottom of the sea. However, soils in the seabed close to shore usually consists of very soft silts, and this reclaimed land must be able to support heavy earthmoving equipment associated with the operation of ground improvement immediately after the reclaimed soil is barely safe under its own weight.

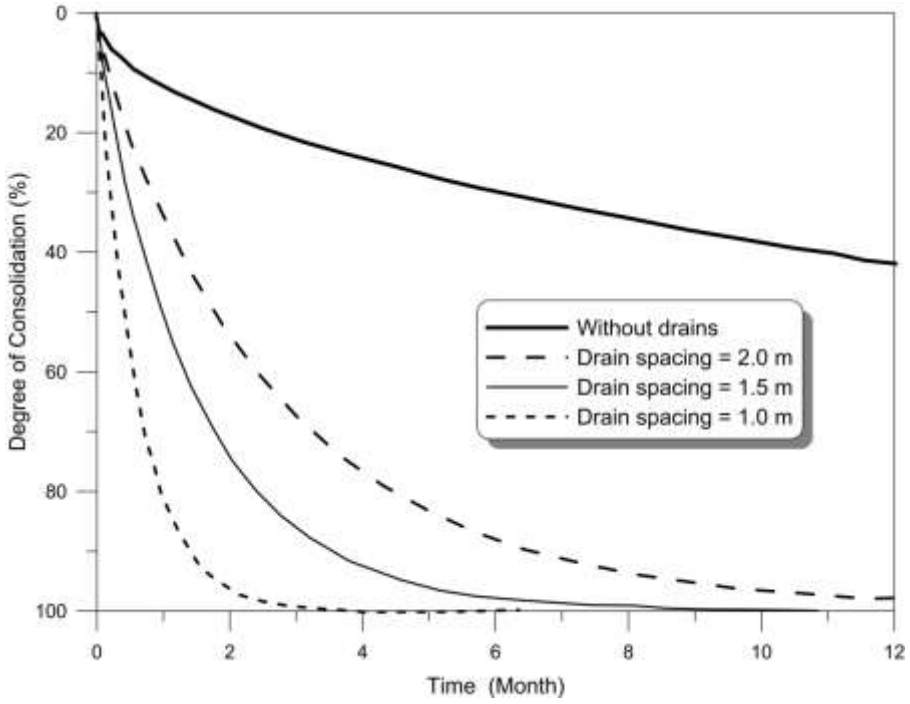

Figure 1.2 : Consolidation rates for the river muds

(Adopted from Lau & Cowland, 2000)

Since the shear strength of reclaimed land is very low, ground improvement must begin before construction can start, but preloading even with vertical drains, may not be ideal because the subsoil is incapable of supporting the surcharge load. In some situations, even finding good quality materials for the surcharge load is challenging due to whether they are available or not, and the accessibility of the site. This is why vacuum preloading with or without vertical drains has become a very good alternative in these situations.

When vacuum pressure is applied it will create a negative pore pressure in the ground and increase the effective stress of the soil without altering its total stress. Theoretically, 100 kPa vacuum pressures can be applied to the ground, but in field conditions the maximum value observed is around 80 kPa. When the required preloading is greater, vacuum preloading can be applied along with the embankment surcharge load because an effective vacuum system will yield almost the same amount of vertical strain obtained by the same magnitude of pressure applied using fill loading. Vacuum pressure can induce isotropic consolidation of the soil such that the resultant lateral movement is compressive and the soil moves inwards (radially towards the drain), unlike the outward lateral strains caused by surcharge embankments. This action may increase the stability of the embankments by reducing the overall lateral shear strains, but care must be taken because it might lead to tensile cracking in the ground in the PVD area.

In ground improvement projects the membrane and membraneless systems are used to apply vacuum pressure with or without vertical drains. In a membrane system, an airtight membrane is used to confine the volume to which the vacuum pressure is applied, and there is no direct connection between the vacuum pump and each single drain. Here a sand mat is used as a drainage layer between horizontal vacuum distribution pipes starts from the vacuum pump and vertical drains installed to drain water out from the soil. The airtight membrane is sealed at the perimeter of the embankment using a bentonite trench and cut off wall. In the membrane less system each and every drain is directly connected to the vacuum pump via a horizontal drainage system.

1.4 Smear effects due to the drain installation

The efficient installation of drains is extremely important in order to ensure that the use of vertical drains is economically viable. Drains are inserted into the ground via a truck mounted steel mandrel where the general installation speeds are in excess of 1m/s. Due to this high speed method of mandrel insertion, the soil around the drain is disturbed and this region is known as the smear zone. Inside the smear zone, the lateral permeability and compressibility of the soil is reduced, and this has an adverse impact on the rate of consolidation.

To predict the rate of consolidation and the magnitude of final consolidation settlement, the smear effect must be estimated accurately. The extent of the smear zone and the ratio of reduced permeability within the smear zone are the main factors affecting the rate of the consolidation due to drain installation. Moreover, this will change the structure of the soil and the coefficient of compressibility which can alter the total settlement.

1.5 Objectives and scope of the study

The effects of smear and well resistance have been implicitly incorporated by Indraratna & Redana (1998), but the variation of soil compressibility within the smear zone was not included in this solution. Constant permeability was assumed within the smear zone in most of the solutions developed until Walker & Indraratna (2006) included the linear variation of permeability in the radial consolidation model. Extent of the smear zone is now calculated based on large scale laboratory experiments using remoulded soil samples. These larger samples were restrained by its rigid boundary, while the scaled down mandrel and slower rates of installation would not represent actual field behaviour.

The main aim of this work is to study the smear effects in the field conditions and incorporate soil disturbance with varying compressibility and permeability into radial consolidation with vacuum preloading. Extent of the smear zone was obtained using the variation of moisture content, void ratio, horizontal permeability, normalised permeability and degree of disturbance along the radius of the drain. Executing a comprehensive study of the smear effects due to drain installation under field conditions is an objective of this work. The variations of permeability and compressibility along the radius of the drain are properly captured in radial consolidation theory with vacuum preloading. The reduction of permeability and compressibility with time due to a reduction in the void ratio was also considered in the analytical solution.

The results of small-scale laboratory experiments with model vertical drains and vacuum pressure are not abundant in literature, so in this study, a new consolidation cell was designed and laboratory experiments were performed using samples of Ballina clay to carry out radial consolation tests with vacuum pressure in a relatively short period of time. The analytical model proposed in this study has been applied to several embankments constructed over soft clay and stabilised with vertical drains and vacuum preloading. The settlement, pore water pressure and lateral strains obtained from the analysis were compared with actual field results. Finally two embankments were simulated using PLAXIS finite element program considering the variations to the characteristics of soil structure due to the drain installation.

1.6 Organisation of the Thesis

Chapter 1 outlines the content, scope, and objectives of this thesis, while Chapter 2 presents a comprehensive literature review. The concepts and analytical models developed for one-dimensional consolidation and radial consolidation are discussed first, and then the aspects of history, development, and use of vertical drain are followed by the smear effects due to drain installation. After that, the prevailing knowledge of soil improvement using vertical drains is presented and the chapter concludes by addressing the effects of viscoelasticity in clay soils.

Chapter 3 presents the field and laboratory procedure used to determine the extent of the smear zone. The variation of compressibility due to the drain installation is examined using the samples collected around the drains installed in an embankment in Ballina, Australia. The effect of the overlapping smear zones was also examined in this study.

In Chapter 4, a new radial consolidation model was developed with vertical drains and vacuum preloading by considering the characteristics of soil structure. The variation of compressibility and horizontal permeability along the radial direction was incorporated into the radial consolidation equation with vacuum preloading. The analysis also considered how, as consolidation evolves, the void ratio and permeability of soil decrease over time.

Chapter 5 describes the procedure for, and results of laboratory experiments with vacuum preloading. A new consolidation cell was developed to conduct tests on 70mm diameter samples of soil with vacuum pressure applied using 6mm diameter vertical drains. Both undisturbed and disturbed samples of Ballina clay were tested

and an empirical relationship of lateral strain with the applied vacuum surcharge ratio is presented.

Chapter 6 presents the application of proposed models to Ballina bypass embankment and Tianjin port embankment where the underlying soft soil at these sites was improved with vacuum pressure and vertical drains. The settlements, pore water pressure, and the lateral strains were then compared with the actual field measurements.

Chapter 7 presents the numerical simulation conducted using the PLAXIS 2D 2015 finite element package. Two embankments built in Tianjin port China were modelled with vacuum pressure whilst considering the soil structure characteristics, and then compared with the actual field data. There was a good agreement with settlement, pore water pressure, and lateral strain between the predicted and observed values.

Chapter 8 presents the conclusions and recommendations for future works, followed by the references.

Chapter 2 Literature Review

2.1 Consolidation of soft clay

2.1.1 Consolidation Settlement

When a layer of saturated clay is subjected to an external load the pore pressures will immediately increase and then gradually decrease as the ground consolidates. Terzaghi (1943) described consolidation as any process that involves a decrease in the water content of a saturated soil without replacing it by water or air. Settlement upon loading is divided into three broad categories known as immediate compression, primary consolidation, and secondary consolidation.

- Immediate compression – Caused by the elastic deformation of dry and saturated soils without any change in the moisture content.
- Primary Consolidation – Pore water pressure of a saturated clay increases immediately after applying an external load. As the excess pore pressure dissipates pore water is expelled, which results in a change in the volume of saturated

cohesive soils. Primary consolidation contributes to most of the settlement caused by an external load.

- Secondary Consolidation – Can be observed in saturated cohesive soils after the end of primary consolidation, and it is the result of the plastic yielding of the soil fabric.

2.1.2 Terzaghi's one dimensional (1D) consolidation Theory

Karl Terzaghi set the first significant benchmark in the theory of consolidation in 1923. The assumptions behind his original theory are as follows,

- Soil is saturated and homogeneous, and the compressibility of solid grains of the soil and the compressibility of the pore water are negligible.
- A unique linear relationship exists between the vertical effective stress (σ') and the void ratio (e) that is independent of the loading history and time.
- The coefficient of permeability is assumed to be constant during the consolidation process.
- The small strain theory and Darcy's low are valid
- The flow of water is only in one (vertical) direction.

Considering the above assumptions and the continuity equation, the following relationship between the void ratio and excess pores pressure can be derived:

$$\frac{k_v}{\gamma_w}\frac{\partial^2 u}{\partial z^2} = \frac{1}{1+e_0}\frac{\partial e}{\partial t} \tag{2.1}$$

$$c_v \frac{\partial^2 u}{\partial z^2} = \frac{\partial u}{\partial t} \tag{2.2}$$

Solving this equation using appropriate boundary condition gives an expression for the degree of consolidation.

$$U_v = 1 - \sum_{m=0}^{\infty} \frac{2}{M^2} exp^{-M^2 T_v} \quad (2.3)$$

where m is an Integer, $M = \frac{\pi}{2}(2m+1)$, T_v is the time Factor for vertical drainage, $T_v = c_v t/H^2$, c_v is the coefficient of consolidation, t is the elapsed time, and H is the length of the drainage path.

2.1.3 Coefficient of vertical consolidation (c_v)

In Terzaghi's theory where a linear relationship among the vertical effective stress (σ'), the void ratio (e) and constant permeability is assumed, the coefficient of consolidation (c_v) controls the consolidation process. The coefficient of consolidation is defined by,

$$c_v = \frac{k_v}{\gamma_w m_v} \quad (2.4)$$

where m_v is defined by;

$$m_v = \frac{\Delta \in_v}{\Delta \sigma'_v} \quad (2.5)$$

The magnitude of c_v is higher in the recompression range than in the compression range. Sudden decrease of c_v after the pre-consolidation pressure in clay reflects the change in m_v as the soil passes from an over-consolidated region into a normally consolidated region. (Terzaghi, 1943)

Researchers have introduced different methods to estimate the c_v value. $\in_v$ – log t curves of a clay sample in a oedometer test typically have an S shaped curve or a continuously increasing slope (Bjerrum, 1967). By using this S shaped curve c_v can be derived using the Casagranade method. When this value is compared with c_v that was obtained using the Taylor square root method, it is generally smaller.

(Lambe & Whitman, 1979; Pelletier et al., 1979). Sridharan & Rao (1981) proposed a rectangular hyperbola fitting method to determine c_v. This value is different from those obtained from the Casagranade and Taylor methods.

The value of c_v can be obtained using equation 2.4 by directly measuring k_v and taking m_v from the EOP e Vs σ' curve. However, c_v could vary considerably depending on the position of the element and the time, so it is better to consider c_v as a curve fitting parameter rather than a fundamental parameter. (Leroueil, 1988)

2.1.4 Soil Permeability (*k*)

Terzaghi's consolidation theory assumes a constant permeability throughout the consolidation process, but as consolidation progresses the permeability of the soil decreases as the pore within the soil mass shrinks.

It is imperative to use the correct permeability value when estimating the consolidation settlements accurately with time. Tavenas et al. (1983a) studied the available laboratory methods to derive the value of permeability and concluded that the constant head of tests performed in the triaxial apparatus in larger samples are the best as they reduce the problem of representative space although, the results from falling head tests conducted in an oedometer also proved to be very reliable, and were much more economical and convenient to perform. Further in this study it has been shown that Darcy's low is valid for hydraulic gradients between 0.1 and 50 in natural soft clays. The permeability of soft clay could also be obtained indirectly by Taylor's (1948) method and Casagrande & Fadum's (1944) methods using the coefficient of consolidation derived from the step loading consolidation tests, but the permeability values derived from these methods were not representative of the actual field permeability encountered.

As the consolidation process continues and the soil voids shrink, the permeability of the soil also decreases. Mesri & Olson (1971) and Samarasinghe et al. (1982) proposed a relationship between the void ratio and the soil permeability. Tavenas et al. (1983b) concluded that the existing void ratios and permeability relationships are generally not valid. However, they did state that for a strain range of 0-20%, which is often encountered in engineering practice, it is reasonable to assume a linear relationship between void ratio and logarithms of permeability. This was based on laboratory experiments performed in undisturbed clay samples obtained from North America and Europe, and is present below as;

$$\bar{e} = e_0 + c_k \log\left(\frac{k}{k_0}\right) \tag{2.6}$$

where e_0 is the in-situ void ratio, k is the coefficient of soil permeability, k_0 is the initial coefficient of soil permeability, and c_k is the permeability change index. The permeability change index can be directly related to the initial void ratio as (Tavenas et al., 1983b):

$$c_k = 0.5\, e_0 \tag{2.7}$$

2.1.5 Vertical consolidation with variable compressibility and permeability

Using $e - \log \sigma_v'$ and $e - \log k$ plots, Lekha et al. (2003) modified the classic Terzaghi theory to incorporate the variation of compressibility and permeability. The modified expressions are;

$$U_v = 1 - \sum_{m=0}^{\infty} \frac{2}{M^2} exp^{-M^2 T_v{}^*} \tag{2.8}$$

$$T_v^* = 0.5\left(1 + \left(1 + \frac{\Delta p}{\sigma'_i}\right)^{1-C_c/C_k}\right)T_v \quad (2.9)$$

where T_v^* is the modified time factor, $\Delta p/\sigma'_i$ is load increment ratio, σ'_i is the initial effective stress, and Δp is the applied preloading pressure. It was found that the C_c/C_k and $\Delta p/\sigma'_i$ ratios governed the rate of consolidation. (Figure 2.1)

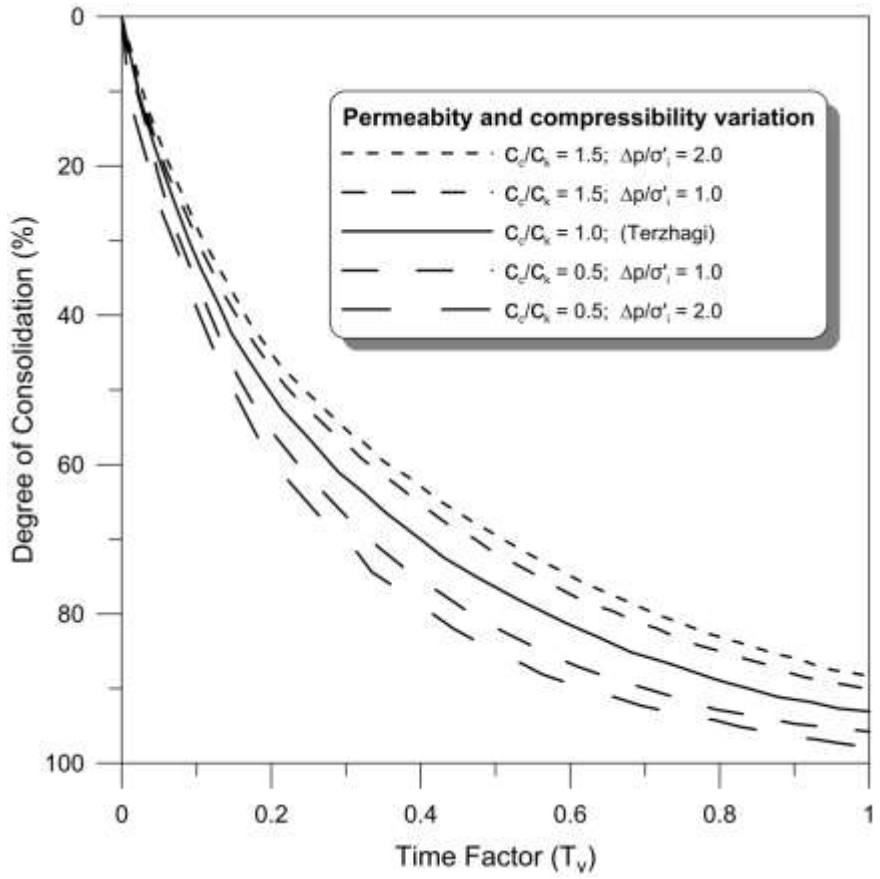

Figure 2.1: Variation of the degree of consolidation with time factor (T_v) for varying values of c_c/c_k and $\Delta p/\sigma'_i$ (after Lekha et al., 2003)

The results indicate that when c_c/c_k approaches unity the solution converges to a well-known Terzaghi consolidation equation, but if c_c/c_k is below 1.0, consolidation would occur at a faster rate and a higher loading ratio would also make consolidation faster.

2.2 Theory of Radial Consolidation

2.2.1 Barron's theory on radial consolidation

Barron (1948) presented the first mathematical solution for radial consolidation using sand drain wells. Both the vertical and radial flow towards the drain was incorporated and the well resistance and smear were also considered in this study. The assumptions on which this solution is based are listed as follows, and they are similar to the assumptions made by Terzaghi for his consolidation theory.

- Applied loads are initially carried by excess pore water pressure
- The vertical load is assumed to be uniformly distributed and all the compressive strain within the soil occurs vertically.
- The influenced zone of the drain is assumed to be circular and axi-symmetric
- Permeability of the drain is infinite compared to the soil
- Darcy's law is valid and small strain theory is applicable.

Barron (1948) considered two possible cases of analysis, known as free strain and equal strain. In the assumptions it was assumed that a uniform load is acting in the circular influenced zone. For the free strain case, it was assumed that differential settlements would not create any redistribution of stresses acting on the soil, due to the arching of the surcharge load. Furthermore, it was assumed that the shear strains that resulted with this differential settlement did not have any effect on consolidation. However, it is understandable that this process would redistribute the load based on the arching created by the surcharge fill load. The most extreme case with this is that the load has been redistributed to an extent that would result in an equal stain without

any differential settlement. This is the fundamental for equal strain case and the constitution equation for both vertical and horizontal consolidation can be given as;

$$\frac{\partial \bar{u}}{\partial t} = c_v \left(\frac{\partial^2 u}{\partial z^2}\right) + c_h \left(\frac{\partial^2 u}{\partial r^2} + \frac{1}{r}\frac{\partial u}{\partial r}\right) \tag{2.10}$$

When considering radial consolidation only, this equation (2.10) is reduced to;

$$\frac{\partial \bar{u}}{\partial t} = c_h \left(\frac{\partial^2 u}{\partial r^2} + \frac{1}{r}\frac{\partial u}{\partial r}\right) \tag{2.11}$$

where t is the time elapsed after the load is applied, u is the excess pore water pressure at radius r and at depth z. c_h is the coefficient of radial consolidation and can be defined as;

$$c_h = \frac{k_h}{\gamma_w m_v} \tag{2.12}$$

Richart (1959) reviewed the theory of vertical drains taking the changing void ratios with the consolidation process in to consideration, and stated that the difference in consolidation time response is negligible. Further, he compare the results obtained from the free stain and equal strain methods and concluded that both results are similar, but the equal strain method is much easier to use in engineering practise.

2.2.2 Hansbo's solution for radial consolidation theory

Yoshikuni & Nakanodo (1974) presented a rigorous solution for radial consolidation that considered the finite permeability and well resistance. Hansbo (1981) proposed an approximate solution for vertical drains based on the equal strain theory where both smear and well resistance were taken into consideration. The average degree of consolidation U_h , of the soil cylinder (Figure 2.2) with a vertical drain is given by;

$$U_h = 1 - exp\left(-\frac{8T_h}{\mu}\right) \tag{2.13}$$

$$\mu = \ln\left(\frac{n}{s}\right) + \left(\frac{k_h}{k_s}\right)\ln(s) - 0.75 + \pi z(2l - z)\frac{k_h}{q_w}\left\{1 - \frac{k_h/k_h' - 1}{(k_h/k_h')(s/n)}\right\} \tag{2.14}$$

Alternatively, in a simplified form,

$$\mu = \ln\left(\frac{n}{s}\right) + \left(\frac{k_h}{k_s}\right)\ln(s) - 0.75 + \pi z(2l - z)\frac{k_h}{q_w} \tag{2.15}$$

The effect of smear only is given by,

$$\mu = \ln\left(\frac{n}{s}\right) + \left(\frac{k_h}{k_s}\right)\ln(s) - 0.75 \tag{2.16}$$

The effect of well resistance only is given by,

$$\mu \approx \ln(n) - 0.75 + \pi z(2l - z)\frac{k_h}{q_w} \tag{2.17}$$

If both smear and well resistance are ignored, the above parameter becomes,

$$\mu = \ln(n) - 0.75 \tag{2.18}$$

where $n = {}^{d_e}/_{d_w}$, $n = {}^{d_s}/_{d_w}$, $d_w = 2r_w$ is the equivalent diameter of the drain, $d_e = 2r_e$ is the diameter of the zone influenced by the drain, $d_s = 2r_s$ is the diameter of the smear zone, l is the length of the drainage path, q_w is the discharge capacity, and z is the depth from the surface. The coefficient of permeability in the vertical

and horizontal directions are k_v and k_h, respectively, and the reduced coefficient of permeability in the smear zone is k_s (See Figure 2.2)

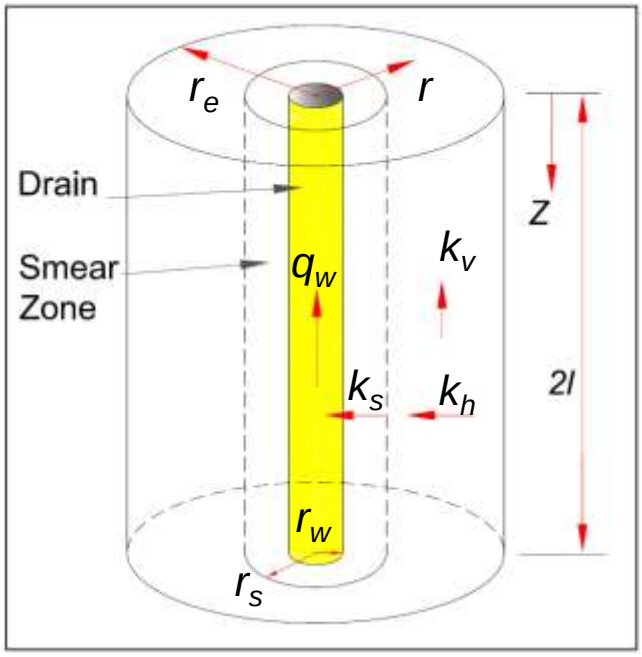

Figure 2.2: Schematic soil cylinder with vertical drains

Onoue (1988) presented a rigorous mathematical solution for drain wells that incorporated both smear and well resistance. It was concluded that the results from this method were similar to the results obtained using Hansbo's (1981) approximate plane strain method.

2.2.3 Numerical modelling using Plane Strain Consolidation model

All the previously mentioned models were developed by considering the consolidation of a single drain in a unit cell in axisymmetric conditions, but analysing an embankment built on soft soil improved by prefabricated vertical drains should be based on plane strain conditions to accurately reflect the consolidation responces. Therefore it is imperative to establish a method that can convert existing axisymmetric models to an equivalent plane strain 2D model to give the same

consolidation response. Indraratna (2010) stated that this equivalent plane strain condition can be achieved by;

- Geometric approach – the spacing the PVD's changes while the permeability of clay remains constant.
- Permeability approach – the drain spacing remains unchanged but the coefficient of permeability is matched.
- Combined permeability and geometry approach – equivalent plane strain permeability is obtained while maintaining convenient drain spacing.

Hird et al. (1992) presented a solution to convert the axisymmetric model to a plane strain model that enabled it to be incorporated in finite element methods. However, this method tends to average out the smear zone across the unit cell hence is an implicit way to incorporate the smear effects. However, Indraratna & Redana (1997) and Indraratna & Redana (1999) were able to include the smear effects to the plane strain model in a novel and explicit way that enhanced its ability to accurately predict the smear effects and its role in consolidation when vertical drains are used in ground improvement projects.

In Indraratna & Redana (1997) and Indraratna & Redana (2000), the permeability approach was used to convert an axisymmetric case into an equivalent plane strain model. The spacing of the plane strain model was kept the same as the diameter of the axisymmetric unit cell (Figure 2.3), but the permeability of the plane strain model was changed to obtain the same degree of consolidation in both axisymmetric ($\overline{U}_h$) and plane strain ($\overline{U}_{h,ps}$) conditions.

$$\overline{U}_h = \overline{U}_{h,ps} \tag{2.19}$$

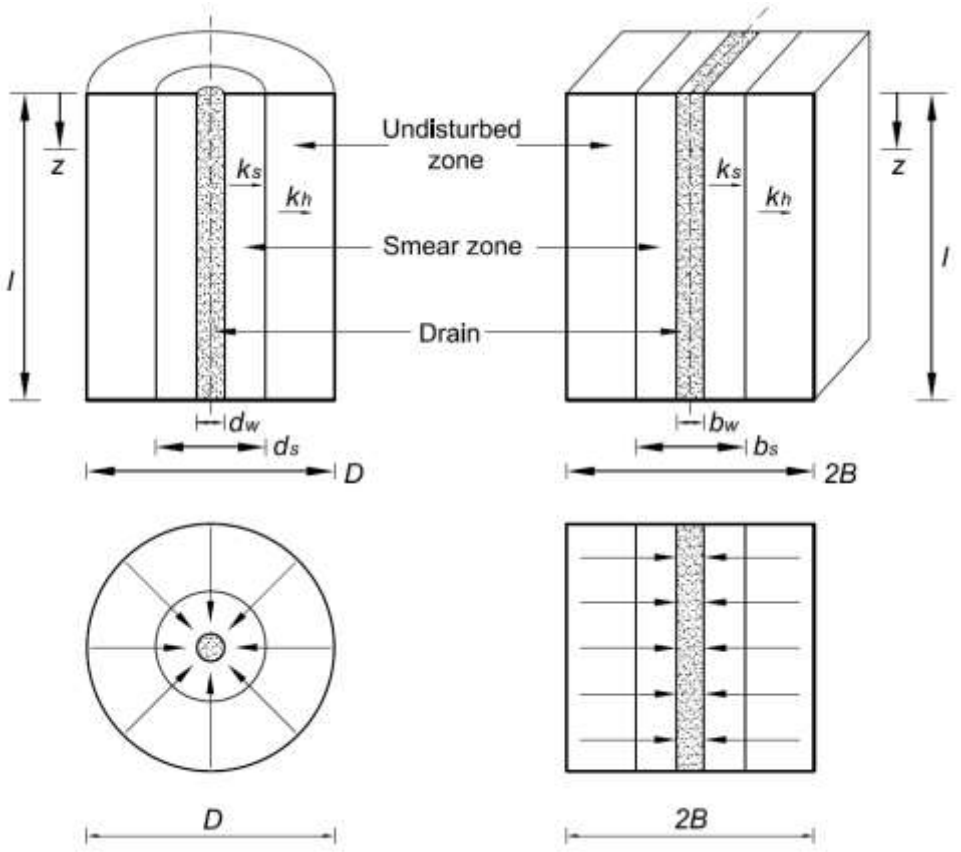

(a) **(b)**

Figure 2.3 : Conversion of an axisymmetric unit cell into a plane strain condition; (a) axisymmetric model (b) plane strain model (After Indraratna & Redana, 1997)

The average degree of consolidation of the plane strain model is;

$$\overline{U}_{h,ps} = 1 - \frac{\overline{u}}{u_0} = 1 - exp\left(-\frac{8T_{hp}}{\mu_p}\right) \tag{2.20}$$

where $U_{h,ps}$ and T_{hp} are the average degree of consolidation and time factor for plane strain conditions, $\overline{u}$ is the average excess pore water pressure at a given time, u_0 is the pore water pressure at the start of consolidation, and

$$\mu_p = \left[\alpha + (\beta)\frac{k_{h,ps}}{k'_{h,ps}} + (\theta)(2lz - z^2) \right] \tag{2.21}$$

In the above,

$$\alpha = \frac{2}{3} - \frac{2b_s}{B}\left(1 - \frac{b_s}{B} + \frac{{b_s}^2}{3B^2}\right) \tag{2.21a}$$

$$\beta = \frac{1}{B^2}(b_s - b_w)^2 + \frac{b_s}{3b^3}(3{b_w}^2 - {b_s}^2) \tag{2.21b}$$

$$\theta = \frac{2{k^2}_{h,ps}}{k'_{h,ps}Bq_z}\left(1 - \frac{b_w}{B}\right) \tag{2.21c}$$

where $k_{h,ps}$ and $k'_{h,ps}$ are the coefficient of permeability of the undisturbed and smear zones respectively, the subscript *ps* represents the plane strain condition, and q_z is the equivalent discharge capacity in plane strain model.

The time factor ratio can be defined by combining Equations 2.19, 2.20 and 2.13 as;

$$\frac{T_{hp}}{T_h} = \frac{k_{h,ps}}{k_h}\frac{R^2}{B^2} = \frac{\mu_p}{\mu} \tag{2.22}$$

R is the radius of the axisymmetric unit cell and *2B* is equal to the spacing of drains in the plane strain model. Initially these were assumed to be equal so the equivalent plane strain coefficient of permeability can be expressed in terms of the permeability of the axisymmetric model as;

$$k_{h,ps} = \frac{k_h\left[\alpha + (\beta)\frac{k_{h,ps}}{k'_{h,ps}} + (\theta)(2lz - z^2)\right]}{\left[\ln\left(\frac{n}{s}\right) + \left(\frac{k_h}{k'_h}\right)\ln(s) - 0.75 + \pi(2lz - z^2)\frac{k_h}{q_w}\right]} \tag{2.23}$$

Neglecting the terms represents well resistance, so an expression can be derived to represent the influence of shear as;

$$\frac{k'_{h,ps}}{k_{h,ps}} = \frac{\beta}{\left[\ln\left(\frac{n}{s}\right) + \left(\frac{k_h}{k'_h}\right)\ln(s) - 0.75 - \alpha\right]} \tag{2.24}$$

If both smear and well resistance is ignored then Equation 2.23 will reduced to the solution proposed by Hird et al. (1992)

$$\frac{k_{h,ps}}{k_h} = \frac{0.67}{[\ln(n) - 0.75]} \tag{2.25}$$

2.3 Use of Prefabricated vertical drains in ground improvement

2.3.1 History of vertical drains

The main advantage of using vertical drain is that they accelerate consolidation by reducing the drainage path. Early work using sand drains to speed up the consolidation was reported in Porter (1936) and Johnson (1970). Kjellman (1948) introduced cardboard wick drains instead of the sand drains, however the top part of the drains decayed rapidly, which reduced the drainage capacity. In 1971 Geodrains introduced a plastic grooved core instead of the cardboard one used before. Wick drains had been used occasionally until then although sand drains were still the most popular type of vertical drains used. (Holtz et al., 1991)

With the rapid development and subsequent urbanisation of eastern Asia during 1980's, the drains and installation methods had to be improved in order to meet the demands. Prefabricated vertical drains made from a corrugated plastic core covered with geo synthetic filter become popular and gradually replaced sand drains as the primary type of vertical drain in use. Recent developments in geotextiles also enabled the production of synthetic geo-materials with higher tensile strength and long term durability. Several types of drains were introduced to the market, such as Geodrain (Sweden), Alidrain (England), Mebradrain (Netherlands). This competition reduced the prices of the drain and made them much more cost effective as time saving installation methods were introduced. Today, PVDs of 30m long can be

installed into the ground within a minute. Details of different types of drains, installation methods, and typical geometric characteristics of drains are listed in Table 2.1. (Jamiolkowski et al., 1983; Holtz et al., 1991) Even though band shaped PVDs are the most popular type of drains, circular drains are also used in some projects, especially where a vacuum pressure is applied. Due to the high demand for environmentally friendly geosynthetic products, Bio-degradable drains have also become popular in recent times. In these drains geotextile made from organic materials such as Jute acts as the filter and stitched coir acts as the vertical drainage path. (Figure 2.4)

Table 2.1: Characteristics of different types of vertical drains. (After Jamiolkowski et al., 1983)

Drain type	**Installation method**	**Drain diameter (m)**	**Typical spacing (m)**	**Maximum length (m)**
Sand drains	Driven or vibratory closed-end mandrel (displacement type)	0.15-0.6	1-5	≤ 30
Sand drains	Hollow stem continuous flight auger (low displacement)	0.3-0.5	2-5	≤ 35
Sand drains	Jetted (non-displacement)	0.2-0.3	2-5	≤ 30
Prefabricated sand drains (sandwicks)	Driven or vibratory closed-end mandrel; flight auger; rotary wash boring (displacement or non-displacement)	0.06-0.15	1.2-4	≤ 30
Prefabricated band-shaped drains	Driven or vibratory closed-end mandrel (displacement or low displacement)	0.15-0.1	1.2-3.5	≤ 60

2.3.2 Equivalent drain diameter

Barron's (1948) radial consolidation theory assumed a circular cross-section drain in the analysis. This can easily be calculated when sand drains have been installed because the mandrel used has a circular cross section. Due to the increased usage of band drains in ground improvement projects it was necessary to come up with a method to estimate an equivalent diameter for a band drains. Kjellman (1948) suggested that the circumference of a drain is more important than its cross sectional area when assessing its water discharge capacity, and if the circumference of the drains are the same then it will lead to the same consolidation response. Hansbo (1979) later verified this using finite element analysis. Hansbo (1981) also proposed an equivalent diameter for band drains having a width of 'a' and a thickness of 'b' as;

$$d_w = \frac{2(a+b)}{\pi} \; ; \; or \qquad r_w = \frac{(a+b)}{\pi} \tag{2.26}$$

Later Atkinson & Eldred, (1981) suggested a reduction factor of $\pi/4$ to cater for the corner effects. This was subsequently proved by Rixner et al. (1986) using the finite difference method, and also by Hansbo (1987). The corrected expression for the equivalent drain diameter (d_w) is;

$$d_w = \frac{(a+b)}{2} \tag{2.27}$$

Pradhan et al. (1993) proposed an equation for the equivalent drain diameter based on the flow nets around the drain influenced area as;

$$d_w = \; d_e - 2\sqrt{(\bar{s}^2)} + b \tag{2.28}$$

$$\bar{s}^2 = \frac{1}{4} d_e^2 + \frac{1}{12} a^2 - \frac{2a}{\pi^2} d_e \qquad (2.29)$$

Long & Covo (1994) determined an equivalent diameter for drain with a rectangular cross section using an electrical analogue field plotter as,

$$d_w = 0.5\, a + 0.7\, b \qquad (2.30)$$

(a) **(b)**

Figure 2.4 : Types of drains available (a) Band drains: Synthetic and bio degradable drains; (b) Circular drains : 54mm & 34mm diameter drains

2.3.3 Filter in Prefabricated vertical drains

Holtz et al. (1991) mentioned that the most important property of a drain is its lateral and vertical permeability and its durability over time. The behaviour of the filter will affect the lateral permeability while the plastic core is responsible for

vertical drainage. The currently contrasting and prevailing views are concerned with how to choose a suitable filter cloth to wrap around the stiffer central core in a PVD. Hansbo (1981 & 1983) stated that it would be better to make the openings of the filter cloth small enough to prevent any particles of soil from passing through whereas Jansen & den Hoedt (1983) and Vreeken (1983) indicated that having a larger opening size would allow the tiny particles to pass through while the larger particles formed a natural soil filter.

When designing a geotextile filter for a vertical drain it is better to assess the, soil retention ability of the geotextile, permeability and the resistance to clogging. (Holtz et al., 1991) A basic guideline for permeability is given by;

$$k_{filter} \geq 10\, k_{soil} \tag{2.31}$$

For a geotextile filter, the apparent opening size (AOS) can be used to characterise its performance. Carroll (1983) presented the generally used criteria as;

$$\frac{O_{95}}{D_{85}} \leq (2-3) \tag{2.32}$$

where the retention ability is given by,

$$\frac{O_{50}}{D_{50}} \leq (10-12) \tag{2.33}$$

Here, O_{95} is the AOS of the geotextile, the pore size of which 95% of the pores in the geotextile are smaller, or the size of the largest particle passing through. D_{85} is the diameter of 85% of soil particles passing through. According to AS 8700 (2011), the AOS (O_{95}) should not be greater than 80 μm.

To prevent the particles from clogging, Christopher & Holtz (1985) suggested the following two criteria should be fulfilled:

$$\frac{O_{95}}{D_{15}} \geq 3 \tag{2.34}$$

$$\frac{O_{15}}{D_{15}} = (2-3) \tag{2.35}$$

2.3.4 Discharge capacity and well resistance of a drain

The discharge capacity of a drain is a very important parameter because it affects the performance of a vertical drain system. According to Holtz et al. (1991) the drain discharge capacity ($q_{w)}$ depends on the following factors;

- The cross sectional area available for water to travel vertically, and the effect of horizontal earth pressure.
- Possible folding and bending of the drain due to high settlement
- Reduction of flow capacity due to the intrusion of fine particles through the geotextile.
- Durability of drains

Chu et al. (2004) calculated the minimum required discharge capacity of a drain to be as;

$$q_{requried} \geq 7.85\, F_s k_h l_m^2 \tag{2.36}$$

Where F_s is the factor of safety which can be taken as 4-6, l_m is the maximum discharged length, and k_h is the lateral soil permeability. The $q_{requried}$ was obtained from Barron (1948) and is given as;

$$q_{requried} = \frac{\varepsilon_f U_{10} l \pi c_h}{4T_h} \tag{2.37}$$

where ε_f is taken as a quarter of the total length of the drain (assumed total settlement), U_{10} is 10% degree of consolidation, c_h is coefficient of radial consolidation, T_h is the times factor for radial consolidation, and l is the length of the drain.

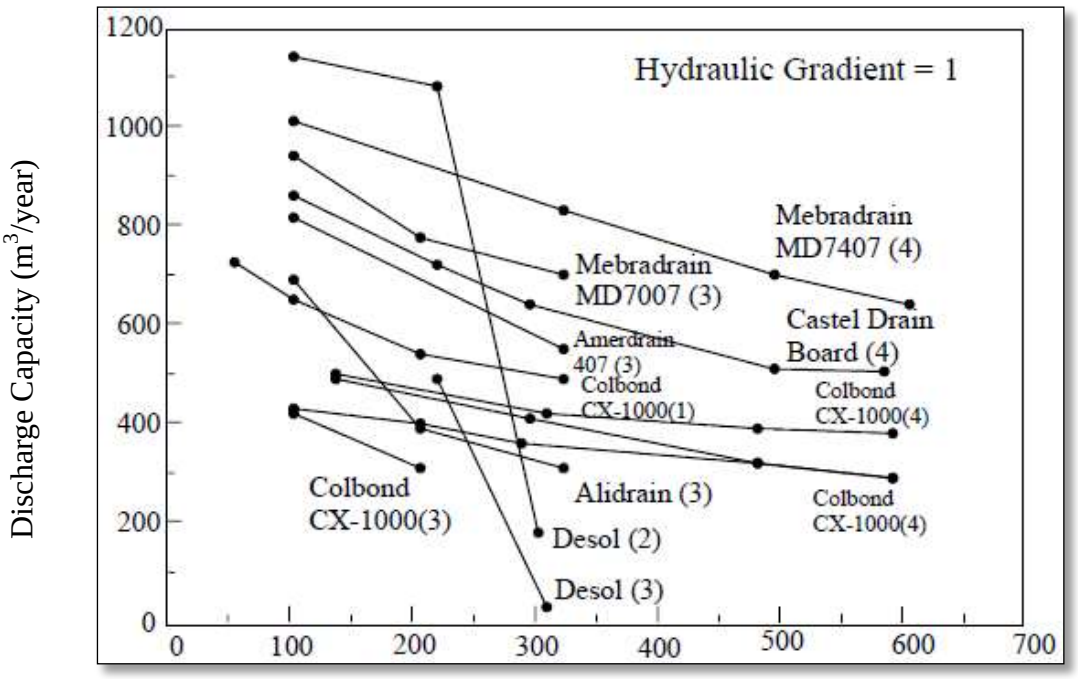

Figure 2.5: Variation of discharge capacity with confining pressure for different drain types. (After Rixner et al., 1986)

Rixner et al. (1986) summarised the discharge capacity of many types of drains, and it is shown in Figure 2.5. The effect of lateral pressure on the discharge capacity is clearly evident from these results. Miura & Chai (2000), Chai & Miura (1999) and Bergado et al. (1996) also investigated the effect of lateral pressure on the discharge capacity and stated that discharge capacity tests should be conducted using clay confinement to obtain satisfactory results.

In their comprehensive report, Holtz et al., (1991) concluded that the effect of well-resistance to the rate of consolidation was negligible in short term conditions, but they did mention that as long as the discharge capacity was around 100-150 $m^3/year$ the rate of consolidation would not change. Den Hoedt (1981) reported a discharge capacity of 90 $m^3/year$ and Kremer (1981) suggested 160 $m^3/year$ to avoid the influence of well resistance. Indraratna & Redana (2000) stated that a discharge capacity of 40-60 $m^3/year$ might introduce well-resistance into vertical drains in long term conditions. Hansbo (1987) also recommended that the discharge capacity should not be below 50-100 $m^3/year$ for long drains.

2.3.5 Influence zone of a drain

In ground improvement projects, vertical drains are installed in both square and triangular patterns, as shown in Figure 2.6. The influence zone of a drain is a primary parameter required in almost all analytical solutions. Hansbo (1981) calculated the influence zone of a drain based on the spacing of drains (S) as follows;

$$d_e = 1.128\,S \qquad \text{for drains installed in square pattern;} \qquad (2.38)$$

$$d_e = 1.05\,S \qquad \text{for drains installed in triangular pattern;} \qquad (2.39)$$

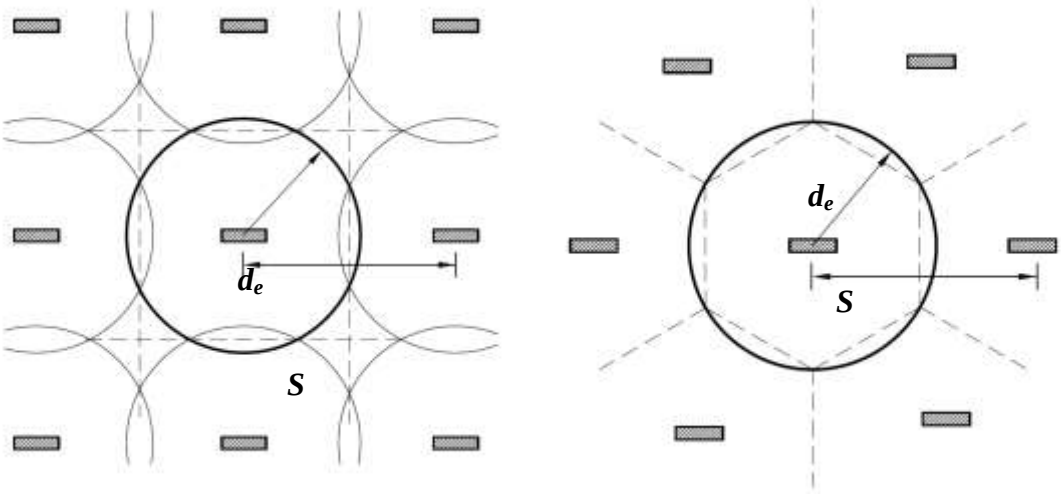

(a) **(b)**

S = spacing of drains

Figure 2.6 : Drain installation pattern and equivalent diameter (d_e) **(a)** Square pattern; **(b)** Triangular pattern

In most conditions a square pattern is preferred because it is easy to lay out and install, although a triangular pattern produces more uniform settlement in between drains.

2.3.6 Drain installation

In ground improvement projects, thousands of drains are usually installed and therefore proper equipment must be used to save time and install the drains efficiently. Slender vertical drains are inserted into the ground inside a stiffer steel mandrel that is driven by a mechanical rig (Figure 2.7). A shoe is attached to the vertical drain to act as an anchor. Bo et al. (2003) stated that selecting the right type of rig for drain installation is very important; the rig is supported by a sand platform placed above the ground to be improved, and while a heavier rig may cause the

equipment to become unstable, a lighter rig may not have enough power to drive the drains smoothly into the ground.

Figure 2.7 : Drain Installation equipment.

2.3.7 Types of Mandrels and Anchors used

Rectangular and rhombic shaped mandrels are commonly used in vertical drain installation while circular mandrels are not used very often (Bo et al., 2003). Smaller rhombic mandrels generate less disturbance of the soil and hence the smear effects are less than rectangular mandrels. However, rectangular mandrels (Figure 2.8) are preferred when drains are installed in stiffer ground because rhombic mandrels tend to buckle under higher soil resistance.

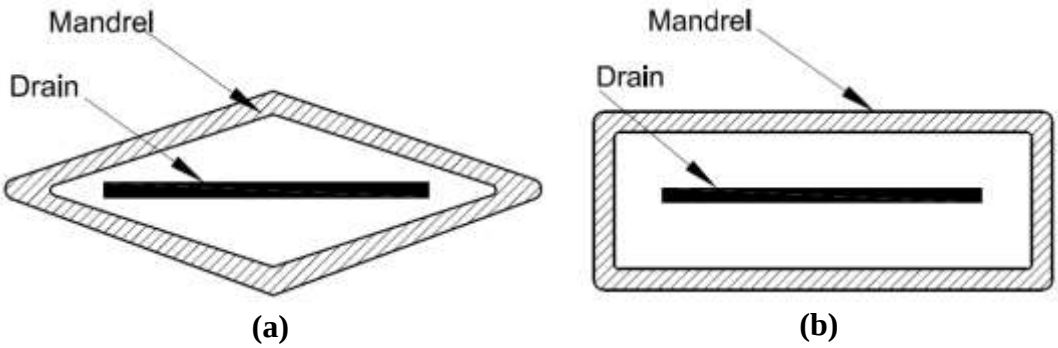

Figure 2.8 : Different shapes of mandrel (a) Rhombic; (b) Rectangular.

Steel bars and rectangular steel plates are the most common types of drain anchors used in vertical drain installation. The anchor should be stiff enough to hold the drain in position when the mandrel is about to be lifted up after the drain has been driven it to the required depth. The anchor plate is also used to prevent any soil from entering the drain whilst it is being driven into the soil.

2.4 Smear effects due to drain installation

2.4.1 General

When vertical drains are installed with a steel mandrel, the soil adjacent to it is disturbed and creates region known as the smear zone where the coefficients of lateral permeability and radial consolidation in the soil are decreased. This will adversely affect consolidation and therefore the extent of this smear zone and the reduction of horizontal permeability must be estimated accurately in order to predict the consolidation responses over time.

Rowe (1968) stated that the amount of disturbance caused by the mandrel intrusion depends on the sensitivity and macro-fabric of the soil. Barron (1948) suggested that smear due to drain installation is somewhat similar to the disturbance

experienced close to the wall of sampling tubes, although the amount of smearing created due to driving a hollow mandrel with a closed cap at one end was much larger than the sampling tubes because it displaces the entire soil.

Barron (1948) and Hansbo (1979, 1981) divided soil into two zones, the smear zone created by the installation of drains, and the undisturbed region beyond that. The smear zone was assumed to be a uniform cylindrical shape where its centreline coincided with the centre of the vertical drain. The diameter of the smear annulus was taken as d_s and a reduced average permeability inside the smear zone was taken as k_s. As a result of this, two new parameters were introduced to the analytical solution for radial consolidation, namely $s = d_s/d_e$ and k_h/k_s (permeability ratio). These two new parameters were difficult to calculate accurately in laboratory conditions. (Holtz et al., 1991)

As reported by Indraratna & Redana (2000), a two zone representation of the smear zone is adequate for practical situations encountered. However, several researchers carried out some extensive laboratory work and then suggested that three definite zones exist due to the installation of drains (Onoue et al., 1991; Madhav et al., 1993; Rujikiatkamjorn et al., 2013). These three zones can be broadly defined as:

- A highly remoulded smear zone near the drain where the permeability and compressibility are significantly reduced.
- A middle transition zone where the permeability is moderately decreased.
- An outer undisturbed zone where drain installation has no impact on the permeability or compressibility of the soil.

2.4.2 Extent of the smear zone and the reduction factor for permeability

The diameter and average permeability reduction factor of the smear zone are the two main factors needed to evaluate the smear effects due to drain installation. The diameter of the smear zone can be stated as a factor of the equivalent diameter of the mandrel used. It is well established that the horizontal permeability continuously increases within the smear zone until it reaches the undisturbed zone permeability at the boundary of the smear zone and undisturbed zone (Onoue et al., 1991; Madhav et al., 1993; Indraratna & Redana, 1998).

Different values for the extent of smear zone can be found in the literature. Holtz & Holm (1973) and Akagi (1977) assumed the following relationship for the extent of the smear zone:

$$d_s = 2d_m \tag{2.40}$$

where d_m is the diameter of a circle where the area is equal to the cross sectional area of the mandrel used. Using the curve fitting method Bergado et al. (1991) also verified this value. Using laboratory experiments Sharma & Xiao (2000) estimated the smear zone to be four times the area of mandrel and 5-8 times the area of the drains used. Jamiolkowski et al. (1983) proposed a slightly different expression where,

$$d_s = \frac{(5-6)}{2} d_m \tag{2.41}$$

Indraratna & Redana (1998) performed large scale consolidation tests to investigate the smear effects due to drain installation. The consolidation cell used had a 450mm inside diameter and was 950mm long. A section of this test equipment is shown in Figure 2.9a. A 50mm sand drain was installed using a 50mm diameter

steel mandrel. After installation, vertical and horizontal samples of soil were collected around the drain in different radial locations (Figure 2.9b), using a tube sampler. These samples were subsequently tested in an Oedometer to obtain the permeability characteristics.

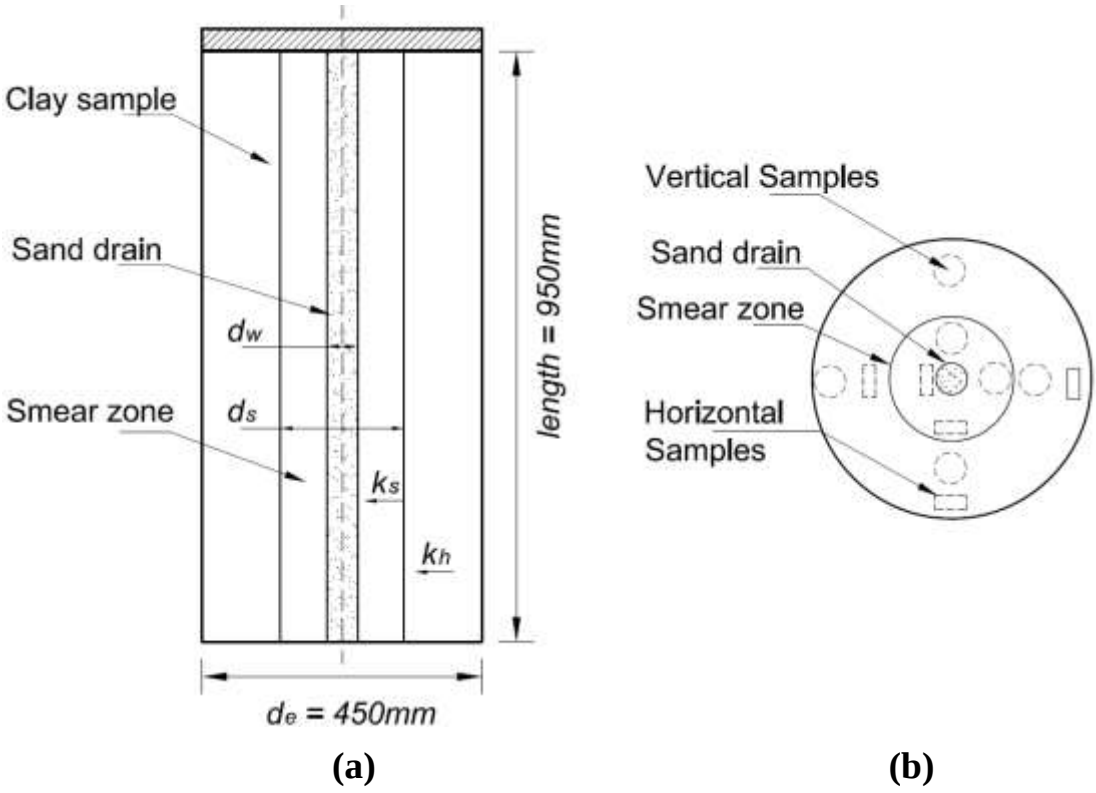

Figure 2.9 : (a) schematic diagram of large scale consolidometer. (b) Sample extraction locations for oedometer tests (Modified after Indraratna & Redana, 1998)

According to laboratory testing, the diameter of the smear zone was estimated to be four to five times the diameter of the mandrel used. It was observed that lateral permeability had sharply reduced in the smear zone towards the sand drain, while the coefficient of vertical permeability remained constant in smear zone and undisturbed zone. The variations of permeability with radial locations are shown in Figure 2.10.

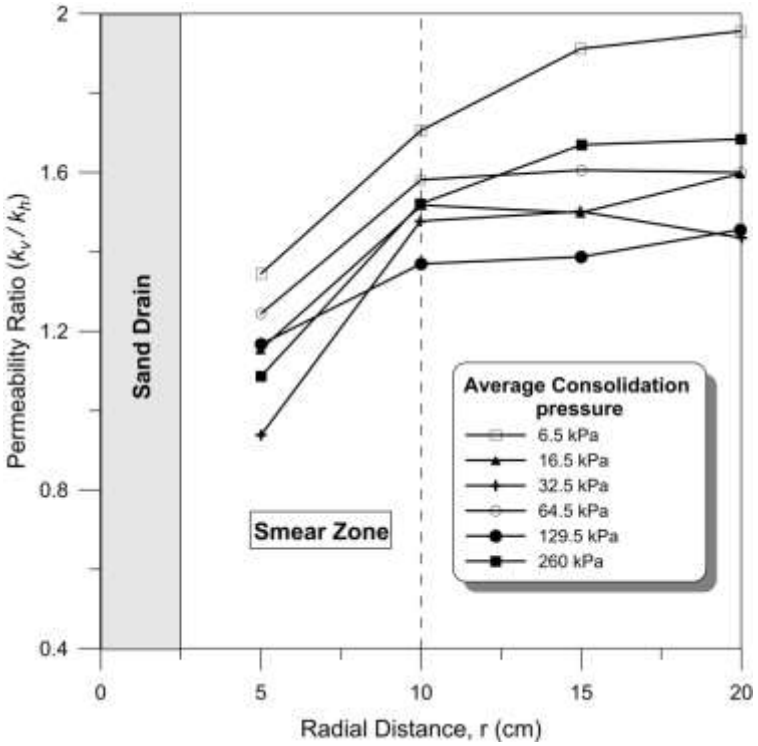

Figure 2.10 : variations in the ratio of vertical permeability/ horizontal permeability along the radius of the drain (Modified after Indraratna & Redana, 1998)

Sathananthan & Indraratna (2006) also performed similar types of large scale consolidation test on remoulded Moruya clay, and they stated that the reduction in the moisture content was also used to estimate the extent of the smear zone. Further, an empirical correlation was proposed for a reduction of permeability in terms of a decrease in the moisture content as:

$$\frac{\Delta k}{k_h} = C\left(\frac{\Delta w}{w_0}\right)^n \qquad (2.42)$$

Where Δk is the reduction in permeability, Δw is the reduction in the moisture content, w_0 is the moisture content of the undisturbed region, and C and n are empirical constants.

Guidelines for the reduction in permeability inside the smear zone have been provided by many researchers. Hansbo (1981) assumed the ratio between undisturbed and smear zone to be 3, while Bergado et al. (1991) used back-analysis and determined this to be only 1.75. Using laboratory experiments Sharma & Xiao (2000) estimated the permeability ratio as 1.3.

2.4.3 Analysis of soil disturbance using cavity expansion theory

Akagi (1977) and Sharma & Xiao (2000) reported a considerable increase in pore water pressure when a closed mandrel was driven into a sample of saturated clay. It is understandable that the horizontal displacement of soil due to the insertion of a closed end mandrel caused this elevated pore pressure. Sathananthan et al. (2008) attempted to establish the extent of the smear zone by the pore pressure generated due to the mandrel, along with established methods such as variations of lateral permeability and the moisture content. The analytical cavity expansion theory of Cao et al. (2001) was used to obtain an expression for the radial variation of pore water pressure (u) as:

$$u = p_0 + \frac{Mp_0'}{\sqrt{3}}\sqrt{(R-1)} - \frac{q}{\sqrt{3}} + \frac{2}{\sqrt{3}}\int_r^{r_p}\frac{q}{r}dr - p' \qquad (2.43)$$

Where *R* is the isotropic over consolidation ratio which can be expressed in terms of the conventional over-consolidation ratio (OCR) as:

$$R = \frac{3(45 - 12M + M^2)OCR}{(6-M)(6+M+2(6-M)OCR^{(3M/6+M)})} \qquad (2.44)$$

Where p_0 is the initial mean stress, $p'$and q are the effective mean stress and deviator stress, *M* is the slope of the critical state line, and *r* is the radial distance.

A good agreement with the predicted pore pressures was derived from the cavity expansion theory and the experimental values obtained using large scale consolidometer are shown in Figure 2.11. The smear zone was about 2.5 times the size of the mandrel and the permeability ratio between the undisturbed zone and the smear zone was between 1.08-1.64.

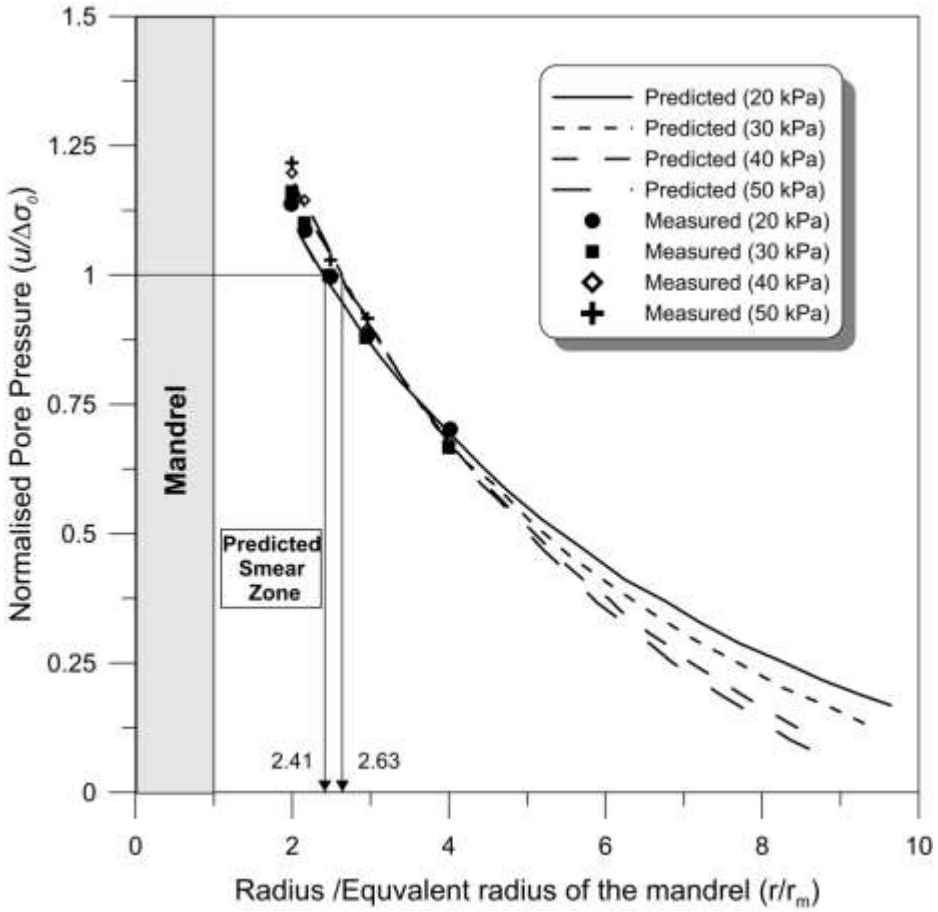

Figure 2.11: Normalised pore pressure variation along the radius

(After Sathananthan et al., 2008).

Ghandeharioon et al. (2010) developed this concept further by introducing an elliptical cavity expansion theory to investigate the smear effects in mandrel driven

vertical drains. An elliptical smear zone was assumed in this solution and the experimental and numerical validation is presented in Ghandeharioon et al. (2012)

2.4.4 Overlapping smear zones

Radial consolidation models such as Hansbo (1981) and Indraratna & Redana (1997) considered the lateral permeability to be a constant but reduced value throughout the smear zone, but it is well understood that the lowest permeability exists near the drain and it increases along the radius of the smear zone until it becomes relatively constant in the undisturbed zone. Walker & Indraratna (2006) modified the radial consolidation equation by considering the permeability as being reduced towards the drain in a parabolic shape.

When vertical drains are used in a ground improvement project, the drainage path of an each drain can be reduced by adding more drains per unit area. However, Saye (2003) recognised there is a minimum drain spacing below which no significant improvements in consolidation responses can be achieved. Walker & Indraratna (2007) proposed a concept of overlapping smear zones to describe the mechanisms responsible for this.

In this model, a linear variation in permeability was assumed inside the smear zone. A schematic diagram of an overlapping smear zone is shown in Figure 2.12 where it was assumed that the radius of the smear zone r_s was larger than the radius of the drain influence area r_e . The permeability of the interaction area was taken as constant and the permeability was equal to the value where the smear zones intersected.

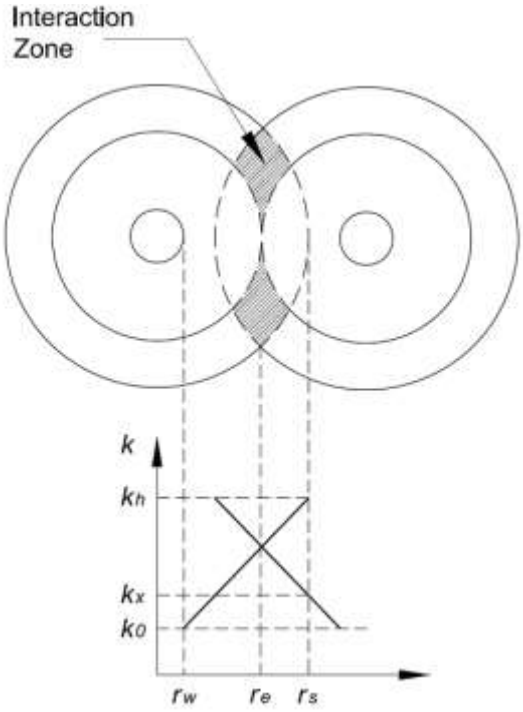

Figure 2.12 : Schematic diagram of an overlapping smear zone (After Walker & Indraratna (2007)

2.4.5 Influence of drain installation to the soil structure

Leroueil & Vaughan, (1990) stated that in-situ soil has a unique structure that will not be available in the reconstituted samples made from the same materials. However, almost all the experiment work conducted in the smear zone study was limited to testing remoulded soils that cannot capture how the soil structure is affected by drain installation using steel mandrels. Chai et al. (2004) discussed about the consolidation characteristics and recently, Yang et al (2014) studied about the nonlinearity of virgin compression lines in structured clay.

To overcome these limitations, Rujikiatkamjorn et al. (2013) presented a conceptual model to describe the destruction of soil structure as a result of drain installation. Details of this conceptual model are shown in Figure 2.13. This concept

was proved using experiments conducted using large scale undisturbed sample tests and numerical analysis.

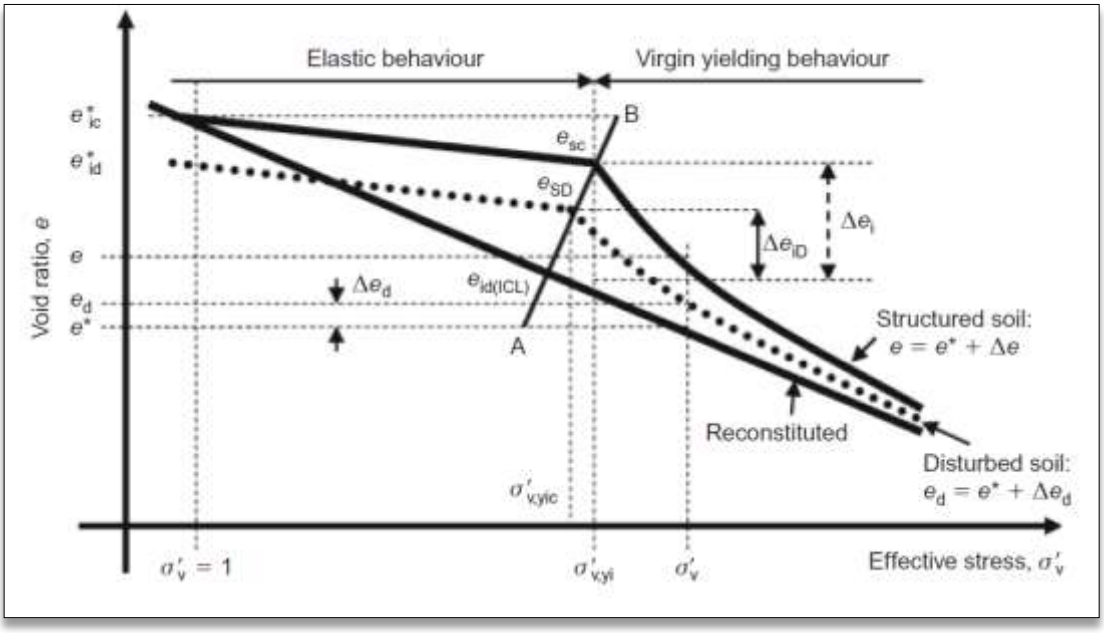

Figure 2.13 : Conceptual model to evaluate smear effects

To quantify the amount of disturbance caused by a new parameter, a degree of disturbance (DD) was introduced as;

$$DD = 1 - \left[\frac{e_{SD} - e_{id(ICL)}}{e_{SC} - e_{id(ICL)}}\right] \tag{2.45}$$

2.5 Soil improvement using Vacuum Preloading

2.5.1 Introduction

The concept of using vacuum preloading as a ground improvement technique was first presented by Kjellman (1952), and since then it has been successfully used in many regions of the world (Holtz, 1975; Bergado et al., 1998; Rujikiatkamjorn & Indraratna, 2007; Indraratna et al., 2011). This method has a distinct advantage in projects like land reclamation where soft soil dredged from sea bed is used as the

land reclamation material which cannot support any additional surcharge fill loads due to its inherent low shear strength.

In typical field conditions, a vacuum pressure of 80 kPa can be transferred to the soil, but when a higher preloading is needed, a vacuum pressure can be applied along with traditional surcharge fill loads. Chu et al. (2000) stated that vacuum preloading could be cheaper and faster than surcharge embankment fill, especially where quality fill materials for embankments were not abundantly available. A vacuum pressure is applied to the ground using two main methods, the membrane system, ex. Menard (Figure 2.14) and the membraneless system, ex. Beaudrian (Figure 2.15).

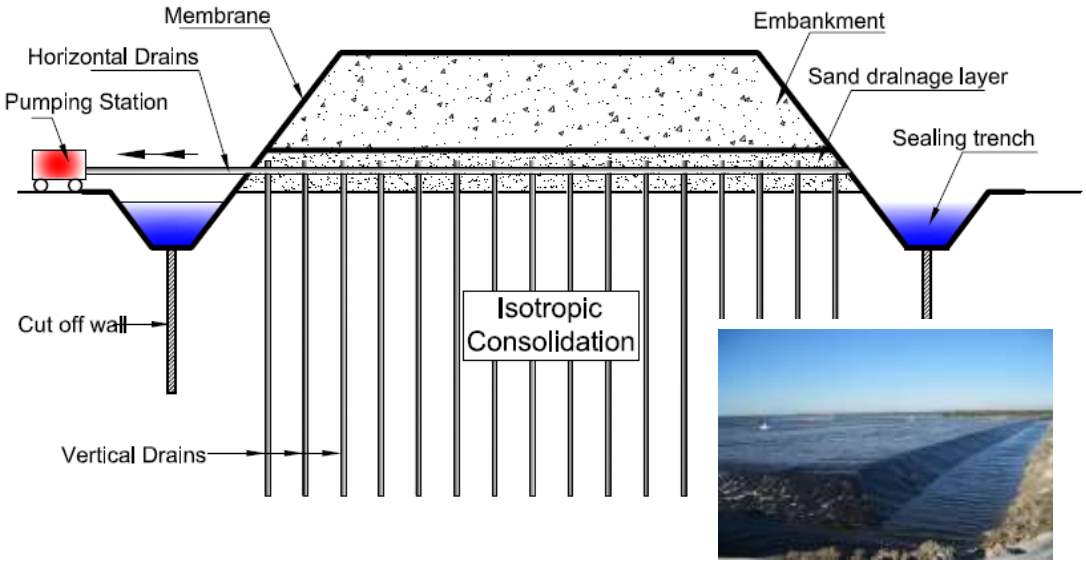

Figure 2.14 : Membrane system

In a membrane system an airtight membrane is placed over a sand drainage layer and then a vacuum pressure is applied using horizontal drains placed inside the sand mat. A horizontal drain is not connected individually to the vertical drains. to ensure a watertight membrane, a Bentonite sealing trench and a cut off wall at the periphery of the embankment is commonly used to prevent vacuum pressure leakage.

This system allows the vacuum pressure to be transmitted to the soft ground through the vertical drains and the top surface of the clay layer, and it also needs less piping so the installation time and costs involved are less (Indraratna et al., 2010).

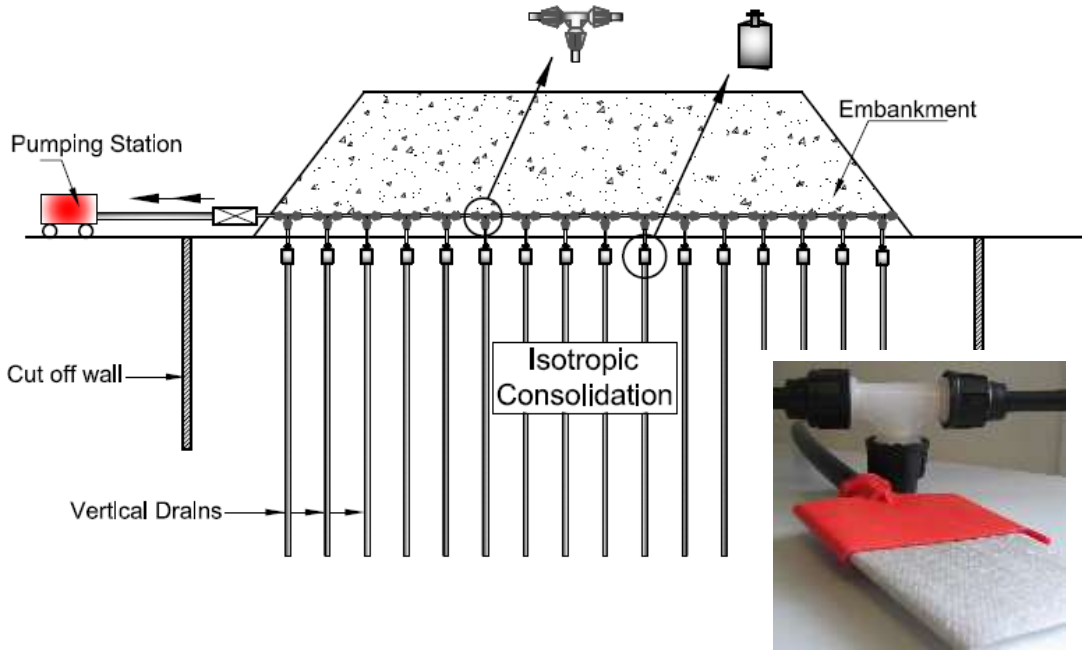

Figure 2.15 : Membrane less system

When vacuum pressure with vertical drains is used close to a marine boundary, it can be difficult to prevent a loss of vacuum through the land layers close to the ground, even with a cut off wall. Applying vacuum pressure using a membraneless system is an ideal solution in these situations. In this system every drain is directly connected to the vacuum pump via a horizontal piping system, and therefore, the vacuum pressure is applied directly to the drain. Other advantages with this system are that a sand drainage blanket is not needed and the vacuum pressure can be applied to a specific section beneath the embankment. However, this system does require more connections and piping which obviously increases the installation time and costs.

2.5.2 Principles of Vacuum preloading with PVD

The effective strength increase of an embankment with a preloading surcharge pressure is well understood. When a vacuum pressure is applied to a layer of soft clay the total stress in the soil will not change. However, the negative pressure applied by the vacuum pump will reduce the pore water pressure by the same amount of vacuum pressure transferred from the mechanical system to the underlying soft clay. Under a constant total load this reduction in pore water pressure will increase the effective stress and hence the stability of weak soils. Figure 2.16 shows how the effective stress transfer would occur in the case of a surcharge only case and combined surcharge and vacuum applied situation. (Indraratna et al., 2005a)

Qian et al. (1992) and Indraratna et al. (2005a) compared the main differences between conventional surcharge preloading and vacuum preloading as:

- With a vacuum pressure the soil is subjected to isotropic consolidation and so the resultant lateral movement is compressive. Consequently, embankment can be rapidly constructed.
- When a vacuum pressure is applied, it is imperative to monitor the 'inward' movements of soil, particularly close to the toe of the embankment, in order to reduce any damage to adjacent structures. This can occur when the vacuum preloading contributes a higher percentage of the preloading applied.
- Vacuum pressure can be propagated to the deeper sub soil layers using prefabricated vertical drains.
- Settlement due to an efficient vacuum system is equal to the same settlement caused by an embankment surcharge, provided the stress applied from the embankment load is equal to the magnitude of vacuum pressure applied.

- Since a vacuum preloading can reduce the height of an embankment, the amount of the excess pore pressure generated would also be reduced increasing its stability. Due to the gap between the mandrel and the actual vertical drain, an unsaturated soil drain interface is created that will retard consolidation; however, a vacuum preloading can negate this effect to a certain degree.

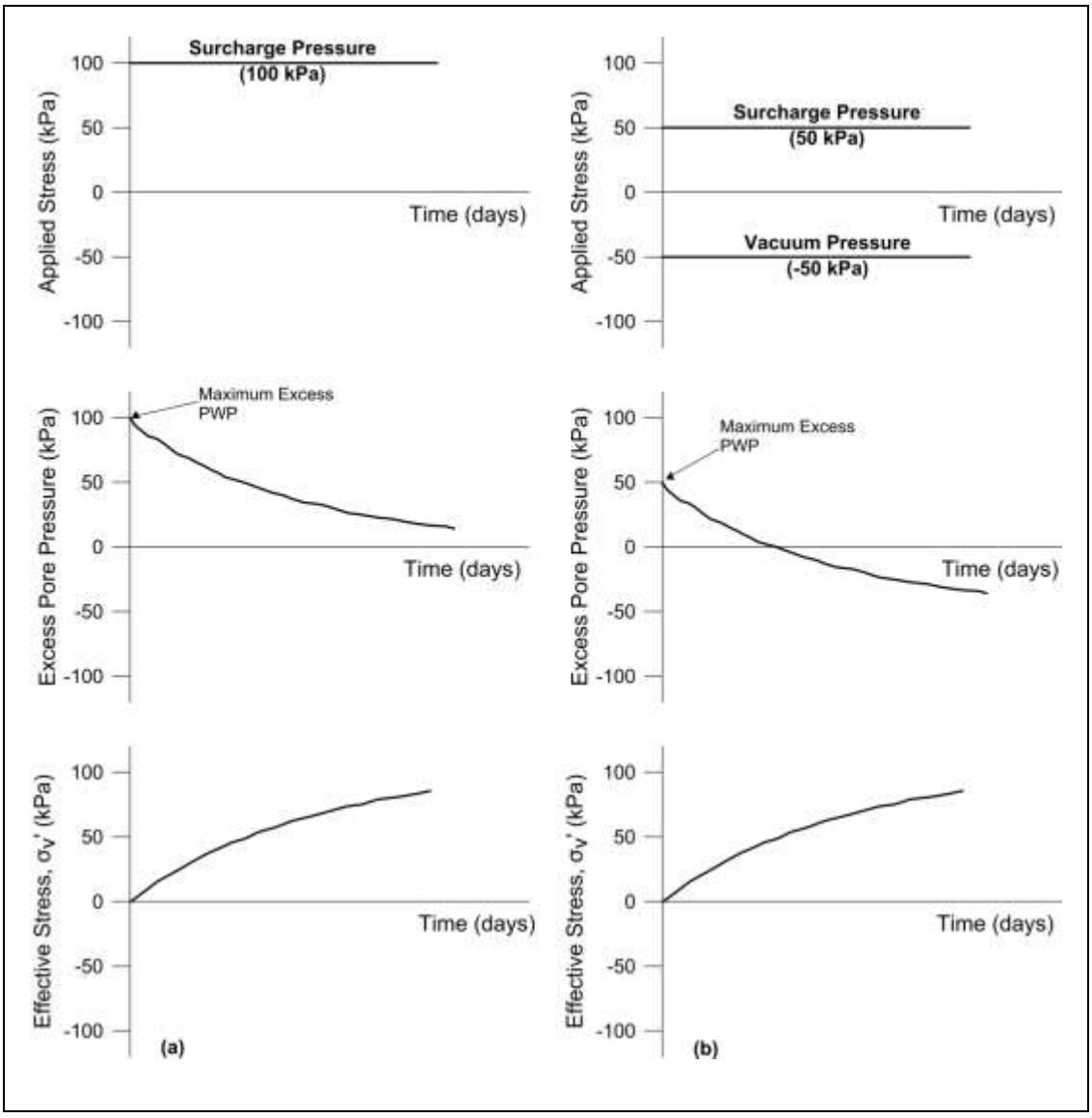

Figure 2.16 : Effective Stress Increase in **(a)** Surcharge loading only; **(b)** Surcharge and Vacuum loading (Adopted from Indraratna et al., 2005a).

2.5.3 Theory of vertical consolidation incorporating vacuum preloading

Based on Terzaghi's consolidation theory Mohamedelhassan & Shang (2002) developed a one dimensional consolidation model that combined a vacuum and surcharge. The average degree of consolidation for a combined surcharge and vacuum preloading can be expressed by,

$$U_{vc} = 1 - \sum_{m=0}^{\infty} \frac{2}{M^2} exp^{-M^2 T_{vc}} \tag{2.46}$$

$$T_{vc} = \frac{C_{vc} t}{H^2} \tag{2.47}$$

where T_{vc} is a time factor for a combined vacuum and surcharge preloading. In this study consolidation apparatus was modified to apply a vacuum preloading and two sets of experiments were carried out using different samples of clay. The same consolidation characteristics were observed from all three loading conditions (vacuum pressure, surcharge pressure, and a combination of vacuum and surcharge pressure) and a good agreement with the proposed model was also observed. It was concluded from this study that the required consolidation parameters can be derived from conventional oedometer tests provided the loading conditions are one dimensional.

2.5.4 Analytical model for vacuum preloading

In most ground improvement projects, a vacuum pressure was applied to the ground using PVDs. Indraratna et al. (2005c) proposed a comprehensive mathematical solution for vacuum preloading with vertical drains that was based on an equal strain assumption (Barron, 1948) and an assumed trapezoidal vacuum pressure distribution along the vertical drain to simulate the possible loss of vacuum.

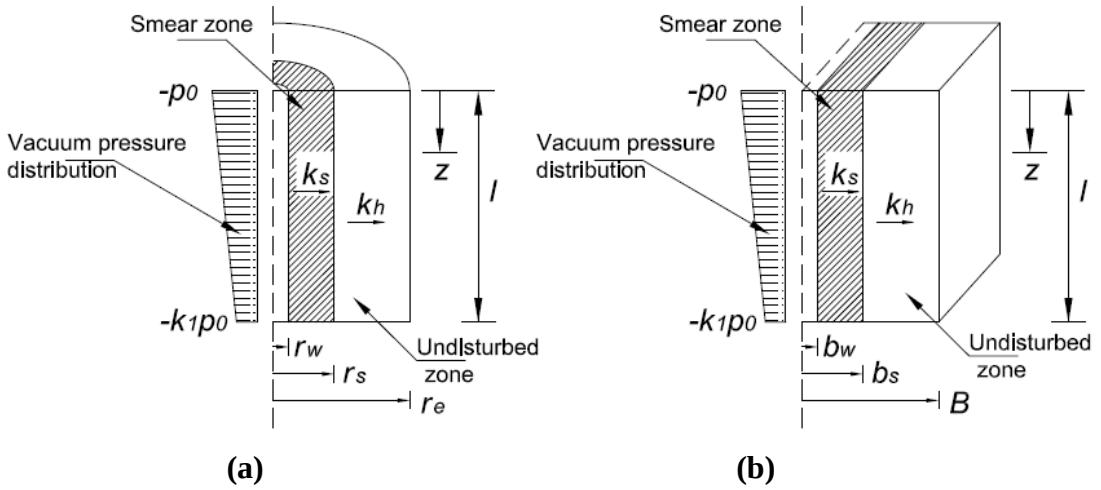

Figure 2.17 : Vacuum pressure distribution in a unit cell (a) Axisymmetric condition; (b) Plane strain condition. (Indraratna et al., 2005c)

The average excess pore water pressure ratio for an axisymmetric soil cylinder (Figure 2.17) can be expressed as;

$$R_u = \left(1 + \frac{p_0}{\bar{u}_0}\frac{(1+k_1)}{2}\right) exp\left(-\frac{8T_h}{\mu}\right) - \frac{p_0}{\bar{u}_0}\frac{(1+k_1)}{2} \qquad (2.48)$$

and

$$\mu = \ln\left(\frac{n}{s}\right) + \left(\frac{k_h}{k_s}\right)\ln(s) - 0.75 + \pi z(2l - z)\frac{k_h}{q_w}\left\{1 - \frac{k_h/k_h' - 1}{(k_h/k_h')(s/n)}\right\} \qquad (2.49)$$

where, p_0 = the vacuum pressure applied at the top of the drain, k_1 = the ratio between the vacuum at the top and bottom of the drain, $\bar{u}_0$ = the average initial excess pore water pressure, k_h = the horizontal permeability coefficient of soil in the undisturbed zone, k_s = the horizontal permeability coefficient of soil in the smear zone, and the value for μ can be further simplified as;

$$\mu = \ln\left(\frac{n}{s}\right) + \left(\frac{k_h}{k_s}\right)\ln(s) - 0.75 + \pi z(2l - z)\frac{k_h}{q_w} \quad (2.50)$$

In the field, a vacuum pressure is applied to the ground using hundreds if not thousands of drains, so it is impossible to apply the axisymmetric model to a numerical analysis and simulate the ground behaviour, even with the most advanced of modern computers. To overcome this problem, an axisymmetric model must be converted into a 2D plane strain model in order to incorporate it into advanced numerical models (Indraratna & Redana, 2000). Indraratna et al. (2005c) converted the axisymmetric model proposed in equation (2.48) into 2D plane strain conditions (Figure 2.17) as:

$$R_{up} = \left(1 + \frac{p_{0p}}{\bar{u}_0}\frac{(1+k_1)}{2}\right)exp\left(-\frac{8T_{hp}}{\mu_p}\right) - \frac{p_{0p}}{\bar{u}_0}\frac{(1+k_1)}{2} \quad (2.51)$$

and,

$$\mu_p = \left[\ \alpha\ + \frac{k_{hp}}{k_{sp}}(\beta) + (\theta)(2lz - z^2)\right] \quad (2.52)$$

$$\alpha = \frac{2}{3}\frac{(n-s)^3}{n^2(n-1)} \quad (2.53)$$

$$\beta = \frac{2(s-1)}{n^2(n-1)}\left[n(n-s-1) + \frac{1}{3}(s^2+s+1)\right] \quad (2.54)$$

$$\theta = \frac{2k_{hp}}{Bq_z}\left(1 - \frac{1}{n}\right) \quad (2.55)$$

This solution was successfully incorporated into numerical models in Indraratna et al. (2005b) and Rujikiatkamjorn et al. (2008) and an excellent agreement with the field data was observed.

2.5.5 Settlement and lateral strains due to vacuum preloading

Outward lateral displacements would occur in soft clay subjected to an embankment loading as a result of the shear stresses generated. However, vacuum preloading will induce inward lateral strains due to its isotropic consolidation that can be used to reduce any lateral deformation (Bergado et al., 1998; Chai et al., 2006). Robinson et al, (2012) also studied lateral strains under vacuum pressure using reconstituted Kaolinite samples in a modified Rowe cell (Rowe & Barden, 1966).

Vertical and lateral ground deformations induced by vacuum preloading were discussed by Chai et al. (2005). Using oedometer tests with a vacuum pressure they observed that if the lateral stress induced by the vacuum pressure was greater than the at-rest horizontal stress, there will be an inward lateral strain in the soil, as shown in Figure 2.18. Furthermore, he stated that in a case of an inward horizontal movement, vacuum pressure would yield less vertical settlements than the settlement induced by the equivalent surcharge load.

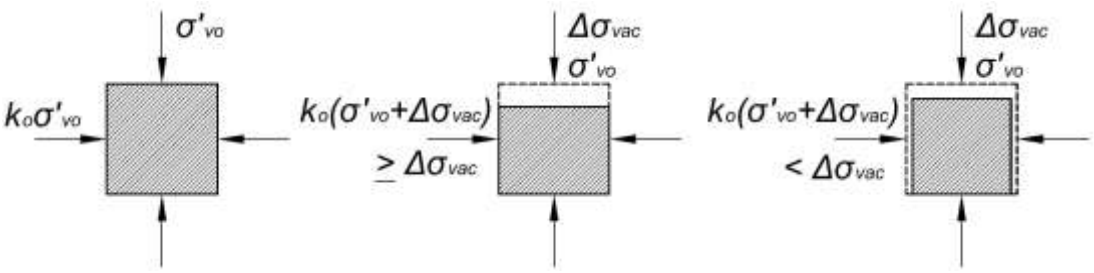

Figure 2.18 : Deformation forms of soil element subjected to a vacuum pressure (a) initial stresses; (b) No lateral displacements; (c) With lateral displacements (Adopted from Chai et al., 2005)

2.5.6 Degree of consolidation (DOC) of vacuum preloading projects.

In any ground improvement project, the degree of consolidation is a vital parameter used to gauge the efficiency of the improvement work, so it is frequently used in design specifications and contract documentation. In projects with vertical drains the settlement data is often used to estimate the DOC and back calculate the coefficient of radial consolidation (Vinod et al., 2010). The Asaoka (1978) method is widely used to obtain ultimate settlement and DOC using the settlement data. Chu & Yan (2005) proposed an expression to evaluate the average degree of consolidation (U_{avg}) using the pore pressure distribution profiles (Figure 2.19) as;

$$U_{avg} = 1 - \frac{\int [u_t(z) - u_s(z)]dz}{\int [u_0(z) - u_s(z)]dz} \tag{2.56}$$

where,

$$u_s(z) = \gamma_w z - s \tag{2.57}$$

$u_0(z)$ is the initial pore water pressure, z is the depth of the soil layer, $u_t(z)$ is a pore water pressure at the depth z at any given time, $u_s(z)$ represents the minimum pore pressure that can be expected when a vacumm pressure is applied, and s is the vacuum pressure applied.

Chu & Yan (2005) and recently Indraratna et al. (2013) studied how the degree of the consolidation varies with the strain based and pore water based methods, and both concluded that at an any given time, settlement based DOC was higher than pore water based DOC.

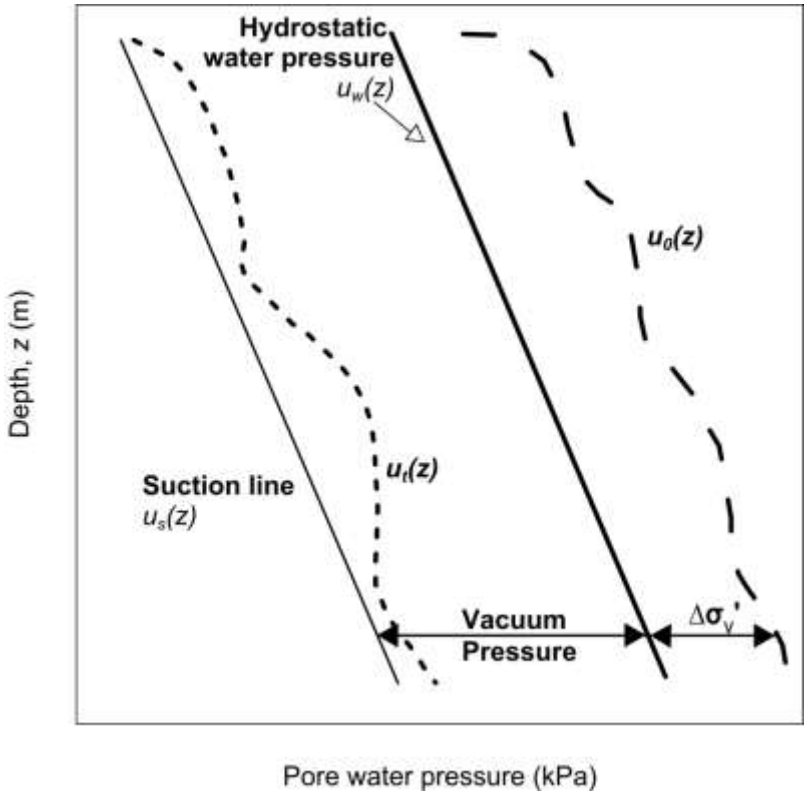

Figure 2.19 : Pore water pressure distribution with depth, Surcharge load with vacuum pressure is applied (adopted from Chu & Yan, 2005)

2.6 Viscous behaviour of soft clay

2.6.1 Hypothesis A and Hypothesis B

Identifying the correct laboratory compression curve that would represent actual in-situ conditions is still remains a challenging task. As indicated by Ladd et al. (1977) and Jamiolkowski et al. (1985), two extreme possibilities exist, that are referred to as hypothesis A and hypothesis B (Figure 2.20). Many researchers have tried to experimentally demonstrate which hypothesis represents the true behaviour of clay, so some have supported hypothesis A while others supported hypothesis B, and some even showed results in between (Aboshi, 1973).

In hypothesis A (Ladd et al., 1977; Mesri & Godlewski, 1977; Mesri & Choi, 1985) the strains arising from transferring pore water pressure into the effective

stress of the soil (primary consolidation) and the strains resulting from viscous deformations (secondary consolidation) were separated. Terzaghi's one dimensional consolidation theory was then used to calculate the primary consolidation settlement, while the coefficient of secondary consolidation (c_α) was used to estimate the resultant viscous deformations that would subsequently occur.

Hypothesis A assumes the relationship between the End of the primary (EOP) void ratio and the effective stress is independent from the thickness of the sample of soil (Figure 2.20), and therefore the compression curve obtained from laboratory experiments were similar to the in-situ stress strain curves.

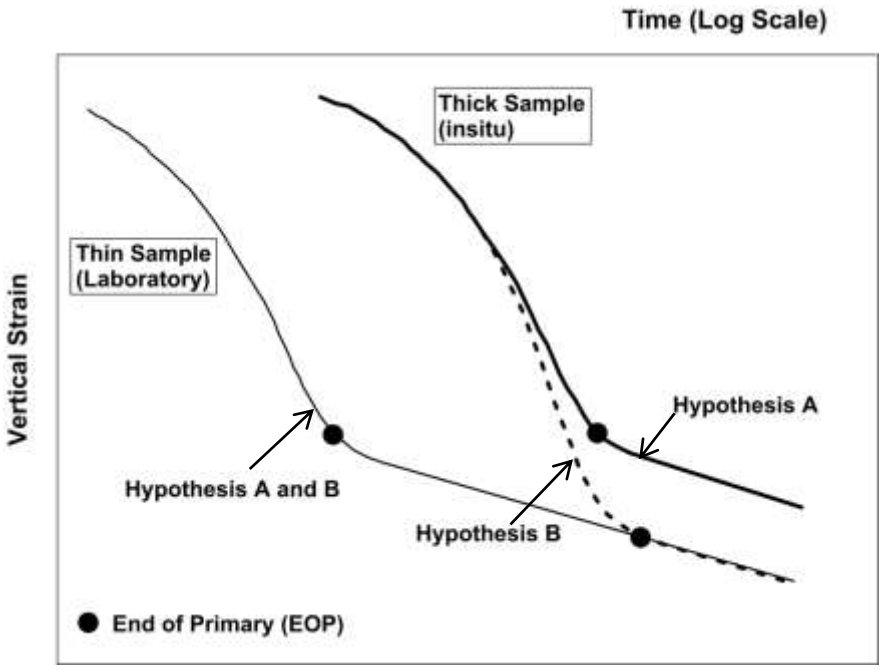

Figure 2.20 : Creep hypothesis A and B. (After Ladd et al., 1977)

In hypothesis B (Suklje, 1957; Bjerrum, 1967; Degago et al., 2011) assumed that some structural viscosity was responsible for creep and this process began within the primary consolidation phase and during pore water dissipation. As a result the strain at the end of primary consolidation increased with the thickness of the sample

and the results obtained using thin samples in the laboratory do not represent the actual in-situ stress strain relationship.

2.6.2 Effects of Delayed Consolidation

The compressibility characteristics of clay that exhibits delayed consolidation cannot be demonstrated using a single curve in $e - log\sigma'$ diagram, but it can be described by a system of lines or curves, as shown in Figure 2.21. Each of these lines represents the equilibrium void ratio for different values of effective stress at a specific time of sustained loading. Consolidation tests done by Crawford (1964) indicated that the rate of delayed consolidation was about the same throughout the depth of clay.

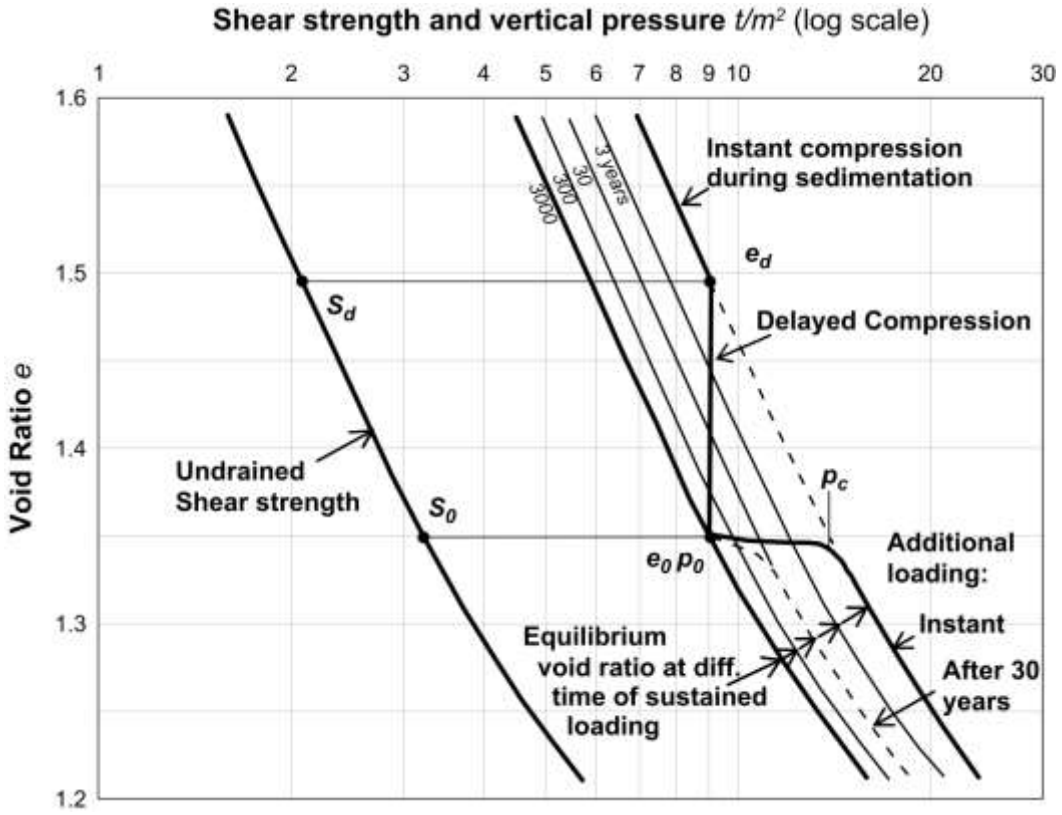

Figure 2.21: Compressibility and shear strength variation of a clay exhibiting delayed consolidation (After Bjerrum, 1967)

Figure 2.21 represents a unique relationship between the void ratio, effective stress and time, which means that at any given value of effective pressure and void ratio there is an equivalent time of sustained loading and a certain rate of delayed consolidation that is independent of the way in which the clay has reached these values. The reduction in the void ratio that occurred in the clay was divided into two components (Bjerrum, 1967).

- Instant compression – that occurred simultaneously with the increase of effective pressure and reduced void ratio.
- Delayed compression - the reduction in the void ratio at constant effective pressure.

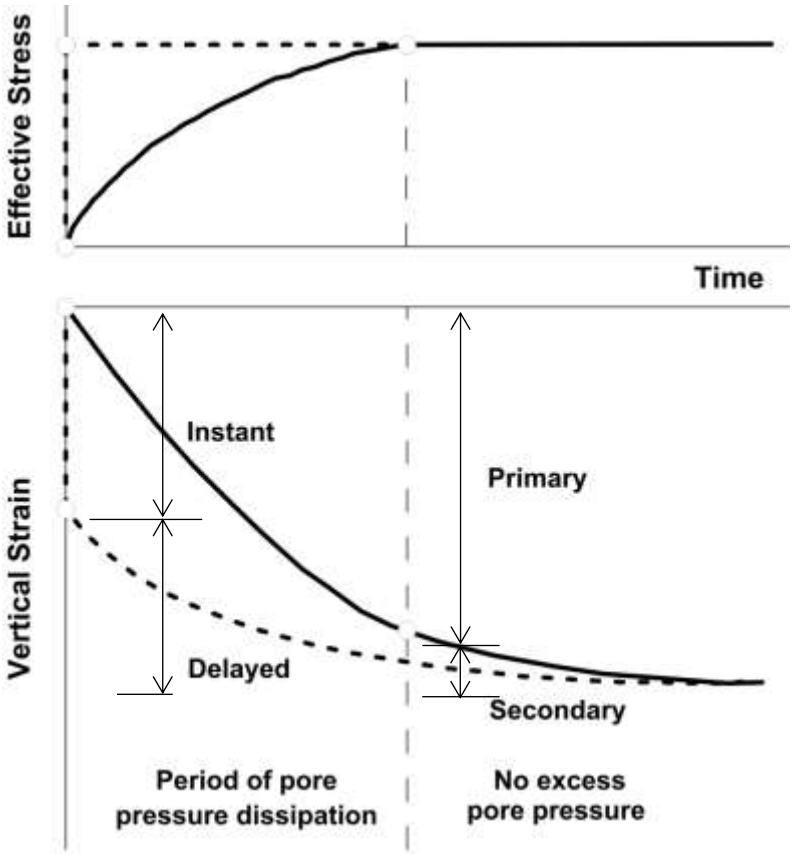

Figure 2.22 : Different with delayed consolidation and primary consolidation (After Bjerrum, 1967)

The concept of delated consolidation describes the reaction of clay to the increase in effective stress; it differs from the well-known primary and secondary compression that separates compression into two sections that occurs before and after the excess pore water has dissipated (Figure 2.22). This reduction in the water content during the delayed compression means the shear strength of the clay will increase and reserve resistance is created against any further compression similar to the pre- consolidation pressure in over-consolidated clay. The amount of reserve resistance against further compression will depend on the reduction of the void ratio and time of the sustained loading. This process was earlier demonstrated in the laboratory by Moretto (1946).

2.6.3 Strain rate effects on consolidation

Based on experiment results, Leroueil et al., (1985) stated that the rheological behaviour of the clay was described by two equations as follows:

$$\sigma_p' = f(\dot{\epsilon_v}) \tag{2.58}$$

$$\frac{\sigma_v'}{\sigma_p'} = g(\epsilon_v) \tag{2.59}$$

Once these two relationships for a given soil are known, any stress-strain-strain rate relationship for the soil can be constructed as shown schematically in Figure 2.23. Equations (2.58) and (2.59) can be combined to obtain a general rheological equation as (2.60) and the behaviour of clay under one dimensional compression is controlled by this unique stress-strain-strain rate relationship.

$$\dot{\epsilon}_v = f^{-1}\left(\frac{\sigma_v'}{g(\epsilon_v)}\right) \tag{2.60}$$

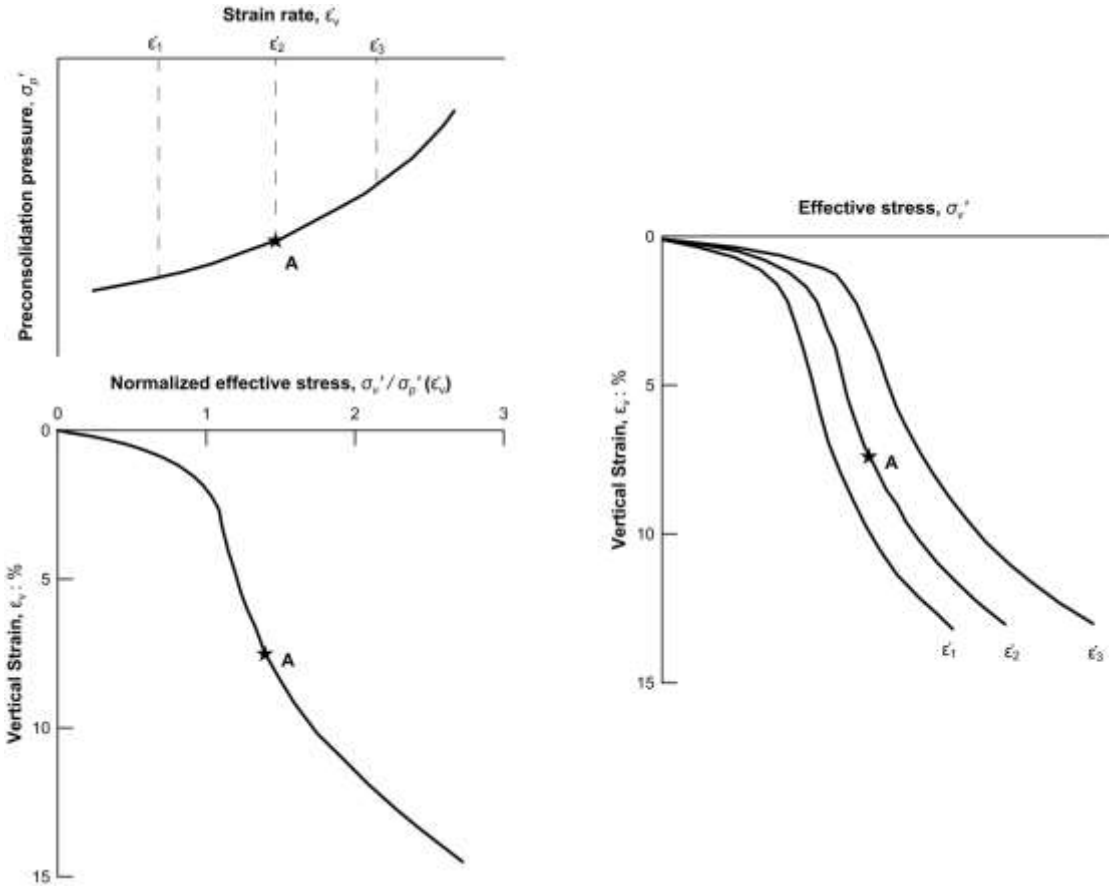

Figure 2.23 : Concept of the rheological model (After Leroueil et al., 1985)

2.6.4 Interrelationship between time and stress-compressibility

Hypothesis A assumes that all the viscous strains (secondary consolidation) occur after primary consolidation is completed. For a given load at an arbitrary time, the magnitude of the total secondary consolidation settlement depends on the time required to complete the primary consolidation. Even though the total primary consolidation settlement increases with the load increment ratio for almost all the soils, no such relationship exists between load increment ratio and the rate of secondary consolidation settlement (Mesri & Godlewski, 1977)

Mesri & Godlewski (1977) stated that the relationship between C_α and C_c holds true for all combinations of time, effective stress, and void ratios. One important

implication of this interrelationship is that the shape of the settlement curve in the secondary consolidation curve can be predicted if the compressibility characteristics of primary consolidation are available. Depending on the shape of that curve C_α may increase, decrease, or remain constant with time.

The existing evidence indicates that the measured values of C_α do not depend on the load increment ratio even though C_α depends entirely on the final effective stress. This study concluded that the constant value of the C_α / C_c together with EOP $e - log\sigma'$curve completely defined the secondary compression behaviour of any soil.

2.6.5 Elastic Visco-Plastic modelling of soft clay

Most of the models (Mesri & Godlewski, 1977; Leroueil et al., 1985; Leroueil, 1988) developed to investigate the time dependent behaviour of clays were obtained by fitting simple functions to the experimental data obtained in the laboratory. Most of these proposed models cannot fully describe procedures such as multi-stage loading, relaxation, and the constant rate of strain testing which generally used in laboratory conditions.

To overcome these limitations based on the concept of equivalent time, an elastic visco plastic model (EVP) was presented by Yin & Graham (1989,1994), where visco plastic behaviour of clay in one-dimensional consolidation can be described as:

$$\dot{\epsilon}_z = \frac{\kappa}{V\sigma'_z}\dot{\sigma}'_z + \frac{\psi}{Vt_0} exp\left(-\frac{\epsilon_z V}{\psi}\right)\left(\frac{\sigma'_z}{\sigma'_{z0}}\right)^{\lambda/\psi} \quad (2.61)$$

Where $\in_z$ is the vertical strain, κ, λ, ψ are the critical state soil parameters obtained in $e - ln\sigma'$ space, V is the specific volume, σ'_z is the effective vertical stress, and σ'_{z0} is the initial effective vertical stress.

Le et al. (2012) summarised the details of different creep mechanisms discussed in previous literature and enhanced explanation for the creep settlements in compression of soft clay is proposed. Using one dimensional oedometer tests performed on dry and saturated kaolinite clay Wong & Varatharajan (2014) investigated the effects of stress level, stress history, pore fluid type, and drainage path on creep settlement resulted by one dimensional consolidation. From experimental results it was concluded that the rate of creep settlement is controlled by the drainage direction along which the viscous flow occurs.

2.7 Summary

Vertical drains have been used as an efficient ground improvement method for a long time. The materials used to manufacture the drains and its durability will ensure the efficiency of the vertical drain system. The quality of the filter materials used and the discharge capacity of the central plastic core are very important parameters that must be considered when selecting a suitable type of drain.

Analytical models developed in the area of vertical drains and vacuum preloading enhance an engineer's capability of predicting the consolidation response. The conversion of axisymmetric models to equal 2D plane strain analysis has led to significant developments in the use of computer programs with finite element codes. Installing drains with a steel mandrel will disturb the surrounding soil and adversely affect the rate of consolidation. To predict the consolidation response accurately, it is

imperative to accurately estimate the extent of and reduction in permeability within the smear (disturbed) zone.

When a vacuum preloading is applied with vertical drains, the construction rate of the surcharge embankment can be accelerated, because, it will induce less lateral strains and reduce the possibility of a shear failure in the embankment. This method can be used with an airtight membrane or with a membrane less system where each drain is individually connected to the vacuum pump using horizontal pipes. The mechanisms of vacuum preloading and how it enhances the effective stress by applying negative pore water pressure is well understood. Analytical solutions are available to predict the vertical settlements due to vacuum preloading, but only empirical relationships are available to estimate the lateral deformations induced.

There is still a debate among researchers about the creep hypothesis and much experimental evidence could be found to support both hypotheses A and B. Most of the methods used to analyse vertical drains and vacuum preloading were developed on the assumptions which Terzaghi based his theory, and hence they are inclined towards Hypothesis A.

Chapter 3 An analysis of soil disturbance in field conditions

3.1 Introduction

Preloading is a simple and economical ground improvement technique however, in very thick layers of clay having low permeability the time needed to complete the final consolidation can be very long. Preloading with prefabricated vertical drains (PVDs) is a popular method of ground improvement because it reduces the drainage path and accelerates consolidation (Bo et al., 2003; Indraratna et al., 2005b). When prefabricated vertical drains are used, they must be driven into the ground using a steel mandrel using a truck mounted hoist. This insertion and removal of the mandrel disturbs the surrounding soil and this creates a disturbed zone known as the smear zone. The horizontal permeability and compressibility of the clay is reduced inside this smear zone such that it adversely affects consolidation (Indraratna & Redana 1998). Therefore an accurate estimation of amount of disturbance caused is very important to correct settlement prediction.

Barron (1948) developed an analytical solution for radial consolidation with sand drains and Hansbo (1981) extended it by incorporating the smear effects and well resistance. According to Chai and Miura (1999) the extent of the smear zone and the ratio between the lateral coefficient of permeability in the undisturbed zone and in smear zone are the main factors needed to characterise the smear effects. Indraratna & Redana (1997) and Sathananthan & Indraratna (2006) stated that the variation of horizontal permeability along the radius of the drain and the moisture content can be used to estimate the size of the smear zone.

Using the laboratory data obtained from remoulded samples of Boston Blue clay, Onoue et al. (1991) identified three distinct zones resulting from drain installation based on the variation of horizontal permeability. Basu & Prezzi (2007) also stated there is a transition zone between the remoulded smear zone and undisturbed zone and incorporated it into a radial consolidation theory. Indraratna and Redana (1998) studied the effects of smear due to the installation of compacted sand drains in a large scale consolidometer and concluded that the radius of the smear zone was about 100mm, which is 4 times the radius of the mandrel used. They also stated that in the soil near the drain, the ratio between vertical and horizontal permeability approaches Unity. Sharma and Xiao (2000) also performed similar experiments using a 1m diameter by 0.4m high consolidation cell and reported that the radius of the smear zone was about 4 times the radius of the mandrel used and its permeability was about 1.3 times lower than the surrounding undisturbed region. During drain installation, a significant increase in the pore water pressure was captured by seven miniature pore water pressure transducers installed in different radial locations inside the clay sample.

The use of cavity expansion theory to predict the extent of the smear zone and associated increase in pore water pressure during drain installation was examined by Ghandeharioon et al (2010), who then concluded that a conical shaped smear zone would be more realistic, although an equivalent cylindrical shape could still provide the same consolidation response based on the equivalent area method. They obtained a smear zone radius that was almost 3.1 times the equivalent radius of the mandrel. Sathananthan et al. (2008) used cylindrical cavity expansion theory to predict the increase in pore pressure during drain installation, while the laboratory experiments showed that the smear zone was about 2.5 times the size of the mandrel and the permeability ratio between the undisturbed zone and the smear zone was between 1.08-1.64.

Hird and Moseley (2000) investigated the smear effects of layered soil consisting of alternative layers of pre-consolidated Kaolin and sand by measuring the loss of hydraulic head, and reported that the smear zone was 1.6 times the radius of the drain. Sathananthan and Indraratna (2006) stated that the variation in the moisture content along the radius of the drain can also be used to estimate the extent of the smear zone. In their study, they reported that the smear zone was 2.5 times the equivalent diameter of the mandrel. Some recommended parameters are extracted from Indraratna et al. (2005a) are given in Table 3.1.

The aim of this work is to investigate the smear effects when soil is subjected to drain installation in actual field conditions by using variations of the coefficients of permeability, water content, and compressibility. the disturbed zone around a rectangular mandrel was characterised using soil samples obtained from the soft clay layer at various locations beneath an embankment built at Ballina, Australia.

Table 3.1 : Extent of the smear zone and variations in permeability

Source	Extent	Permeability	Notes
Barron (1948)	$r_s = 1.6\ r_m$	$k_h/k_s = 3$	Assumed in the analysis
Hansbo (1979)	$r_s = 1.5 \sim 3\ r_m$	Open	Based on available literature
Hansbo (1981)	$r_s = 1.5\ r_m$	$k_h/k_s = 3$	Assumed in case history
Bergado et al. (1991)	$r_s = 2\ r_m$	$k_h/k_v = 1$	Laboratory tests and back analysis
Onoue et al. (1991)	$r_s = 1.6\ r_m$	$k_h/k_s = 3$	From test interpretation
Almeida & Ferreira (1993)	$r_s = 1.5 \sim 2\ r_m$	$k_h/k_s = 3 \sim 6$	based on experience
(Indraratna & Redana, 1998)	$r_s = 4 \sim 5\ r_m$	$k_h/k_v = 1.15$	laboratory investigation
Chai & Miura (1999)	$r_s = 2 \sim 3\ r_m$	$k_h/k_s = C_f\ (k_h/k_s)$	C_f ratio between lab and field value
Hird & Moseley (2000)	$r_s = 1.6\ r_m$	$k_h/k_s = 3$	Recommend for design
Xiao (2000)	$r_s = 4r_m$	$k_h/k_s = 1.3$	Laboratory investigation

3.2 Site characteristics

The samples used in this study were extracted from a test embankment constructed at Ballina, New South Wales over an area where conventional prefabricated and new, environmentally friendly jute drains had been installed. The site is near the newly constructed Ballina bypass on the Pacific Highway that runs along the east coast of Australia, between Sydney and Brisbane. The area the embankment was built on is situated in the middle of a low lying flood plain that consists of saturated and very soft clay. The basic properties of the soil obtained from the samples tested are given in Table 3.2.

Table 3.2 : Soil properties of Ballina Clay

Property	**Values**
Liquid Limit, LL (%)	98
Plastic Limit, PL (%)	32
Plasticity Index, PI	66
Specific Gravity, G_s	2.58
Water Content, (%)	94.7
Void Ratio, e	2.44
Wet Unit Weight (kN/m^3)	16.5

According to the geotechnical investigation report the subsoil conditions were relatively uniform throughout the site and the top soil was about 0.2m thick and contains the organic material of decomposing sugar cane plants. There is a 1.0m thick layer of sandy silty alluvium crust below the layer of organic clay followed by a layer of dark grey high plasticity silty clay from 1.5-9.5m deep that was deposited in an estuarine environment. A 4m thick transition layer was encountered, underlain by a 5m thick layer of fine grained sand layer, below which there is a Pleistocene layer of stiff to hard clay. According to the Unified Soil Classification System, the samples of soil can be classified as high plasticity clay (CH). Indraratna et al. (2012) reported a comprehensive soil profile that relates to the Ballina Bypass project, and

they are presented in Figure 3.1. The Ballina Bypass was close to the embankment from which the samples for this study were taken.

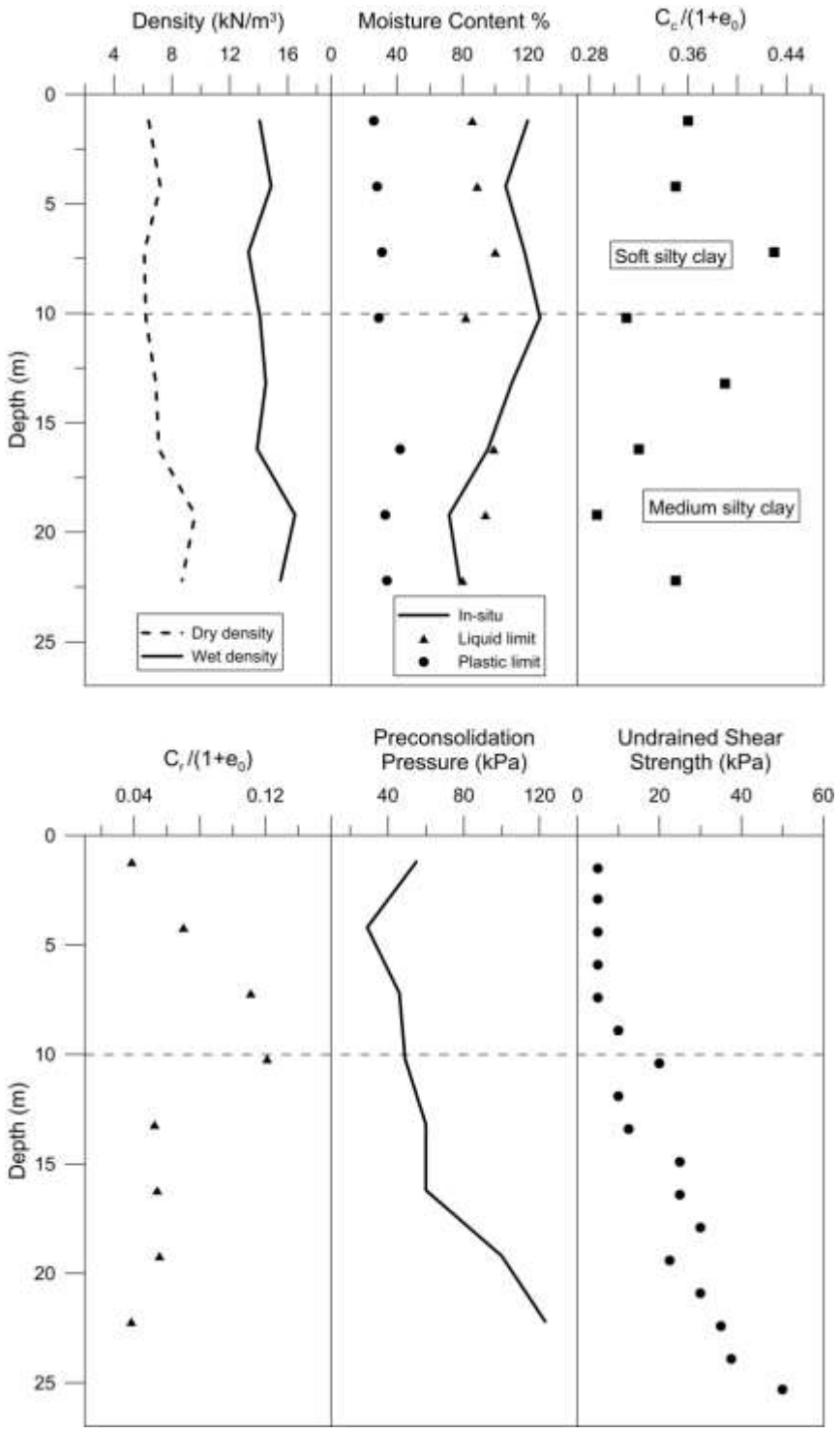

Figure 3.1 : General soil profile and properties of Ballina clay (Modified after Indraratna et al. 2012)

3.3 PVD installation and recovery of undisturbed samples

In the test embankment, vertical drains were installed in a square pattern 1.2m apart, to a depth of 15m. Before installing the drains, vibrating wire piezometers and horizontal push in pressure gauges were installed at different depths to record the soil response during installation. Conventional wick drains and bio-degradable jute drains were installed under the embankment using the same mandrel, so this would result in the same smear effects. A truck mounted 80-tonne excavator equipped with 20m long mandrel was used to insert the drains into the ground at approximately 1.5m/s. The rectangular shoes were 140mm long x 90mm wide x 1mm thick. The cross section of a typical instrumentation plan is shown in Figure 3.2

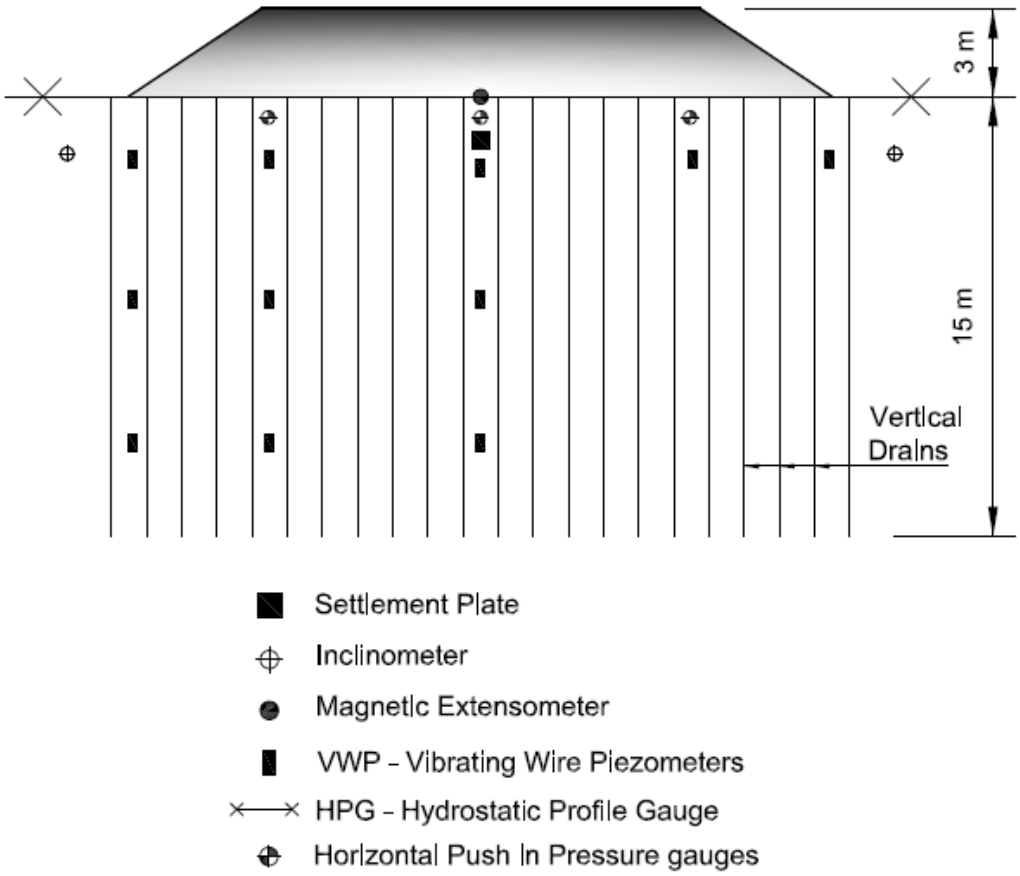

Figure 3.2 : Typical instrumentation plan

The smear effects due to the installation patterns of a single drain and multi drains were investigated during this study. For the single drain analysis (Single-drain Case), two vertical drains were installed (W1 & W2) and then samples of soil were collected from around both drains, as shown in Figure 3.3. Multiple drain installation (Multi-drain Case) was used to analyse the effects of overlapping smear zones. Samples were extracted between two rows of 14 installed drains with a spacing of 1.2m, as per Figure 3.4.

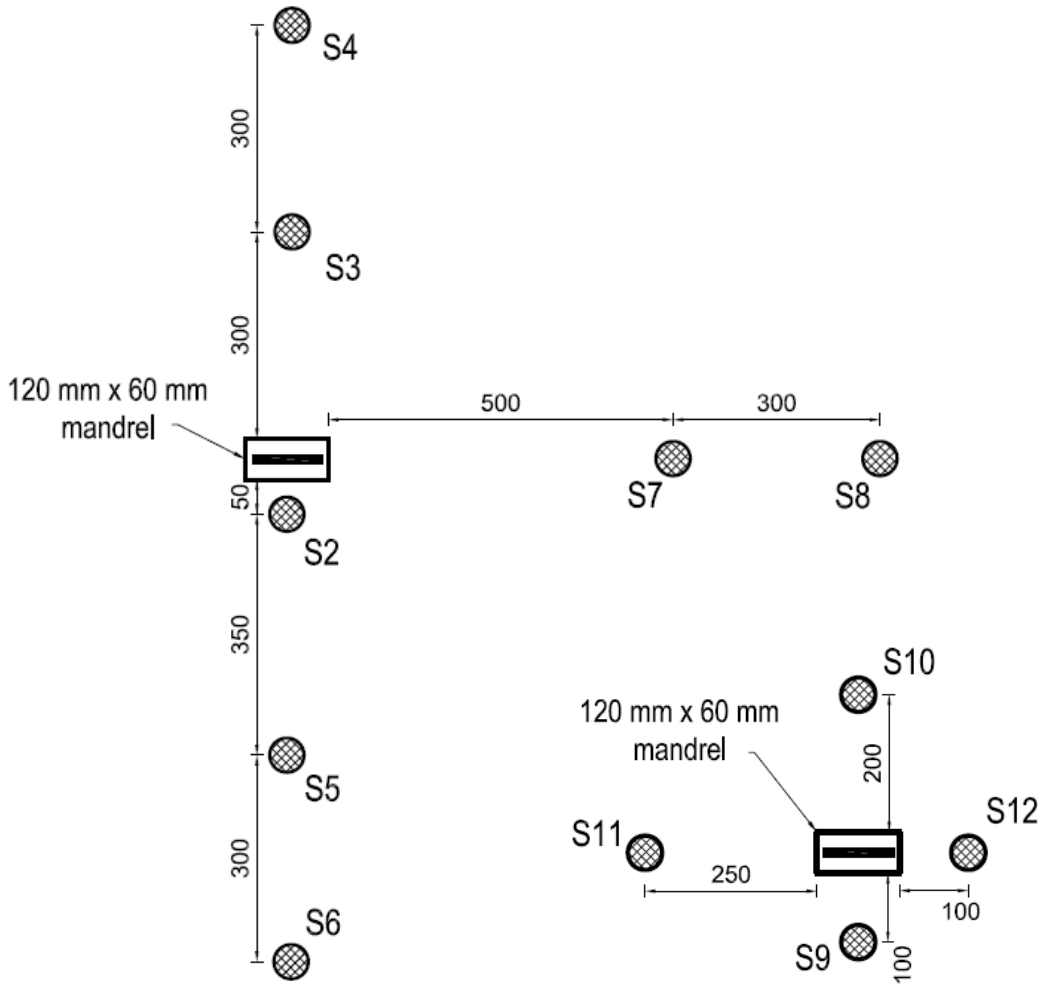

Figure 3.3: Sampling locations for single drain installation, (a) W1 and (b) W2

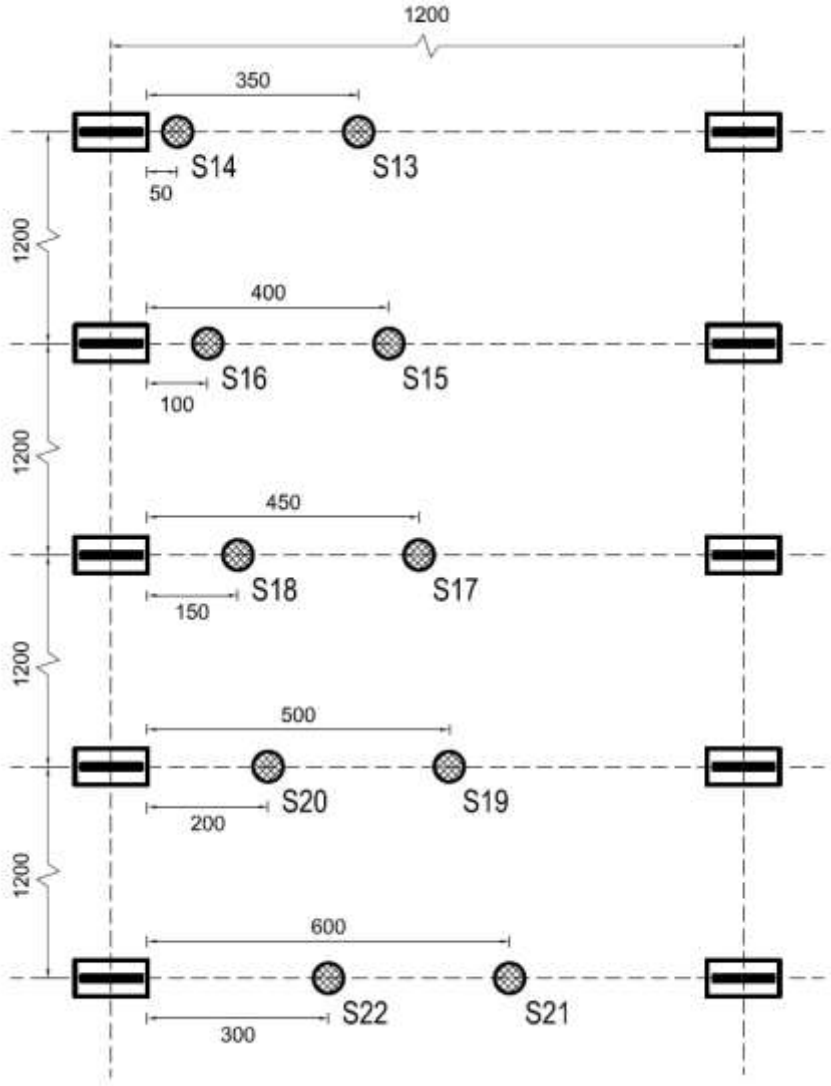

Figure 3.4: Sampling locations for multi drain installation, W3

Samples of undisturbed soil were extracted from a depth of 2.5 to 2.95 below the 600mm thick working platform. All the samples were recovered within 45 minutes of installing the vertical drains. Shelby tubes (50mm diameter by 450mm long) were used to extract the samples. Due to the low shear strength of the soil and lack of space, block samples could not be taken. The tubes used for sampling were in accordance with the recommendations made by Hvorslev (1949). The parameter of

the area ratio (C_a), the outside clearance ratio (C_o), and the inside clearance ratio (C_i) are defined as follows:

$$C_a = \frac{D_w^2 - D_e^2}{D_e^2} \tag{3.1}$$

$$C_o = \frac{D_w - D_t}{D_t} \tag{3.2}$$

$$C_i = \frac{D_s - D_e}{D_e} \tag{3.3}$$

Where, D_s and D_t are the inside and outside diameter of the tube above the cutting edge respectively. D_w is the outside diameter of the cutting edge that enters the ground and D_e is the inside diameter. In the tubes used, the outside diameter was 49.4mm while the inside diameter was 47.8mm, and it did not have a tapered cutting edge. In order to extract a good quality sample, an inside clearance ratio between 0% and 1.5% and outside clearance ratio between 0% and 3% were recommended by Hvorslev (1949). For the tubes used, both these values were 0% because the cutting edge was not chamfered. Increasing the area ratio creates more disturbances when sampling the soil, so the area ratio should be less than 10%, as per Hvorslev (1949). The area ratio of the sampler used was 6.88% so it was clearly within the allowable limits followed in practice worldwide.

To minimise soil disturbance during sample preparation and extraction from the tubes, it was decided to fit the tube sample directly to the oedometer apparatus, so a smaller diameter sample tube had to be used to obtain samples from the ground. The samples were taken from along the radial distance from the drain, so the smaller

diameter sample tubes were better because they represented the soil conditions better in that particular location. To avoid any disturbance caused by extraction, samples were extracted 300mm apart; 11 samples were extracted for single drain analysis and 10 samples for multi-drain analysis.

After the vertical drain had been installed, the location where samples required to be extracted was selected by measuring the distance from the center of the drain. The ground was then pre-bored to the desired depth using rotary driller and then Shelby tubes were inserted into the ground via a system mounted on a truck (Figure 3.5). Steady and uninterrupted force was applied to the tubes to ensure a smooth and continuous motion. When the tube reached the desired depth, it remained stationary for about 5 minutes, and then it was slowly rotated and withdrawn at a steady speed to minimise any disturbance. The sample was then cleaned and paraffin wax was applied to each end of the tube. Two plastic caps were attached to protect the wax seal and then the tubes were labeled, wrapped in shock absorbing bubble wrap, and then transported to the lab. The sampling tubes were immediately stored in a humidity controlled room at 10C temperature and above 95% of humidity to prevent any moisture loss from the samples.

3.4 Laboratory experimental program

The variations in the moisture content along the radius of the drain can be used to characterise the extent of the smear zone so the moisture content of the samples was measured as soon as they reached the laboratory. To do this, the plastic cap at the bottom of the each tube was removed and about 3cm of soil was emptied out. Three moisture tests were carried out from each sampling tube and then average of

them was taken for analysis. After the test the tubes were re- sealed and stored in the humidity room.

(a) (b)

Figure 3.5 : Sample extraction: (a) Pre-boring; (b) insertion of Shelby tube

Oedometer tests were performed on the samples extracted vertically and horizontally from the sample tubes. The samples extracted vertically were used to investigate the variations of vertical compressibility, while the horizontal samples were used to investigate any variations in horizontal permeability along the radius. Indraratna et al. (2012) reported that the undrained shear strength of Ballina clay in the samples taken from depth was around 5kPa. The relatively small diameter sample tube caused the clay to adhere to the wall so extracting the whole sample would be difficult and leave disturbed soil near the wall, thus a 20mm long piece of the tube was cut off with a pipe cutter. After cutting the tube the soil was trimmed with a

thin wire and the samples were then fitted directly into the oedometer. Then it was tested according to the procedure set out in ASTM (2011)

To obtain a horizontally orientated sample the clay had to be completely extracted from the tube so a 75mm long length of tube was cut off with a pipe cutter. Once the tube was cut around its circumference, the soil was trimmed with a thin wire. Even though the sample length is relatively short it could subjected to disturbance during extraction due to the adhesion between the tube wall and clay sample. Therefore a very thin wire was inserted along the inside of the Shelby tube to separate the sample from the tube. After that the soil sample was slowly pushed out from the tube and then trimmed to fit into a thin wall 42.1mm diameter oedometer for a stepped loading consolidation test (ASTM, 2011). To examine whether the sample preparation disturbed the soil, a Vane shear test was carried out before and after the soil sample was prepared and revealed that the corresponding shear strengths were similar. After placing the sample into the oedometer a seating stress of 3.4 kPa was applied to the vertical specimen and this load was doubled each day until it reached 218.7kPa.

3.5 Test results and analysis

3.5.1 Characterisation of the Smear Zone: Permeability and Water Content Perspective

The extent of the smear zone can be estimated by methods such as the variation of water content, permeability and compressibility along the radius from the drain. Fig. 3.6a shows the variation of water content along the radial distances for the single drain and multi drain cases.

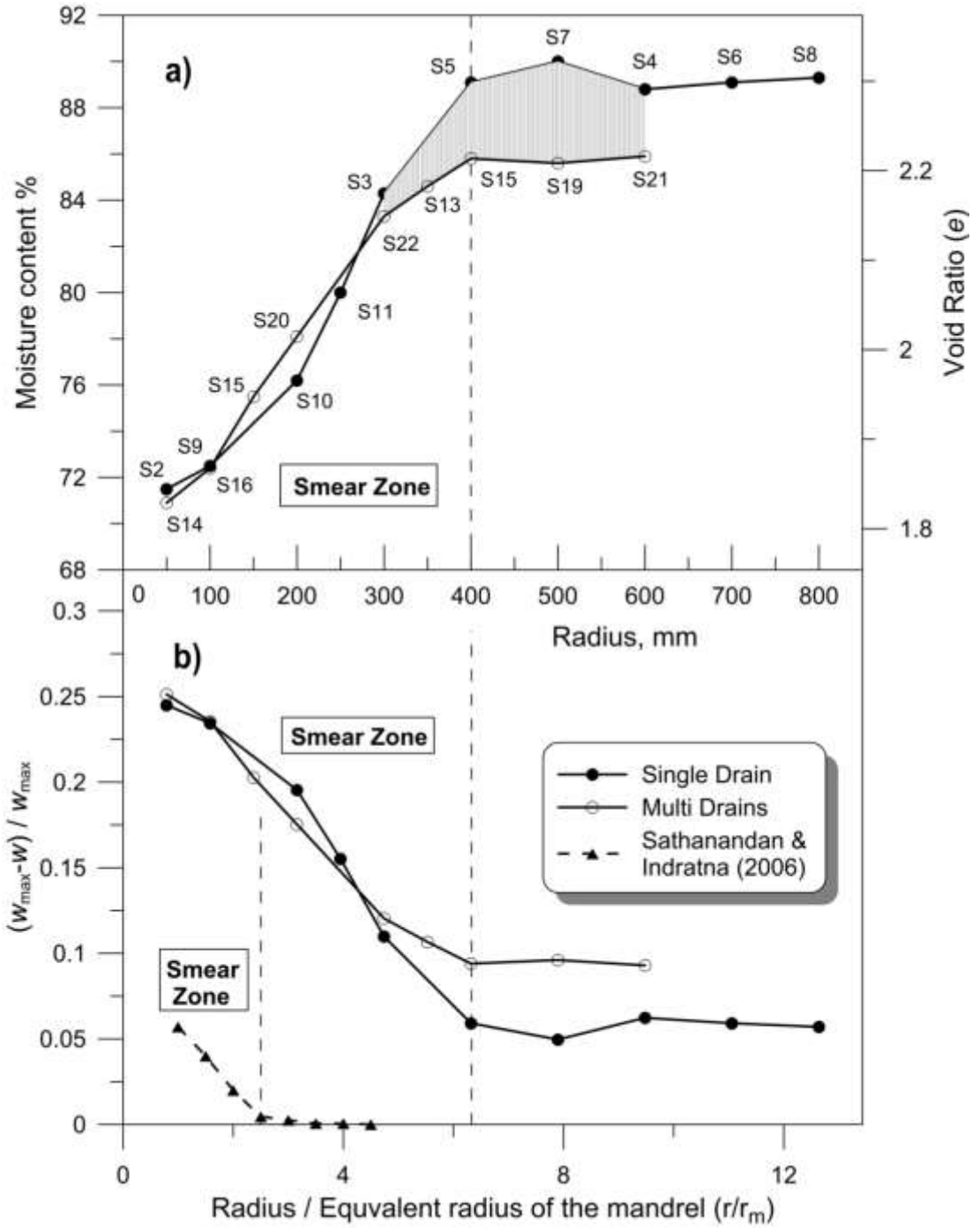

Figure 3.6 : (a) Variation of moisture content along the distance away from the drain (b) Variation of normalised moisture content reduction with normalised distance with equivalent mandrel radius (radius of a circular mandrel with same cross sectional area) for both single drain and multi-drain cases

The in-situ moisture content of the clay specimens from which samples were retrieved (2.5 – 2.95 m) was approximately 93-95%. According to Figure 3.6(a) the moisture content had gradually increased up to 89-90% within the first 400mm from the drain and then remained relatively constant. Disturbance as a result of the rapid insertion of a rigid steel mandrel in soft clay leads to fabric remoulding that is not caused by any reduction in moisture. Further information and discussion on disturbance and moisture reduction has been carried out by Sathananthan and Indraratna (2006) and Rujikiatkamjorn et al. (2013).

With the single drain case, the water content beyond 400mm from the PVD was less affected by drain installation, but with the multi-drain case the water content had decreased by about 4% beyond 400mm from the PVD; this was caused by the overlapping smear zone. The mandrel was 140mm x 90mm which gives an equivalent diameter of 126.6mm. The tests for moisture content indicated that the radius of the smear zone was 400mm which was almost 6.3 times the equivalent mandrel diameter.

Figure 3.6(b) shows the variation of normalised moisture content $(w_{max}-w)/w_{max}$ with the ratio between the radius to the equivalent radius of the mandrel. w_{max} and w are the maximum water content and the water content at any radial location. The experimental data obtained by Sathananthan and Indraratna (2006) was also plotted along with the results from this study. Even though the plots appear to follow the same trend, the extent of the smear zone and reduction in the water content appears to be more in field conditions than the values obtained by

Sathananthan and Indraratna (2006), who estimated the diameter of the smear zone to be 2.5 times the equivalent mandrel diameter.

The variations in the void ratio, permeability, and normalised permeability away from the vertical drain are shown in Figure 3.7 (a) to (c) for the single drain case, and (d) to (e) for the multi- drain case, respectively. All the trends were similar to the variations in water content shown in Figure 3.6. The Casagrande log time method was used to derive the coefficient of consolidation in a horizontal direction (c_h) from those samples extracted horizontally, and Terzaghi's one dimensional theory was used to back calculate the horizontal permeability values (k_h). The horizontal permeability was constant beyond the 400mm radial distance from the vertical drain and was visibly reduced towards the drain inside 400mm.The lateral permeability in the multi-drains also confirmed the possibility of an overlapping smear zone, because, the permeability at a given location more than 400mm away were less than those obtained from the single drain case. At least 3 samples at a given location were tested to confirm the soil properties.

Normalised permeability was defined as the ratio between the horizontal permeability (k_h) and lateral permeability of the undisturbed zone (k_h(undisturbed)) to characterise the smear zone. Variations of this with the radial distance are plotted in Figs. 3.7(c) and 3.7(e). The normalised permeability ratio was close to 1 beyond the smear zone in the single drain and was reduced to 0.9 in the multi drain case. Inside the smear zone the normalised permeability ratio decreased rapidly with the radial distance close to the drain boundary (highly disturbed zone). Irrespective of the pressure applied, all the curves in both the single drain case and multi drain case were confined within a relatively narrow band characterising the smear zone. This

data revealed that the normalised lateral permeability ratio within the smear zone varied from 0.2 and 1 (an average of 0.6).

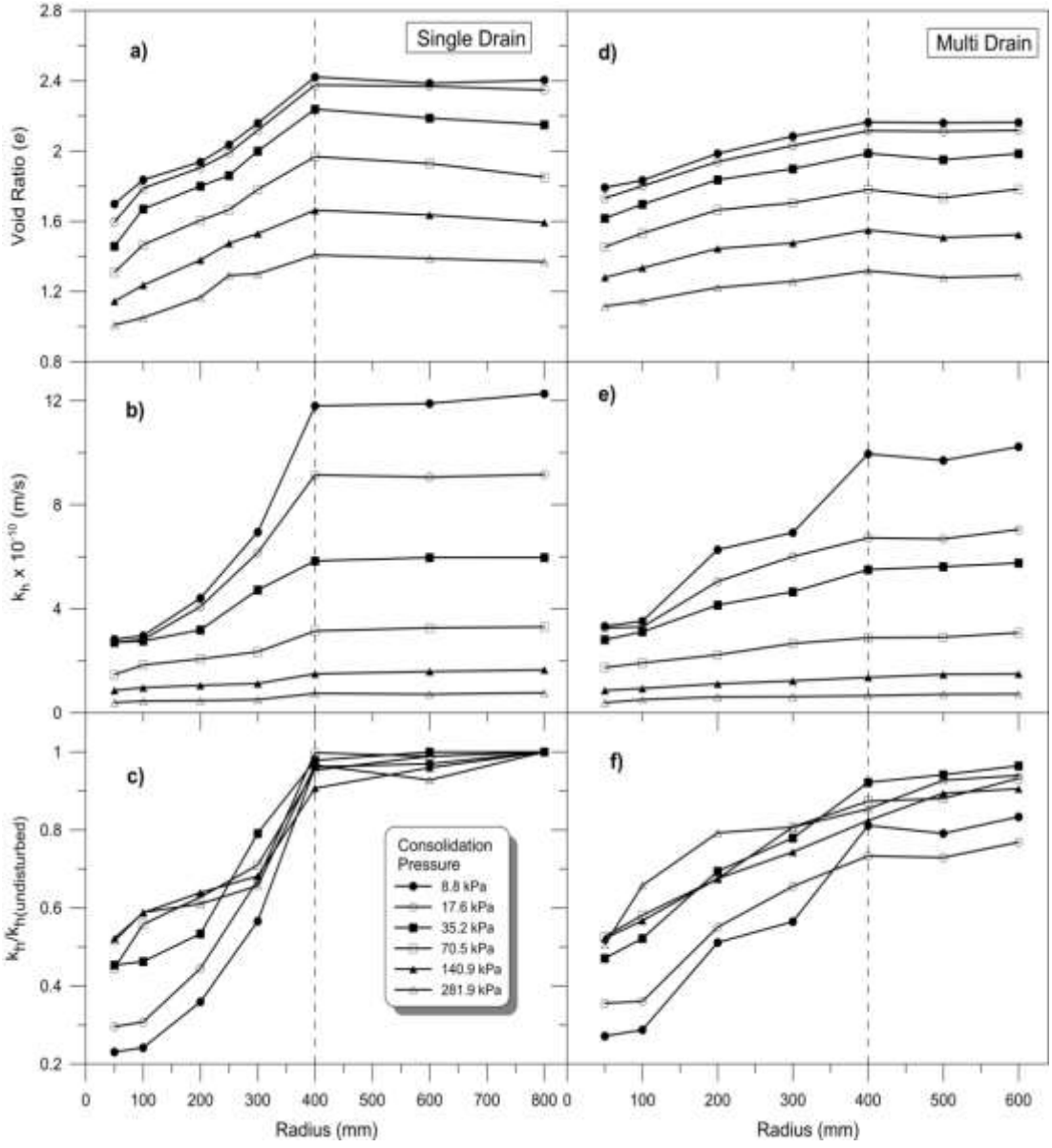

Figure 3.7 : Variations of the void ratio, permeability, and normalised permeability away from the vertical drain for the single drain and multi-drain cases

According to the variations in the moisture content, void ratio, and permeability, the smear zone was about 6.3 times larger than the equivalent dimension of the mandrel, which was much higher than the previous values assumed and obtained in the laboratory. This work proves that in field conditions, soil can be subjected to more disturbances when longer vertical drains are installed at higher installation speeds because the soil can experience a longer period of shearing during installation. However, the samples used in this study were extracted from less than 3m from the ground surface where soil is subjected to maximum shearing and hence the area of maximum soil disturbances. It has been observed that the smear zone was much smaller at deeper layers where the clay was stiffer and the confining pressure was higher with depth. The analogy of pile driving in relation to mandrel intrusion is useful to further clarify the concept (Gavin et al., 2010).

3.5.2 Characterisation of the Smear Zone: Perspective of Soil Compressibility

According to Burland (1990), and Leroueil & Vaughan (1990) the behaviour of in- situ soil can differ from its remoulded state due to its distinctive structure because when a remoulded sample is prepared the in-situ structure of the soil is totally destroyed. Drain installation alters the structure of the soil and this leads to different compression behaviour. By using the monitored settlement data of an embankment where vertical drains were installed using two different size mandrels, Bergado et al. (1991) observed a higher settlement and faster rate of consolidation in the area where a smaller diameter mandrel was used.

Rujikiatkamjorn et al. (2013) proposed a conceptual model to capture the degree of disturbance (Figure 3.8) due to the installation of vertical drains by carrying out undisturbed large scale testing. They suggested using a 3-zone model

around the vertical drain, but a characterisation of the smear zone in relation to actual field conditions was not included in their study. The degree of disturbance (DD) due to soil de-structuration was based on the change in the void ratio of partially disturbed soil at each respective point of maximum yield stress along the yield points line AB, and can be quantified as follows:

$$DD = 1 - \left[\frac{e_{SD} - e_{id(ICL)}}{e_{SC} - e_{id(ICL)}}\right] \tag{3.4}$$

where e_{SD} is the void ratio of the partially disturbed soil at yield stress, e_{SC} is the void ratio of the undisturbed soil at yield stress, and $e_{id(ICL)}$ is the void ratio on the isotropic compression line (ICL) at the intercept of Line AB and the isotropic compression line.

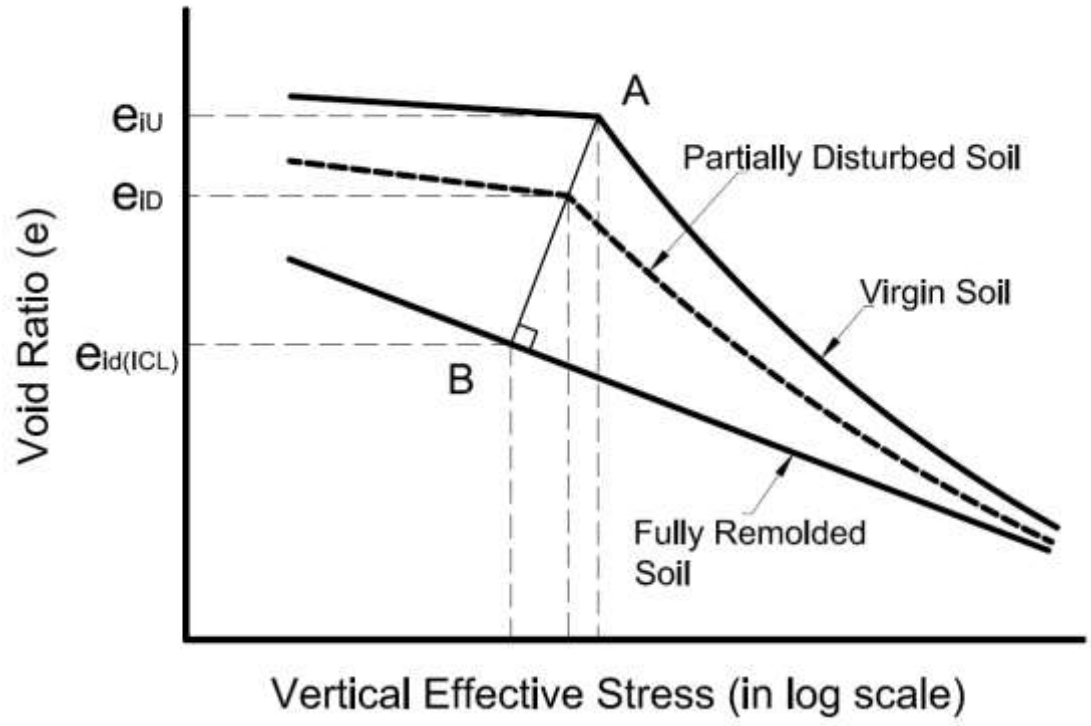

Figure 3.8 : Concept to assess the degree of soil disturbance

Figures 3.9 and 3.10 show how the void ratio varied with the effective stresses (compression curves) in the vertical and horizontal samples respectively. It is evident that soil is subjected to a severe remoulding close to the drain, but the amount of remoulding decreased along the radius of the drain, while the compression beyond the smear zone was almost constant. A compression curve for the undisturbed sample was generated from a sample extracted more than 3 m away from the vertical drain, using the same method of sample preparation. If the samples were disturbed by extraction and the preparation methods were significant, there would not have been any visible change in the pre-consolidation pressure. The compression plots in Figures 3.9 and 3.10 indicate that the pre-consolidation pressure had decreased notably close to the drain, thus confirming there were minimal effects due to sample preparation.

The compression curves for the multi-drain case at an influence zone 600mm away from the vertical drains were generally lower than for the single drain curves. This may be attributed to the effects of installing adjacent vertical drains. Before installing the drains, vibrating wire piezometers and total pressure gauges that can measure any increase in lateral pressure were installed between the proposed drain lines. An increase of 3-5kPa in the in-situ pore pressures and total lateral pressures was detected by field instrumentation, but they returned to their original in-situ state 6-18 hours after installation

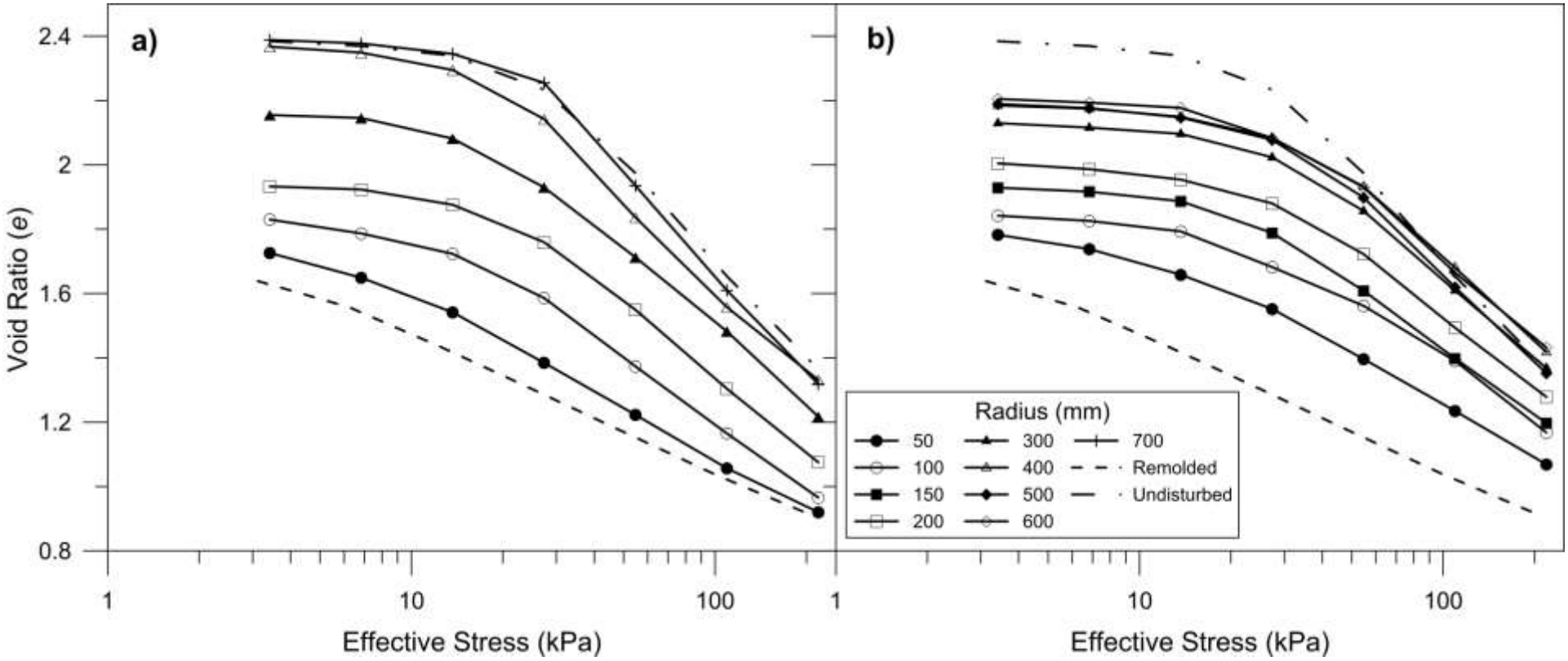

Figure 3.9 : Compression curves for vertical samples, (a) Single-drain case and (b) Multiple-drain case

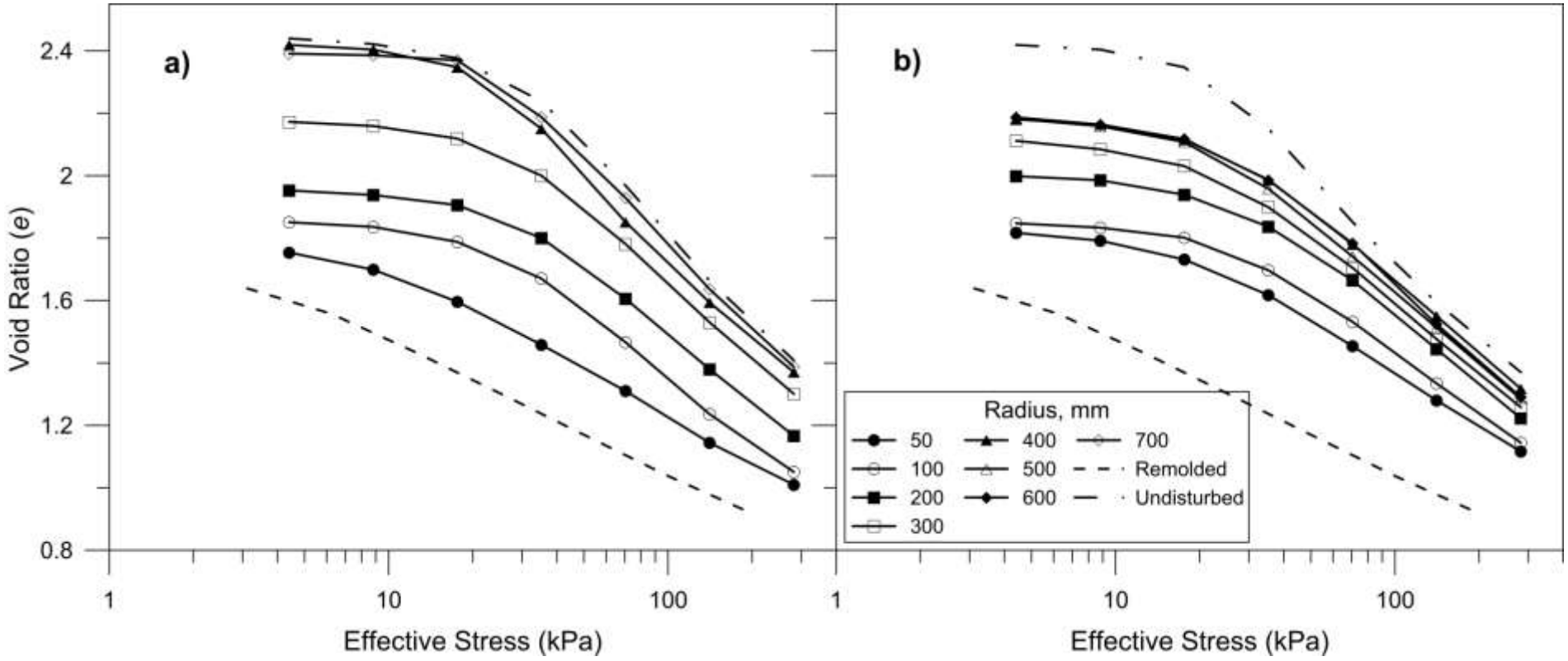

Figure 3.10 : Compression curves for horizontal samples, (a) Single-drain case and (b) Multiple-drain case

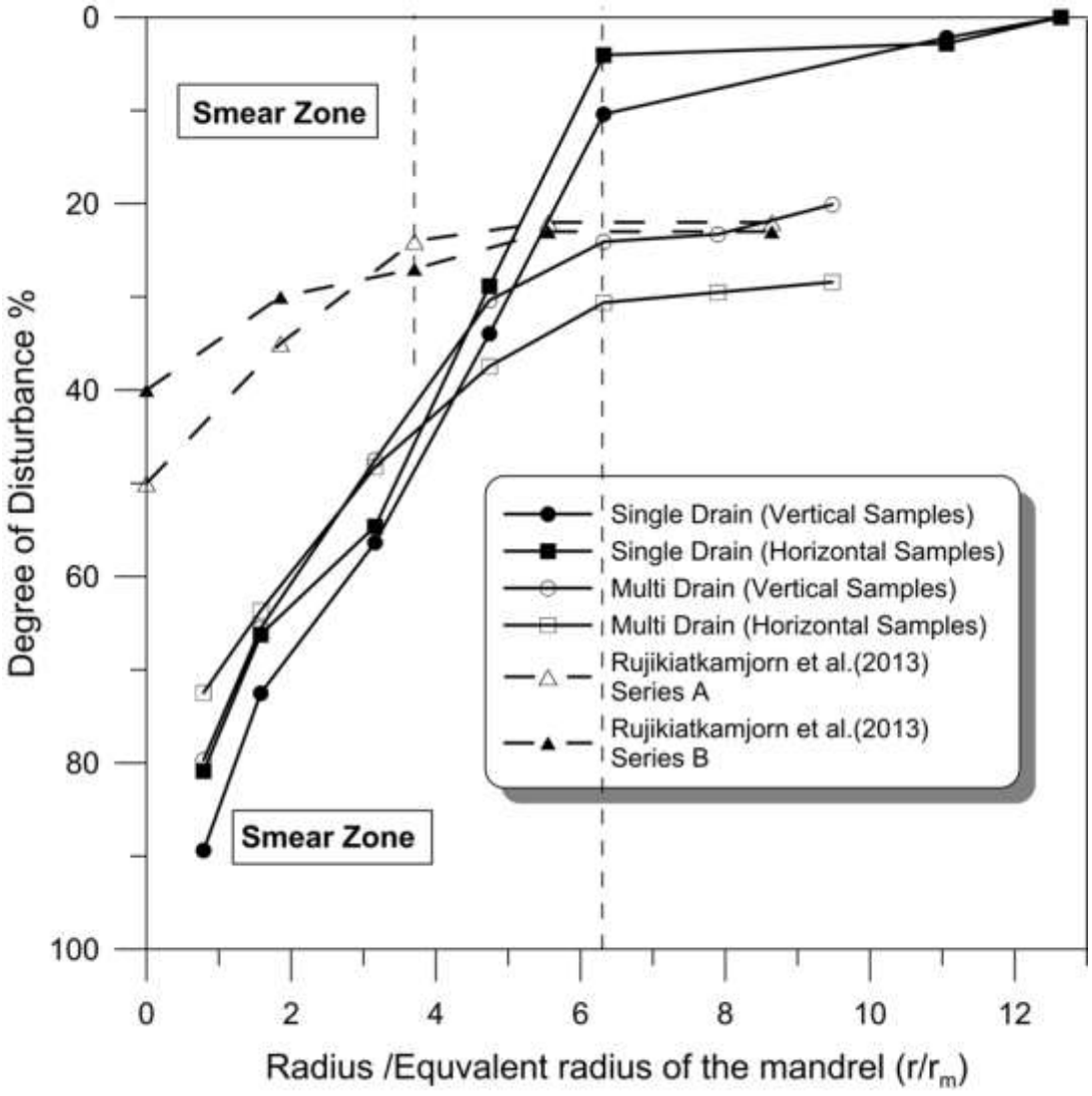

Figure 3.11 : Degree of disturbance

The variation in the degree of disturbance given by Equation (3.4) along with the normalised radius is shown in Figure 3.11 above, and indicates there was more disturbances in the soil closer to the drain. The degrees of disturbance for the vertical samples beyond the smear zone were 10.4 % and 24.1% for single drain and multi-drain cases, respectively, while the degrees of disturbance for the horizontal samples in the same region were 4.1% and 30.6% for single drain and multi-drain cases, respectively. The degrees of disturbance 50mm away from the drain were

89.4% and 79.7% for single drain and multi-drain cases, reflecting a severe disturbance and remoulding close to the drain. The laboratory results were also plotted along with the current study data. Rujikiatkamjorn et al. (2013) used undisturbed samples, however, a scaled-down mandrel and drain used in the laboratory experiments with 350mm diameter sample in the experimental investigation. This means the samples subjected to less shearing time at lower speeds, which resulted in lesser disturbances, as is evident from the low degree of disturbance values.

3.6 Effect of Drain Installation on Soil Anisotropy

Anisotropy can be developed during the deposition of soft clays and it can be preserved until they are disturbed by external forces. Leroueil & Vaughan (1990), Larsson (1981) and Tavenas et al. (1983b) stated that marine clay exhibits very little or no anisotropy. It was expected that compressibility and permeability anisotropy would be altered during the installation of vertical drains. Volume compressibility anisotropy in one dimensional consolidation can be defined as the ratio of the coefficient of volume compressibility obtained from a horizontal specimen to that obtained from a vertical specimen at the same location. Permeability anisotropy is also defined as the ratio of the lateral permeability to the permeability of vertical direction of soil.

Figure 3.12 shows the variation of the volume compressibility anisotropy and permeability anisotropy with the distance away from a vertical drain at an effective stress of 24-54kPa. For this site, the degree of anisotropy of volume compressibility and permeability for the undisturbed soil was 1.2 and 1.1, respectively and is well within the values stated in Tavenas et al. (1983b). The volume compressibility

anisotropy obtained from the single drain case was higher than that for the multi-drain case, although these values diminished when approaching the close vicinity of the drain. A similar trend was also observed for permeability anisotropy.

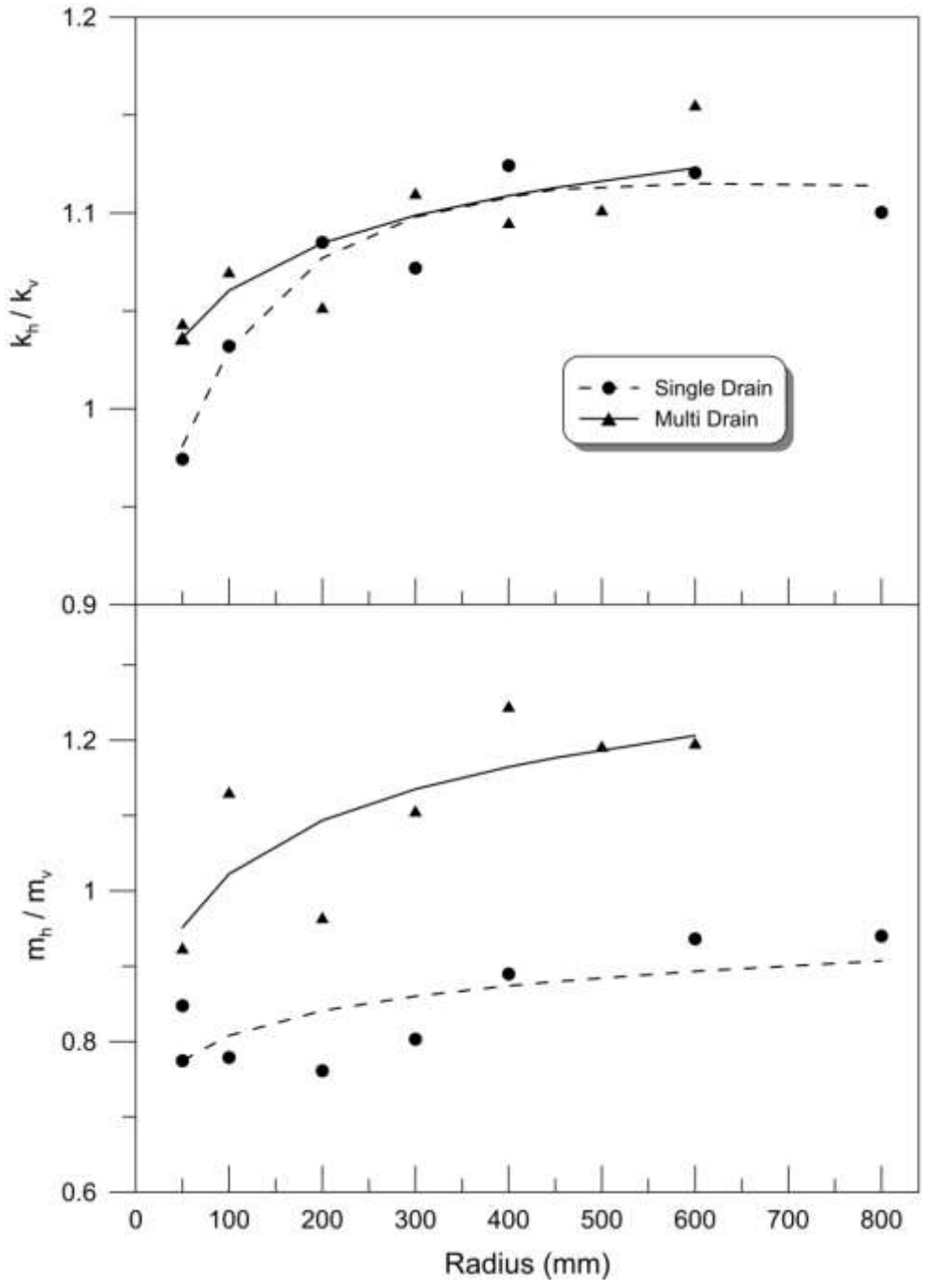

Figure 3.12 : Volume compressibility anisotropy and permeability anisotropy along the distance away from vertical drain

3.7 Practical Implications

The radial consolidation theory proposed by Walker and Indraratna (2007) was used to investigate the effects of drain installation. Linear variation of permeability within the smear zone was assumed to capture the various properties of soil within the smear zone. Figure 3.13 presents the unit cell together with variations in linear permeability in the smear zone.

The degree of consolidation (U_h) can be expressed as:

$$U_h = exp\left(\frac{-8T_h}{\mu}\right) \tag{3.5}$$

$$T_h = \frac{c_h t}{d_e^2} \tag{3.6}$$

$$c_h = \frac{k_{hi}}{m_v \gamma_w} \tag{3.7}$$

$$\mu = ln\left(\frac{n}{s}\right) - \frac{3}{4} + \frac{K(S-1)}{(S-K)} ln\left(\frac{s}{K}\right) \tag{3.8}$$

$$K = \frac{k_{hi}}{k_0} \tag{3.9}$$

$$n = \frac{r_e}{r_w} \tag{3.10}$$

$$s = \frac{r_s}{r_w} \tag{3.11}$$

where T_h is the time factor, r_s is the radius of the smear zone, r_w is the equivalent radius of the vertical drain, r_e is the radius of the influence zone, k_{hi} is the coefficient of horizontal permeability in the undisturbed zone, k_0 is the coefficient of horizontal permeability at the soil drain interface, c_h is the coefficient of consolidation in the

horizontal direction, m_v is the average coefficient of volume compressibility from the vertical samples, and γ_w is the unit weight of water.

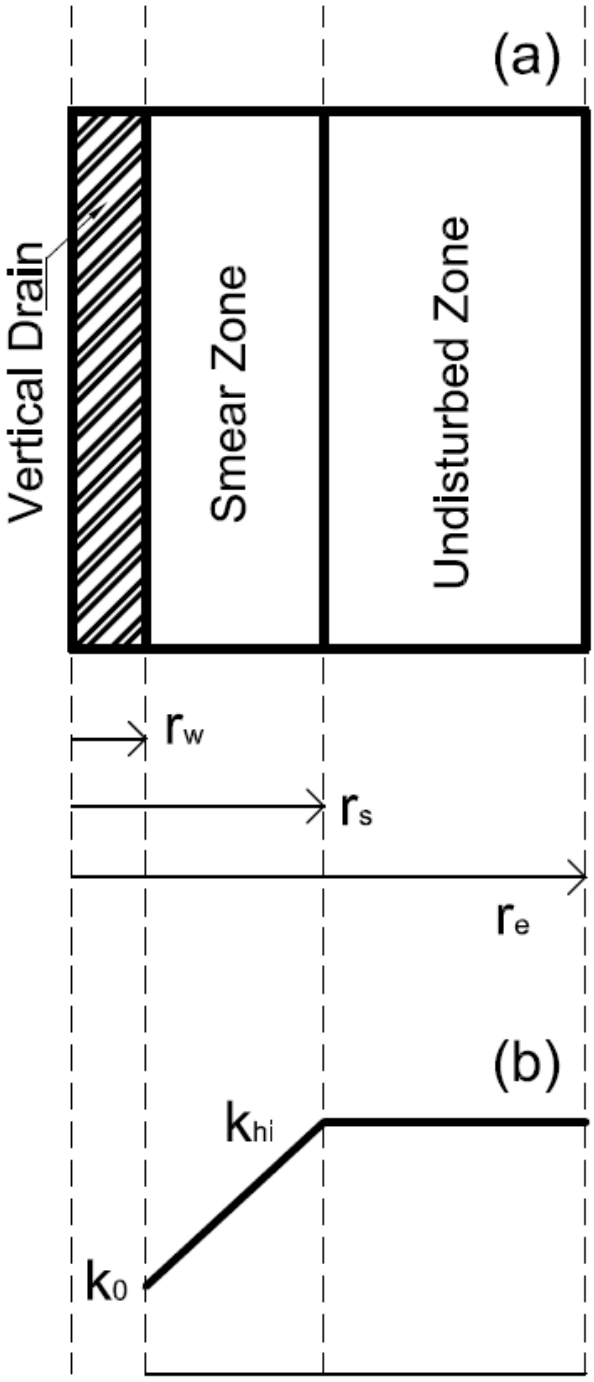

Figure 3.13 : (a) Cross section of unit cell with vertical drain and (b) permeability variation

Total settlement, $S(t)$, at a given time can be obtained by;

$$S(t) = U_h m_v \Delta\sigma_v H \tag{3.12}$$

And the excess pore water pressure by;

$$u(t) = U_h \Delta\sigma_v \tag{3.13}$$

where $\Delta\sigma_v$ is the vertical applied effective stress and H is the thickness of the soil.

The performance of this test embankment is currently being monitored, so the field data will not available to the writer until end of 2015, so for this analysis the following parameters were used to simulate the behaviour of the embankment as closely as possible; the parameters are r_s =400mm, r_e =678mm, r_w =51.5mm, $\Delta\sigma_v$ = 29.1 kPa, and H =15m. The following 3 cases were examined: (a) CASE A (Single Drain Case), CASE B (Multi-drain Case), and CASE C (Ideal Case: No smear). The parameters are tabulated in Table 3.3.

Figure 3.14 (a) presents the variation of the average degree of consolidation and the associated excess pore pressure, while Figure 3.14(b) presents the settlements with time based on 3 cases. As expected, the consolidation rate based on Case C was the highest, followed by Case B and Case A. In Case B the lower coefficient of compressibility led to a higher rate of consolidation than Case A. All three cases yielded different final settlement values due to the effects of drain installation, while Case C produced the highest ultimate settlement. The final settlement was independent of the drainage type (radial or vertical or both), but directly related to the compressibility parameter (m_v or C_c), the effective stress increment and thickness

of clay, so any change in the compressibility parameter due to disturbance will affect the final settlement

These three cases resulted in different settlement values due to the effect of installation and they all resulted in different values of ultimate settlement. The unit cell analyses showed that by including the variations in compressibility and permeability due to the degree of disturbance, a more realistic prediction of consolidation can be obtained. Variations in the properties compressibility, due to drain installation should also be considered during design, apart from the variations in permeability.

Table 3.3 : Soil parameters used in analysis

Parameter	**Single Drain CASE A**	**Multi Drain CASE B**	**Ideal Drain CASE C**
k_{hi} ($\times 10^{-10}$m/s)	7.97	6.88	7.97
k_0 ($\times 10^{-10}$m/s)	2.96	2.96	7.97
m_v (m^2/kN)	0.00290	0.00188	0.00336
n	13.165	13.165	13.165
s	7.767	7.767	7.767
K	2.696	2.329	1.000
C_h (m^2/Day)	0.00242	0.00323	0.00209

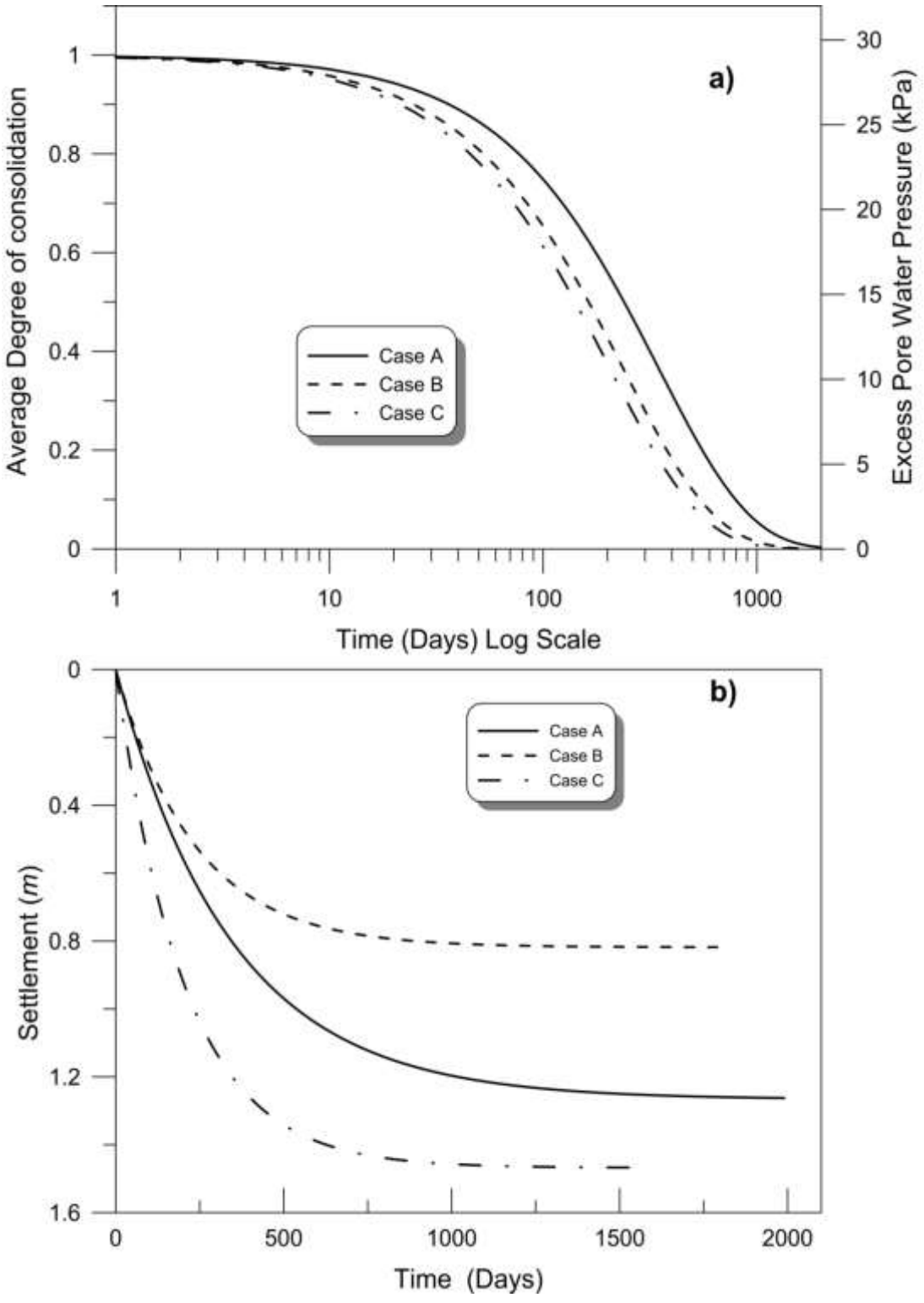

Figure 3.14 : (a) Excess pore pressure predictions and degree of consolidation (b) comparison of vertical displacements.

3.8 Summary

In this study, the effects of drain installation on consolidation was investigated using samples obtained from a test embankment constructed over a soft clay site in Ballina, NSW, and by studying the alterations to the permeability, compressibility, and anisotropy of the soil. The variations in the lateral and vertical directions were obtained using a standard oedometer test of samples retrieved around PVDs installed in different radial locations. The extent of the smear zone can be explained on the basis of either variations of normalised permeability, soil compressibility, or a change in the water content.

It was evident from the moisture content tests that the smear zone had extended 400mm away from the vertical drain. The water content was lowest near the drain, but it gradually increased in the smear zone and then remained relatively constant at a distance greater than 400mm away from the drain. The water content was almost unaffected by the installation of the single drain, but it decreased even beyond 400mm away in the in multi-drain case. The samples for the single drain and multi-drain cases were taken from the same area and same depth where the clay was homogeneous within a close proximity to each other, and therefore the effect of spatial variation can be ignored. Figure 3.6(a) also showed that the water content was almost the same inside the smear zone, within a distance of 400mm, but beyond the smear zone in the multi-drain case, the water content and horizontal permeability decreased further compared to those obtained from the undisturbed samples; this result supports the existence of an overlapping smear zone. The apparent reduction in the region beyond the smear zone was about 4%, and similar trends also occurred in the variation of permeability and void ratios. These observations can be attributed to

a probable overlapping smear zone where the permeability or water content at a given location greater than 300mm was less than those obtained from the single drain case.

All the methods used to evaluate the extent of the smear zone suggested a smear zone that was 6.3 times larger than the equivalent mandrel dimension, which was much higher than that 2-4 times observed in the laboratory using reconstituted specimens. As expected, the volume compressibility and permeability anisotropy also provided similar trends and the anisotropy next to the installed drain changed markedly. Moreover, in field conditions the soil can be subjected to a higher degree of disturbance when longer vertical drains are installed, indeed the compression curves revealed that the soil became more disturbed towards the drain as the soil close to the drain experienced severe remoulding due to installation.

The numerical analysis using the unit cell analogy and linear variation of permeability inside the smear zone showed that by incorporating compressibility and permeability due to the degree of disturbance, the degree of consolidation could be predicted more realistically. In the disturbed region the lateral permeability, co efficient of consolidation, compressibility and pre-consolidation pressure, were adversely affected, so it is imperative that the effects of variations in compressibility be included in the analytical solution apart from the variations of permeability. These variables significantly affected the rate of settlement and dissipation of excess pore pressure, so it is suggested as the basis of this study that these parameters should be assessed using undisturbed samples obtained at different distances from the vertical drains. Since same drain installation methods are used when vacuum pressure is

applied with vertical drains, results obtained in this chapter for smear zone can be used with vacuum preloading projects as well.

In conclusion, The installation of mandrel driven vertical drains creates a disturbed region (the smear zone) around the drain. To predict the rate of consolidation accurately, the extent of the smear zone and the ratio of the horizontal coefficient of permeability in the undisturbed zone over the smear zone must be estimated correctly. However, the effects of soil disturbance under field conditions have not been captured properly by previous work carried out in this area. Indeed, most prior work was limited to laboratory experiments where relatively shorter drains were driven into the soil with scaled down mandrels. In this study, the characteristics and extent of the smear zone were investigated using samples obtained from around a vertical drain installed beneath an embankment built at Ballina, Australia, and then the normalised permeability (k_h/k_{hu}), water content, and the volume compressibility across the smear zone was used to determine the properties of the smear zone. According to this study, the smear zone observed under field conditions was larger than the smear zone identified in the laboratory studies, and therefore a convenient method of calculating the extent of the smear zone is also proposed.

Chapter 4 Development of analytical model

4.1 General

Vacuum preloading was introduced by Kjellman (1952) and since then it has become a very popular ground improvement method, especially in reclamation projects. In most cases vacuum pressure is applied to the ground along with traditional surcharge fill loads, but when thick layers of soft clay are encountered, it is general practise to use vertical drains with or without a vacuum pressure to accelerate the consolidation. Vacuum pressure is applied to the ground either with or without membranes where the vacuum pump is connected directly to each drain (membrane less system) or vacuum pressure is applied into an air tight membrane (membrane system). Both methods have their inherent advantages and disadvantages although the membrane method applies a suction force to the surface below the air tight cover and the vacuum pressure is also propagated through the length of the

drain; latter is the only way a vacuum pressure is transferred in a membrane less technique (Indraratna et al., 2005a).

Barron (1948) and Hansbo (1981) laid a platform for the analytical modelling of radial consolidation. When vertical drains are installed using a steel mandrel it creates a disturbed region known as the smear zone where the lateral permeability decreases and the rate of consolidation is adversely affected. Analytical models for radial consolidation such as those developed by Hansbo (1981) and Indraratna & Redana (1997) assumed a constant but reduced permeability inside the smear zone. However the horizontal permeability inside the smear zone changes from a minimum value near the drain to a maximum value at the boundary of the smear zone and in Walker & Indraratna (2006) and Walker & Indraratna (2007) considered a parabolic and linear variation of permeability within the smear zone respectively, and modified the analytical solution for radial drainage accordingly. Indraratna et al. (2005a) and Indraratna et al. (2005c) successfully extended the radial consolidation theory to incorporate vacuum preloading, but they consider only a constant permeability within the smear zone in that solution.

The main assumptions based on Barron (1948) and Hansbo (1981) theories are similar to the assumptions made in the Terzaghi consolidation theory where a constant value for the coefficient of volume compressibility and lateral permeability is assumed during consolidation; these values are the average stress increment values. However, as consolidation continues the void ratio of the soil gradually decreases which causes the coefficient of volume compressibility and lateral permeability to vary (Tavenas et al., 1983). To better predict the pore pressure and ground settlement, the variation of compressibility and permeability must be

considered in the analysis. Lekha et al., (2003) modified the Terzaghi consolidation equation to include the variations of compressibility and permeability, and then Indraratna et al., (2005b) incorporated this into their radial consolidation equation.

Leroueil & Vaughan, (1990) stated that natural soil has a distinct structure that would not be available in reconstituted clay samples. The installation of a rigid mandrel during drain installation alters the structure of the soil such that the compressibility and the lateral permeability are affected (Chai & Miura, 1999). Most of the earlier laboratory studies carried out to investigate the smear effects were performed on large reconstituted samples of soil therefore the analytical solutions developed for radial consolidation considered the variation of lateral permeability due to the effects of drain installation effects, but the effect of compressibility was not captured properly in those solutions. After testing large scale undisturbed samples Rujikiatkamjorn et al. (2013) provided a concept to incorporate this variation in compressibility, and then Rujikiatkamjorn & Indraratna (2014) presented an analytical model for radial consolidation that incorporated the changes to the soil structure and lateral permeability due to the installation of mandrel driven drains. This variation of compressibility will alter the consolidation responses when vacuum pressure is applied with vertical drains. However, the current analytical models developed for vacuum preloading do not capture the effects of the soil structure characteristics on its compressibility and permeability due to the drain installation.

In this chapter, a new analytical solution for vacuum preloading with vertical drains that incorporates the variation of compressibility and permeability due to the destruction of soil during drain installation will be developed. This solution assumed a linear variation of vacuum pressure along the length of the drain while the

associated pore pressure distribution and settlement was obtained from both normally consolidated and lightly over-consolidated clays. Inside the smear zone, the linear variation of permeability was assumed with a minimum value close to the drain and a gradual increase to a maximum value of in-situ permeability at the boundary of the smear zone. This analysis also considered the effects of varying coefficients of compressibility and lateral permeability with reducing void ratios. The proposed model was verified using selected case studies in Chapter 6.

4.2 Assumptions made in the analysis

The following assumptions were made while the analytical solution for radial consolidation with vacuum pressure was being derived.

- Soil is saturated and homogeneous and Darcy low is valid for flow relationships. In the perimeter of the assumed unit cell, where $r = R$, no flow was allowed. $\frac{\partial u}{\partial r}(r = R) = 0,$ and the vertical drain was much longer than the unit cell radius and therefore the vertical flow of water in the clay was insignificant.

- Small strain theory is valid and the equal strain concept presented in Barron (1948) was used in the analysis. Compressive strains were only allowed to occur in a vertical direction, and total settlement at the ground surface at any given time was uniform.

- Permeability within the smear zone was taken as varying linearly from a minimum value of $k_{0(rw)}$ to a maximum value k_h at the boundary of the smear zone and the undisturbed zone. Beyond the smear zone the lateral permeability is a constant value of k_h (Undisturbed lateral permeability)

-

- Variations of vacuum pressure along the depth of the drain were linear.

4.3 Compression characteristics of structured clay

Most deposits of natural clay were formed by sedimentation and subsequent one dimensional consolidation under its own weight for thousands of years. These deposits exhibit permeability and compressibility anisotropy due to factors such as distinct soil structure, nature of deposition, effective overburden pressure, stress history, and the cementation bonds (Gibson & Lo, 1961; Randolph & Wroth, 1979). Natural soils are different forms of reconstituted soils due to the influence of macro and micro 'structures' inherent in natural soils (Burland, 1990; Leroueil & Vaughan, 1990). Mitchell (1976) described this 'structure' as a combination of the arrangement of particles known as the fabric, and bonds between the inter-particles.

Numerous constitutive models have been developed to simulate the behaviour of structured clay, such as Gens & Nova (1993); Whittle (1993); Wheeler (1997); Rouainia & Muir Wood (2000) and Liu & Carter (2002). The compressibility and strength obtained by the reconstituted samples are intrinsic because they do not depend on the relevant characteristics of the natural soils (Burland, 1990). Therefore the properties of reconstituted soils can be used as reference properties to measure the influence of soil structure. Based on this, Liu & Carter (1999,2000) proposed a model to describe the virgin compression behaviour of structured soils where the structure was assessed using variations of the void ratio, and the additional void ratio due to the soil structure was inversely proportional to the present mean effective stress. They also stated the difference in behaviour between reconstituted soils and structured soils as follows, and it is shown graphically in Figure 4.1.

- Natural soils are relatively stiffer at low stress levels and for a given effective stress; structured soil has a higher void ratio than the reconstituted clay obtained from the same natural clay. When the effective stress increases, soil is subjected to destruction and the additional void ratio occupied by the natural soil decreases.

- The influence of the soil structure seems to have reduced with the increasing stress while the compression curve of structured soil moves closer to the reconstituted soil curve with increasing stress.

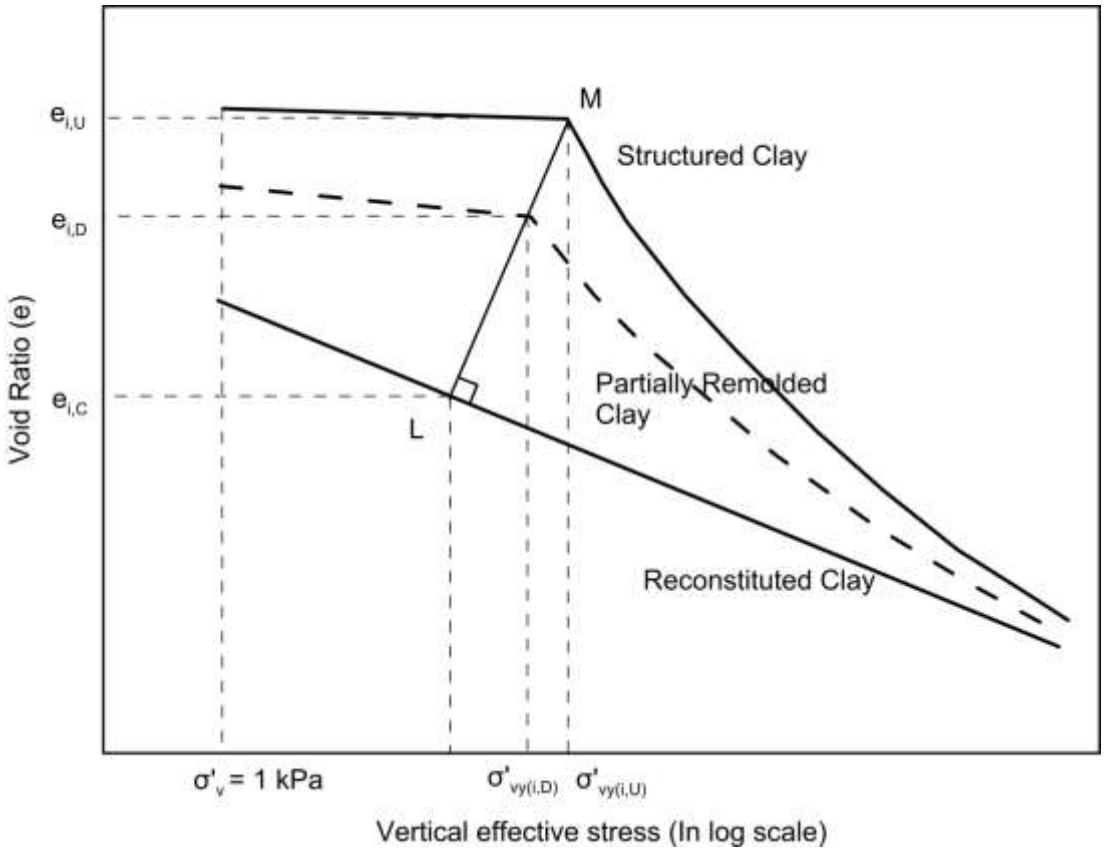

Figure 4.1 : Schematic of the compression behaviour of clay (After Rujikiatkamjorn et al., 2013)

4.4 Characteristics of the conceptual model

The structured curve represents the undisturbed soil beyond the smear zone is subjected to very little or no disturbance due to drain installation. Soil within the smear zone can be represented by the partially remoulded clay shown in Figure 4.1 and then the reconstituted soil can be taken as the severely disturbed region near the drain. Detailed mathematical formulations related to Figure 4.1 are presented in Liu & Carter (1999); Rujikiatkamjorn et al. (2013) and Rujikiatkamjorn & Indraratna (2014), and they are expressed as follows.

- The intrinsic properties of soil are represented by the reconstituted clay and the compression curve of reconstituted clay will act as the reference compression curve given by;

$$e^* = e_{ic}^* - c_c^* \log \sigma'_{\mathrm{v}} \tag{4.1}$$

Where σ'_v is the current effective vertical stress, e_{ic}^* is the void ratio corresponding to the vertical stress of 1 kPa, e^* is the current void ratio at the vertical stress of σ'_v in the reconstituted compression curve, and c_c^* is the gradient of compression line of the reconstituted soil in one dimensional consolidation.

- The variations in the void ratio during the consolidation of a undisturbed soil are given by following equations,

$$e = e_{ic}^* + \Delta e_{i,u} \left[\frac{\sigma'_{\mathrm{vy}(i,U)}}{\sigma'_{\mathrm{v}}}\right]^b - c_c^* \log \sigma'_{\mathrm{v}} \quad \sigma'_{\mathrm{v}} \geq \sigma'_{\mathrm{vy}(i,U)} \tag{4.2}$$

$$e = e_{i,u} - c_s^* \log \frac{\sigma'_{\mathrm{v}}}{\sigma'_{\mathrm{vy}(i,U)}} \quad \sigma'_{\mathrm{v}} < \sigma'_{\mathrm{vy}(i,U)} \tag{4.3}$$

$$\Delta e_{i,u} = e_{i,u} - e_{ic}^{*} + c_c^{*} \log \sigma'_{vy(i,U)} \quad (4.4)$$

where $\sigma'_{vy(i,U)}$ is the yield stress of the virgin compression curve, $e_{i,u}$ is the relevant void ratio at the yielding, b represents the index of de-structuring, and c_s^{*} is the recompression index when $\sigma'_v < \sigma'_{vy(i,U)}$

- Nagaraj (1990) stated that the loci of the yield stress for curves with different degree of disturbances are perpendicular to each other. It was assumed that the initial yield stress of partially disturbed soil within the smear zone lies in the line LM in Figure 4.1. Line LM is perpendicular to the one dimensional consolidation curve of reconstituted soil, so the initial yield stress of partially disturbed soil can be calculated as;

$$\sigma'_{vy(i,D)} = \left(10^{[c_c^{*}(e_{i,D} - e_{i,u})]}\right) \sigma'_{vy(i,U)} \quad (4.5)$$

The initial yield stress of partially disturbed soil is given by $\sigma'_{vy(i,D)}$ and the corresponding void ratio is $e_{i,D}$. This point lies in the line LM.

- The yield stress of partially disturbed soil can be obtained from equation 4.5 where the compression curve of that particular soil is given by,

$$e = e_{ic}^{*} + \Delta e_{i,D} \left[\frac{\sigma'_{vy(i,D)}}{\sigma'_v}\right]^{b} - c_c^{*} \log \sigma'_v \qquad \sigma'_v \geq \sigma'_{vy(i,D)} \quad (4.6)$$

$$e = e_{i,D} - c_s^{*} \log \left[\frac{\sigma'_v}{\sigma'_{vy(i,D)}}\right] \qquad \sigma'_v < \sigma'_{vy(i,D)} \quad (4.7)$$

$$\Delta e_{i,D} = e_{i,D} - e_{ic}^{*} + c_c^{*} \log \sigma'_{vy(i,D)} \quad (4.8)$$

4.5 Experimental data to fit the conceptual model

The effects of drain installation on the structure of clay in actual field conditions were studied in Chapter 3. The samples used for testing were extracted under an embankment stabilised with vertical drains in low lying flood plains at Ballina, Australia. Before the embankment was built, vertical drains were installed and samples were collected from around a single drain and between two rows of drains, to simulate a multi drain case. The locations from where the samples were extracted are shown in Figures 3.3 and 3.4. The variation in the void ratio and lateral permeability is shown in Figure 3.7. From that data and the moisture content distributions and degree of disturbance data presented in Figures 3.6 and 3.11 it is evident that the smear zone was located 400mm away from the drain.

The compressibility characteristics were studied via stepped loaded laboratory oedometer consolidation tests carried out on samples extracted from single drain and multi drain configurations. Vertical and horizontal specimens were taken from each location and then the compressibility of each sample was measured. The experimental data from the vertical samples is shown in Figure 3.9 and from the horizontal samples in Figure 3.10. The data shows how the compressibility of the soil changed along the radius of the area of influence in the drain; it was then fitted to the conceptual model described in section 4.4, and the fitted curves are shown in Figure 4.2.

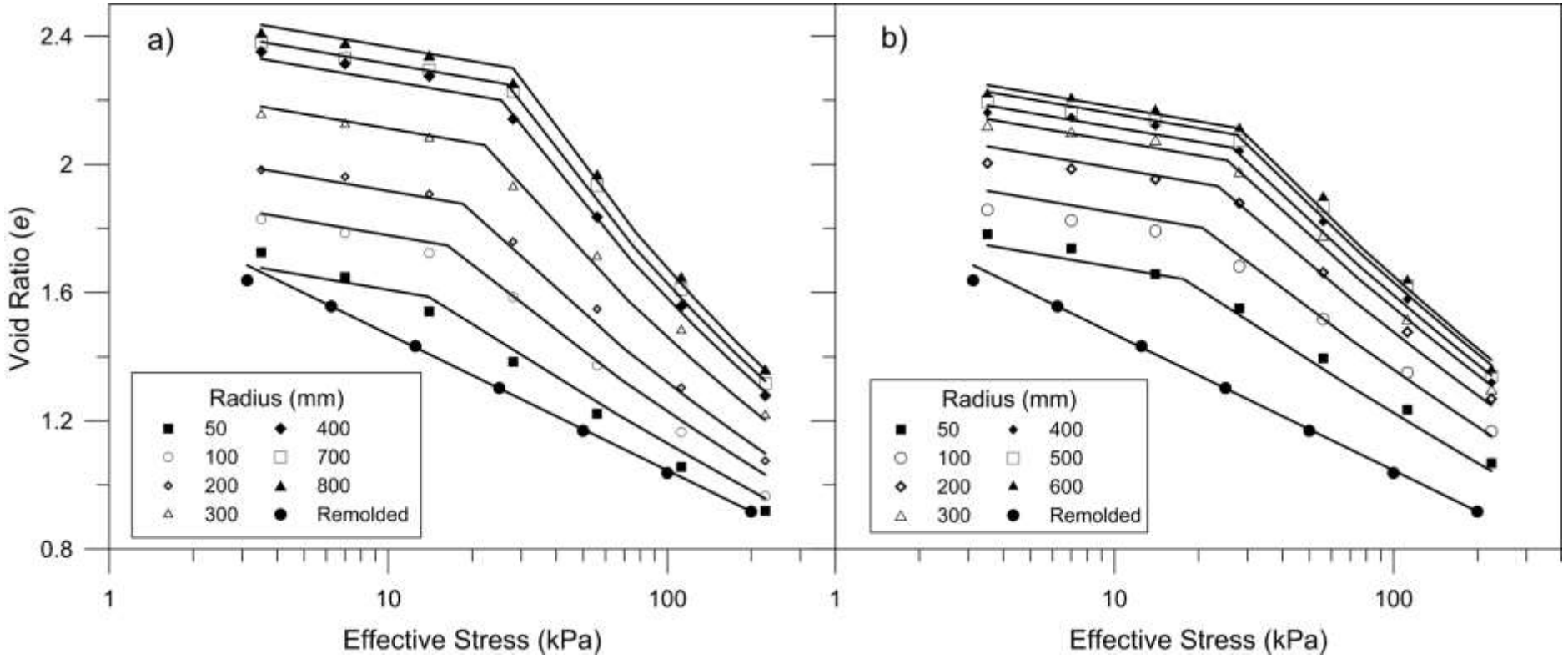

Figure 4.2 : Compressive curves with fitted data; a) Single drain case; b) Multi drain case

For the single drain analysis, the yield stress of the undisturbed curve ($\sigma'_{vy(i,U)}$) was 28 kPa, but it decreased to 13.9 kPa in the curve obtained 50mm away from the drain where the soil was subjected to the maximum amount of remoulding. ($\sigma'_{vy(i,D)}$) the de-structuring index value was taken as 0.38 to fit the curves to the available data. In the multi drain analysis the relevant values were taken as follows: as $\sigma'_{vy(i,U)}$ was 28 kPa, $\sigma'_{vy(i,D)}$ was 17.6 kPa ,and b was taken as 0.25.

4.6 Normalising the soil parameters for the Analysis

4.6.1 Average void ratio and compressibility parameters

The experimental investigation in Chapter 3 revealed that the permeability and compressibility of the intact clay had altered after the drain was installed. Moreover, the samples extracted from different distances away from the drain indicated that within the smear zone the initial void ratio and yield stress also varied. The initial void ratio and yield stress, or the pre-consolidation pressure of a soil is very important in calculating the ultimate settlement and time-settlement response of a layer of soft clay. Therefore, it is important to use the average compression curve to simulate the behaviour of soil cylinder around a vertical drain after smear zone is created due to the drain installation. This average curve will represent the actual soil condition in the field and will yield a realistic consolidation response. (Rujikiatkamjorn & Indraratna, 2014)

Take $\bar{e}$ as the average void ratio at any average vertical effective pressure $\bar{\sigma}'$, $\bar{e}_0$ as the average void ratio at the initial stage at an effective vertical stress of σ'_0, and $\bar{e}_f$ as the average void ratio at the final stage when the effective stress is σ'_f. The pre-consolidation stress (yield stress) of the average curve is denoted by $\bar{\sigma}'_i$.

Figure 4.3 shows the average compressive curve and the compressive curve for the undisturbed region and soil near the vertical drain.

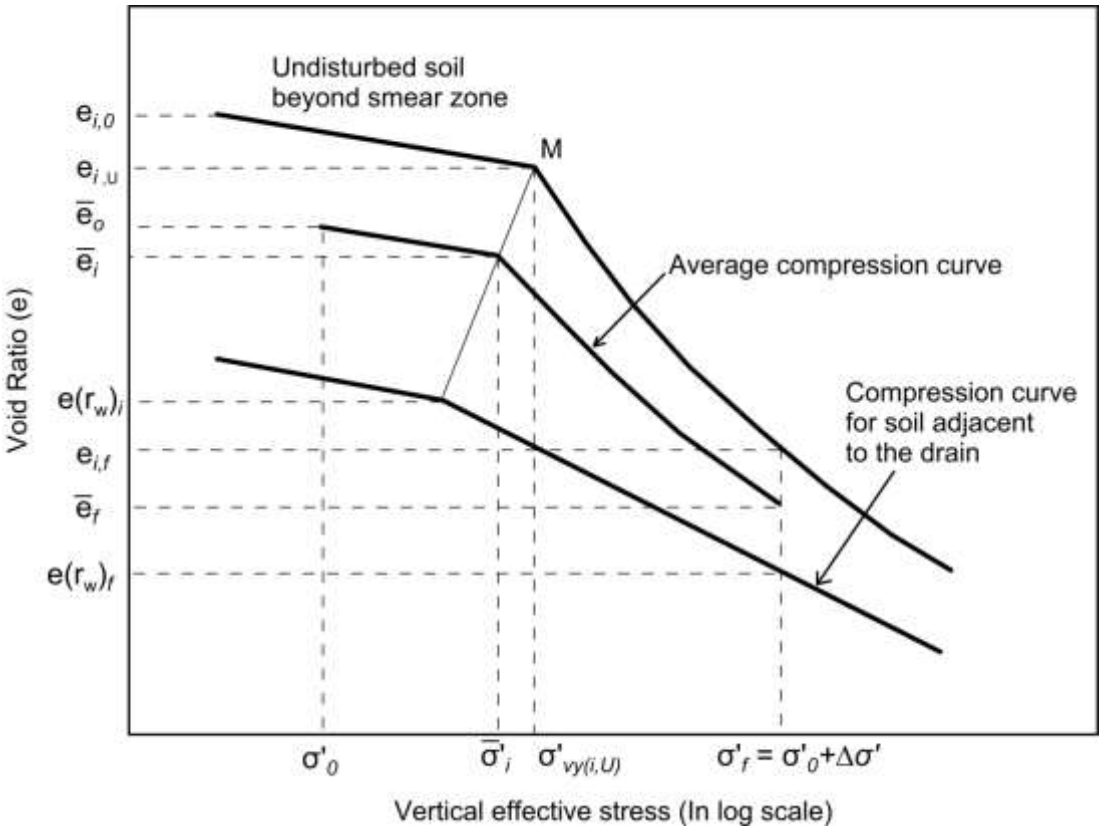

Figure 4.3 : Average compression curve for a disturbed soil.

The change in the void ratio change the average compression curve can be described by the following equations,

$$\bar{e} = \bar{e}_0 - c_s \log\left(\frac{\bar{\sigma}'}{\sigma'_0}\right) \qquad \bar{\sigma}' \leq \bar{\sigma}'_i \qquad (4.9)$$

$$\bar{e} = \bar{e}_0 - c_s \log\left(\frac{\bar{\sigma}'_i}{\sigma'_0}\right) - \bar{c}_c \log\left(\frac{\bar{\sigma}'}{\bar{\sigma}'_i}\right) \qquad \bar{\sigma}' > \bar{\sigma}'_i \qquad (4.10)$$

where, $\bar{c}_c$ is the average compressibility index for a given stress range in a normally consolidated region, and c_s is the recompression index in over-consolidation region.

It was noted that the average recompression index (c_s) was the same as the recompression index of undisturbed curve, so according to Tavenas et al., (1983b) the void ratio can be related to permeability as,

$$e = e_0 + c_k \log\left(\frac{k_h}{k_{h0}}\right) \tag{4.11}$$

where c_k is the permeability index. The semi-log, permeability–void ratio relationship with the assumed void ratio parameters are shown in Figure 4.4, while the actual permeability void ratio relationships observed during the single drain case and multi-drain case are shown in Figure 4.5.

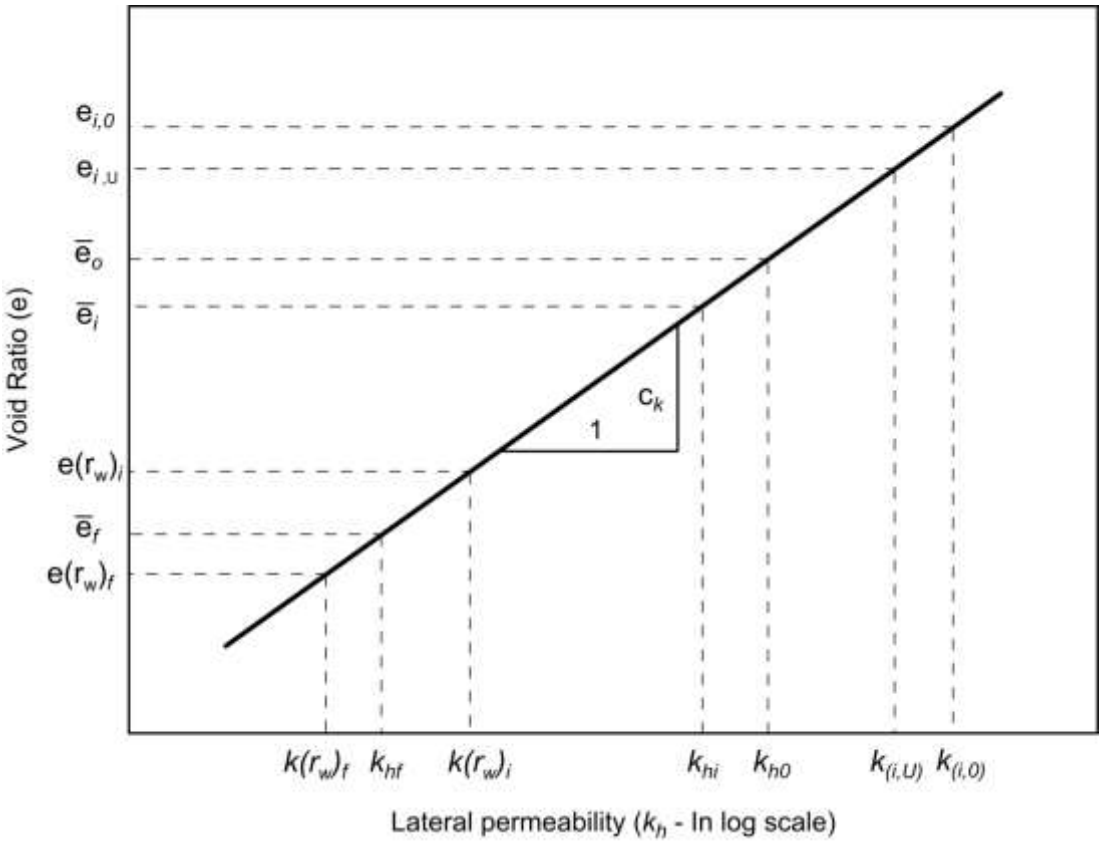

Figure 4.4: Variation of permeability with void ratio (model assumptions)

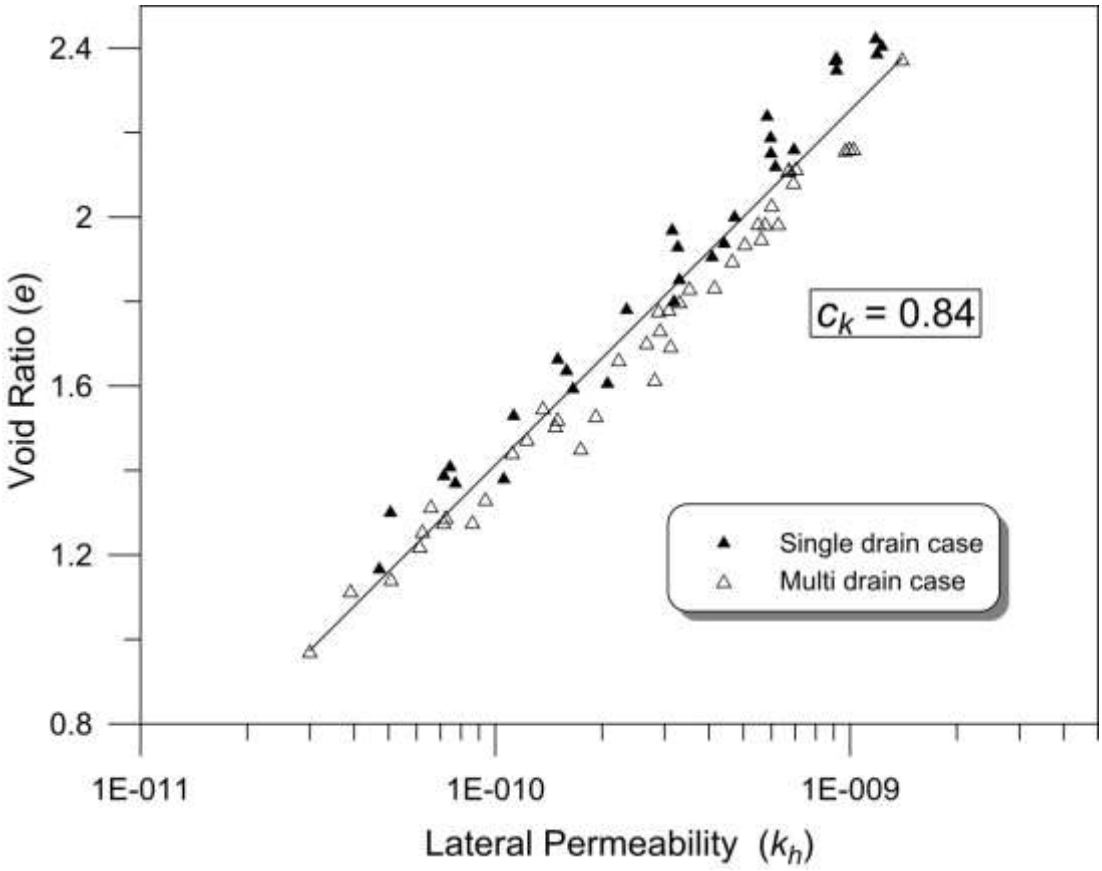

Figure 4.5 : Variation in permeability with the void ratio observed in experiments

Along the line LK in Figure 4.1 lays the yield stresses of partially disturbed curves that were obtained from the consolidation tests performed on samples obtained within the smear zone. The expression for the void ratio at the yield of clay along the radius of the drain's effective area can be obtained as;

$$e_i(r) = e_{i,U} + c_k \log\left(\frac{k(r_w)i}{k_{i,U}}\right) \qquad r \le r_s \qquad (4.12)$$

$$e_i(r) = e_{i,U} \qquad r_s < r \le R \qquad (4.13)$$

The void ratio at the yield stress of the soil cylinder was at its lowest value next to the drain samples but it will increase linearly along the radius until it reaches the boundary of the smear zone where it will attain the void ratio of undisturbed pre-consolidation pressure ($e_{i,U}$). Beyond the limit of the smear zone, the yield stress is equal to $e_{i,U}$. This variation can be represent by,

$$e(r)_i = \frac{e_{i,U}}{f_i}\left[\frac{A}{r_w}r + B\right] \tag{4.14}$$

$$A = \frac{f_i - 1}{s - 1} \tag{4.14a}$$

$$B = \frac{s - f_i}{s - 1} \tag{4.14b}$$

$$f_i = \frac{e_{i,U}}{e(r_w)i} \tag{4.14c}$$

$$s = \frac{r_s}{r_w} \tag{4.14d}$$

where, r_s is the radius of the smear zone and r_w is the equivalent radius of the drain. By combining the integrating equations 4.12, 4.13, and 4.14 we can obtain an expression for the void ratio ($\bar{e}_i$) at the yield stress ($\bar{\sigma'}_i$) in the averaged curve,

$$\bar{e}_i(R - r_w) = \int_{r_w}^{r_s}\left(\frac{e_{i,U}}{f_i}\left[\frac{A}{r_w}r + B\right]\right)dr + \int_{r_s}^{R} e_{i,u}dr \tag{4.15}$$

$$\bar{e}_i(R - r_w) = \frac{e_{i,U}}{f_i}\left[\frac{A}{2r_w}(r_s^2 - r_w^2) + B(r_s - r_w)\right] + e_{i,u}(R - r_s) \tag{4.16}$$

The void ratio in the average curve at yield stress can be given by,

$$\bar{e}_i = \frac{e_{i,U}}{(n-1)}\left(\frac{1}{f_i}\left[\frac{(f_i+1)(s-1)}{2}\right]+(n-s)\right) \tag{4.17}$$

where

$$n = \frac{R}{r_w} \tag{4.17a}$$

and R is the radius of the soil cylinder considered in the analysis. The yield stress that relates to this average void ratio can be calculated from this equation,

$$\bar{\sigma'}_i = \left(10^{[c_c^*(\bar{e}_i - e_{i,u})]}\right)\sigma'_{\mathrm{vy}(i,U)} \tag{4.18}$$

The external applied stress of $\Delta\sigma'$ was applied to the embankment from an initial stress of σ'_0 to a final stress of σ'_f. The average void ratio of the initial stage and the final stage can be derived in a similar manner to equation 4.17 as follows,

$$\bar{e}_0 = \frac{e_{0,U}}{(n-1)}\left(\frac{1}{f_0}\left[\frac{(f_0+1)(s-1)}{2}\right]+(n-s)\right) \tag{4.19}$$

$$f_0 = \frac{e_{0,U}}{e(r_w)0} \tag{4.19a}$$

$$\bar{e}_f = \frac{e_{f,U}}{(n-1)}\left(\frac{1}{f_f}\left[\frac{(f_f+1)(s-1)}{2}\right]+(n-s)\right) \tag{4.20}$$

$$f_f = \frac{e_{f,U}}{e(r_w)f} \tag{4.20a}$$

The average compression curves obtained for the single drain case and the multi-drain case using equations 4.17 to 4.20 is shown in Figure 4.6

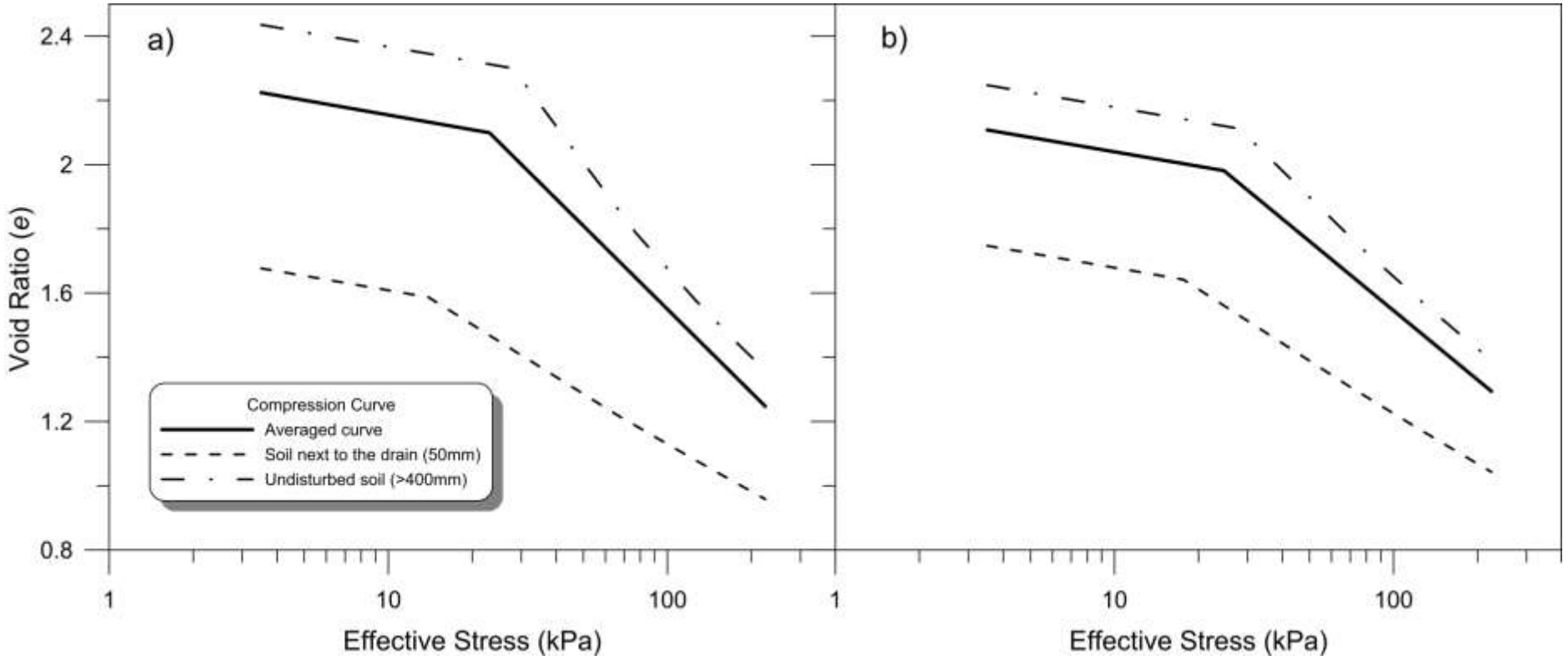

Figure 4.6 : Averaged compression curves for a) Single drain case b) Multi-drain case

The compression index in a normally consolidated range of an averaged compression curve can be obtained by the following equation,

$$\bar{c}_c = \frac{\bar{e}_i - \bar{e}_f}{log\left(\frac{\sigma'_0 + \Delta\sigma'}{\bar{\sigma}'_i}\right)} \tag{4.21}$$

4.6.2 Distribution of Permeability in the smear zone

The linear distribution of permeability within the smear zone stated in Walker & Indraratna (2007) was used to simulate the variation of lateral permeability in this analysis. The variations in permeability and the void ratio along the radius of the unit cell are shown in Figure 4.7. This permeability variation in the smear zone is given by,

$$k_h(r_w) = k(r_w)_0 \tag{4.22}$$

$$k_h(r_s) = k_h \tag{4.23}$$

Equation 4.24 will satisfy the boundary conditions of equations 4.22 and 4.23

$$k_h = \frac{k_h}{\kappa}\left[\frac{C}{r_w}r + D\right] \qquad r \le r_s \tag{4.24}$$

$$C = \frac{\kappa - 1}{s - 1} \tag{4.24a}$$

$$D = \frac{s - \kappa}{s - 1} \tag{4.24b}$$

$$\kappa = \frac{k_h}{k(r_w)_0} \tag{4.24c}$$

$$k_h = k_h \qquad r_s < r \le R \tag{4.24d}$$

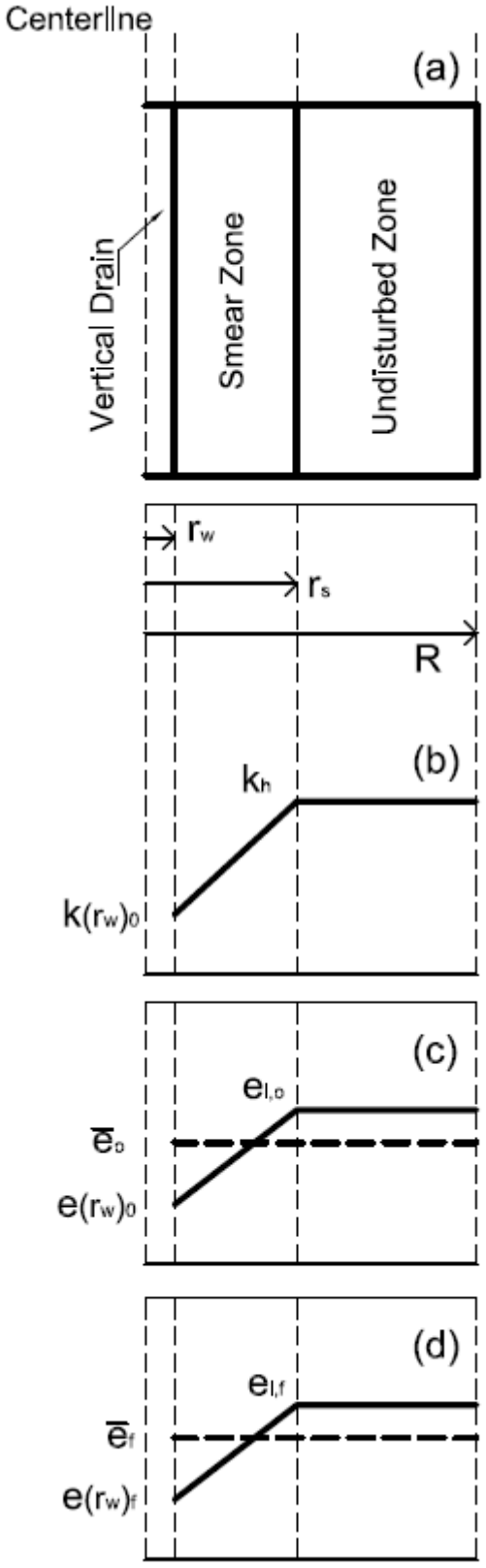

Figure 4.7 : Variation of b) Permeability; c) initial void ratio; d) final void ratio of a unit cell with a vertical drain (Modified from Rujikiatkamjorn & Indraratna, 2014)

4.7 Vacuum consolidation model considering soil structure characteristics

A vacuum pressure with vertical drains has been a popular method of ground improvement used all over the world. Indraratna et al. (2005a, 2005c) presented comprehensive analytical models for radial consolidation with vacuum preloading. Chu et al. (2000) observed in field conditions that the distribution of a vacuum pressure along the depth of the drain was not uniform and later Indraratna et al. (2005a) reported a loss of vacuum with the depth of a drain in laboratory experiments with large scale samples. The presence of intermediate layers of thin sand may be one reason why the vacuum pressure can be leaked from these layers, while another possibility is that when the drains are long, the higher lateral stress compresses drains at greater depths, which causes resistance to the vacuum propagating. Therefore, a linear variation of vacuum pressure was assumed in this analysis, and the axisymmetric unit cell and vacuum pressure distribution is shown in Figure 4.8.

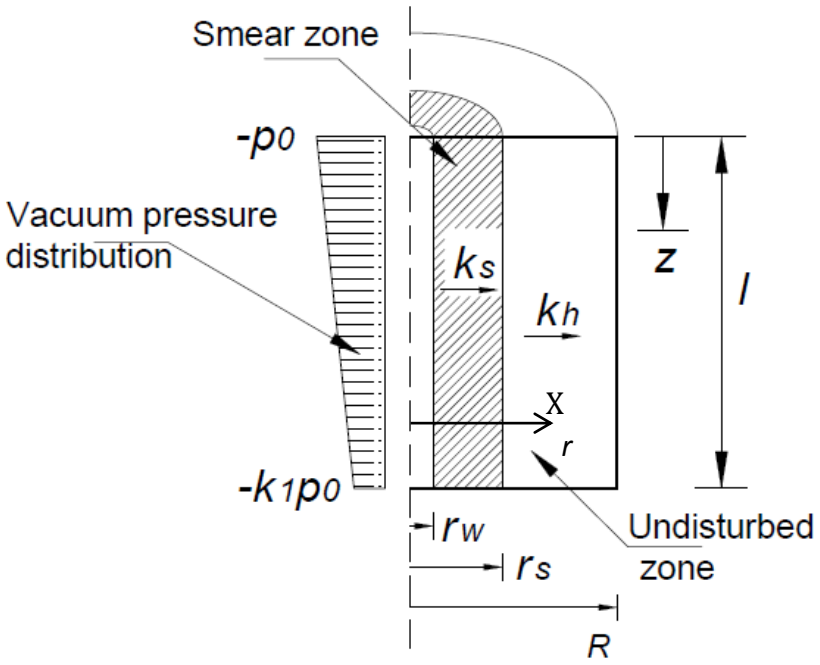

Figure 4.8 : Vacuum pressure distribution in an axisymmetric unit cell

The variation of vacuum pressure along the depth of the drain can be expressed as;

$$p(z) = p_0\left[1 - (1 - k_1)\frac{z}{l}\right] \tag{4.25}$$

Where *z* is the depth measured from the top of the surface, p_0 is the vacuum pressure applied from the top of the drain, and k_1 is the vacuum pressure reduction factor. By considering the flow through the point *X* and the distance *r* away from the centreline of the drain shown in Figure 4.8, an expression for the rate of discharge using Darcy's equation can be written as,

$$\frac{\partial Q}{\partial t} = kiA \tag{4.26}$$

$$\frac{\partial Q}{\partial t} = \frac{k_{h(r)}}{\gamma_w}.\frac{\partial u}{\partial r}.2\pi r\ dz \tag{4.27}$$

where *Q* is the discharge through point *X* of a strip of thickness *dz* and *u* is the excess pore water pressure. The rate of discharge through point *X* is equal to the rate of change of strain of the soil volume beyond that point.

$$\frac{\partial \mathrm{Q}}{\partial t} = \frac{\partial \epsilon}{\partial t}.\pi(R^2 - r^2)\ dz \tag{4.28}$$

By 4.27 and 4.28,

$$\frac{\partial u}{\partial r} = \frac{\partial \epsilon}{\partial t}\frac{\gamma_w}{2k_{h(r)}}\frac{(R^2 - r^2)}{r} \tag{4.29}$$

ϵ is the vertical strain and the $k_{h(r)}$ represent the variation of lateral permeability with the radius of the influenced area of the drain *R* given in equation 4.24. By

applying the variation of permeability to equation 4.29, two expressions for the excess pore water pressure inside the smear zone and the undisturbed zone beyond it can be obtained as,

Within the smear zone $r_w < r \leq r_s$ assumes the excess pore water pressure to be u'

$$\frac{\partial u'}{\partial r} = \frac{\partial \epsilon}{\partial t} \frac{\gamma_w}{2\left\{\frac{k_h}{\kappa}\left[\frac{C}{r_w}r + D\right]\right\}} \frac{(R^2 - r^2)}{r} \tag{4.30}$$

Integrating equation 4.30 w.r.t the radius r;

$$u' = \frac{\partial \epsilon}{\partial t}\frac{\gamma_w \kappa R^2}{2k_h}\left[\begin{array}{c}\left(\frac{D}{C^2 n^2} - \frac{1}{D}\right) ln\left(\frac{Cr}{r_w} + D\right) + \\ \frac{1}{D}\ln(r) - \frac{r}{Cr_w n^2}\end{array}\right] + c_1 \tag{4.31}$$

Applying the boundary condition, when $r = r_w$, $u = -p_0\left[1 - (1 - k_1)\frac{z}{l}\right]$ to the above equation 4.31,

$$u' = \frac{\partial \epsilon}{\partial t}\frac{\gamma_w \kappa R^2}{2k_h}\left[\begin{array}{c}\left(\frac{D}{C^2 n^2} - \frac{1}{D}\right) ln\left(\frac{Cr}{r_w} + D\right) + \\ \frac{1}{D}\ln\left(\frac{r}{r_w}\right) - \frac{(r - r_w)}{Cr_w n^2}\end{array}\right] - p_0\left[1 - (1 - k_1)\frac{z}{l}\right] \tag{4.32}$$

Outside the smear zone $r_s < r \leq R$ expression for the excess pore water pressure (u) can be written as;

$$\frac{\partial u}{\partial r} = \frac{\partial \epsilon}{\partial t}\frac{\gamma_w}{2k_h}\frac{(R^2 - r^2)}{r} \tag{4.33}$$

Integrating the equation 4.33 w.r.t the radius r;

$$u = \frac{\partial \epsilon}{\partial t}\frac{\gamma_w R^2}{2k_h}\left[\frac{1}{r} - \frac{r}{R^2}\right] + c_2 \tag{4.34}$$

To obtain the pore pressure (u_s) at the boundary of smear zone substitute $r = r_s$ in the equation 4.32,

$$u_s = \frac{\partial \epsilon}{\partial t}\frac{\gamma_w \kappa R^2}{2k_h}\left[\begin{matrix}\left(\frac{D}{C^2 n^2} - \frac{1}{D}\right) ln(\kappa) + \\ \frac{1}{D}\ln(s) - \frac{(s-1)}{Cn^2}\end{matrix}\right] - p_0\left[1 - (1 - k_1)\frac{z}{l}\right] \tag{4.35}$$

Applying the above boundary condition $u_s = u_{(r=r_s)}$ to the equation 4.34 the excess pore pressure beyond the smear zone can be obtained as,

$$u = \frac{\partial \epsilon}{\partial t}\frac{\gamma_w \kappa R^2}{2k_h}\left[\begin{matrix}\ln\left(\frac{r}{r_s}\right) + \frac{1}{2n^2}\left(s^2 - \left\{\frac{r}{r_w}\right\}^2\right) + \\ \kappa\left\{\begin{matrix}\left(\frac{D}{C^2 n^2} - \frac{1}{D}\right) ln(\kappa) + \\ \frac{1}{D}\ln(s) - \frac{(s-1)}{Cn^2}\end{matrix}\right\}\end{matrix}\right] - p_0\left[1 - (1 - k_1)\frac{z}{l}\right] \tag{4.36}$$

Excess pore pressure distribution within the smear zone and the undisturbed zone beyond it is given in equations 4.32 and 4.36. The expression for the average pore pressure in the unit cell considered at any given time can be given as,

$$\bar{u}_t = \frac{1}{\pi(R^2 - r_w^2)l}\left[\int_0^l \int_{r_w}^{r_s} u' 2\pi r \, dr dz + \int_0^l \int_{r_s}^{R} u 2\pi r \, dr dz\right] \quad (4.37)$$

$$\bar{u}_t = \frac{2}{(R^2 - r_w^2)l}\left[\int_0^l \int_{r_w}^{r_s} u' r \, dr dz + \int_0^l \int_{r_s}^{R} u r \, dr dz\right] \quad (4.38)$$

Where $\bar{u}_t$ is the average excess pore pressure of the soil cylinder at depth *z*, for vertical drain length *l* and for a given time *t*

Substituting the pore pressure expression in equation 4.38 and integrating,

$$\bar{u}_t = \frac{\partial \epsilon}{\partial t}\frac{R^2 \mu}{2k_h}\gamma_w - \frac{(1 + k_1)}{2}p_0 \quad (4.39)$$

After ignoring the lesser important terms the value of μ can be given by,

$$\mu = ln\left(\frac{n}{s}\right) - \frac{3}{4} + \frac{\kappa(s-1)}{s-\kappa} ln\left(\frac{s}{\kappa}\right) \quad (4.40)$$

Excess pore water pressure ratio is taken as R_u defined as,

$$R_u = \frac{\bar{u}_t}{\Delta\sigma'} \quad (4.41)$$

Equation 4.39 was modified using equation 4.41 as,

In an over-consolidated state $\bar{\sigma}' \leq \bar{\sigma}'_i$ and t $\leq t_i$

$$R_u = \frac{\partial \bar{e}}{\partial \bar{\sigma}'} \frac{\partial(\sigma - \bar{u}_t)}{\partial t} \frac{d_e^2 \mu}{8k_h(1+\bar{e}_0)\Delta\sigma'} \gamma_w - \frac{(1+k_1)}{2} \frac{p_0}{\Delta\sigma'} \tag{4.42a}$$

Where $d_e = 2R$ is the diameter of the effective soil cylinder, and t_i is the time need for soil to change from an over consolidated state to a normally consolidated state.

In a normally consolidated state $\bar{\sigma}' > \bar{\sigma}'_i$ and t $> t_i$

$$R_u = \frac{\partial \bar{e}}{\partial \bar{\sigma}'} \frac{\partial(\sigma - \bar{u}_t)}{\partial t} \frac{d_e^2 \mu}{8k_h(1+\bar{e}_i)\Delta\sigma'} \gamma_w - \frac{(1+k_1)}{2} \frac{p_0}{\Delta\sigma'} \tag{4.42b}$$

A surcharge load and vacuum preloading was applied instantaneously to the top of the unit cell and it was assumed that these loads do not vary with time. Therefore the total stress applied was constant and $\partial\sigma/\partial t$=0 where $\partial\sigma$ is the total stress applied was equal to the surcharge load and magnitude of the vacuum pressure. From equation 4.41a

$$R_u = -\frac{\partial \bar{e}}{\partial \bar{\sigma}'} \left(\frac{\partial \bar{u}_t}{\partial t} \frac{1}{\Delta\sigma'} \right) \frac{d_e^2 \mu}{8k_h(1+\bar{e}_0)} \gamma_w - \frac{(1+k_1)}{2} \frac{p_0}{\Delta\sigma'} \tag{4.43}$$

Differentiating equation 4.41,

$$\frac{\partial R_u}{\partial t} = \frac{\partial \bar{u}_t}{\partial t} \frac{1}{\Delta\sigma'} \tag{4.44}$$

From equations 4.43 and 4.44 and modifying further,

$$\frac{\partial R_u}{\partial t} = -\left(R_u + \frac{(1+k_1)}{2}\frac{p_0}{\Delta\sigma'}\right)\left(\frac{(1+\bar{e}_0)}{\partial\bar{e}/_{\partial\bar{\sigma}'}}\right)\frac{8k_h}{\mu d_e^2 \gamma_w} \tag{4.45}$$

$$\frac{\partial R_u}{\partial t} = \frac{\partial R_u}{\partial T_{h0}}.\frac{\partial T_{h0}}{\partial t} \tag{4.46}$$

$$T_{ho} = \frac{c_{ho} t}{d_e^2} \tag{4.47a}$$

$$\frac{\partial T_{h0}}{\partial t} = \frac{c_{ho}}{d_e^2} \tag{4.47b}$$

$$c_{ho} = \frac{k_{ho}}{m_{vo}\gamma_w} \tag{4.47c}$$

$$m_{vo} = \frac{(\partial\bar{e}/\partial\sigma'_{\mathrm{v}})_{t=0}}{(1+\bar{e}_0)} \tag{4.47d}$$

and

$$m_v = \frac{\partial\bar{e}/\partial\bar{\sigma}'}{(1+\bar{e}_0)} \tag{4.47e}$$

by equations 4.45 to 4.47, for $\bar{\sigma}' \leq \bar{\sigma}'_i$;

$$\frac{\partial R_u}{\partial T_{ho}} = -\frac{8}{\mu}\frac{m_{vo}}{m_v}\frac{k_h}{k_{ho}}\left(R_u + \frac{(1+k_1)}{2}\frac{p_0}{\Delta\sigma'}\right) \tag{4.48a}$$

For an over consolidated state (when $\bar{\sigma}' > \bar{\sigma}'_i$) a similar equation can be derived as;

$$\frac{\partial R_u}{\partial T_{hi}} = -\frac{8}{\mu}\frac{m_{vi}}{m_v}\frac{k_h}{k_{hi}}\left(R_u + \frac{(1+k_1)}{2}\frac{p_0}{\Delta\sigma'}\right) \tag{4.48b}$$

Where

$$T_{hi} = \frac{c_{hi}(t-t_i)}{d_e^2} \tag{4.49a}$$

$$c_{hi} = \frac{k_{hi}}{m_{vi}\gamma_w} \tag{4.49b}$$

$$m_{vi} = \frac{(\partial \bar{e}/\partial \sigma'_{\mathrm{v}})_{t=t_i}}{(1+\bar{e}_i)} \tag{4.49c}$$

$$m_v = \frac{\partial \bar{e}/\partial \sigma'_{\mathrm{v}}}{(1+\bar{e}_i)} \tag{4.49d}$$

Differentiating equation 4.9 with respect to the effective stress gives;

$$\frac{m_{vo}}{m_v} = \frac{\bar{\sigma}'}{\sigma'_0} \tag{4.50}$$

and,

$$\bar{\sigma}' = \sigma'_0 + u_0 - \bar{u}_t \tag{4.51}$$

where u_0 is the pore pressure increment due to the surcharge load only, and $\bar{u}_t$ is average excess pore water pressure. Combining equations 4.50, 4.51 and 4.41,

$$\frac{m_{vo}}{m_v} = 1 + \frac{u_0}{\sigma'_0} - \frac{R_u \Delta\sigma'}{\sigma'_0} \qquad \bar{\sigma}' \le \bar{\sigma}'_i \tag{4.52a}$$

Similarly,

$$\frac{m_{vi}}{m_v} = \frac{\sigma'_o}{\bar{\sigma}'_i} + \frac{u_0}{\bar{\sigma}'_i} - \frac{R_u \Delta\sigma'}{\bar{\sigma}'_i} \qquad \bar{\sigma}' > \bar{\sigma}'_i \tag{4.52b}$$

Combining equations 4.9, and 4.11,

$$-c_s \log\left(\frac{\bar{\sigma}'}{\sigma'_0}\right) = c_k \log\left(\frac{k_h}{k_{h0}}\right) \qquad \bar{\sigma}' \le \bar{\sigma}'_i \tag{4.53a}$$

$$\frac{k_h}{k_{ho}} = \left(\frac{\bar{\sigma}'}{\sigma'_0}\right)^{-c_s/c_k} = \left(\frac{m_{vo}}{m_v}\right)^{-c_s/c_k} \qquad \bar{\sigma}' \le \bar{\sigma}'_i \tag{4.53b}$$

Similarly, combining 4.10 and 4.11

$$\frac{k_h}{k_{hi}} = \left(\frac{\bar{\sigma}'}{\sigma_i'}\right)^{-\bar{c}_c/c_k} = \left(\frac{m_{vi}}{m_v}\right)^{-\bar{c}_c/c_k} \qquad \bar{\sigma}' > \bar{\sigma}_i' \qquad (4.53c)$$

By equations 4.52 and 4.53,

$$\frac{k_h}{k_{ho}} = \left(1 + \frac{u_0}{\sigma_0'} - \frac{R_u \Delta\sigma'}{\sigma_0'}\right)^{-c_s/c_k} \qquad \bar{\sigma}' \leq \bar{\sigma}_i' \qquad (4.54a)$$

$$\frac{k_h}{k_{hi}} = \left(\frac{\sigma'_o}{\bar{\sigma}_i'} + \frac{u_0}{\bar{\sigma}_i'} - \frac{R_u \Delta\sigma'}{\bar{\sigma}_i'}\right)^{-\bar{c}_c/c_k} \qquad \bar{\sigma}' > \bar{\sigma}_i' \qquad (4.54b)$$

By substituting Equations 4.53 and 4.54 to 4.48,

$$\frac{\partial R_u}{\partial T_{ho}} = -\frac{8}{\mu} P \left(R_u + \frac{(1+k_1)}{2} \frac{p_0}{\Delta\sigma'}\right) \qquad (4.55)$$

Where the function P is defined by,

$$P = \left(1 + \frac{u_0}{\sigma_0'} - \frac{R_u \Delta\sigma'}{\sigma_0'}\right)^{1-\left(c_s/c_k\right)} \qquad \bar{\sigma}' \leq \bar{\sigma}_i' \qquad (4.55a)$$

$$P = \left(\frac{\sigma_0'}{\bar{\sigma}_i'} + \frac{u_0}{\bar{\sigma}_i'} - \frac{R_u \Delta\sigma'}{\bar{\sigma}_i'}\right)^{1-\left(\bar{c}_c/c_k\right)} \qquad \bar{\sigma}' > \bar{\sigma}_i' \qquad (4.55b)$$

Equation 4.55 describes the radial consolidation of vertical drains with vacuum preloading under an instantaneous surcharge load and vacuum pressure, where the changes to the compressibility and permeability due to drain installation are

incorporated. However, this nonlinear finite difference equation does not have a general solution and the value P varies with R_u. In the over consolidation region R_u will vary from $u_0/\Delta\sigma'$ to $(\sigma_0' + u_0 - \bar{\sigma}_i')/\Delta\sigma'$ and in the normally consolidated region from $(\sigma_0' + u_0 - \bar{\sigma}_i')/\Delta\sigma'$ to $-p_0/\Delta\sigma'$. The value of P is taken as the average of these separate regions and is given by;

$$P = P_{av,0} = 0.5\left[\left(\frac{\bar{\sigma}_i'}{\sigma_0'}\right)^{1-\left(c_s/c_k\right)} + 1\right] \qquad \bar{\sigma}' \le \bar{\sigma}_i' \qquad (4.56a)$$

$$P = P_{av,i} = 0.5\left[\left(\frac{\sigma_0' + \Delta\sigma'}{\bar{\sigma}_i'}\right)^{1-\left(\bar{c}_c/c_k\right)} + 1\right] \qquad \bar{\sigma}' > \bar{\sigma}_i' \qquad (4.56b)$$

To modify equation 4.55 a new parameter, T_h^* is defined as,

$$T_{h0}^* = P_{av,0}T_{h0} = 0.5\left[\left(\frac{\bar{\sigma}_i'}{\sigma_0'}\right)^{1-\left(c_s/c_k\right)} + 1\right]T_{h0} \qquad \bar{\sigma}' \le \bar{\sigma}_i' \qquad (4.57a)$$

$$T_{hi}^* = P_{av,i}T_{h0} = 0.5\left[\left(\frac{\sigma_0' + \Delta\sigma'}{\bar{\sigma}_i'}\right)^{1-\left(\bar{c}_c/c_k\right)} + 1\right]T_{hi} \qquad \bar{\sigma}' > \bar{\sigma}_i' \qquad (4.57a)$$

And the modified equation can be given as,

$$\frac{\partial R_u}{\partial T_h^*} = -\frac{8}{\mu}\left(R_u + \frac{(1+k_1)}{2}\frac{p_0}{\Delta\sigma'}\right) \qquad (4.58)$$

In an over consolidated state $\bar{\sigma}' \leq \bar{\sigma}'_i$ and t $\leq t_i$

$$\frac{\partial R_u}{\left(R_u + \frac{(1+k_1)}{2}\frac{p_0}{\Delta\sigma'}\right)} = -\frac{8}{\mu}\partial T^*_{h0} \tag{4.59}$$

$$ln\left(R_u + \frac{(1+k_1)}{2}\frac{p_0}{\Delta\sigma'}\right) = -\frac{8}{\mu}T^*_{h0} + c_3 \tag{4.59a}$$

when $t = 0, T^*_{h0} = 0$ and $R_u = {u_0}/{\Delta\sigma'}$

Applying above boundary conditions to equation 4.59a;

$$R_u = \left(\frac{u_0}{\Delta\sigma'} + \frac{(1+k_1)}{2}\frac{p_0}{\Delta\sigma'}\right)exp\left(-\frac{8T^*_{h0}}{\mu}\right) - \frac{(1+k_1)}{2}\frac{p_0}{\Delta\sigma'} \tag{4.59c}$$

In a normally consolidated state $\bar{\sigma}' > \bar{\sigma}'_i$ and t $> t_i$;

when $t = t_i, T^*_{hi} = 0$ and $R_u = {(\sigma'_0 + u_0 - \bar{\sigma}'_i)}/{\Delta\sigma'}$

Applying above boundary conditions to equation 4.59a;

$$R_u = \left[\left(\frac{(\sigma'_0 + u_0 - \bar{\sigma}'_i)}{\Delta\sigma'} + \frac{(1+k_1)}{2}\frac{p_0}{\Delta\sigma'}\right)exp\left(-\frac{8T^*_{h0}}{\mu}\right) - \frac{(1+k_1)}{2}\frac{p_0}{\Delta\sigma'}\right] \tag{4.59d}$$

When a vacuum pressure is not applied $u_0 = \Delta\sigma'$, and the value of c_c/c_k for normally consolidated soil approaches unity, then equations 4.59c and 4.59d will converge to the Walker and Indraratna (2007) solutions for radial consolidation.

From equations 4.59 and 4.57;

$$R_u = \begin{bmatrix} \left(\frac{u_0}{\Delta\sigma'} + \frac{(1+k_1)}{2}\frac{p_0}{\Delta\sigma'}\right)\times \\ exp\left\{-\left[\left(\frac{\bar{\sigma}_i'}{\sigma_0'}\right)^{1-\left(c_s/c_k\right)}+1\right]\frac{4T_{h0}}{\mu}\right\} \\ -\frac{(1+k_1)}{2}\frac{p_0}{\Delta\sigma'} \end{bmatrix} \qquad \begin{matrix} \bar{\sigma}' \le \bar{\sigma}'_i \\ t \le t_i \end{matrix} \qquad (4.60a)$$

$$R_u = \begin{bmatrix} \left(\frac{(\sigma_0' + u_0 - \bar{\sigma}_i')}{\Delta\sigma'} + \frac{(1+k_1)}{2}\frac{p_0}{\Delta\sigma'}\right)\times \\ exp\left\{-\left[\left(\frac{\sigma_0' + \Delta\sigma'}{\bar{\sigma}_i'}\right)^{1-\left(\bar{c}_c/c_k\right)}+1\right]\frac{4T_{hi}}{\mu}\right\} \\ -\frac{(1+k_1)}{2}\frac{p_0}{\Delta\sigma'} \end{bmatrix} \qquad \begin{matrix} \bar{\sigma}' > \bar{\sigma}'_i \\ t > t_i \end{matrix} \qquad (4.60b)$$

t_i can be obtained from equation 4.60a by substituting $R_u = {(\sigma_0' + u_0 - \bar{\sigma}_i')}/{\Delta\sigma'}$

$$t_i = \frac{\mu d_e^2}{4c_{ho}\left[\left(\frac{\bar{\sigma}_i'}{\sigma_0'}\right)^{1-\left(c_s/c_k\right)}+1\right]}\ ln\left(\frac{u_0 + \frac{(1+k_1)}{2}p_0}{\sigma_0' + u_0 - \bar{\sigma}_i' + \frac{(1+k_1)}{2}p_0}\right) \qquad (4.61)$$

In a vacuum preloading project the degree of consolidation can be measured from the excess pore water pressure as well as the settlement data. Chu & Yan (2005) proposed an expression (Figure 2.19) to evaluate the average degree of consolidation (U_p) using the pore pressure distribution profiles as,

$$U_p = 1 - \frac{\int [u_t(z) - u_s(z)]dz}{\int [u_0(z) - u_s(z)]dz} \tag{4.62}$$

$$u_s(z) = \gamma_w z - s \tag{4.63}$$

where $u_0(z)$ is the initial pore water pressure, z is the depth of the soil layer, $u_t(z)$ is a pore water pressure at depth z at any given time, $u_s(z)$ represents the minimum pore pressure that can be expected when a vacumm pressure is applied, and s is the vacuum pressure applied. The equation 4.62 can be changed to include R_u as,

$$U_p = 1 - \left(\frac{\bar{u}_t + p_0}{u_0 + p_0}\right) = 1 - \left(\frac{\bar{u}_t + p_0}{\Delta\sigma'}\right) \tag{4.64a}$$

$$U_p = 1 - \left(R_u + \frac{p_0}{\Delta\sigma'}\right) \tag{4.64b}$$

Rujikiatkamjorn and Indraratna (2014) stated that if the surcharge fill is assumed to be a ramp loading excess pore pressure ratio during ramp loading (R_u^*) can be taken as,

$$R_u^* = \frac{\Delta\sigma_t'}{\Delta\sigma'} R_u \tag{4.65}$$

Where, $\Delta\sigma_t'$ is the applied surcharge load at time t during ramp loading and $\Delta\sigma'$ is the final surcharge load. By selecting the applied vacuum pressure as zero the equation 4.60 and 4.64 can be used for non-vacuum areas with vertical drains.

4.8 Settlement analysis of thick multilayered clay with vacuum pressure and vertical drains

Use of vacuum preloading along with vertical drains as a ground improvement method is economically feasible only when very thick clay layers with high compressibility and low shear strength are encountered. Most of these clay deposits are a result of sedimentation, sometimes even extended to around 10,000 years. As a result of that, these thick clay layers usually comprise of distinct layers with different geotechnical properties such as coefficients of consolidation, compressibility and secondary consolidation.

Most of the analytical methods developed to assess the consolidation responses are only limited to one soil layer and when calculating the settlements the stress values of mid-depth are usually considered. However, the initial effective stress varies linearly along the depth of the soil, and in a thick layer there will be significant difference in the initial stress in the lower clay layers. Even though the total effective stress increment is accurately estimated, the resulting strain calculation will be incorrect if the actual initial stress has not been selected in the analysis. This is due to the nonlinear relationship of soil stiffness with the effective stress, and in lower effective stresses the soil yields more strains (resulting larger settlements) compared to the higher initial effective stresses experienced in deeper clay layers, when both layers are subjected to the same external load. Therefore, it is imperative to consider this behaviour of natural clay deposits in order to accurately predict the surface settlements. Another problem associated with this is when vacuum pressure is applied to the surface; it is not fully transmitted in to the deeper soil layers due to

vacuum loss. In such cases the total effective stress applied to the soil is reduced along the depth of the vertical drain and this has to be taken in to consideration when final settlements are estimated.

Walker et al. (2009) proposed a comprehensive mathematical model to analyse consolidation of a stratified soil with vertical and radial drainage with both instantaneous and ramp loading and in Walker & Indraratna (2009) vacuum preloading is also included in the solution. Soil properties are assumed to be constant and do not vary with time within the layer considered. Darcy's low is used to describe the flow relationship however, in the vertical direction the average hydraulic gradient to be used is given in Tang & Onitsuka (2000) and Wang & Jiao (2004). The effect of varying initial effective stress with the depth and the variation of soil stiffness in higher effective stresses to the resultant strains were not considered in their solution.

The following method coupled with the analytical model described in Section 4.7 describes how to estimate the settlements in layered soil considering the variation of initial stress and soil stiffness due to increasing depth and the reduction of the total stress applied due to vacuum loss. Stress distribution of a thick clay deposit comprises of n number of distinctive layers with a total thickness of H is shown in Figure 4.9 (not to scale). Vacuum pressure is reduced along the depth of the drain from a value of $-p_o$ from the surface level to a $-k_1 p_o$ at the bottom of the clay deposit (k_1 < 1). Initial stress varies linearly and it was assumed that the ground water level is at the surface level. Yield stress is taken as over-consolidation Ratio (OCR) × initial strass and the load added to the embankment at the surface level is equal to $u_0 + p_o$, where u_0 is taken as the surcharge load. Total applied pressure is

reduced along the depth of the soil due to the vacuum loss. Soil layer, i of thickness z_i is considered at a depth $z = i - 1$ from the ground level.

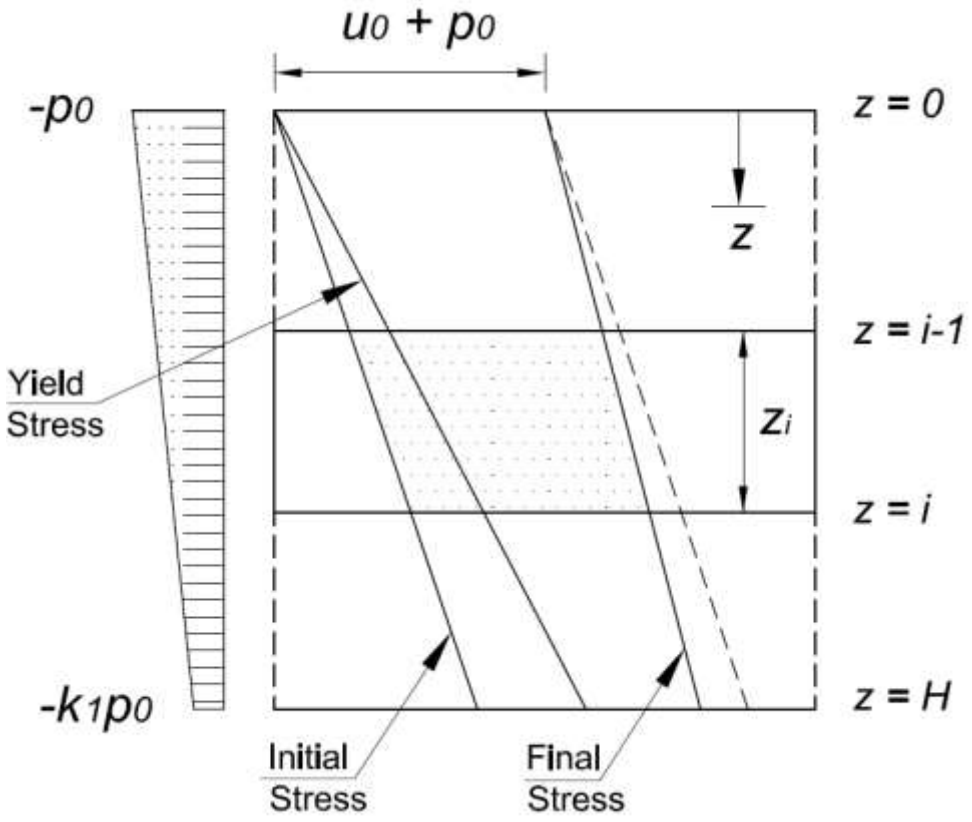

Figure 4.9 : Stress levels of an intermediate clay layer in a thick clay deposit

The vacuum pressure along the drain depth can be taken as,

$$p(z) = p_0 \left[1 - (1 - k_1)\frac{z}{H}\right] \tag{4.66}$$

Then the total effective stress increment along the depth of the drain is,

$$\Delta\sigma = u_0 + p_0 \left[1 - (1 - k_1)\frac{z}{H}\right] \tag{4.67}$$

The effective unit weight of the soil is defined as,

$$\gamma = \gamma_{sat} - \gamma_w \tag{4.68}$$

Assume the layer i shown in Figure 4.9 is over-consolidated and the total settlement in a thin strip of thickness δz due to the external load applied by both surcharge and vacuum pressure can be expressed as; when $\bar{\sigma}' < \bar{\sigma}_i'$; in over-consolidated state,

$$\delta\rho_{zi} = \frac{c_s}{(1+\bar{e}_0)} log\left(\frac{\sigma_0'(z)+\Delta\sigma'(z)}{\sigma_0'(z)}\right) \times \delta z \tag{4.69}$$

Where $\bar{c}_s$ is average recompression index. Intregating the equation 4.69 over the depth the total settlement in the layer z_i can be calculated as,

$$\rho_i = \frac{c_s}{(1+\bar{e}_0)} \int_{i-1}^{i} log\left(\frac{\sigma_0'(z)+\Delta\sigma'(z)}{\sigma_0'(z)}\right) dz \tag{4.70}$$

$$\rho_i = \frac{c_s}{(1+\bar{e}_0)} \int_{i-1}^{i} 0.43\, ln\left(\frac{\gamma z + u_0 + p_0\left[1-(1-k_1)\frac{z}{H}\right]}{\gamma z}\right) dz \tag{4.70a}$$

$$\rho_i = \frac{0.43 c_s}{(1+\bar{e}_0)} \int_{i-1}^{i} ln\left(1+\frac{\Delta u}{\gamma}\frac{1}{z}-\frac{(1-k_1)p_0}{\gamma H}\right) dz \tag{4.70b}$$

Where $\Delta u = u_0 + p_0$ and the solution will yield the total settlement in the layer i as;

$$\rho_i = \frac{0.43 c_s}{(1+\bar{e}_0)} \left[\begin{array}{c} \left[z\, ln\left(1+\frac{\Delta u}{\gamma}\frac{1}{z}-\frac{(1-k_1)p_0}{\gamma H}\right)\right]_{z=i-1}^{z=i} \\ + \frac{\Delta u}{\gamma\left\{1-\frac{(1-k_1)p_0}{\gamma H}\right\}} \times \\ \left[ln\left(\left\{1-\frac{(1-k_1)p_0}{\gamma H}\right\} z + \frac{\Delta u}{\gamma}\right)\right]_{z=i-1}^{z=i} \end{array}\right] \tag{4.70c}$$

when $\overline{\sigma'} < \bar{\sigma}_i'$; in normally consolidated state,

$$\rho_i = \frac{0.43}{(1+\bar{e}_0)} \int_{i-1}^{i} \left[c_s ln\left(\frac{\sigma_0'(z) \times OCR}{\sigma_0'(z)}\right) + \bar{c}_c ln\left(\frac{\sigma_0'(z) + \Delta\sigma'(z)}{\sigma_0'(z) \times OCR}\right)\right] dz \qquad (4.70d)$$

$$\rho_i = z_i \frac{0.43\ ln(OCR)^{(c_s - \bar{c}_c)}}{(1+\bar{e}_0)}$$

$$+ \frac{0.43\bar{c}_c}{(1+\bar{e}_0)} \left[\begin{array}{l} \left[z\ ln\left(1 + \frac{\Delta u}{\gamma}\frac{1}{z} - \frac{(1-k_1)p_0}{\gamma H}\right)\right]_{z=i-1}^{z=i} \\ + \frac{\Delta u}{\gamma\left\{1 - \frac{(1-k_1)p_0}{\gamma H}\right\}} \times \\ \left[ln\left(\left\{1 - \frac{(1-k_1)p_0}{\gamma H}\right\} z + \frac{\Delta u}{\gamma}\right)\right]_{z=i-1}^{z=i} \end{array} \right] \qquad (4.70e)$$

Where, $\bar{c}_c$ is average compression index and the average recompression index ($\bar{c}_s$) is replaced by the insitu recompression index (c_s) since both values are almost the same.

Having accurately calculated the final consolidation settlement it is now important to obtain the total settlement variation with time. This can be achieved by coupling the ρ_i obtained in Equation 4.70 with the degree of consolidation obtained in Equation 4.64 using the unit cell analysis. It is possible to obtain a solution for degree of consolidation considering all layers of the soil at once, using spectral method (Boyd, 2001). This method is extremely useful when soil is drained in vertical direction with perpendicular to the stratified soils. Clearly it will reduce the computational time when used with radial consolidation however, it will not

necessarily improve the accuracy of the settlement calculations. This is especially true when the vertical drainage is insignificant in thick clays considered here and the effects of initial stresses and total stress reduction due to vacuum loss is not considered when calculating the final settlements.

In radial consolidation, the smear zone created due to the drain installation will act as a different soil layer orientated perpendicular to the drainage path. Therefore, the accurate assessment of the characteristics of the smear zone is much more important when estimating the degree of consolidation of clay with radial drainage. This is partly due to the fact that the radial consolidation of a particular intermediate soil layer is not dependent on the soil properties of the layers vertically adjacent to it. For example an averaging technique derived to assess predominantly vertical consolidation in two layered soil could underestimate the settlement with radial consolidation if one layer has significantly higher permeability and lower compressibility parameters compared to the other. Therefore, the settlement analysis done by coupling of degree of consolidation derived using the unit cell framework for individual layers with the total settlement calculated using Equation 4.70 is an excellent and accurate tool which can be used in analysis of embankments built over a thick clay deposits.

The settlement variation with time for the whole clay layer of thickness H can be obtained as;

$$\rho(t) = \sum_{i=1}^{n} U_i \rho_i \tag{4.71}$$

4.9 Parametric analysis

4.9.1 Effects of pre consolidation pressure and load increment ratio

The development of a radial consolidation analytical model for vacuum pressure with vertical drains was shown in the previous section. The change in the soil structure due to drain installation and variations in permeability within the smear zones observed in Chapter 3 was incorporated into this analysis. The aim of this section is to perform a sensitivity analysis to demonstrate how the model reacts to the varying model parameters and how the solution would be changed from previously developed models.

The performance of the model with varying load increment ratios was studied with normally consolidated clay and lightly over consolidated clay. It was assumed that drains were installed in a square pattern with a spacing of 1.2m and the drains were 100mm in width and 3mm in thickness. The drain parameters used are listed in Table 4.1 and the soil parameters obtained for multi drain analysis in Chapter 3 were used as the parameters required in the analysis and tabulated in Table 4.2. The relevant compression curves are given in Figures 4.2 and 4.6. The analytical model used to predict the vacuum pressure with vertical drains is presented in Indraratna et al. (2005a) and this model was used to compare the performance of the current model. In the case of normal consolidated clay the samples were loaded with an initial stress of 28kPa to a final stress of 68 kPa in case A, 108 kPa in case B, and 148 kPa in Case C. This meant the load increment ratio was 2.4, 3.9, and 5.3 respectively. In each loading step, half of the total stress was applied using vacuum preloading, and Figure 4.10 shows the simulation results.

Table 4.1 : Drain parameters

Parameter	Value
r_w *(mm)*	51.5
r_s *(mm)*	400
d_e *(mm)*	1356
s	7.77
n	13.17

Figure 4.10a shows the compression curves for undisturbed, close to drain and averaged samples. According to Figure 4.10b all the loading cases considered in the analysis, the proposed model has yielded lesser settlement. It is clearly visible from Figure 3.9, compressibility of the soil is reduced within the smear zone due to drain installation. As a result of that ultimate settlement of the ground will be reduced since average compressibility parameter derived in Equation 4.21 is used. In the Indraratna et al. (2005) model, a virgin compression curve was used to calculate the settlements whereas in the proposed model a more realistic average compression curve that considered soil disturbance due to drain installation was used. Indraratna et al. (2005) showed higher rates of pore water dissipation hence the degree of consolidation compared to the proposed model in Figure 4.10c was greater due to the accurate distributions of permeability and compressibility captured in the proposed model. This clearly demonstrated the important of the proposed model in predicting the consolidation parameters in vacuum preloading projects.

Table 4.2 : Soil parameters used in the sensitivity analysis for normally consolidated clay

Soil Parameters	Current Model			Indraratna et al. (2005)		
	Case A	**Case B**	**Case C**	**Case A**	**Case B**	**Case C**
$\boldsymbol{\sigma'_0}$ *(kPa)*	28.0	28.0	28.0	28.0	28.0	28.0
$\boldsymbol{\sigma'_f}$ *(kPa)*	68.0	108.0	148.0	68.0	108.0	148.0
$\boldsymbol{u_0}$ *(kPa)*	20.0	40.0	60.0	20.0	40.0	60.0
$\boldsymbol{p_0}$ *(kPa)*	20.0	40.0	60.0	20.0	40.0	60.0
$\boldsymbol{\bar{e}_0}$, $\boldsymbol{e_{o,U}}$	1.949	1.949	1.949	2.112	2.112	2.112
$\boldsymbol{\bar{e}_f}$, $\boldsymbol{e_{f,U}}$	1.653	1.509	1.415	1.783	1.625	1.522
$\boldsymbol{f_0}$	1.38	1.38	1.38	N/A	N/A	N/A
$\boldsymbol{f_f}$	1.35	1.35	1.34	N/A	N/A	N/A
$\boldsymbol{\bar{c}_c}$, $\boldsymbol{c_c}$	0.77	0.75	0.74	0.85	0.83	0.82
$\boldsymbol{c_k}$	0.84	0.84	0.84	0.84	0.84	0.84
$\boldsymbol{P_{av,0}}$	1.038	1.076	1.110	0.991	1.009	1.030
$\boldsymbol{k_{h0}}$, $\boldsymbol{k_{o,U}} \times \mathbf{10^{-10}}(m/s)$	4.35	4.35	4.35	6.79	6.79	6.79
$\boldsymbol{k(r_w)_0} \times \mathbf{10^{-10}}(m/s)$	1.37	1.37	1.37	N/A	N/A	N/A
$\boldsymbol{k_h/k'_h} \times \mathbf{10^{-10}}(m/s)$	N/A	N/A	N/A	1.67	1.67	1.67
$\boldsymbol{\kappa}$	3.182	3.182	3.182	N/A	N/A	N/A
$\boldsymbol{\mu}$	3.969	3.969	3.969	3.195	3.195	3.195

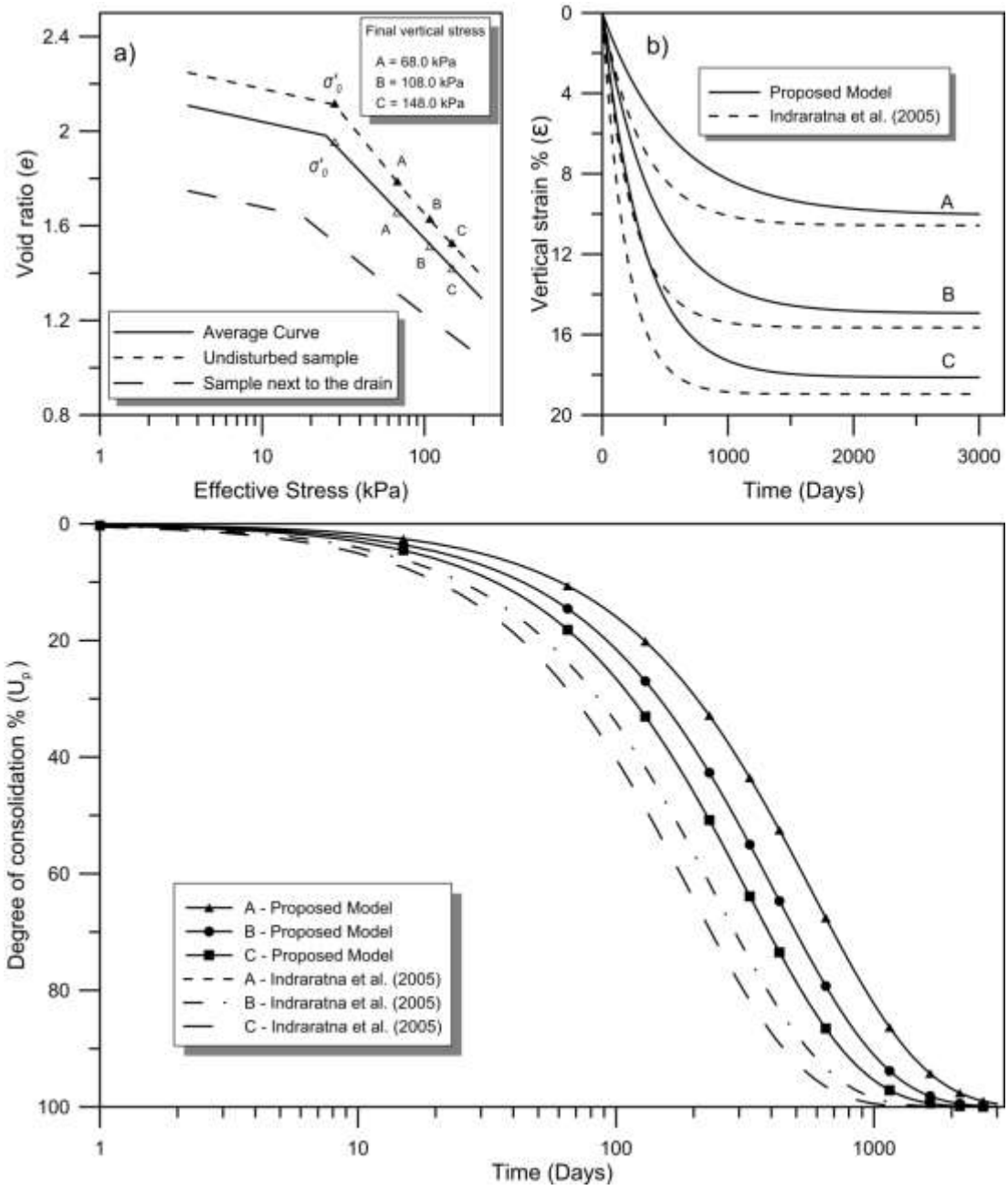

Figure 4.10 : Consolidation response of normally consolidated clay with the predicted model compared to Indraratna et al. (2005) results: (a) the relationship between the Void ratio and effective stress, and (b) vertical strain with time, and (c) the degree of consolidation with time

The proposed model was simulated with lightly over consolidated clay and the soil parameters used in the analysis are shown in Table 4.3. The drain parameters were the same as those used in the simulation of normally consolidated clay shown in Table 4.2. The initial stress of the soil was 10 kPa, and cases D, E, and F were analysed with a final effective stress of 50 kPa, 90 kPa, and 130 kPa; this resulted in 5.0, 9.0, and 13.0 load increment ratios respectively. The vacuum pressure applied was half of the total stress increment applied to the soil. The consolidation responses are shown in Figure 4.11. In Figure 4.11a relevant compression curves are shown for the undisturbed, Close to the drain and averaged samples and the change in pre-consolidation pressure can be clearly observed. Figure 4.11b shows how the settlement is varying with time for the proposed model and compared with the Indraratna et. al (2005) and the degree of consolidation with time is shown at the bottom of Figure 4.11c.

In lightly over consolidated soils the geological pre -consolidation pressure and compressibility was reduced due to the de-structuring of clay when installing the drains. The reduction of pre consolidation pressure will increase the total vertical settlements while a decrease in the compressibility index will cause it to decrease. The final vertical consolidation settlement calculated using the proposed method will depend on the two parameters mentioned above because the soil structure was incorporated into this solution. Figure 4.11 b shows that in the lower load increment ratios the proposed model yielded more settlement than Indraratna et al. (2005), and when the load increment ratio increased the latter method tended to produce comparatively larger settlements.

Table 4.3: Soil parameters used in the sensitivity analysis for over consolidated clay

Soil Parameters	Current Model			Indraratna et al. (2005)		
	Case D	Case E	Case F	Case D	Case E	Case F
$\boldsymbol{\sigma'_0}$ *(kPa)*	10.0	10.0	10.0	10.0	10.0	10.0
$\boldsymbol{\bar{\sigma}'_i}$, $\boldsymbol{\sigma'_{vy(i,U)}}$ *(kPa)*	24.7	24.7	24.7	28.0	28.0	28.0
$\boldsymbol{\sigma'_f}$ *(kPa)*	50.0	90.0	130.0	50.0	90.0	130.0
$\boldsymbol{u_0}$ *(kPa)*	20.0	40.0	60.0	20.0	40.0	60.0
$\boldsymbol{p_0}$ *(kPa)*	20.0	40.0	60.0	20.0	40.0	60.0
$\boldsymbol{\bar{e}_0}$, $\boldsymbol{e_{o,U}}$	2.040	2.040	2.040	2.179	2.179	2.179
$\boldsymbol{\bar{e}_i}$, $\boldsymbol{e_{i,U}}$	1.981	1.981	1.981	2.112	2.112	2.112
$\boldsymbol{\bar{e}_f}$, $\boldsymbol{e_{f,U}}$	1.752	1.564	1.453	1.893	1.686	1.564
$\boldsymbol{f_0}$	1.30	1.30	1.30	N/A	N/A	N/A
$\boldsymbol{f_i}$	1.29	1.29	1.29	N/A	N/A	N/A
$\boldsymbol{f_f}$	1.36	1.35	1.34	N/A	N/A	N/A
$\boldsymbol{c_s}$	0.15	0.15	0.15	0.15	0.15	0.15
$\boldsymbol{\bar{c}_c}$, $\boldsymbol{c_c}$	0.75	0.74	0.73	0.87	0.84	0.82
$\boldsymbol{c_k}$	0.84	0.84	0.84	0.84	0.84	0.84
$\boldsymbol{P_{av,0}}$	1.551	1.551	1.551	0.980	1.000	1.022
$\boldsymbol{P_{av,i}}$	1.041	1.082	1.119	N/A	N/A	N/A
$\boldsymbol{k_{h0}}$, $\boldsymbol{k_{o,U}} \times \mathbf{10^{-10}}(m/s)$	5.58	5.58	5.58	8.16	8.16	8.16
$\boldsymbol{k(r_w)_0} \times \mathbf{10^{-10}}(m/s)$	2.07	2.07	2.07	N/A	N/A	N/A
$\boldsymbol{k_{hi}}$, $\boldsymbol{k_{i,U}} \times \mathbf{10^{-10}}(m/s)$	4.75	4.75	4.75	8.37	8.37	8.37
$\boldsymbol{k_h/k'_h} \times \mathbf{10^{-10}}(m/s)$	N/A	N/A	N/A	1.67	1.67	1.67
$\boldsymbol{\kappa}$	2.690	2.690	2.690	N/A	N/A	N/A
$\boldsymbol{\mu}$	3.579	3.579	3.579	3.195	3.195	3.195

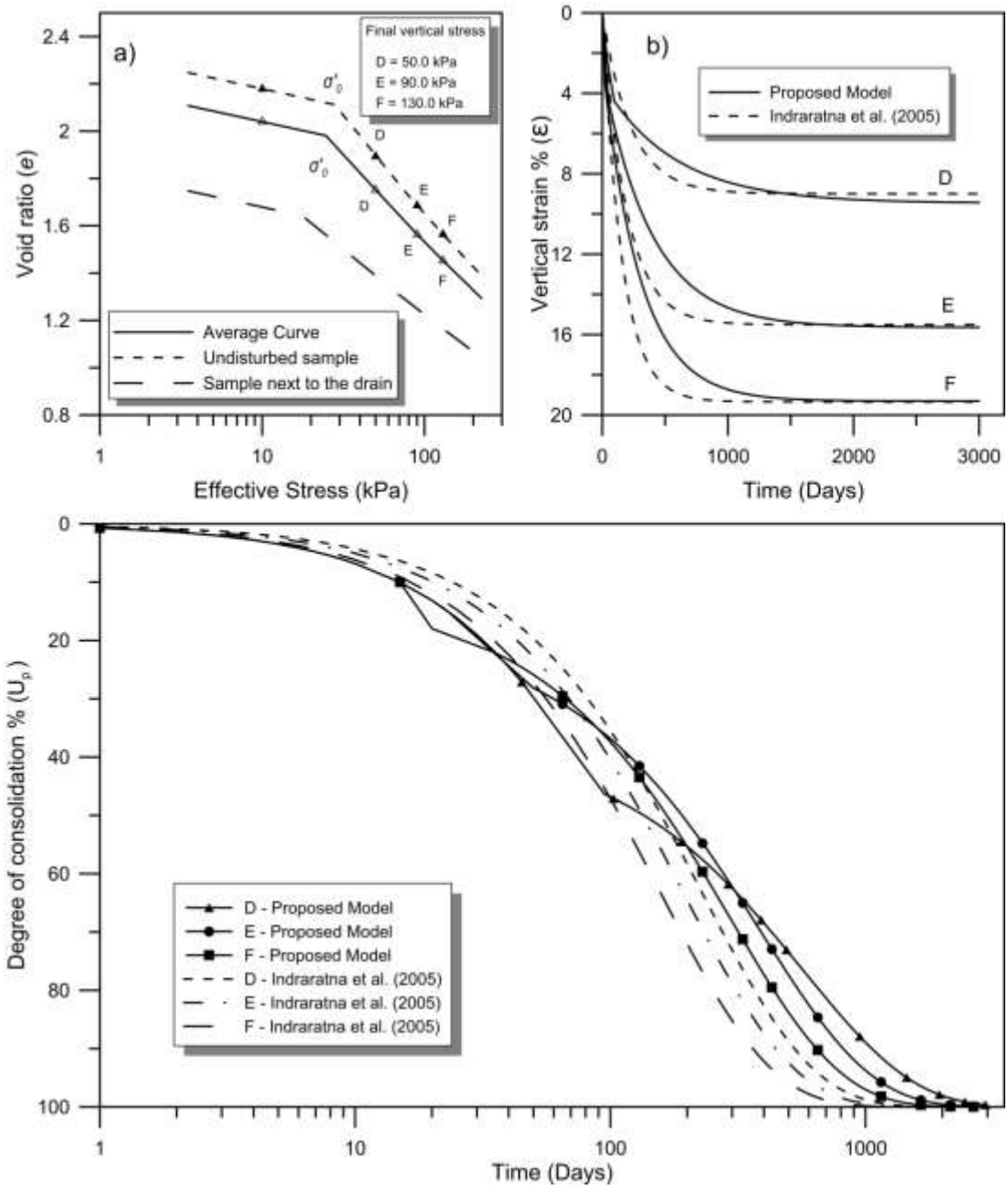

Figure 4.11 : Consolidation with lightly over consolidated clay by the predicted model compared with Indraratna et al. (2005) results showing: (a) the relationship between the Void ratio and effective stress, (b) the vertical strain with time, and (c) the degree of consolidation with time

Figure 4.11c shows that the degree of consolidation in the over consolidated state (where, $\sigma' \leq \bar{\sigma}_i'$) was almost similar in all the consolidation curves, case F with the highest stress ratio would yield first, followed by a slight reduction in the rate of consolidation. The other two cases were still in the recompression region and with a higher co-efficient of consolidation they consolidated faster than case F. However, after about 100 days, all the cases were in a normally consolidated stage, albeit the degree of consolidation in case F was sometimes higher than the other two cases.

In the degree of consolidation curves obtained from the proposed method there is a 'kink' close to time t_i in Figure 4.11c. Rujikiatkamjorn & Indraratna, (2014) stated that this due to a change in the compressibility index from c_s to $\bar{c}_c$ at pre consolidation pressure. However, in actual field conditions, this transition is smooth and such an abrupt drop in pore water pressure would not be observed. It was suggested that this can be overcome by using an average compression index around time t_i in the proposed model (similar to the pseudo-λ described in Indraratna et al., 1992) in actual field consolidation predictions, however it was not adopted in this parametric analysis.

4.9.2 Effects of vacuum loss

When a vacuum pressure is applied using longer vertical drains the total pressure applied by the vacuum pumps may not propagate to the tip of the drain. The factor of vacuum pressure transferred to the bottom of the drain is given in the model in parameter k_1. The presence of layers of permeable sand and higher horizontal stresses present in deeper layers of clay may explain the loss of the vacuum. When vacuum pressure is lost during consolidation the amount of total stress applied would decrease and hence reduce final settlement. The proposed model was simulated with

different factors of vacuum loss in normally consolidated and lightly over consolidated clay.

Figure 4.12 and Figure 4.13 show how the vacuum pressure distribution along the depth of the drain affects normally consolidated and over consolidated clay respectively. The parameters of the soil, the drain characteristics, and loading conditions used in this analysis were identical to the values used in case B and case E in the proposed model simulation described in the previous section. The total pressure applied was 80 kPa, with half of it being vacuum pressure. Vacuum pressure distributions considered in the simulation were rectangular, ($k_1 = 1.0$), triangular ($k_1 = 0$), and trapezoidal, where $k_1 = 0.25, 0.50$ and $k_1 = 0.75$.

Figures 4.12a and 4.13a shows how the pore pressure varied over time with different levels of vacuum loss; as expected, more loss of vacuum would create less effective stress increment in the soil. As with Figure 4.11c, there was a change in the pore pressure around t_i in Figure 4.13a and the reasons and remedial actions are same as those described in the previous section. Figure 4.12b and 4.13b show how the settlement changed over time with different vacuum pressure distributions, and clearly show that more vacuum loss yields less settlement.

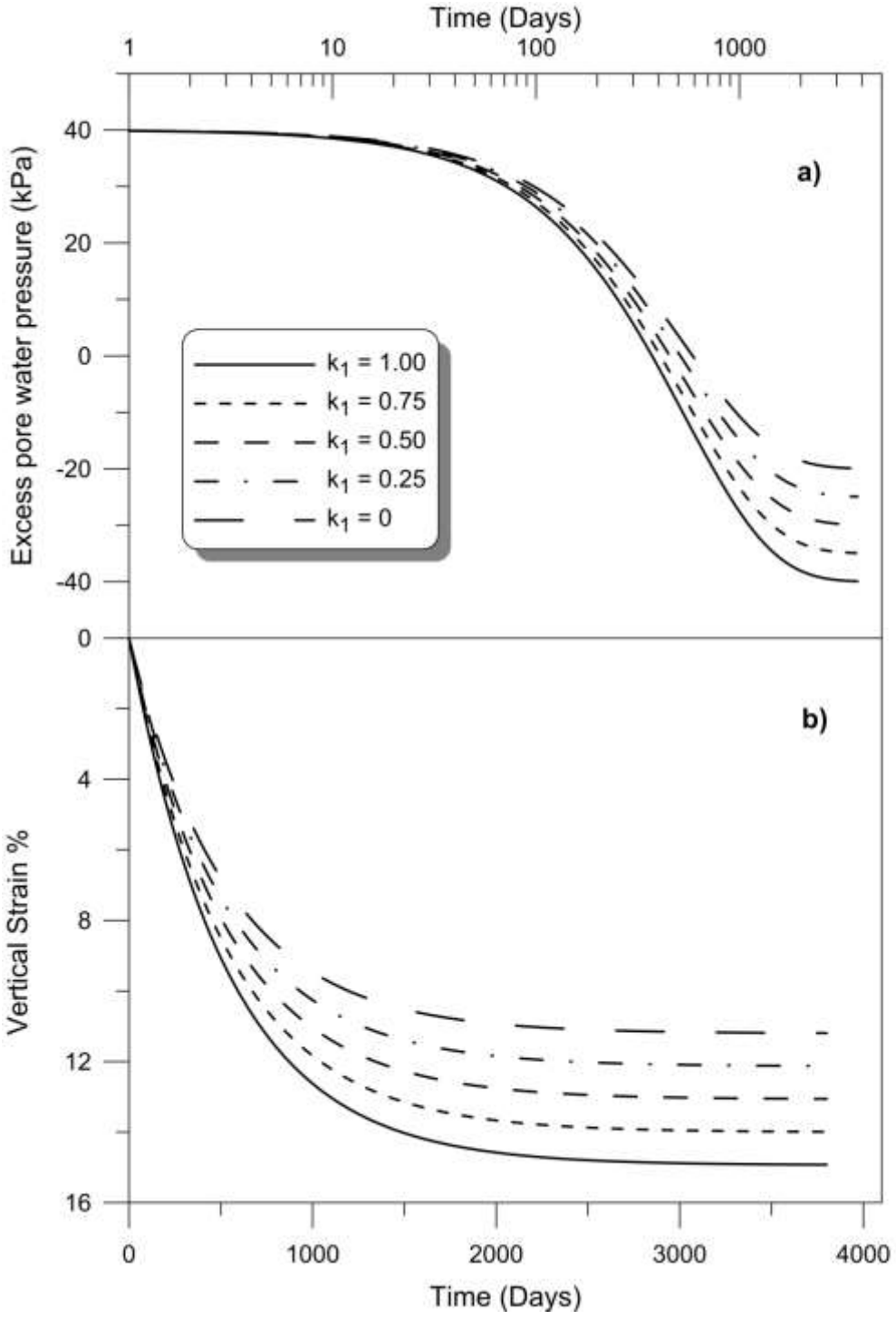

Figure 4.12 : Effects of vacuum distribution inside the drain to the consolidation parameters in normally consolidated clay: a) Excess pore water pressure; b) Vertical strain

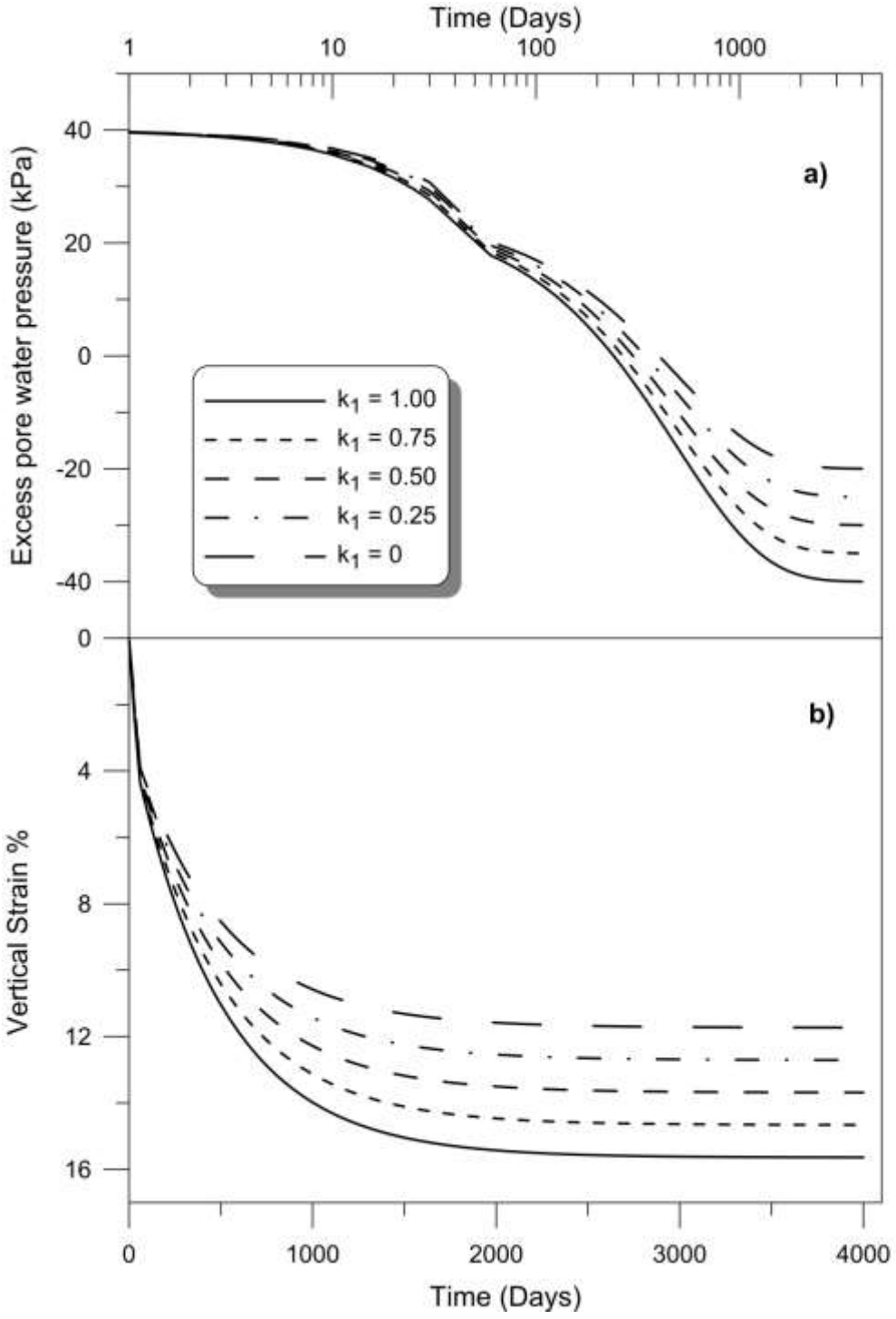

Figure 4.13 : Effects of vacuum distribution inside the drain to the consolidation parameters in lightly over consolidated clay: a) Excess pore water pressure; b) Vertical strain

4.10 Summary

An analytical solution for radial consolidation with vertical drains and vacuum preloading that incorporated the effects of soil disturbance was developed, even though the change in permeability within the smear zone was included in the previous analytical models such as Indraratna et al. (2005), changes in soil compressibility within the smear zone due to the effect of de-structuring and linearly varying permeability was not included in the previous models. The average compression curve was used to represent the partially disturbed smear zone and the intact region beyond it, and the variations in permeability and compressibility with the void ratio was also considered in this analytical model.

The effects of soil disturbance due to drain installation were studied using samples obtained beneath a soft clay embankment constructed at Ballina. Using the analytical model, the degree of consolidation and variation in settlement over time can be obtained and then the results obtained from Indraratna et al. (2005) were compared with this model in a parametric study. This comparison revealed that the current model can be used with normally consolidated and lightly over consolidated models. It was observed that previous models overestimated the consolidation settlements and degree of consolidation compared to the proposed model, and they also ignored all the variations in compressibility variation within the smear zone.

Different vacuum pressure distributions could occur due to the loss of vacuum pressure and would create different pore pressure distributions and settlement values. The proposed model can simulate different vacuum pressure distributions and also predict lesser effective stress increase and total settlement with increasing vacuum

loss. This model leads to more realistic and more accurate consolidation responses that will be of benefit to ground improvement projects with vacuum preloading.

Chapter 5 Laboratory Experiments

5.1 Oedometer testing

Laboratory experiments are a vital part of geotechnical engineering because they are widely used to determine the soil parameters and to understand the soil behaviour. There are basic experiments to derive soil parameters such as the Atterberg limits, the specific gravity and permeability, while oedometer consolidation and triaxial testing have been used extensively in industrial projects and research work to simulate the appropriate stress combinations and ground behaviour, and obtain the relevant design parameters.

Oedometer tests have been used to determine the soil characteristics in one dimensional consolidation (ASTM, 2011) and swelling, where a 50mm diameter and a 20mm high fixed ring is typically used to fit the sample to the apparatus, which is then sandwiched between two saturated porous disks to facilitate free drainage from the top and bottom of the sample. A dead weight lever system is then used to apply a

load to the sample; the load is generally doubled in each day until it reaches the desired load. Consolidation settlement is measured with either a transducer or a manual dial gauge attached to the top of the sample, although some modified oedometers have pore pressure transducers connected to the impermeable bottom plate to measure the variations in excess pore pressure during consolidation. Oedometer tests have been used extensively to characterise the smear zone and to facilitate consolidation tests on undisturbed Ballina clay that are presented in this thesis. However, conventional oedometer tests cannot be used for radial consolidation tests. A traditional oedometer apparatus among many available at the University of Wollongong is shown in Figure 5.1.

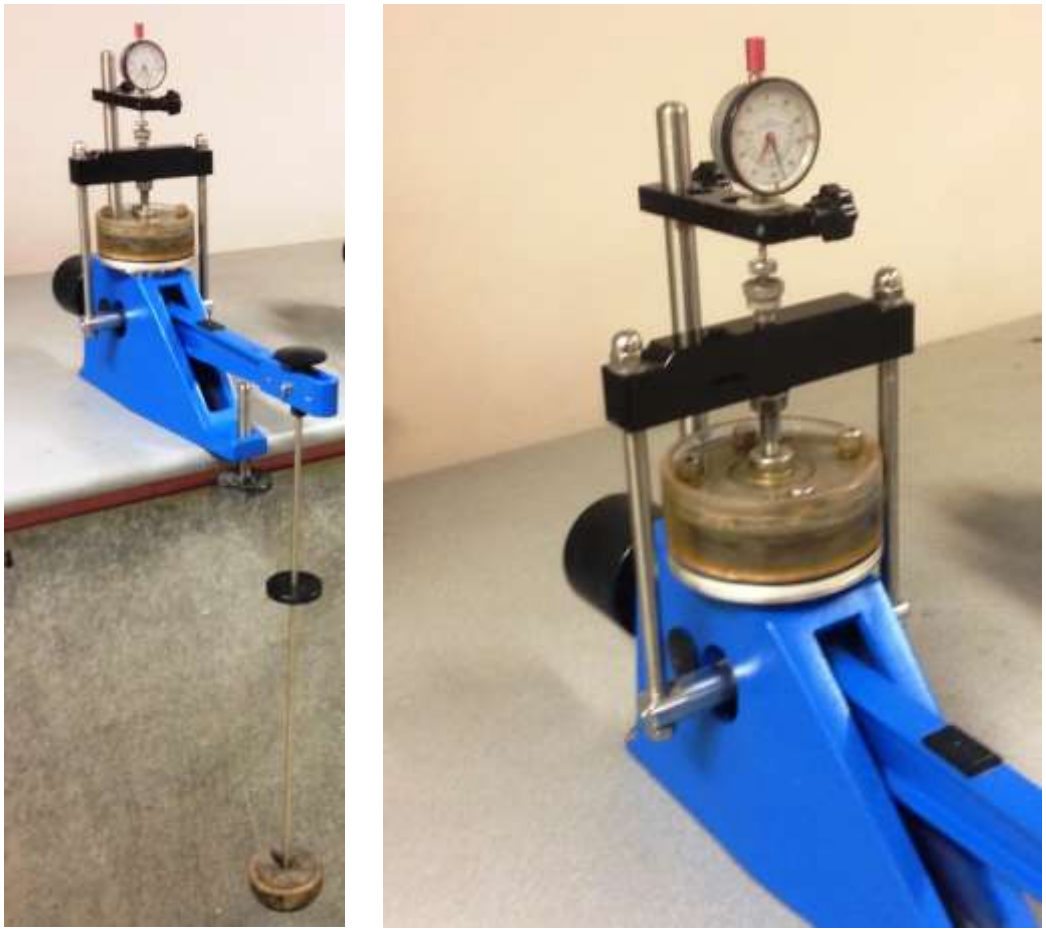

Figure 5.1 : Oedometer apparatus with manual dial gauge

5.2 Rowe and Barden consolidation apparatus

Using the oedometer apparatus, only one-dimensional consolidation test can be performed using relatively small samples, and then only with vertical drainage during consolidation. To overcome this problem, Rowe & Barden (1966) designed a new consolidation cell; a schematic diagram of which is shown in Figure 5.2

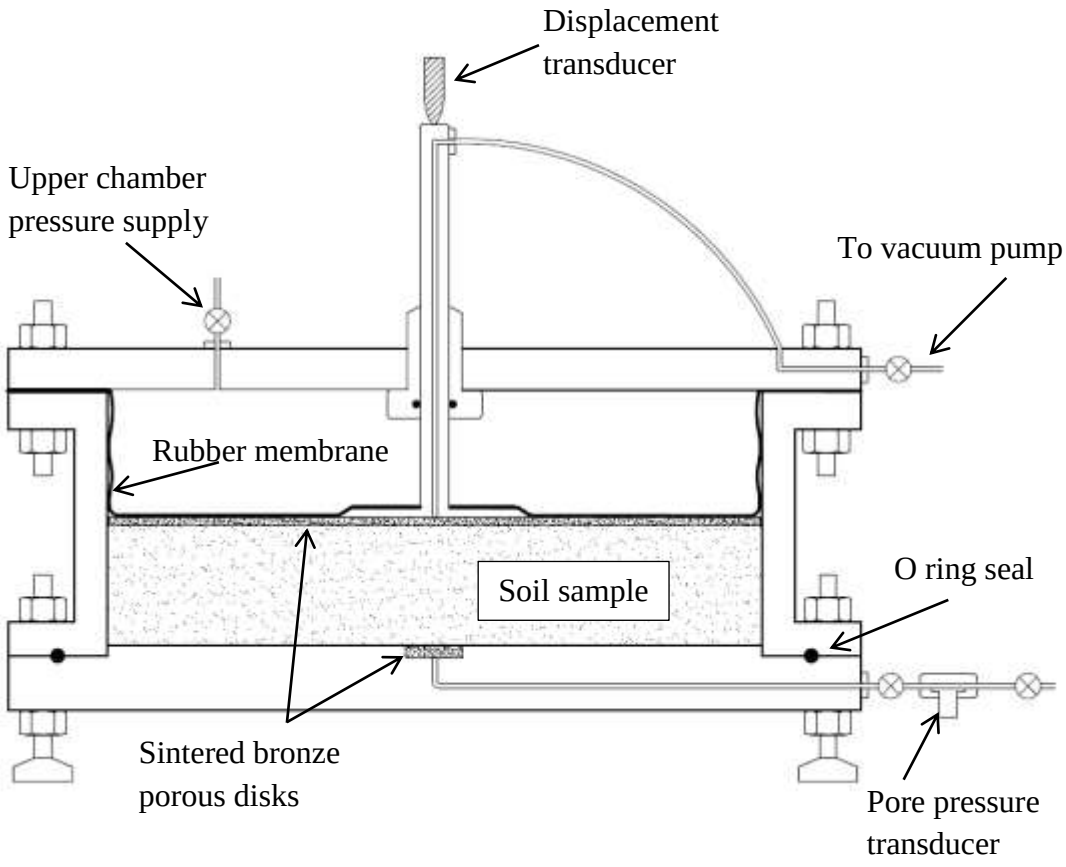

Figure 5.2 : Schematic diagram of a Rowe cell
(Modified from Rowe & Barden, 1966)

In the Rowe cells the pressure that was applied with a lever system in the oedometer apparatus is replaced with a hydraulic loading system that uses a pressure controller to apply the normal stress into a convoluted rubber membrane that sits above the soil sample. In recent versions, this flexible rubber membrane with a floating ring was introduced to further minimise fiction, when stress from the

pressure controller is applied directly onto the sample. Since the dead weight system was eliminated, samples with much larger diameters can now be tested with higher applied stresses. Moreover, the enclosed space in the Rowe cell makes it possible to apply back pressure during consolidation, while by closing the control valves an undrained condition can be created before consolidation commences, thus enabling an accurate estimation of initial pore water pressure in the clay sample.

These recently developed Rowe cells have a rim drain that can act like a horizontal drainage path. This means that by closing the top and bottom drainage paths, a radial consolidation test can be performed as water is drained through the wall of the cell and exits from the rim drain. Another advantage of this type of Rowe cell is that it provides a lateral stress in the vacuum preloading tests. Robinson et al. (2012) installed a thin membrane between the wall of the cell and the sample to enable lateral stress to be applied via a pressure controller connected to the rim drain during vacuum consolidation tests. Radial consolidated tests with vertical drains can also be carried out using a standard Rowe cell. A vertical drain was simulated using a sand compacted drain installed in the middle of the clay sample. It is possible to simulate both free strain and equal strain during consolidation using either a flexible or a rigid porous top plate.

Indraratna et al. (2013) and Kianfar et al. (2013) used a modified Rowe cell to conduct radial consolidation tests with vertical drains and vacuum preloading. They modified a 150mm Rowe cell with an increased height to accommodate very soft soils and placed three pressure transducers at the base of the cell to capture the flow relationship during consolidation using vacuum preloading.

5.3 Modified consolidometer to perform vacuum preloading tests

To conduct vacuum preloading tests with radial consolidation, a new consolidometer has been design and built at the University of Wollongong. The salient aspects of a conventional oedometer apparatus and those of a more advanced Rowe cell were used in the design of this new cell; a schematic diagram of the cell is shown in Figure 5.3, and the parts and setup of the equipment are shown in Figure 5.4.

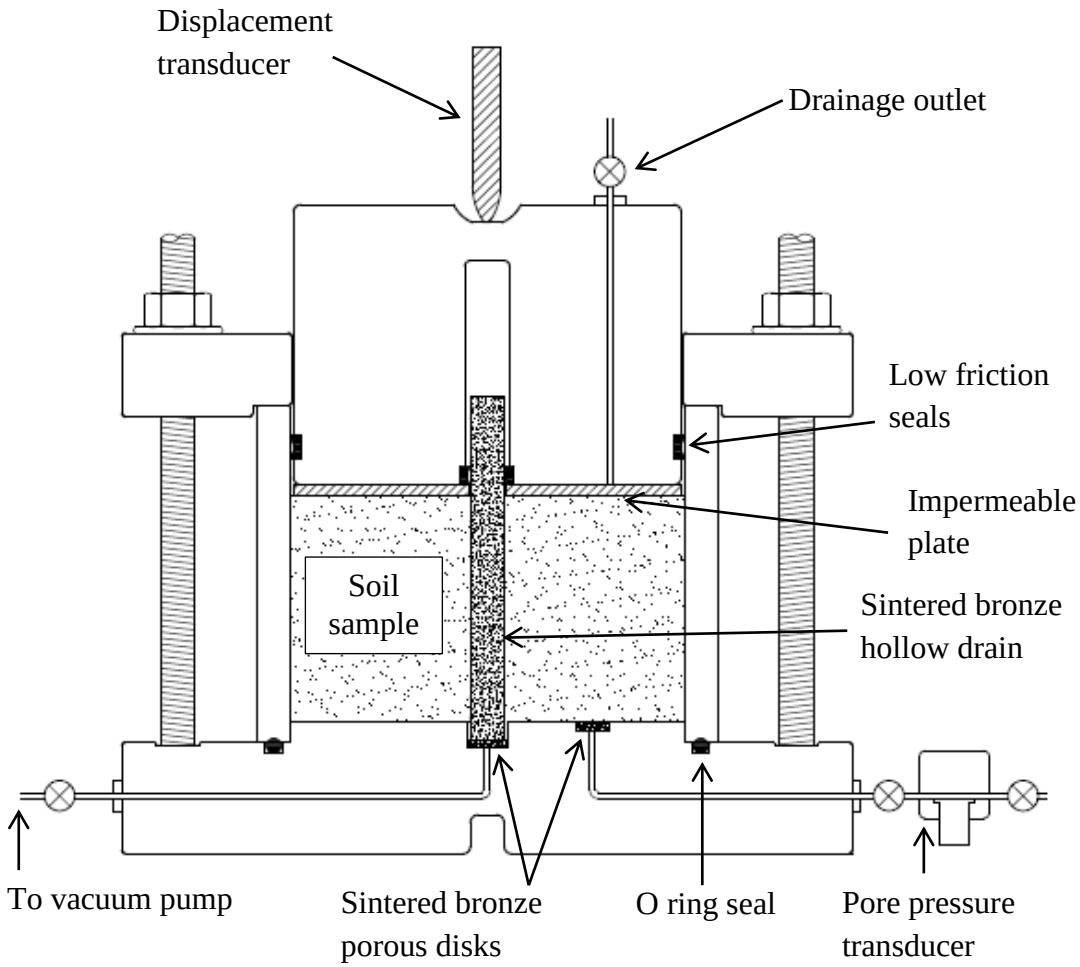

Figure 5.3 : Schematic diagram of the new consolidation cell

This new consolidation cell was designed to overcome several problems which were encountered using the conventional and modified Rowe cells. Ballina clay was the primary material tested using this equipment, and being marine clay, it inherits a very low permeability. Had the modified 150mm cell been used, primary consolidation would have taken a much longer time and thereby increasing the duration of log time cycles when secondary consolidation is measured. A 70mm diameter sample can be used in this equipment, however, if conventional vertical sand drains have been used with vacuum preloading, such as in the Rowe cell, making the drain uniform and well compacted would have been difficult because the drain is only 6mm in diameter. Therefore, the 6mm diameter sand drain is replaced with a hollow, sintered bronze drain with an external diameter of 6mm and an internal diameter of 2.4mm. This ensured that the diameter of drain during consolidation would be constant and eliminate any possibility of resistance posed to clay settlement by the sand column.

A portion of the sintered bronze drain is shown in Figure 5.4 and it can be fixed tightly to the bottom plate of this equipment. All the parts were made from brass to minimise corrosion. The rigid drain prevented the utilisation of a flexible membrane similar to the one used in the 75m diameter Rowe cell, so the flexible membrane was replaced by a rigid piston that sits on top the sample. It was important to separate the top cap and the sample with a thin but rigid impermeable plate to make sure no vertical drainage could occur inside the clay sample, but only allow radial drainage towards the sintered bronze drain. A thin layer of silicon lubricant was applied to the top of the base plate and the bottom of the impermeable disk to help the sample mover laterally, while preventing any drainage at the interface between the sample and the horizontal surfaces.

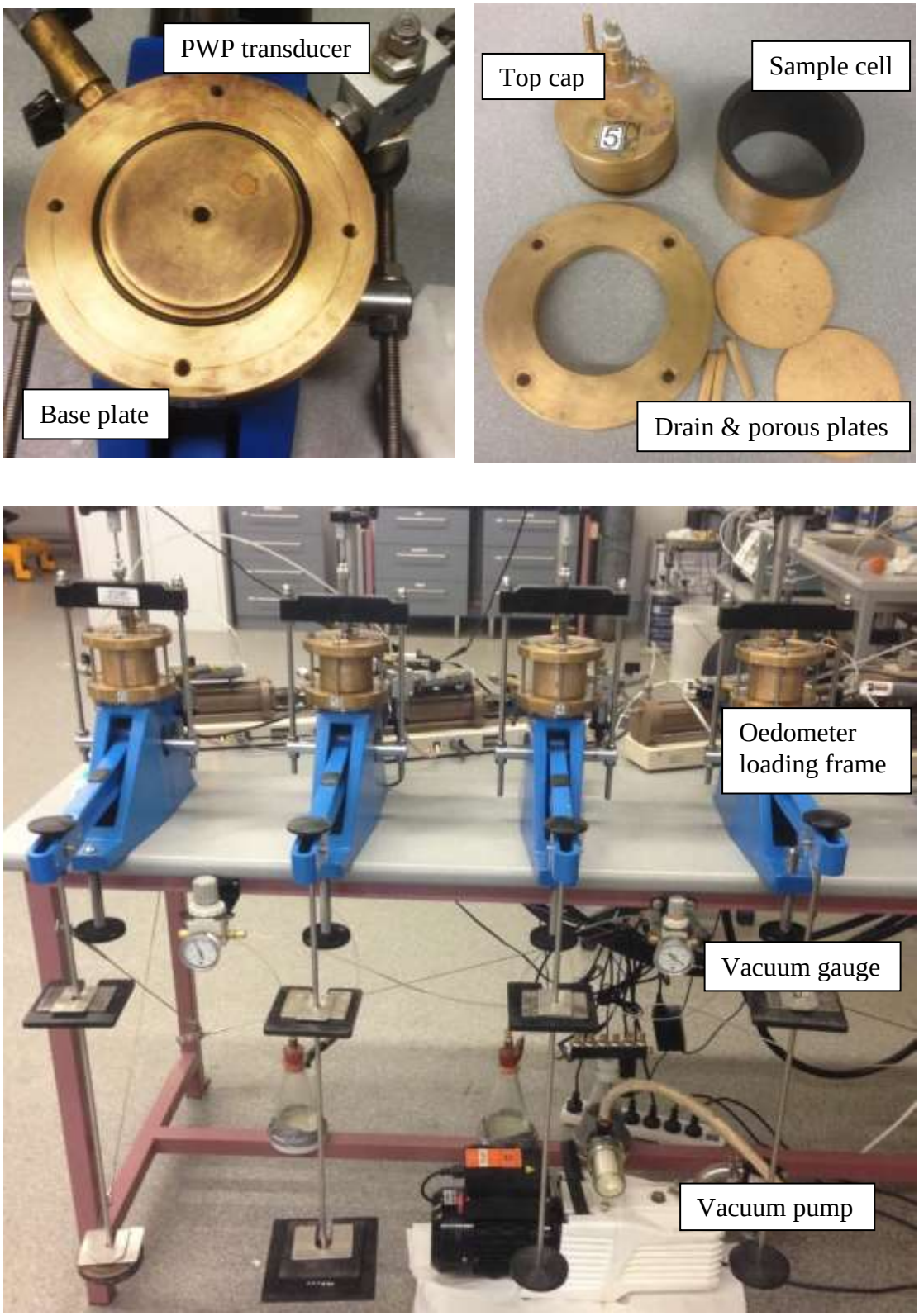

Figure 5.4: consolidometer setup for vacuum preloading tests.

Because of the rigid top cap, any friction between the moving parts of the equipment should be minimised, and this was achieved via the following methods. The inside of the sample cell was coated with thin and even layer of Teflon, and then a purpose designed low friction ring seal was attached to the top cap. This seal will prevent air from entering the sample cell while a vacuum is being applied, and also avoid any water leaks during radial consolidation tests without a vacuum pressure acting as two way seals, which they were specially designed to minimise friction. Another seal was inserted in the interface cavity in the top cap in the vertical drain to stop any friction arising from possible contacts, and also prevent any soil being squeezed from the hole in the impermeable plate. A porous, sintered bronze disk was placed at the midpoint between the drain and the cell boundary in the bottom plate, and then connected to a pore pressure transducer to measure the pore water pressure during consolidation.

The sample cell was pushed towards the bottom plate using a top ring and screw system and an O ring seal, to ensure there would be no leaks between the bottom plate and sample cell. After preparing the sample, the consolidation cell was mounted in a conventional oedometer loading arm and then loaded using dead weights, as shown in Figure 5.4. A displacement transducer was attached to the top of the top piston to measure the vertical settlement during consolidation. Before the consolidation tests commenced, the equipment was calibrated and all the seals were tested by pressurising de-aired water poured into the sample chamber. The water was pressurised by adding dead weights to the oedometer arm and measuring the actual increase in pore pressure using the pore pressure transducers. This would ensure that the load applied by dead weights had transferred entirely onto the sample during consolidation. A vacuum pressure was supplied using the laboratory vacuum pump

rated for continuous running while the applied pressure was controlled by a vacuum gauge connected between the pump and the sample. To ensure the exact vacuum pressure was applied to the sample, two pressure transducers were connected to the vacuum line, in both sides of the sample, capable of measuring suction up to -100kPa. Settlement, excess pore water pressure, and the suction pressure values were monitored in real time by the GDS software interface, which also recorded and downloaded the experimental data.

5.4 Sample extraction and preparation for testing

Soil samples for consolidation test were obtained close to a test embankment built over a low-lying floodplain at Ballina, New South Wales, Australia. The sub-soil generally consisted of highly compressible marine clay inherent with very high compressibility and very low permeability. Over a couple of centuries sugar cane plantations have been a common feature in the surrounding area, thus the top soil contains an approximately 0.2m thick layer of recent organic materials that consist of decomposing sugar canes, below which lies a 1m thick silty clay alluvium that has been deposited during flood events, followed by a 9m thick soft estuarine, clay of high plasticity soft (dark brown). Below the very soft clay there is a 4m thick transition with increasing clay content, underlain by a 5m thick layer of fine sand, At the bottom is a Pleistocene layer of stiff to hard clay.

The embankment was stabilised using vertical drains and U90 piston samples were used to extract undisturbed samples with thin stainless steel tubes. The sample tubes were 700mm long, with an inside diameter of 85.9mm and a wall thickness of 1.96mm. Samples were collected at 500mm vertical intervals. The soft sub-surface soils were extracted using the piston sampler, and they were predominantly marine

soils containing some shells. The results interpreted via laboratory experiments on relatively small samples varied significantly because the consistency of the soil was affected by larger objects such as shells. The sample tubes were received at the University of Wollongong were immediately subjected to CT scan tests; some of the CT scan images are shown in Figure 5.5 below.

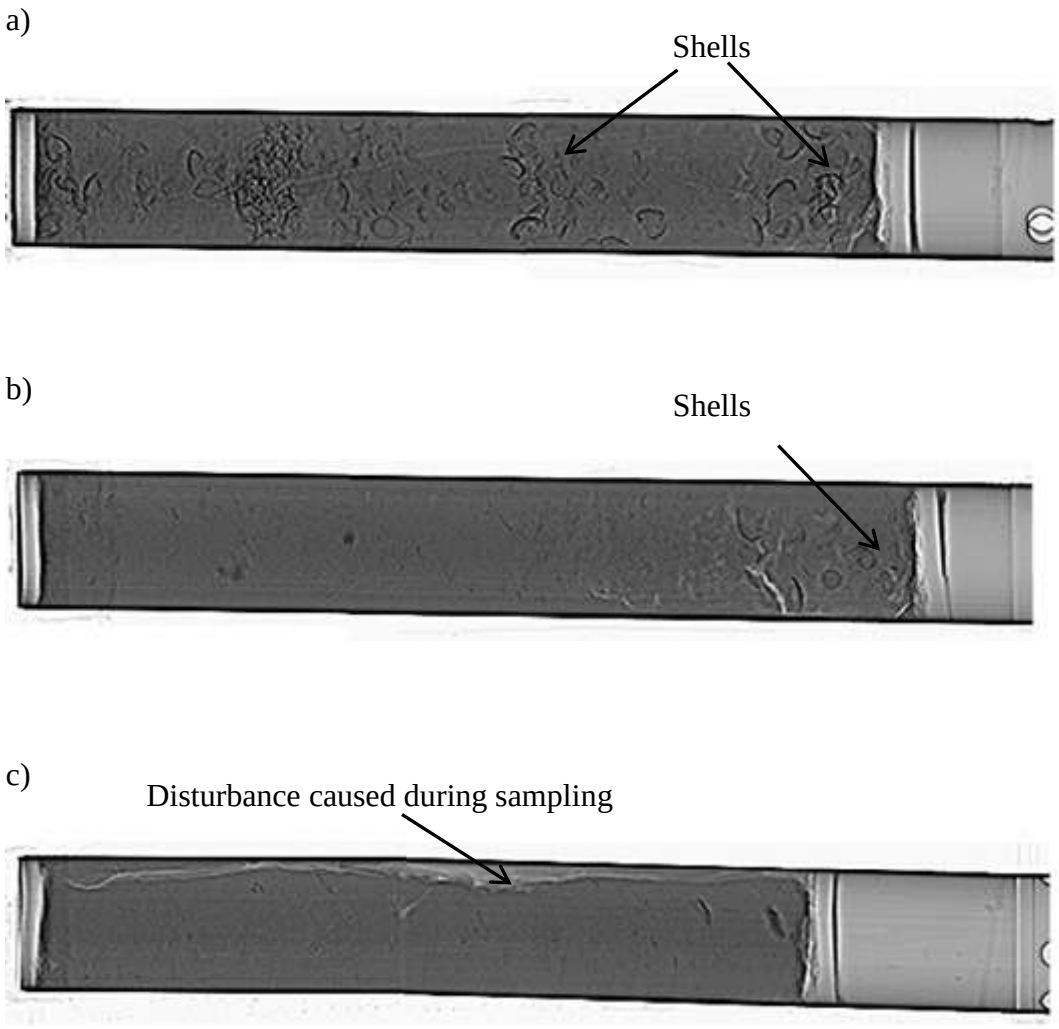

Figure 5.5 : CT scan results of sampling tubes extracted from the depths of a) 3.0-3.5m b) 5.0-5.5m and c) 6.5m-7.0m

The CT scan images proved very useful because they helped us to select the correct samples before cutting the sample tubes. Figure 5.5a shows that the soil extracted from depths of 3.0m to 3.5m contained large amounts of marine shells. Figure 5.5b shows that the samples obtained at 5.0m to 5.5m were in good condition, while Figure 5.5c shows that even though the samples obtained at depths of 6.5 m to 7.0 m were free of shells, they had been disturbed severely during sampling and thus were not suitable for undisturbed consolidation tests. The basic soil properties obtained from tube 5.5b are tabulated in Table 5.1.

Table 5.1: Basic soil properties

Parameter	**Value**
Liquid Limit, LL (%)	126
Plastic Limit, PL (%)	34
Plasticity Index, PI	92
Specific Gravity, Gs	2.58
Water Content, (%)	107.9
Void Ratio, *e*	2.784
Wet Unit Weight (kN/m^3)	13.9

For consolidation tests using an undisturbed sample it is imperative to extract the samples from the tube and then trim them and fit then into the consolidometer rings with minimum disturbance. The sampling techniques used are shown in Figure 5.6 a) to d)

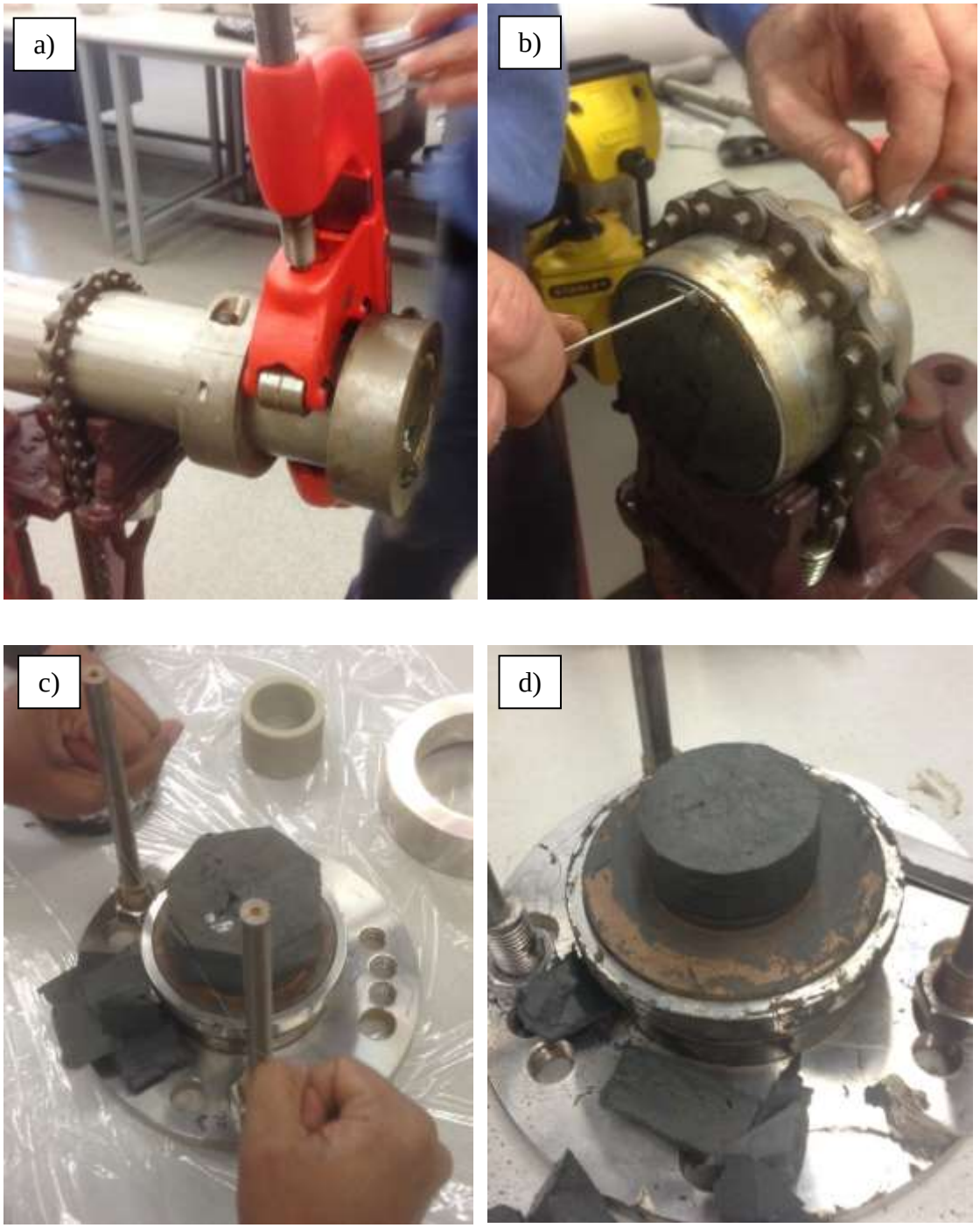

Figure 5.6 : Sample preparation for consolidation tests; a) sample tube clamped and cut using a pipe cutter; b) extracting the sample from the tube; c) Sample trimming; d) 50mm diameter sample trimmed for the oedometer test.

One sample tube had to be used in several tests so it was better not to extract the whole sample. Since the sample tube was very long, extracting the whole sample could create more disturbance as well. To minimise soil disturbance, the sample tube was held securely and the pipe cutter, which did not generate heat during cutting, was used to cut through the wall of the steel tube (Figure 5.6a). Two rigid, adjustable steel rings were attached to both sides of the pipe cutter to prevent the pipe from flexing and a sharp stainless steel cutting disc was used in pipe cutter to ensure smooth cutting. Once the tube was cut peripherally the specimen was sliced using sharp wire. Immediately afterwards, the remaining sample tube was removed, sealed with paraffin wax and placed in a humidity controlled room.

To obtain a 20 mm thick sample, a 40-50mm thick portion was cut from the sampling tube and then placed into the pipe vice. Because the sample adhered to the wall of the tube, a thin but strong wire was inserted through the sample, close to the tube, and then rotated around the internal periphery; this separated the sample and eased the extraction.

The sample was trimmed to the required diameter using a turning trimmer made at UOW; this device can trim samples to 70mm and 50mm in diameter. The extracted sample was placed on the trimming device and a wet, thin wire was used to slice the unwanted portions away while manually rotating the pedestal. This process is shown in Figure 5.6c, while the 50mm diameter trimmed sample is shown in Figure 5.6d. The samples were then fitted to the relevant consolidation rings and transferred to the loading apparatus for consolidation tests.

5.5 Oedometer tests to study compression behaviour of Ballina clay

Oedometer tests were carried out on samples obtained from depths of 5.0 – 5.5m. Samples were prepared as described in section 5.4 and a trimmed vertical consolidation sample is shown in Figure 5.6d. An initial seating pressure of 3.12 kPa was applied to the sample after it was fitted to the oedometer apparatus, and then this load was doubled until the stress reached 800 kPa. Vertical settlement was measured at each loading step with dial gauges attached to the top of the oedometer.

Variations in the void ratio with effective stress for the samples extracted vertically and horizontally are shown in Figure 5.7a; the results indicated that the vertical sample had more resistance to compression within the over-consolidated region than the horizontally extracted samples. This may be due to the effects of particle orientation during the deposition of clay. In the vertical sample, the yield point was more prominent and the yield stress was higher than in the horizontal sample and the compressibility was also higher next to the yield point. However, as the effective stress increased, the compression curve for the vertical sample converged to the other curve. This behaviour was also observed by Parry & Nadarajah (1974). The variation of the coefficient of secondary consolidation (c_α) with effective stress is plotted in Figure 5.7b, and it shows that the c_α variation pattern is the same in both samples. In the over-consolidation region, c_α was very small and it would significantly increase the onset of soil yielding, but as the effective stress increased it seemed to flatten out to a relatively constant intermediate value. In the normally consolidated region, the ratio c_α/c_c where c_c is the coefficient of compressibility was about 0.4 and was relatively constant, as previously demonstrated by Mesri & Godlewski (1977) for an array of soils.

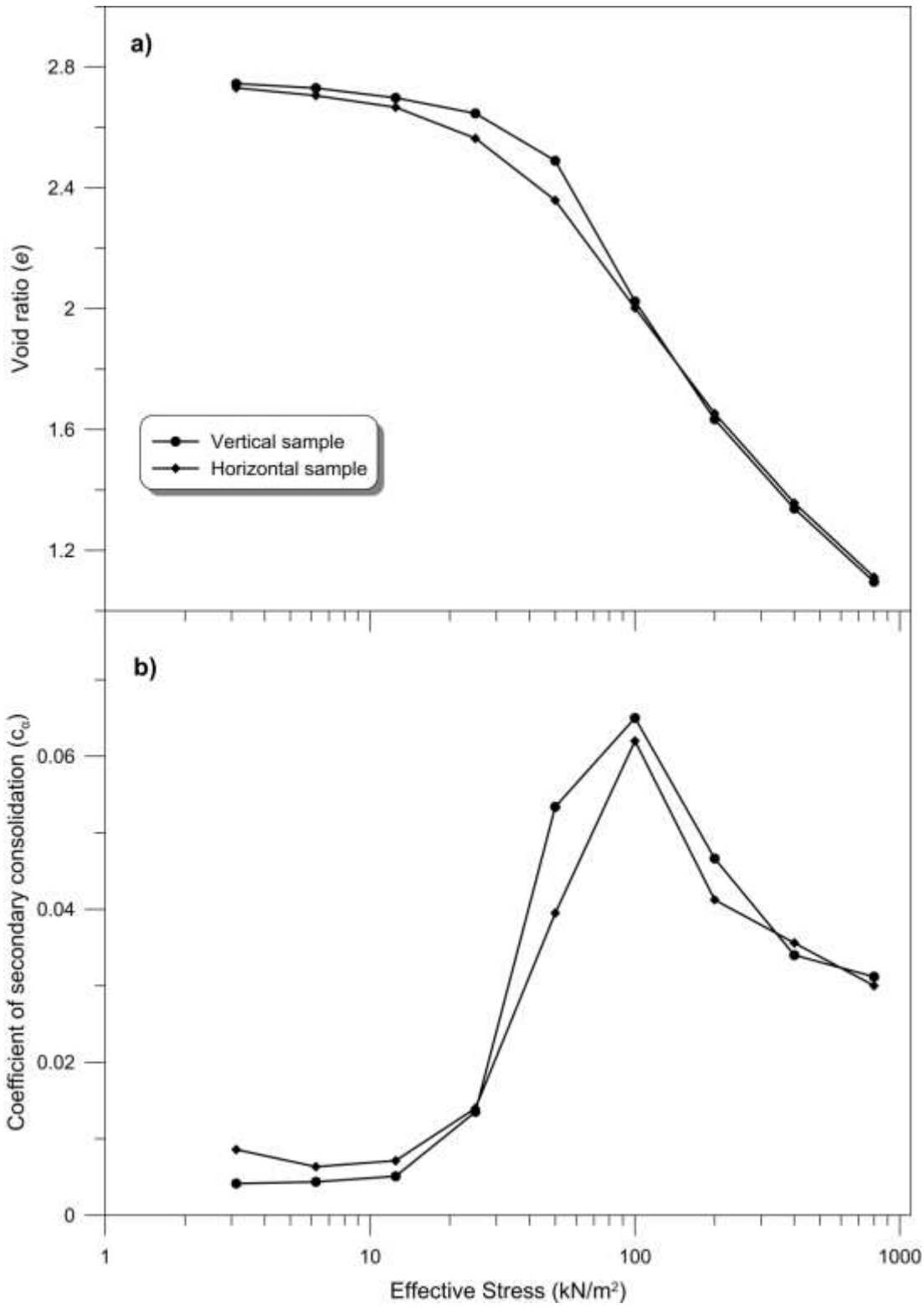

Figure 5.7: Variation of a) the void ratio, and b) the coefficient of secondary consolidation with effective stress, in the vertical and horizontal samples.

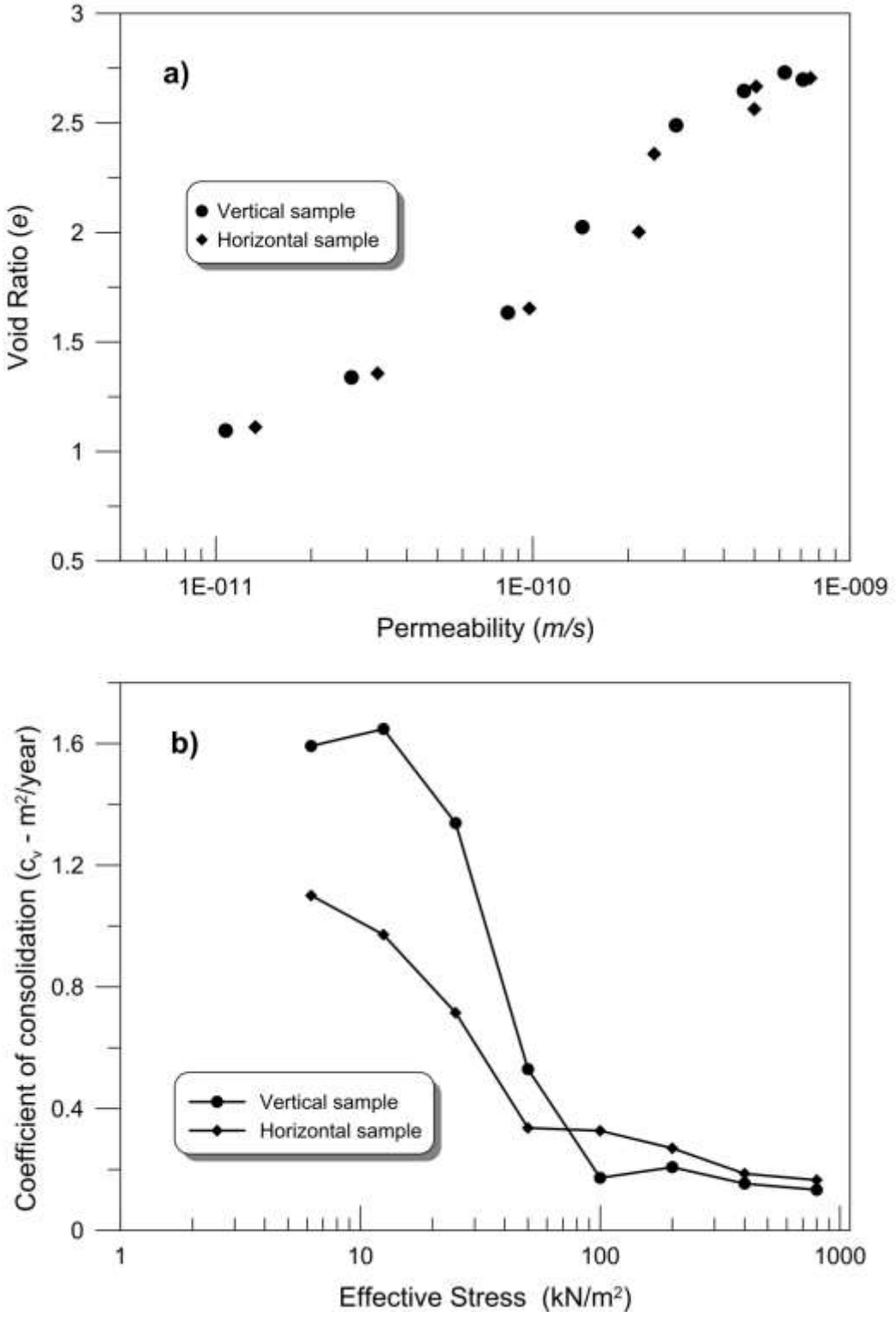

Figure 5.8 : Variation of a) Permeability with void ratio, and b) the coefficient of consolidation with effective stress, in the vertical and horizontal samples.

The variation in permeability with a reducing void ratio, and the change in the coefficient of consolidation with effective stress are shown in Figure 5.8. The vertical and horizontal permeability values were calculated using the Terzaghi consolidation theory, and the coefficients of consolidation were obtained using the Casagrande log-time method. Anisotropic permeability can be observed from the values obtained in the normally consolidated region, the ratio between the horizontal and vertical permeability was 1.20, whereas the values obtained in the over-consolidated region were inconclusive. As expected, the coefficient of consolidation was also higher in the normally consolidated region for the horizontal sample, compared to the vertical sample, even though both samples were obtained adjacent to each other and the identical extraction and trimming method was used in preparing the samples.

5.6 Vacuum consolidation tests performed using remoulded Ballina clay

To investigate how the inward lateral strains effect consolidation due to vacuum preloading, experiments were carried out using remoulded Ballina clay. First, a small amount of clay was scooped out from the sampling tube and the moisture content was measured. Generally, samples prepared for remoulded consolidation tests usually have water added, so that the sample attains a moisture content that is twice the liquid limit of the clay. However, the sample of Ballina clay was highly plastic and the in-situ water content was very high, so to save time and limit the settlement, the pre- consolidation clay was mixed with water to a moisture content of 1.5 times the liquid limit. At that moisture content, the soil was like a slurry and all the shell particles and small incompressible lumps could be removed. The clay sample was then mixed in with the laboratory soil mixture and transferred

to a vacuum apparatus to remove any air entrapped in the sample. The sample was then poured into air tight bags and left in the humidity controlled room for a minimum of 48 hours.

The clay sample was poured directly into the consolidation cell and then stirred well to remove any entrapped air. Then the top cap was attached, the consolidation cell was connected to the oedometer loading apparatus and a pre-consolidation pressure of 17.3 kPa was applied to the sample. Consolidation settlement and variations in excess pore water pressure were monitored, and once the primary consolidation was completed, the sample was removed from the apparatus and the sample cell was connected to the special platform previously used to trim the undisturbed samples. The base of the sample trimmer was exactly the same as the base of the consolidometer; a 6mn hole was made in the centre of the sample by pushing a thin walled steel tube guided by a plastic mould to ensure vertical penetration. The sample was attached to the consolidometer again, and the sintered bronze drain was then inserted and fitted to the base plate through the pre- drilled hole in the sample. The previous pre-consolidation pressure of 17.3 kPa was applied again to check whether the inserted drain had created any further settlement due to disturbance and after about one hour the pre-consolidation pressure was increased to 34.6 kPa and the sample was allowed to consolidate radially (Figure 5.3 & 5.4).

Once primary consolidation was completed, a total consolidation pressure of 80 kPa was applied to the sample using vacuum pressure, a surcharge pressure, and a combination of both. First, top drainage valve was closed and a surcharge load was applied to the sample until the pore water pressure increased at least 90% of the total pressure applied. After that the vacuum pressure was applied to the sample and the

pore pressure and vertical settlement were recorded. Five different vacuum surcharge ratios (*VSR*) were used in the experimental program, with the applied vacuum pressures varying from 0 kPa, 20 kPa, 40 kPa, 60 kPa, and 80 kPa; these resulted in *VSR* values of 0, 0.25, 0.50, 0.75, and 1, respectively. In the first four tests, an additional surcharge load was also applied to make the total consolidation pressure 80 kPa. The vacuum pressure was measured at the top and bottom of the drain to ensure an accurate vacuum pressure application. The variations of vertical settlement and pore water pressure are shown in Figures 5.9 and 5.10, respectively.

Figure 5.9 shows that with an increasing vacuum surcharge ratio (*VSR*), the total vertical strain decreases. When the sample was removed from the consolidation cell it was apparent that it had separated from the wall due to an inward moment caused by isotropic consolidation due to vacuum preloading. When the final void ratio (Figure 5.10) was measured, it was similar in all the samples, confirming that the volumetric strains induced by the both methods were the same (Chai et al., 2005). Figure 5.9 (b) shows the normalised vertical strain variation with the VSR. Normalised vertical strain is defined as the ratio between vertical strains to the vertical strain at the end of primary consolidation (EOP), as calculated by the Casagrande method. As observed from Figure 5.9 all the curves were confined in a thin band, although the strain plotted here was only in a vertical direction as no lateral strains could be included. By inspecting the time taken for EOP, it was oblivious that as the vacuum pressure increased, so too did the rate of consolidation; this was also clear in the pore water pressure plots shown in Figures 5.10a and 5.10b. However, the degree of consolidation obtained using the settlement data was higher than that obtained by the pore pressure data at any given time.

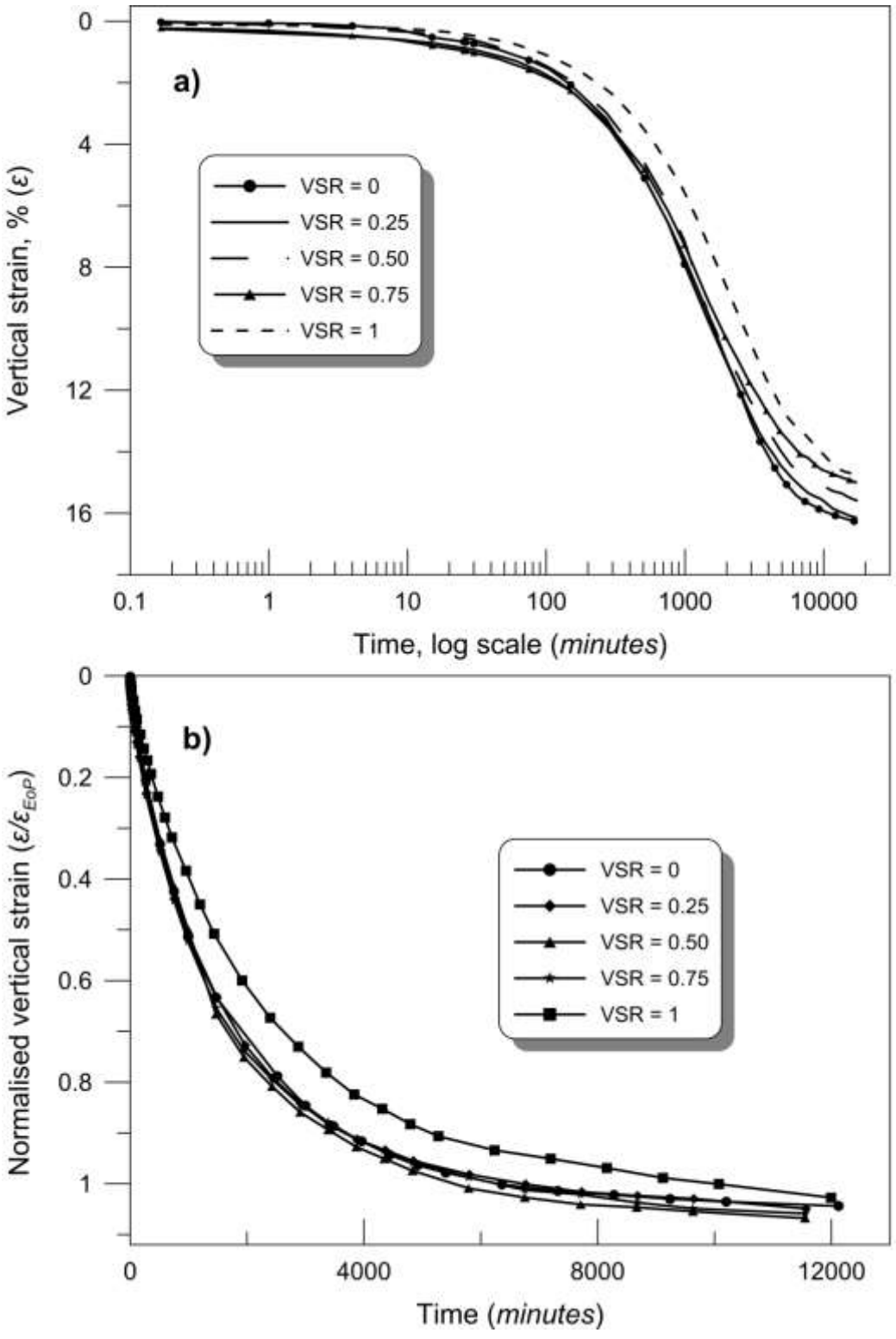

Figure 5.9 : a) Vertical strain, and b) Normalised vertical strain, variation with *VSR* in remoulded Ballina clay.

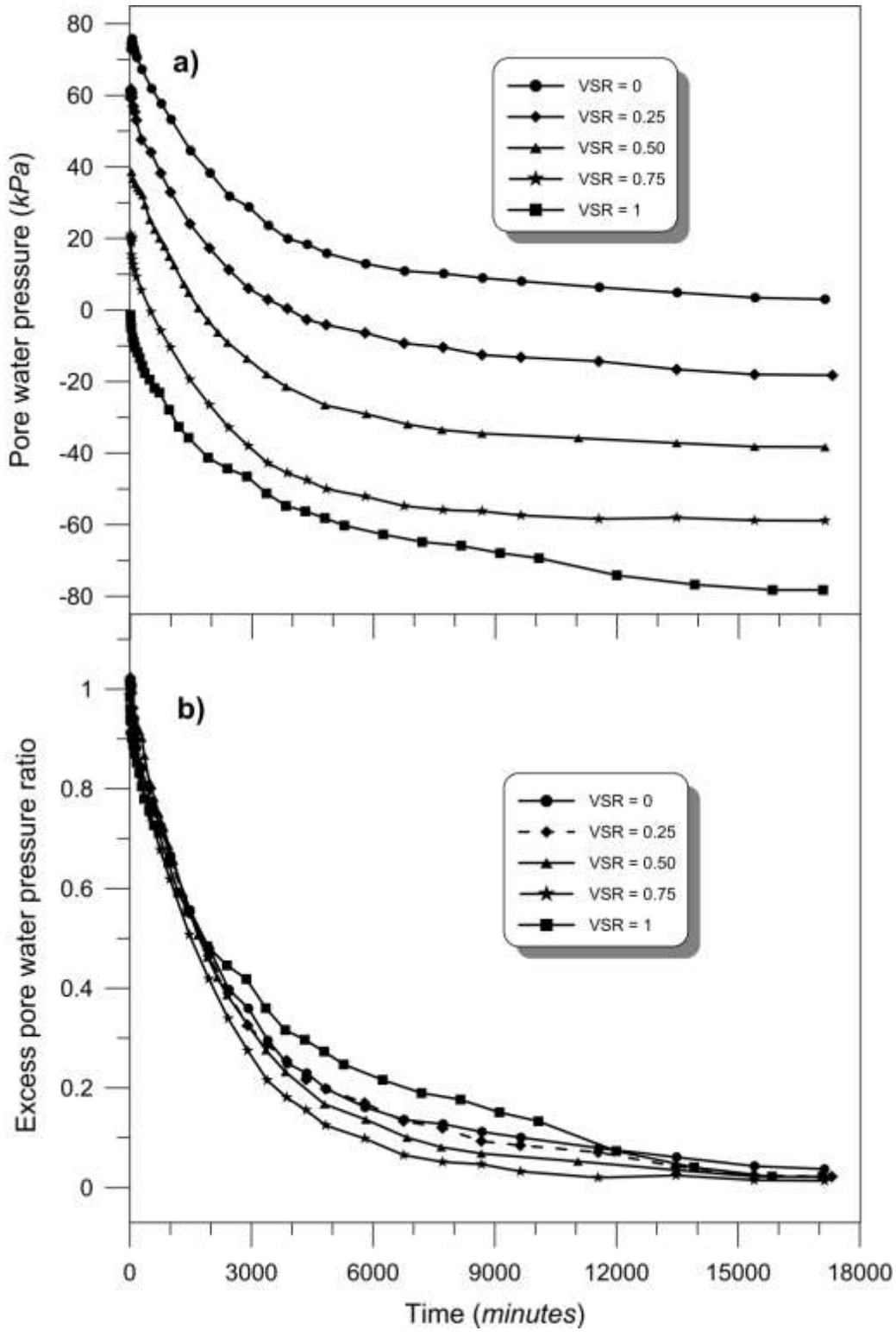

Figure 5.10 : a) Pore water pressure, and b) Excess pore pressure ratio, variation with *VSR* in remoulded Ballina clay.

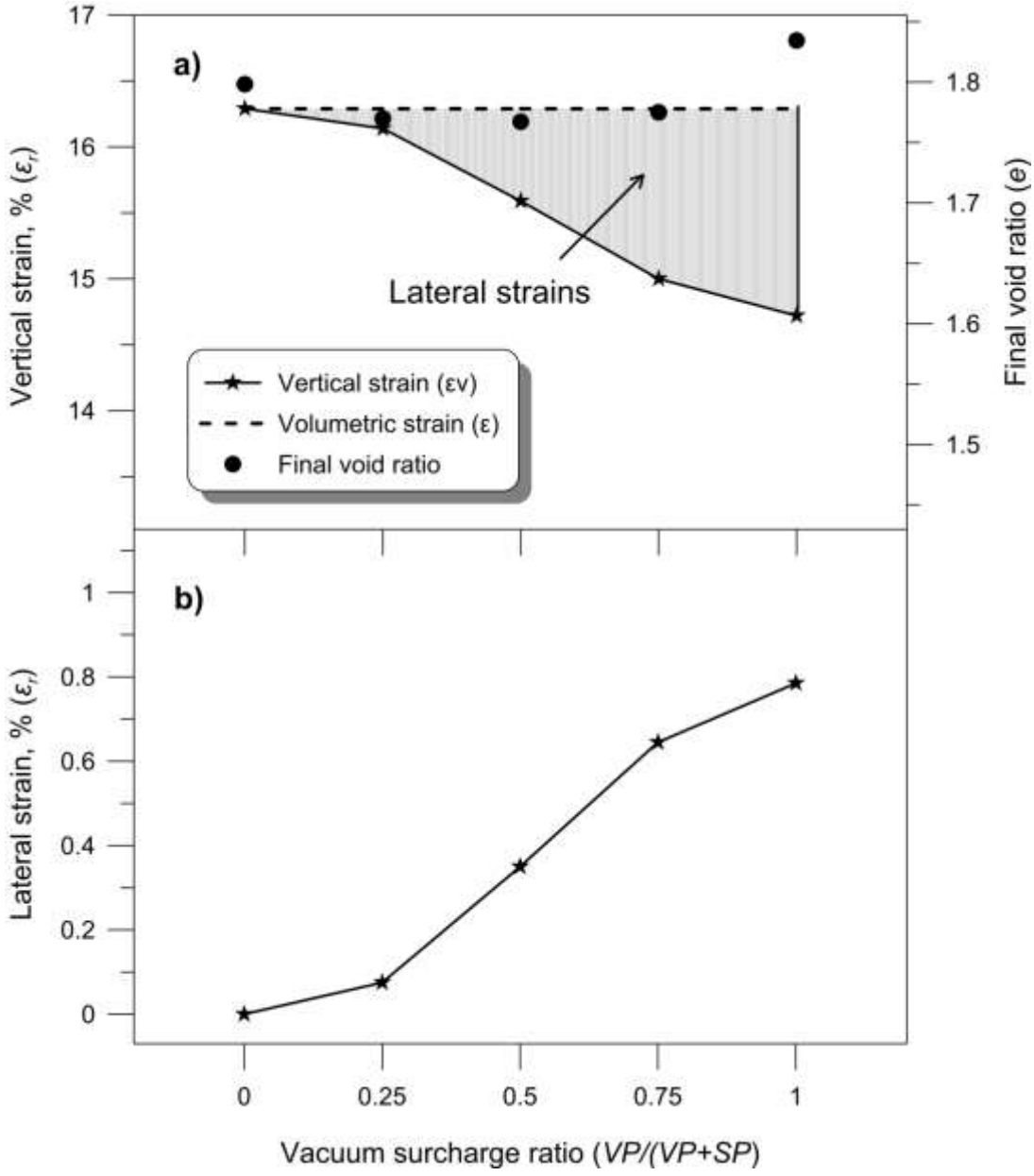

Figure 5.11: a) Vertical strains and final void ratio, and b) Lateral strain, variation with varying *VSR* in remoulded Ballina clay.

Figure 5.11a shows the variation of ultimate vertical strain with *VSR* applied in the enlarged graph for clarity. Since the soil was consolidated to a similar volumetric void ratio at the end of the test, it was assumed that the total volumetric strain in all

the experiments with different *VSR* was the same. Lateral strain was obtained using the following expression and was plotted with varying *VSR* in Figure 5.11b.

$$\epsilon_{volumetric} = \epsilon_{vertical} + 2 \times \epsilon_{radial} \quad (5.1)$$

Indraratna et al., (1997) investigated the settlement and lateral strains of two full scale embankments built over soft clay, and a dimensionless parameter α was defined as the ratio between the maximum lateral displacement at the toe to the maximum settlement at the centre of the embankment. This ratio was found to be 0.185 for the embankment stabilised by sand compaction piles, 0.141 for the Geogrid + vertical drains installed at 2.0m spacing square pattern, and 0.123 for the vertical band drains in a triangular pattern at 1.3m spacing respectively. A similar α value was also calculated for the data presented here, and the values for the inward lateral movement over maximum vertical settlement are 0.187, 0.151 and 0.079 for *VSR* values of 1, 0.75 and 0.5, respectively. The values obtained for a *VSR* of 0 and 0.25 were not considered because the outward lateral movement which would occur was restricted by the confined cell used in the laboratory. The diameter of the sample was 70mm and its initial height was 20.6mm.

5.7 Vacuum consolidation tests performed using undisturbed samples

The same experiments described in Section 5.6 were repeated using samples of undisturbed Ballina clay that were extracted between 5.0-5.5m below from the ground surface. The water table was 0.3m below the surface and first two metres of clay consisted of weathered, over-consolidated clay with a density of 18 kN/m^3 followed by soft compressible clay with a bulk saturation density of 14.5 kN/m^3. The average effective overburden pressure was estimated to be 34.6 kN/m^3 and the

vertical pre-consolidation pressure of 38 kN/m^{3}was obtained using the compression curve given in Figure 5.7, which was very close to the effective overburden pressure. Therefore, the clay can be considered as normally consolidated marine clay. The method used to extract and prepare the sample is described in Section 5.4, and the loading sequence and the experimental plan were similar to the tests described in Section 5.6, although the drain was installed before preloading step 1 instead of after applying a pre-consolidation pressure of 17.3 kPa. The sample with a drain fitted before the consolidation test commenced is shown in Figure 5.12. Variations in the vertical strains and pore water pressure are shown in Figures 5.12 and 5.13, respectively. Since the samples obtained from the ground have more variations than the remoulded samples, the results were not as conclusive as they were in the previous case, although the vertical strain had generally decreased as the vacuum pressure increased.

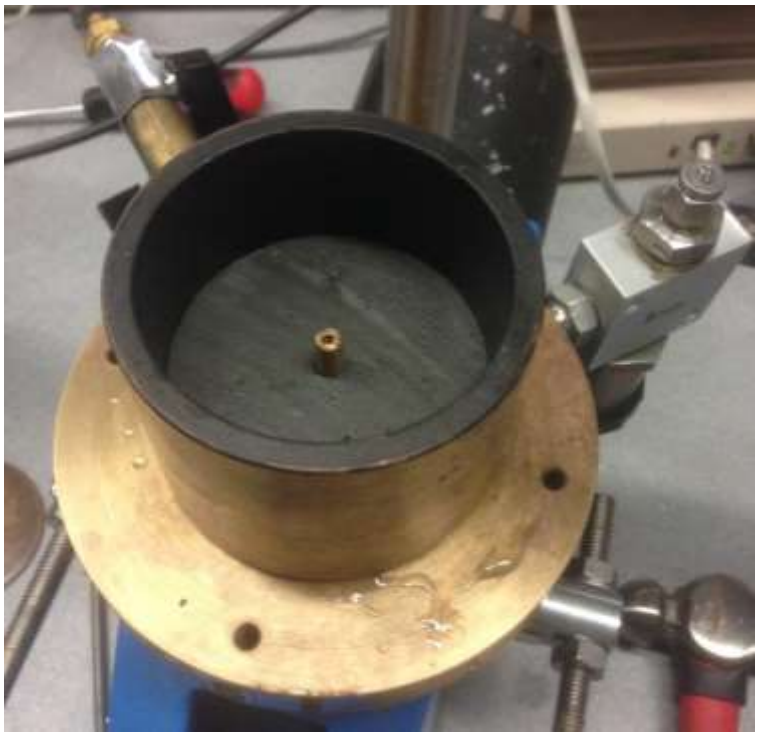

Figure 5.12 : Drain installed undisturbed sample before starting consolidation.

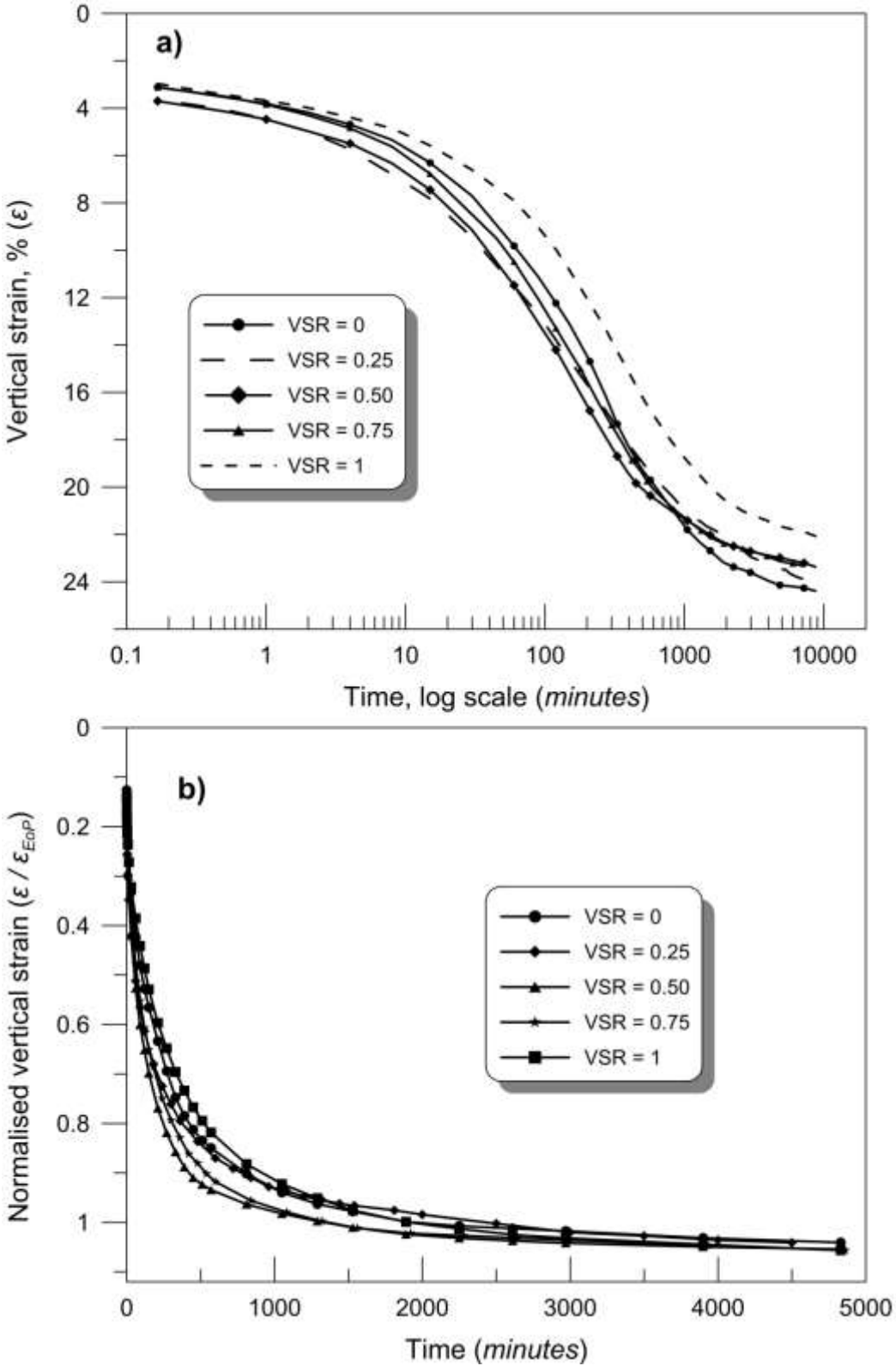

Figure 5.13 : a) Vertical strain; b) Normalised vertical strain; variation with *VSR* in undisturbed Ballina clay

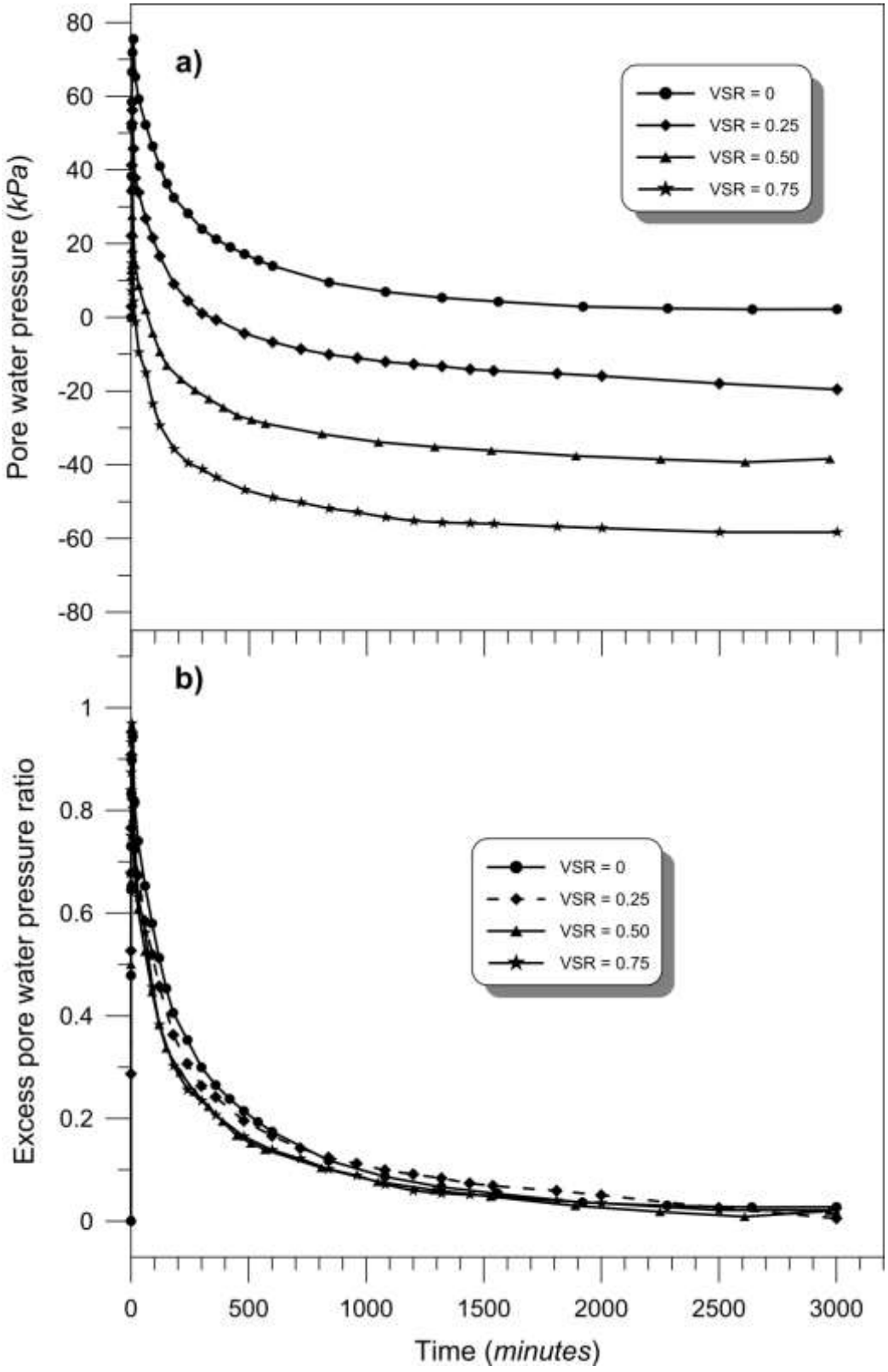

Figure 5.14 : Pore water pressure; b) Excess pore pressure ratio; variation with *VSR* in undisturbed Ballina clay

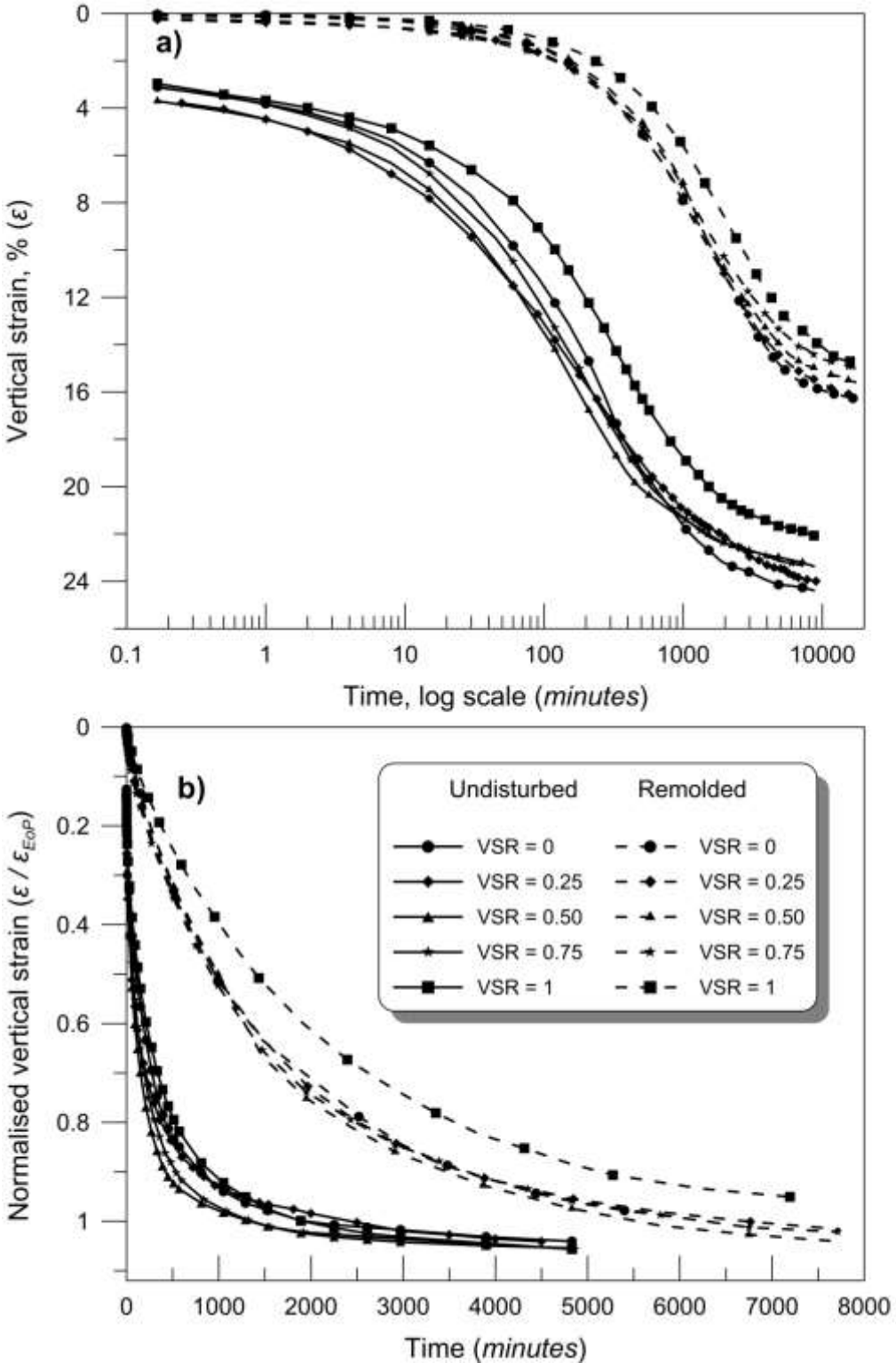

Figure 5.15 : a) Vertical strain; b) Normalised vertical strain; variation with VSR in undisturbed and remolded Ballina clay

Since the permeability of the in-situ samples was much higher than the remoulded samples, primary consolidation was completed quickly. Normalised settlement and pore water pressure plots indicated that vacuum pressure enhanced the rate of consolidation. An attempt was made to investigate the secondary consolidation behaviour with vacuum pressure. Despite the slight reduction observed in secondary consolidation settlement, when the vacuum pressure was increased beyond VSR value of 0.5, it was not conclusive and was not representative of the coefficient of secondary consolidation determined. It is suggested that a consolidation test be carried out with a thicker undisturbed sample to compare the small settlements associated with secondary consolidation for better reliability. The reason for this hypothesised behaviour could be the change in the shape of the consolidation curve due to the enhanced rate of the consolidation attributed to the vacuum pressure. Figure 5.15 shows the variation in vertical strain and normalised vertical strain between undisturbed and remolded samples.

5.8 Summary

A new consolidometer was designed and built at UOW to conduct vacuum preloading tests with vertical drains. It shared common features with a conventional oedometer and the more sophisticated Rowe cell. Consolidation tests were carried out for both remoulded and undisturbed samples obtained from a soft clay site in Ballina. An improvised method was used to extract and prepare undisturbed samples for the consolidation tests. The tests revealed that vertical settlement was reduced when the vacuum pressure ratio was increased, possibly due to the inward movement created by the isotropic consolidation of vacuum preloading. By assuming same volumetric strain, the amount of lateral strain observed with varying vacuum

surcharge ratios was estimated, and an empirical ratio of maximum lateral strains to the maximum vertical strains with varying *VSR* was presented.

Variation in vertical strain and the normalised strain between the in-situ undisturbed soil and remolded soil is clearly seen in Figure 5.15. It can be observed that undisturbed soils are subjected to more settlements compared to remolded soils made of same materials and loaded with same stress range. Rate of consolidation is also higher in undisturbed samples due to higher in-situ permeability.

Chapter 6 Application to Case history

6.1 Ballina bypass road embankment

6.1.1 Introduction

The Pacific Highway runs along the eastern coast of Australia between Sydney and Brisbane. To reduce traffic congestion in the busy town of Ballina, situated along the Pacific highway, an alternate bypass was built over a low lying flood plain, consisting of very soft and compressible marine clay up to 30m thick in some locations (Indraratna et al., 2009; Indraratna et al., 2012). Due to the low shear strength of the underlying soft clay, the time required to stabilise the embankment with vertical drains and step loading took longer than the allowed construction period. Moreover, the use of other ground improvement methods such as soil mixing, pile embankments, and stone columns were not considered because of high cost associated with the deep layers of soil that would be encountered. Preloading the embankment using a surcharge load and vacuum pressure with vertical drains was

the ground improvement method chosen, because, it allowed for rapid embankment construction and was more economical than the other methods. This was the first time that vacuum pressure was used successfully in Australia in a ground improvement project (Kelly & Wong, 2009).

6.1.2 Site characteristics

According to Kelly et al. (2008), the soil underlying the trial embankment consisted of uniform layers of soft to firm estuarine and alluvial clays above residual soils and bedrock. The soft clay varied in thickness from almost zero to a maximum depth of 25m close to the southern approach to Emigrant creek. The clay under the vacuum preloading embankment was almost 25 metres thick. The basic soil parameters used in the analysis and shown in Figure 6.1 were extracted from Indraratna et al. (2012). The 25m thick soil deposit was divided into four distinct layers to obtain an accurate prediction of the consolidation responses. The original ground water table was observed at 0.2m below the surface.

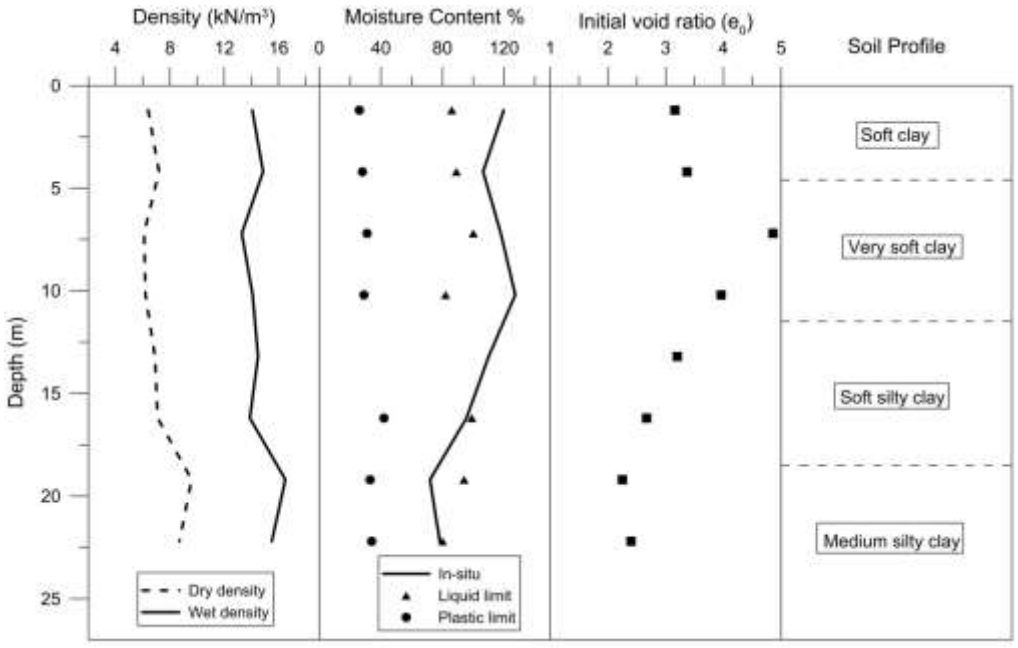

Figure 6.1 : General soil profile and basic soil parameters (Adopted from Indraratna et al., 2012)

Layer 1 is a grey colour, highly plastic clay (CH) that contains decomposing organic materials underlain by grey, highly plastic and very soft estuarine deposits with some traces of shells. A layer of mottled yellow- brown and grey, highly plastic soft clay with traces of sand sits below that, while the bottom layer is a mottled orange and grey, highly plastic clay that is less compressible as the amount of sand increases. The yellow mottles are due to the presence of acid sulphate constitutions or pyrites. The moisture content of the top three layers exceeded 100%, but this decreased to 80% in the bottom layer. The liquid limit of soils is generally between 80-100% and the plastic limits are between 30-40%. The strength and compressibility of these soils are shown in Figure 6.2 below.

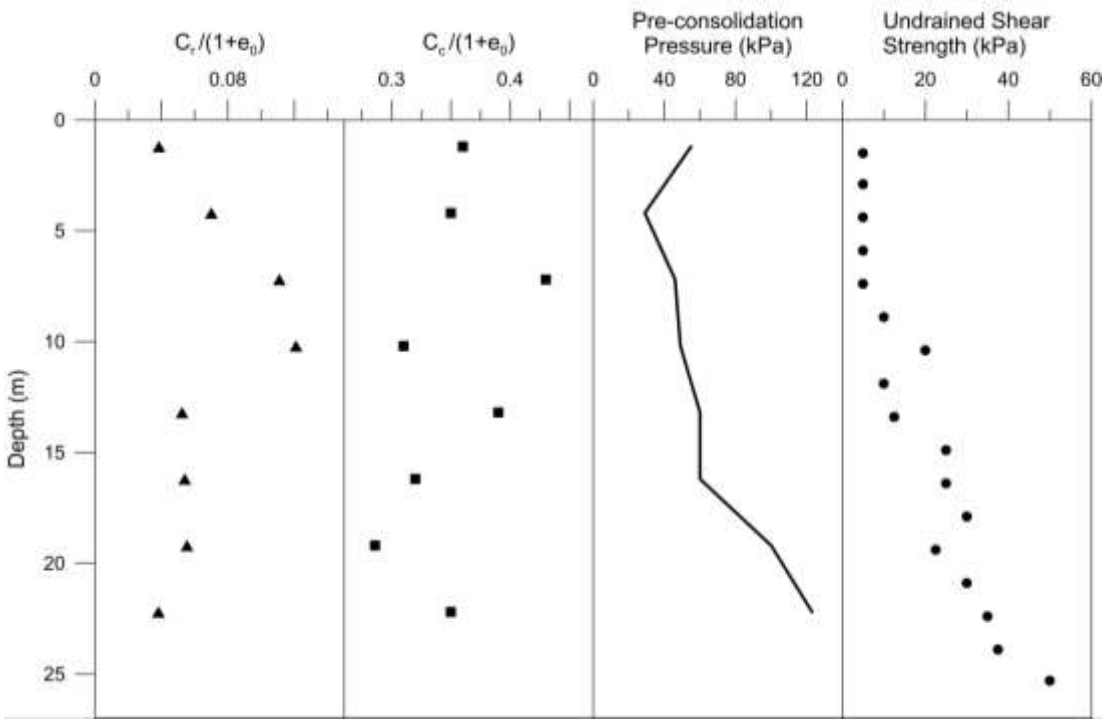

Figure 6.2 : Average Compressibility and strength parameters of Ballina clay

(Adopted from Indraratna et al., 2012)

The Ballina clay was fully saturated and had very low undrained shear strength. The values recorded from field shear tests were between 0-40 kPa. The top layer of soil displayed a higher pre-consolidation pressure, possibly due to a crust at the top that was created by changes to the water table and suction from the tree roots. The underlying layers were almost normally consolidated, while the small amount of over consolidation was due to the delayed consolidation experienced after the clay was deposited. The compressibility values were adopted from Indraratna et al. (2012) and checked with the laboratory oedometer tests performed using samples of undisturbed Ballina clay. The bottom layer showed less compressibility but a higher shear strength and low initial void ratio than the layers above.

6.1.3 Drain installation and embankment construction

According to Kelly & Wong (2009), to limit the post-construction settlement to 50mm, it was estimated that a total surcharge thickness of 11.2m was required, assuming that the density would be 20 kN/m^3. To shorten the construction time and enhance the stability of the embankment, vacuum preloading with conventional surcharge was used. To shorten the drainage path and also distribute the vacuum pressure to the lower layers of clay, 34mm diameter vertical drains were installed at a spacing of 1m in a square pattern using a wick drain rig with a 110mm square base plate. Drains were installed to a total area of 9500m^2 that was then divided into two sections with a vacuum preloading zone (section A), and a non-vacuum section B. The plan of the embankment is shown in Figure 6.3, the section of the embankment with SP1 and SP2 settlement plates and a P1 pore pressure transducer was only treated with a conventional surcharge, while the area between SP3 and SP4 (settlement plates) and the I5 and I6 (inclinometers) were treated with both surcharge and vacuum pressure. The underlying layer of soft soil varied in thickness over the

length of the embankment while the variation below each settlement plate was extracted from Indraratna et al. (2012) and presented in Table 6.1. The thickness of the layer of soft soil below settlement plates SP11 and SP12 was the maximum encountered, so an 8.5m surcharge embankment combined with 70kPa vacuum pressure was proposed to improve this ground section.

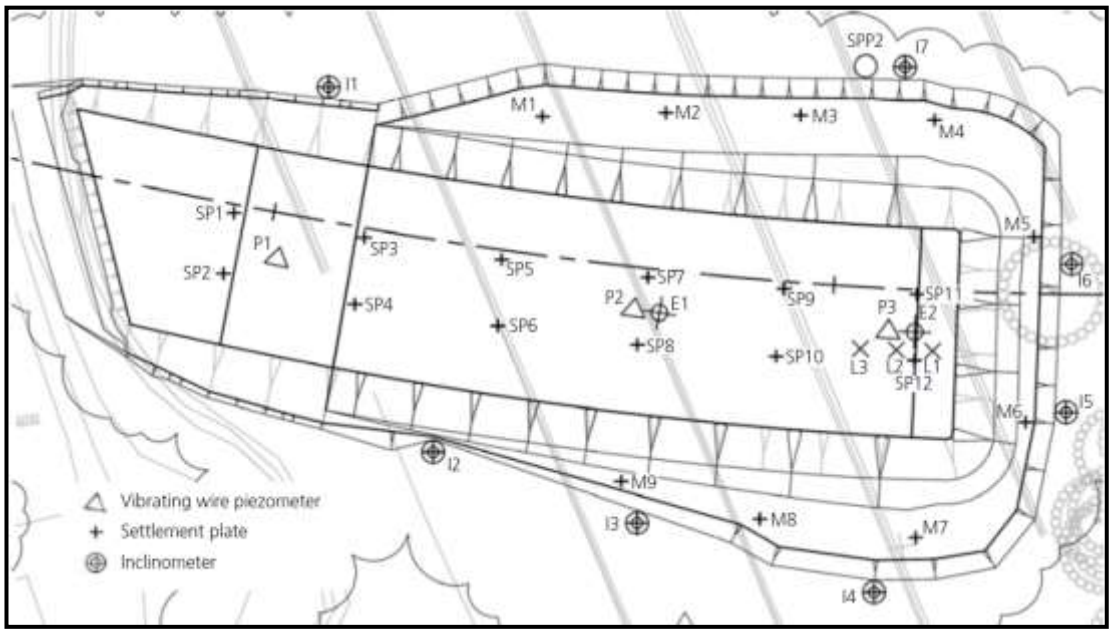

Figure 6.3: Plan view of the embankment and Instrumentation layout

Table 6.1 : Bottom level of soft soil beneath each settlement plate

Settlement Plate	SP 1 SP 2	SP 3 SP 4	SP 5 SP 6	SP 7 SP 8	SP 9 SP 10	SP 11 SP 12
Bottom level (m)	2.7-6.7	6.7-9.7	9.7-11.7	11.7-14.7	14.7-17.7	17.7-24.7

Vertical drains 34mm in diameter and horizontal drains 50mm in diameter, along with a 1mm thick membrane were used in the area improved with vacuum pressure. The edges of the membrane were submerged into a soil-bentonite slurry

trench to eliminate any air leaks, while the vacuum pressure was applied. The horizontal and vertical drains were not connected to each other, so the hydraulic conductivity was provided by a sand blanket below the air tight membrane. All the construction details for the embankment were presented by Kelly et al. (2008) and are also summarised below in Table 3.2. The long delay between the installation of the drainage blanket and starting the vacuum pump was due to constructing treatment ponds adjacent to the area where the vacuum was applied.

Table 6.2 : Construction sequence of the embankment

Construction Stage	Start Date	End date	Duration (Days)
Construction of 1.5m sand drainage layer	8 Nov 2006	24 Nov 2006	16
install vertical and horizontal drains	13 Dec 2006	21 Dec 2006	8
Install instrumentation (I,E, P*)	11 Jan 2007	7 Feb 2007	27
Increase fill to 2.0 m	15 Jan 2007	2 Feb 2007	18
Placement of vacuum membrane	2 Feb 2007	7 Feb 2007	5
Place 0.3m layer of protective sand	7 Feb 2007	11 Feb 2007	4
Install Settlement plates	11 Feb 2007	11 Feb 2007	1
consolidation with vacuum preloading	2 Mar 2007	3 Dec 2007	276
Increase fill to 8.5m	19 Mar 2007	6 Jul 2007	109
consolidation without vacuum preloading	3 Dec 2007	11 Dec 2008	374
additional filling	11 Dec 2008	20 Feb 2009	71

* I- Inclinometer; E- Magnetic Extensometer; P- Vibrating wire piezometer

6.1.4 Embankment instrumentation and observed responses

Settlement plates (SP), permanent monuments (M), magnetic extensometers (E), inclinometers (I), vibrating wire piezometers (P), standpipes (SPP), Load cells (L) and vacuum pressure gauges were installed in the ground to record the consolidation responses; their locations are shown in Figure 6.3. Stage construction with ground settlement and excess pore water pressure observed in the embankment is shown in Figures 6.4 and 6.5 respectively.

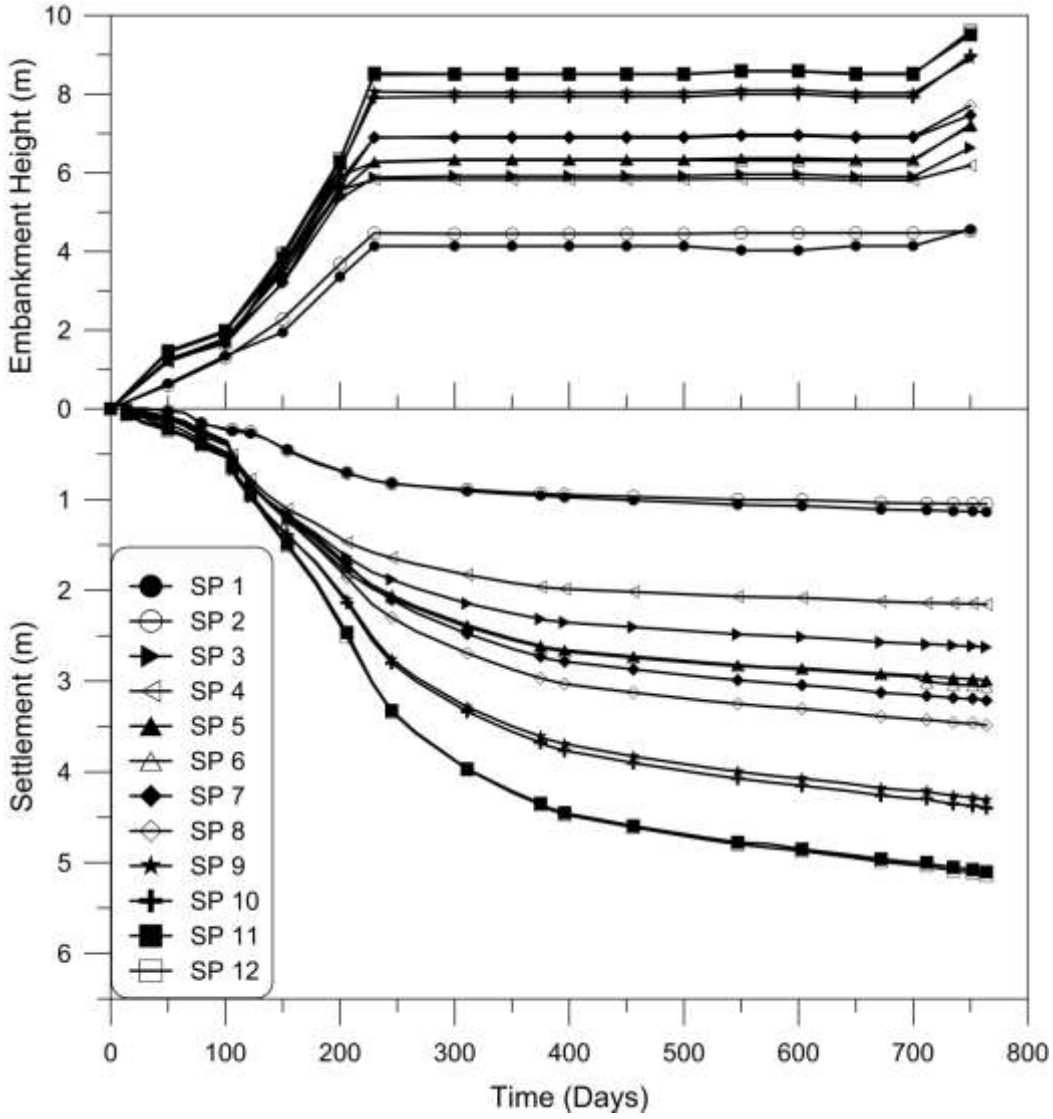

Figure 6.4: Construction stages for the embankment and settlements observed (adopted from Kelly & Wong, 2009)

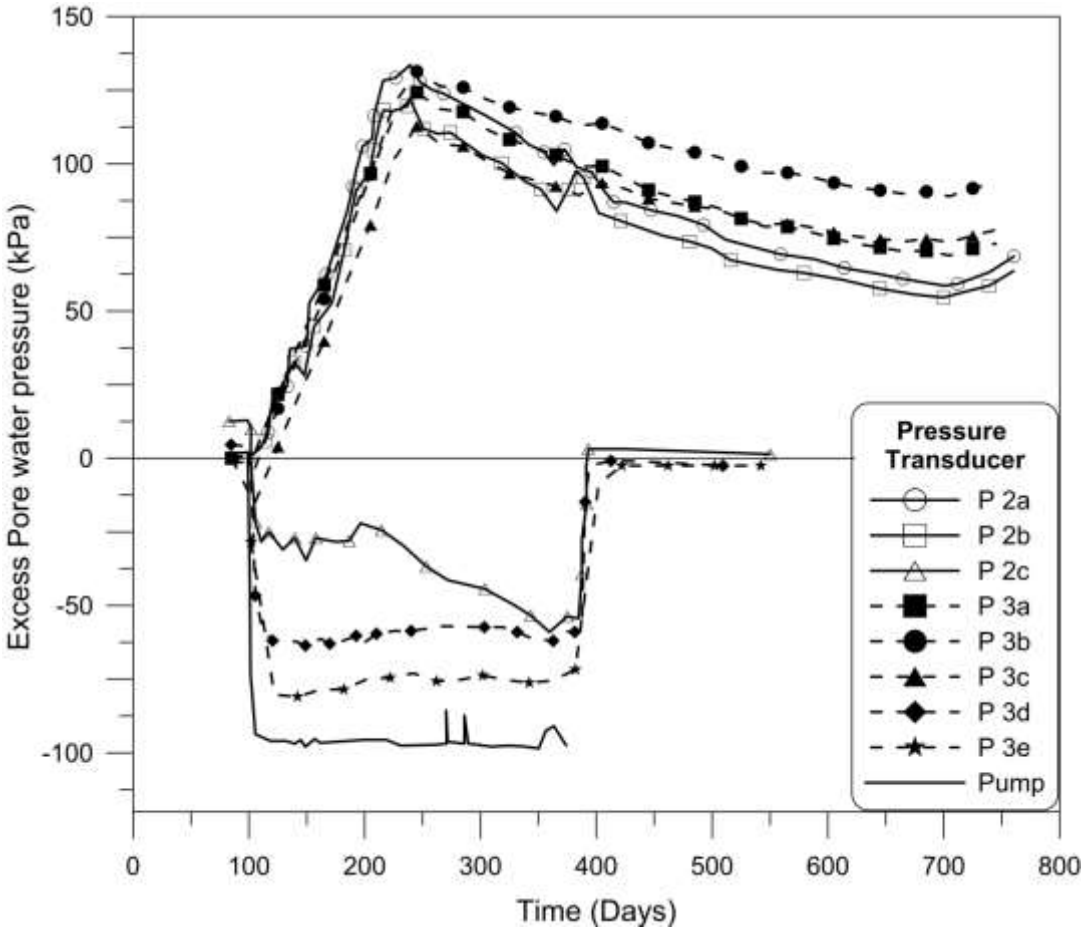

Figure 6.5 : Excess pore pressure distribution (adopted from Kelly & Wong, 2009)

The settlements recorded in SP1 and SP2 are related to the area where a vacuum pressure was not applied to the ground, while the results of the other 10 settlement plates represent the section where a surcharge and vacuum pressure in tandem was applied to improve the ground. The different final settlement value was attributed to the different thickness of compressible subsoil and the surcharge load applied to it. Settlement data began to be recorded on 20th of November, so some initial consolidation settlement was not included in the readings.

Three Pore water pressure transducers were installed close to settlement plates SP7; P2a was installed 8.3m below the surface, P2b was installed 4.8m below the

surface, and P2c was installed 1.3m below the existing ground level. Another four pore pressure transducers were inserted close to SP11; P3a was installed 11.8m below the surface, P3b was installed 8.3m below the surface, P3c was installed 4.8m below the surface, and P3d was installed 1.3m below the surface. All seven pore pressure transducers were installed at the centre of the square drain installation pattern to obtain the highest pore pressure in the layer of clay. Another pressure transducer (P3e) was installed inside a vertical drain 18.3m below the ground level to study vacuum propagation along the depth of the drain.

The pressure measured at the vacuum pump was a constant -98 kPa, except in several instances where the pumps ran out fuel. That was the maximum possible suction that could be generated with a vacuum pump, however, the suction pressure measured below the membrane was -80kPa, but decreased to -70 kPa before the vacuum pump was switched off. This was closely matched by the pressure transducer connected inside the drain (P3e); it confirmed that the full vacuum pressure applied inside the membrane was transmitted to the lower levels of the drain. The average pressure applied while the vacuum pump was operating was estimated to be -75.5 kPa. The excess pore pressure values obtained from P2c and P3d indicated that the vacuum pressure had propagated instantaneously to where the transducers had been installed 1.3m from the surface

However, other pore pressure transducers installed at 4.8m, 8.3m, and 11.8m below the surface only seem to represent only the increased pore pressure due to the surcharge load with minimum effect from the vacuum. Kelly et al. (2008) suggested that this could be due to suction pressure that did not travel up to the transducer, because the soil had a low permeability.

6.1.5 Consolidation analysis using the proposed analytical model

The consolidation settlement and excess pore water pressure were estimated using the proposed method and then compared with the observed field data and the results obtained from previously developed analytical models. According to the construction schedule shown in Table 6.2, the vacuum pumps were switched on after 102 days of settlement recordings, and then switched off on the 378th day, and therefore, only the consolidation responses of first 378 days were considered in the simulation. The drain installation parameters are summarised in Table 6.3, and the extent of the smear zone was taken as 6 times the equivalent diameter of the mandrel as obtained in Chapter 3 along with the void ratio relationships f_o, f_i and f_f.

Table 6.3 : Vertical drain and installation parameters

Parameter	r_w *(mm)*	r_s *(mm)*	d_e *(mm)*	s	n	f_0	f_i	f_f
Value	17	300	1130	17.65	33.24	1.38	1.38	1.35

Using the proposed model, Figure 6.6 shows the calculated settlements at settlement plates SP 4, 8, 10 and 12, which were then compared with the measured field data. The soil parameters in each layer that were used for analysis at SP12 are tabulated in Table 6.4, and the thicknesses of the layers of compressible soil under the relevant settlement plates are given in Table 6.1. An excellent match between the predicted and measured settlement values was obtained, especially when the layer of clay was very thick. Even though the total settlement of SP4 matched well, the consolidation rates were underestimated in the prediction, possibly due to increased vertical drainage encountered in shallow clay layers.

Table 6.4 : Soil parameters used in the analysis at SP12

Depth (m)	λ	κ	γ (kN/m^3)	e_0	k_h (m/s)	*OCR*	c_k
0.0-4.4	0.57	0.10	14.5	2.90	10×10^{-10}	3.0	1.45
4.4-11.5	0.67	0.26	13.7	3.25	10×10^{-10}	1.2	1.63
11.5-19.0	0.63	0.09	14.2	2.90	10×10^{-10}	1.2	1.45
19.0-25.0	0.37	0.09	15.8	2.60	3.3×10^{-10}	1.1	1.30

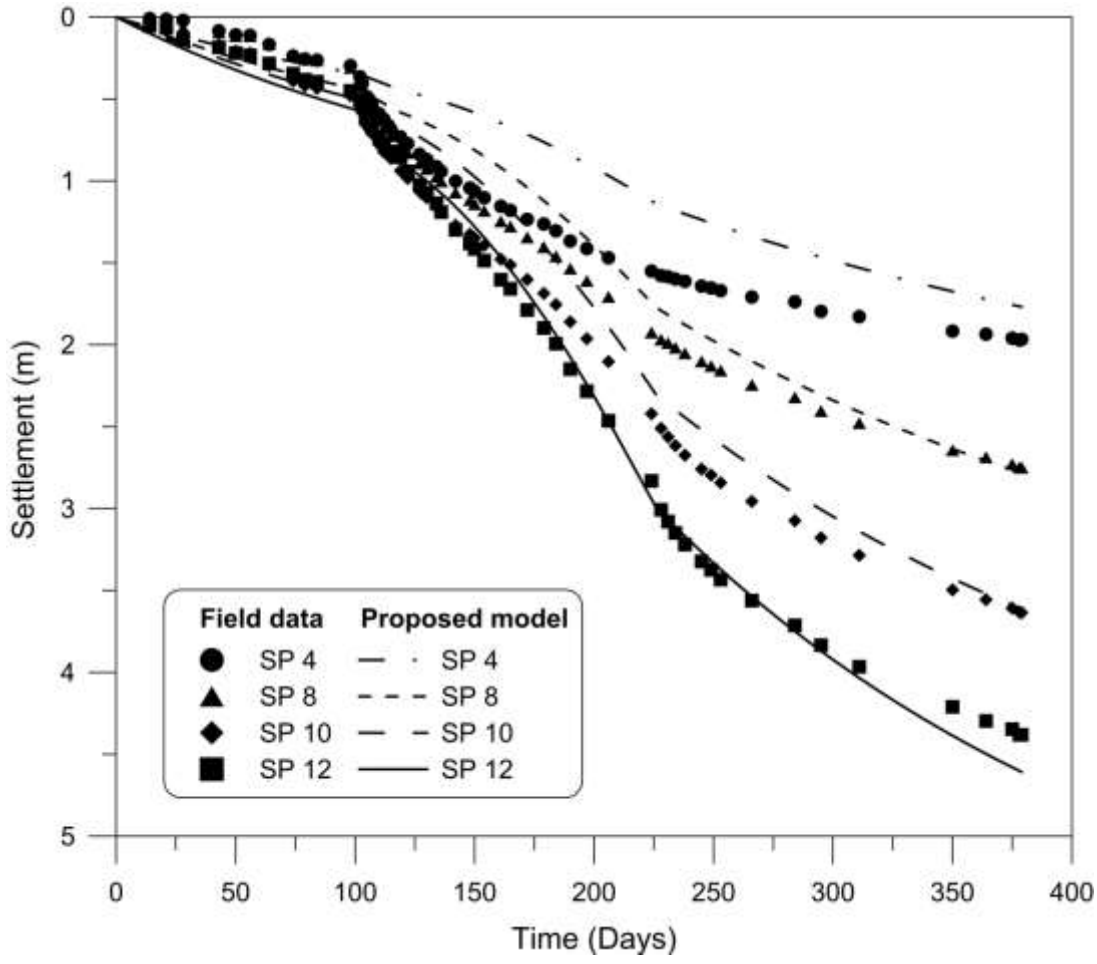

Figure 6.6 : Surface settlement prediction at different settlement plates

Figure 6.7 compares the settlement obtained using the proposed methods along with predictions of Indraratna et al. (2005) and Kianfar et al. (2013) for the settlement recorded at SP12. The vacuum pumps were switched on after 102 days; this is marked as Point A in the Figure. The final construction stage of the embankment (8.5m high) commenced 17 days after switching on the vacuum pumps, and even though they were switched off at point C, analysis continued by assuming that the applied total effective stress after Point B remained unchanged in order to compare the ultimate settlements using all three methods. These hypothetical curves are shown in the Figure after 378 days.

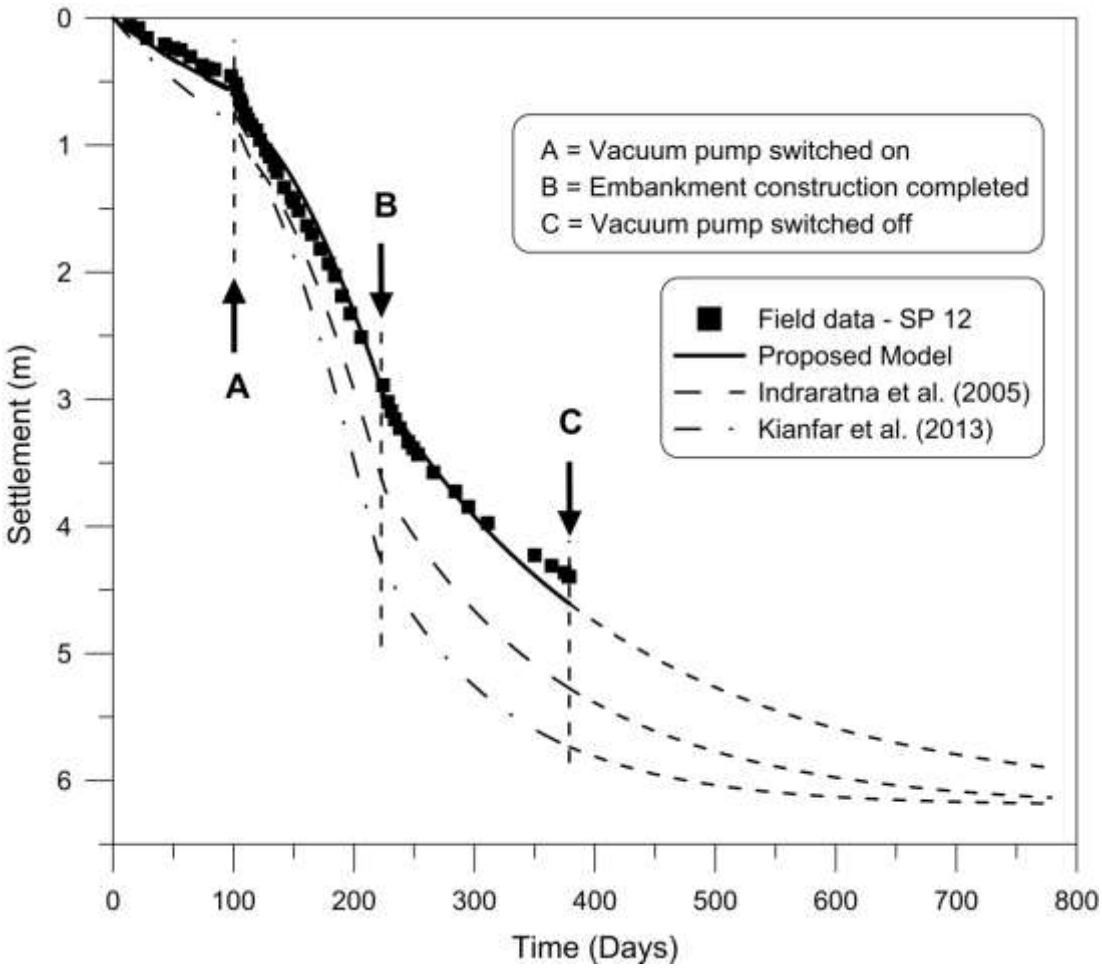

Figure 6.7 : Settlement at SP12 compared to other analytical methods.

Here the proposed method agreed with the field data very well compared to the other methods, because, in the other methods the effects of soil de-structuring due to drain installation was not considered. As a result, the actual permeability and compressibility within the smear zone were overestimated, which led to higher ultimate settlements and consolidation rates. In Kianfar et al. (2013), non-Darcian flow was considered and the velocity of drained water in a lateral direction was increased by approximately 50%, this resulted in even higher consolidation rates compared to other two models. The permeability ratio between the undisturbed zone and the smear zone was taken as 2.0 and the value β for non-Darcian flow was taken as 1.1.

Figures 6.8 shows the variations in excess pore water pressure over time, as seen at P2 (P2a at -8.3m and P2b at -4.8m), as well as the predictions based on the proposed model and Indraratna et al. (2012). The final section of the embankment was raised within 107 days, after which the pore water pressure was increased to a maximum value. Then the excess pressure began to dissipate and the excess pore water pressures observed after 100 days were compared in the simulation with the available field data. Indraratna et al. (2012) generally predicted there would be less excess pore water pressure compared to the proposed model, and there was good agreement with the measured values and predictions from the proposed model. Kelly & Wong (2009) reported that the pore pressure readings were less affected by the vacuum pressure, and those criteria were considered in the analysis of excess pre water pressure when both methods were used.

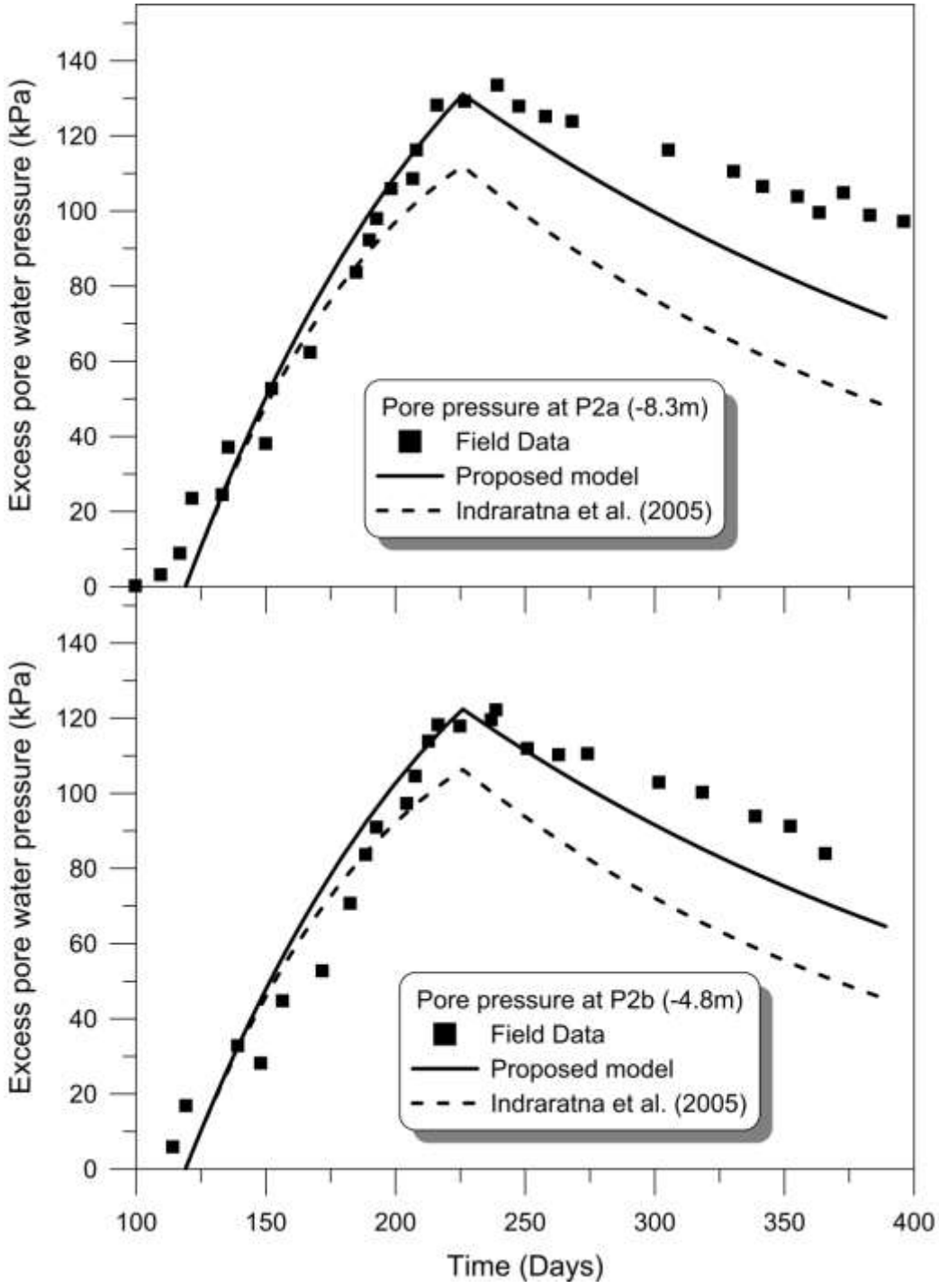

Figure 6.8 : Observed and predicted distributions of excess pore water pressure for a) P2a (8.3m below the ground surface) and b) P2b (4.8m below the ground surface)

6.2 Storage yard at the Port of Tianjin, China

6.2.1 Introduction

Tianjin port is one of the largest ports in mainland China and is situated 100km away from the capital, Beijing. Expansion work at this port included the construction of new infrastructure facilities over recently reclaimed land where 3-4 metres of dredged soft soils sit on top of the original sea bed that consisted of other layers of soft soil 16-19m thick. The original ground and the dredged fill were still were still undergoing consolidation due to additional applied fill loads. A high embankment surcharge load could not be used because the soil had very low undrained shear strength. It was therefore decided to use vacuum preloading. However, the preloading pressure needed to improve the soil could not be provided solely by vacuum pressure, so a combination of vacuum pressure with vertical drains and surcharge loading was applied to successfully improve the ground (Chu et al., 2000; Yan & Chu, 2005).

6.2.2 Site characteristics

The conditions of the sub-soil around the port of Tianjin have been reported in Shang et al., 1998; Yan & Chu, 2003; and Rujikiatkamjorn et al., 2007. A typical cross-section of this subsoil is presented in Figure 6.9, as adopted from Yan & Chu (2003). The top 3-4 m of soil consists of dredged clay from the harbour basin and it is still consolidating due under its own weight. The clay is highly compressible and the undrained shear strength of this layer is typically less than 10 kPa. Below this sits a 5m thick soft muddy layer underlain by a 7.5 m thick layer of soft silty clay located at a depth of 8.5-16m, and below that is a 6m thick layer of stiff silty clay. The

groundwater table was situated at the surface and the moisture content of all the layers varied with the liquid limit, which resulted in fully saturated clay.

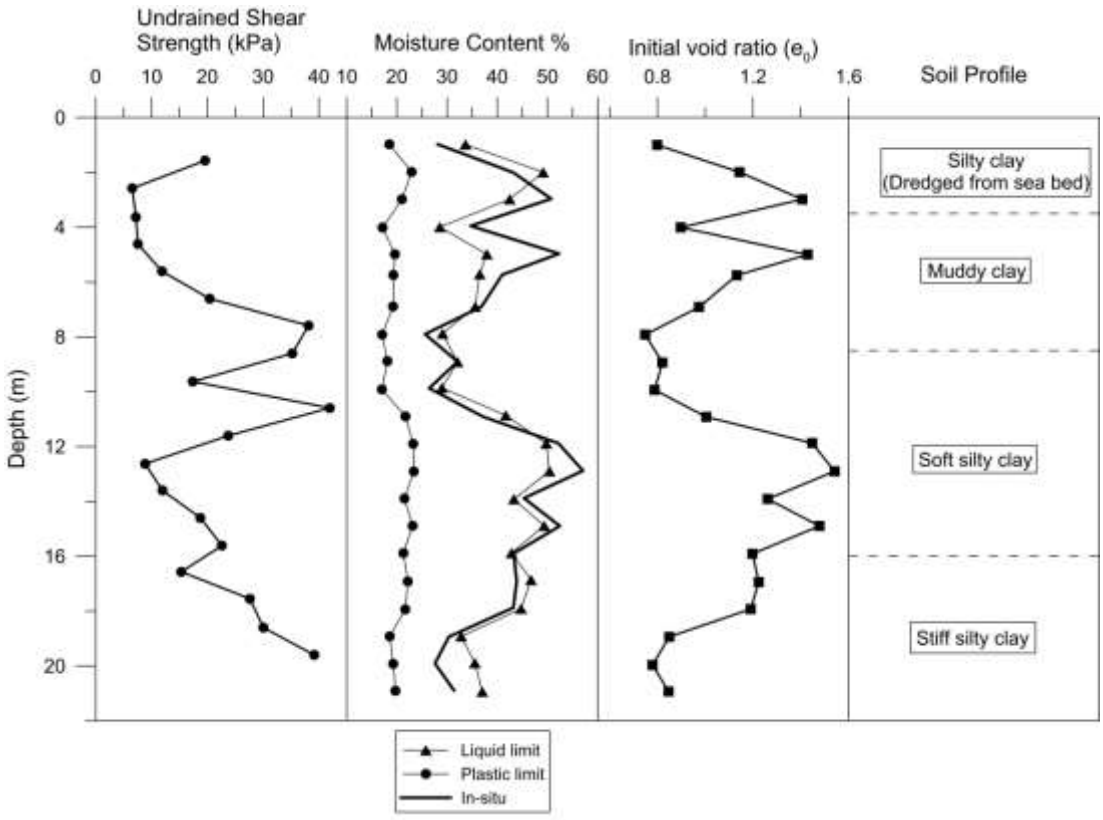

Figure 6.9 : General soil profile and basic soil parameters of soils around the port of Tianjin (Adopted from Yan & Chu, 2003)

6.2.3 Soil improvement procedure and instrumentation

To improve the soil, a 0.3m thick layer of soil was first placed on top of the ground as a platform to install vertical drains, into which 3mm thick by 100mm wide by 20m long band shaped vertical drains were installed in a square pattern at 1m spacing. A mandrel was used to drive the drains into the soil, but rather than pushing the drains dynamically, a static load was preferred given the in-situ soil consistency. This method minimised the smear effects and helped the soil to consolidate quickly.

Surface settlement plates, multi-level settlement gauges, pore water pressure transducers, and inclinometers were installed in the ground to accurately measure consolidation due to external loads. A plan view of the locations of the instruments is shown in Figure 6.10.

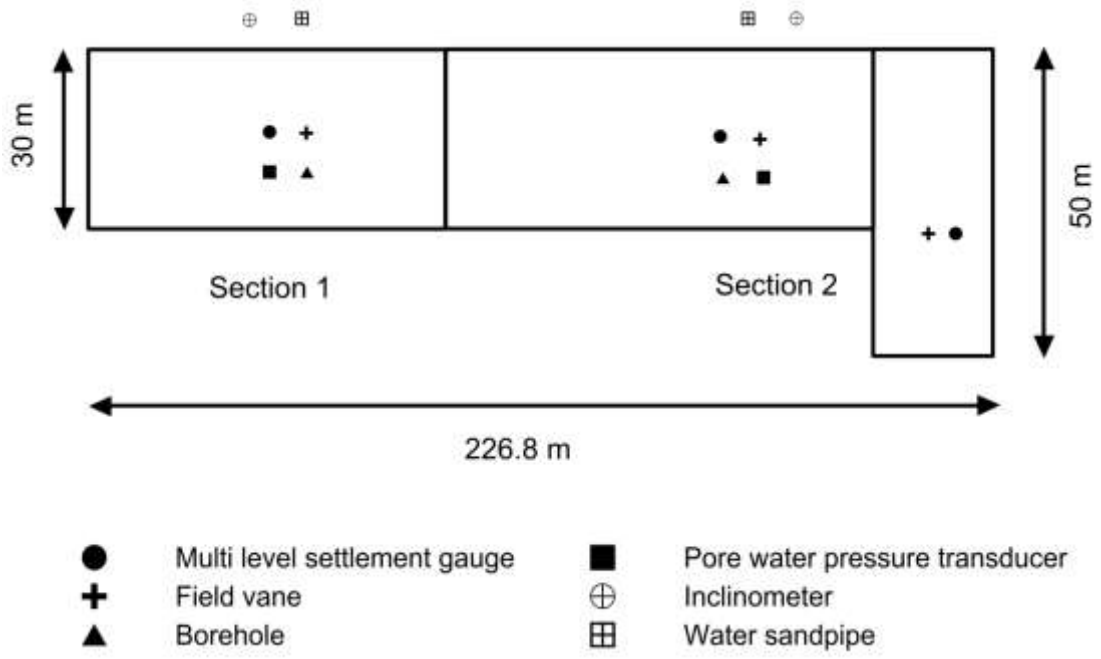

Figure 6.10 : Plan view of the area of improved soil, and the instrumentation (adopted from Chu & Yan, 2005)

Intermediate settlement gauges and pressure transducers were installed at depths of 3.5m, 7.0m, 10.5m, and 14.5m below the surface to measure the settlement of the subsoil layers and at depths of 4.0m, 6.0m, 8.5m, 11.0m, 14.5m and 18.0m, to measure the intermediate pore pressures, respectively. After all the instruments had been installed, 100mm diameter perforated pipes wrapped with a geotextile were placed in perpendicular directions inside the sand blanket to transmit the vacuum pressure to the vertical drains. This area was then covered with three layers of thin

PVC membranes, each of which was sealed properly at the perimeter to maintain an airtight system beneath the membranes. Finally, a vacuum pressure was applied to the surface below the air-tight membrane using jet pumps (Yan & Chu, 2005).

6.2.4 Predicting consolidation using the proposed analytical model

Ground settlement and distribution of excess pore water pressure were estimated using the proposed model, and the results were then compared with the actual field measurements and previously developed models. Lateral strain observed during embankment loading was predicted using the emperical relationship developed in Chapter 5. The drain and subsoil parameters required for the analysis were extracted from Yan & Chu (2003); , Chu & Yan (2005) and Rujikiatkamjorn et al. (2007), and are presented in Table 6.5 and Table 6.6, respectively.

Table 6.5 : Drain parameters – Tianjin port embankment

Parameter	r_w *(mm)*	r_s *(mm)*	d_e *(mm)*	s	n	f_0	f_i	f_f
Value	51.5	287	1130	5.57	10.95	1.38	1.38	1.38

Table 6.6 : Soil parameters used in the analysis of section 1

Depth (m)	λ	κ	γ *(kN/m^3)*	e_0	k_h *(m/s)*	*OCR*	c_k
0.0-3.5	0.12	0.03	18.3	1.10	20×10^{-10}	1.0	0.55
3.5-8.5	0.14	0.03	18.8	1.00	40×10^{-10}	1.2	0.50
8.5-16.0	0.20	0.04	17.5	1.35	20×10^{-10}	1.2	0.67
16.0-20.0	0.10	0.02	18.5	0.90	5×10^{-10}	1.1	0.45

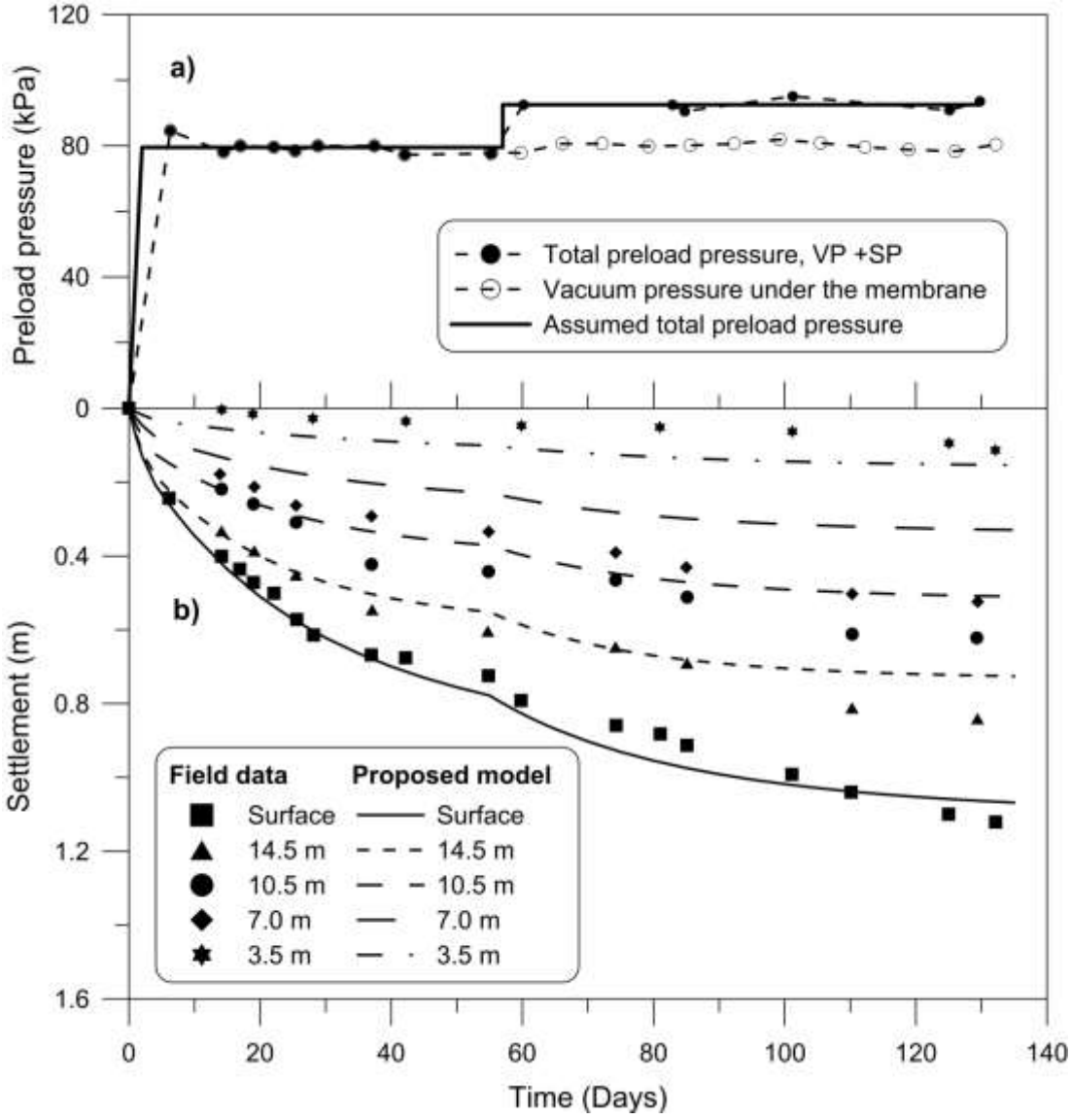

Figure 6.11 : a) Embankment construction; b) Subsurface settlement prediction with field data

The application of preloading pressure with time is shown in Figure 6.11a for section 1. A vacuum pressure was applied and maintained for 55 days, and then a surcharge load of 13 kPa was added to the ground surface in conjunction with the vacuum preloading. The average vacuum pressure under the membrane was -79.5

kPa, and did not vary much with time, thus confirming a satisfactory air-tight vacuum system. Even though the surcharge load had gradually increased due to the comparatively small magnitude, an instantaneous load was assumed in the analysis. Figure 6.11b shows the field settlements measured at each depth and the settlement profile predicted by the proposed model, and it reveals that there is a good agreement between the measured and predicted data. The settlement data measured 7.0m below the surface appears to be higher than the predicted values; this may be due to an incorrectly placed settlement plate, because, it is impossible to have such a small settlement between 7.0m and 10.0m below the surface.

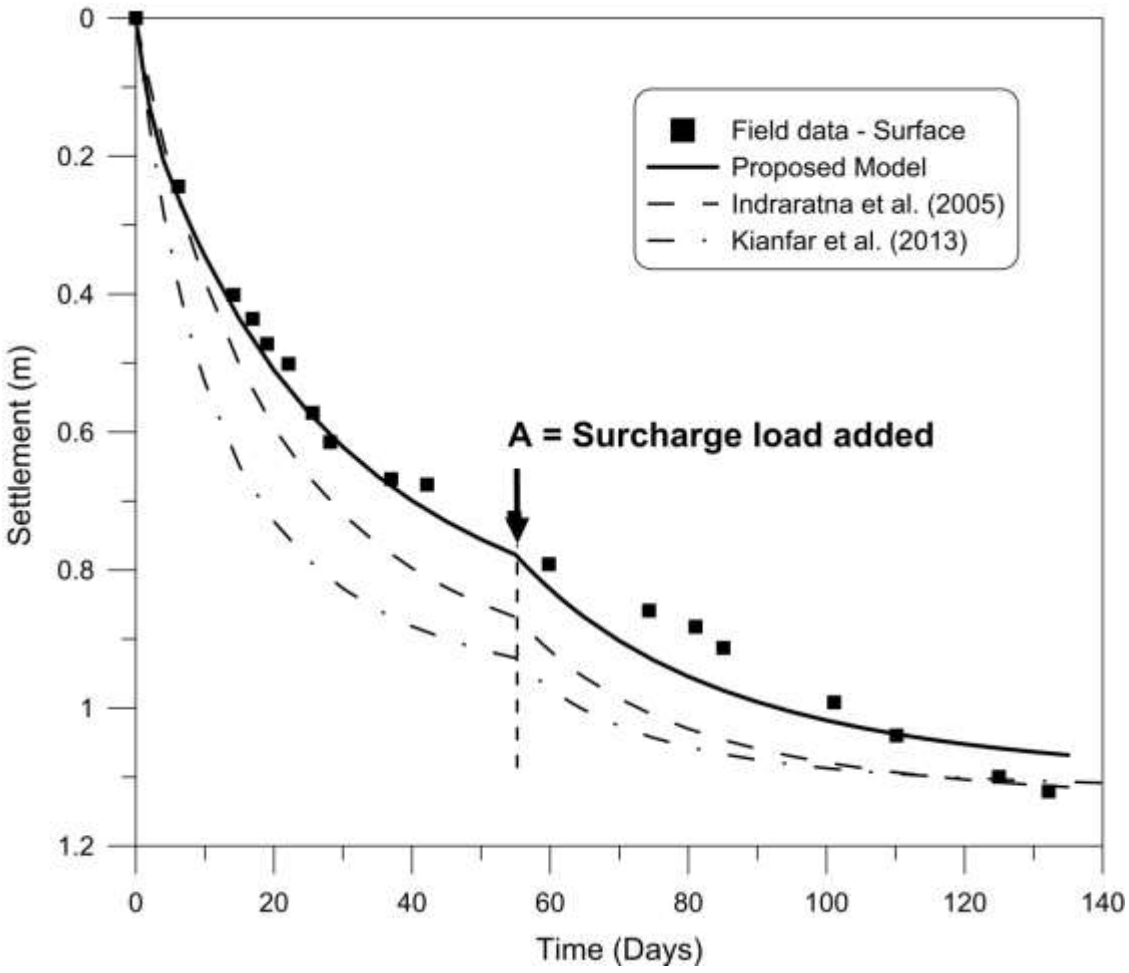

Figure 6.12 : Settlement predictions using different analytical models compared with actual field data

Figure 6.12 shows a comparison of the settlements obtained using the proposed method with predictions using Indraratna et al. (2005) and Kianfar et al. (2013) for the settlement recorded for section 1. Here, point A indicates the time where the additional surcharge load was added. Note that the proposed method matched the actual ground settlement better than other models, however, the final settlement measured by the other method was more accurate. The permeability ratio between the undisturbed zone and the smear zone was taken as 2.0 and the value β for non-Darcian flow was taken as 1.3.

Yan & Chu (2003) presented the pore water pressures for the area considered in the analysis. The variations in excess pore water pressure with time at depths of 18.0m and 14.5m are shown in Figure 6.13a & 6.13b, respectively, as well as the excess pore pressures predicted by the proposed method. Generally, there was a good agreement between the predicted and observed values, but at the initial stages of consolidation the proposed model over-predicts the excess pore water pressures, possibly due to the time taken for the vacuum pressure to propagate through the soft soil layers. In the proposed method, there was a sharp rise in the pore pressure when a surcharge load was applied to the soil; this is not clearly seen in the field data, possibly due to the ramp load applied, although a change in the pore water pattern can be observed.

Figure 6.14 shows the predicted and measures lateral displacements of the embankment after 177 days of consolidation. The field data was extracted from Rujikiatkamjorn et al. (2007) and the predictions were made based on the emperical relationships derived in Chapter 5. After 177 days of consolidation, the applied

vacuum pressre was 79.5 kPa and the surcharge load was 13kPa, which gave a vacuum surcharge ratio *(VSR)* of 0.86.

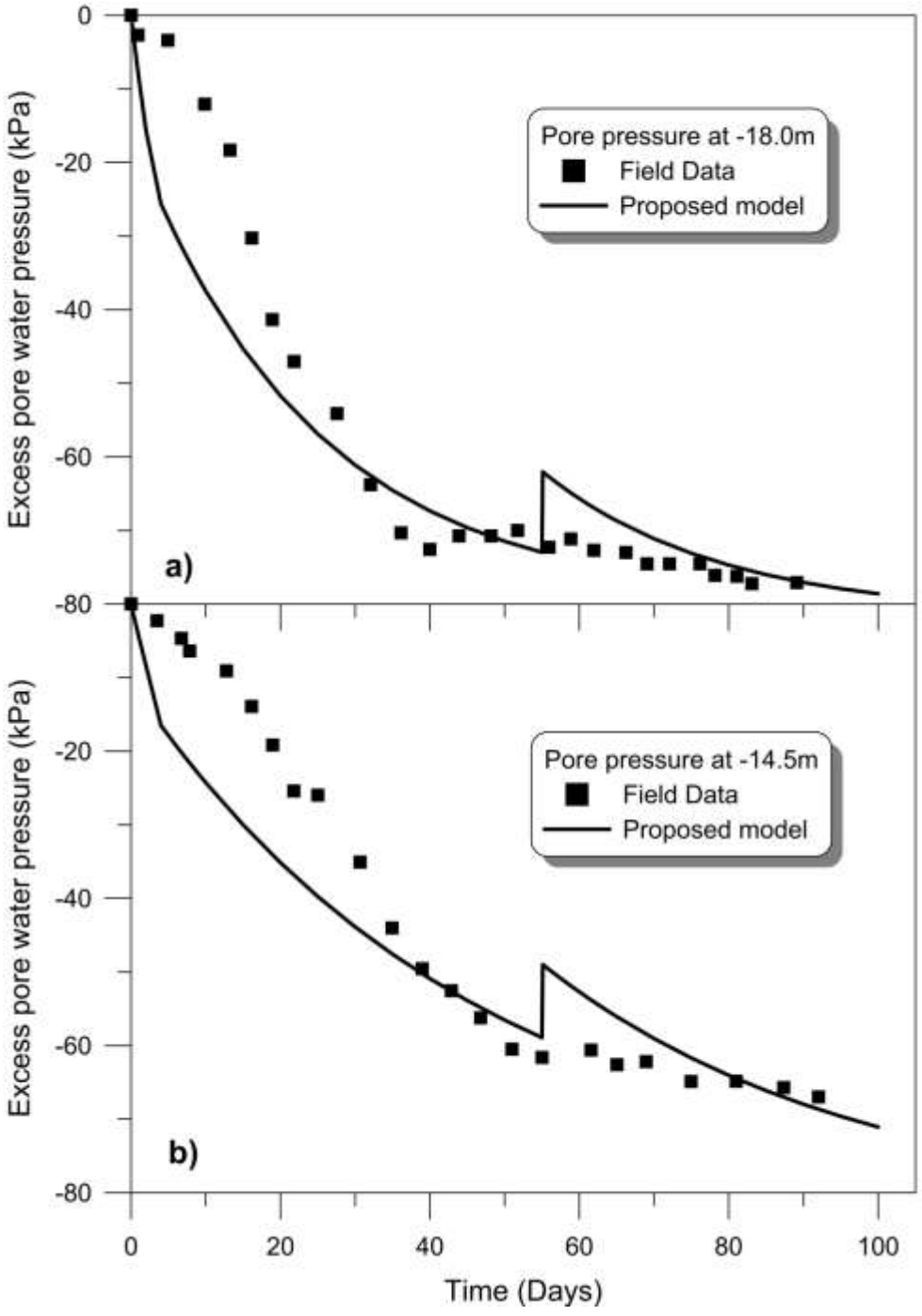

Figure 6.13 : Observed and predicted excess pore water pressure distributions for a) 18.0m and b) 14.5m; below the ground surface

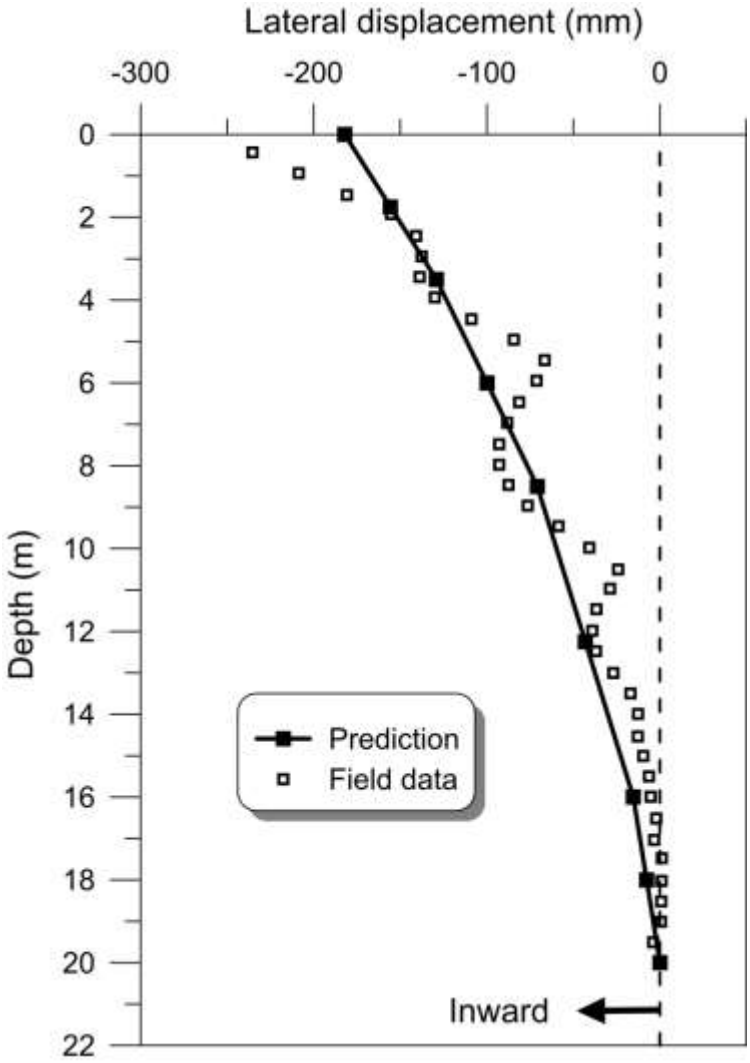

Figure 6.14 : Predicted and measured lateral displacements at toe of the embankment after 177 days of consolidation.

According to the values obtained from Chapter 5, the ratio between maximum settlement at the centre of the embankment and lateral displacenet at the toe of the embankment was 0.187, where *VSR* =1 and 0.151 when the *VSR* was equal to 0.75. By interpolation, this ratio can be estimated as 0.167 for the loading condition applied in the embankment. The lateral displacement at any point was calculated as 0.167 times the total settlement that occurred in a horizontal plane at the centreline of the embankment.

6.3 Ballina test Embankment constructed for the prediction symposium 2016

6.3.1 Construction of the embankment

It was mentioned previously in Chapter 3, that the samples for a field study were obtained from beneath a test embankment constructed at Ballina. This test embankment was constructed so it could be used in the 2016 prediction symposium.

The constructed embankment is 3m in height and the crest of the embankment is 80m long and 15m in width. Sides of the embankment are sloped at 1.5:1. Working platform of 95m x 25m was initially constructed with a thickness of 0.6m and 0.4m thick sand blanket was placed over it to cover the foot print of the embankment. Total length of the embankment was divided in to three sections, two 30m sections with conventional PVD's and bio degradable jute drains and one 20m section with the conventional PVD's however without installing the sand drainage layer. After laying the sand platform the relevant type of vertical drains were installed to the ground in square pattern with a spacing of 1.2m. Drains were driven to the ground to a depth of 15m.

Construction of the 3m high preload embankment was completed within 60 days. Density of 0.4m thick drainage layer was measured as 15.89 kN/m^3 and the rest of the embankment density was measured at 20.55 kN/m^3 resulting a surcharge load of 59.8 kN/m^2, acting on the top of the soil layers. To measure the consolidation responses settlement plates, vibrating wire piezometers, horizontal profile gauges, Magnetic extensometers and inclinometers are installed mainly along the centreline of the section with conventional and jute vertical drains. Layout of the embankment and the instrumentation plan is shown in Figure 6.15

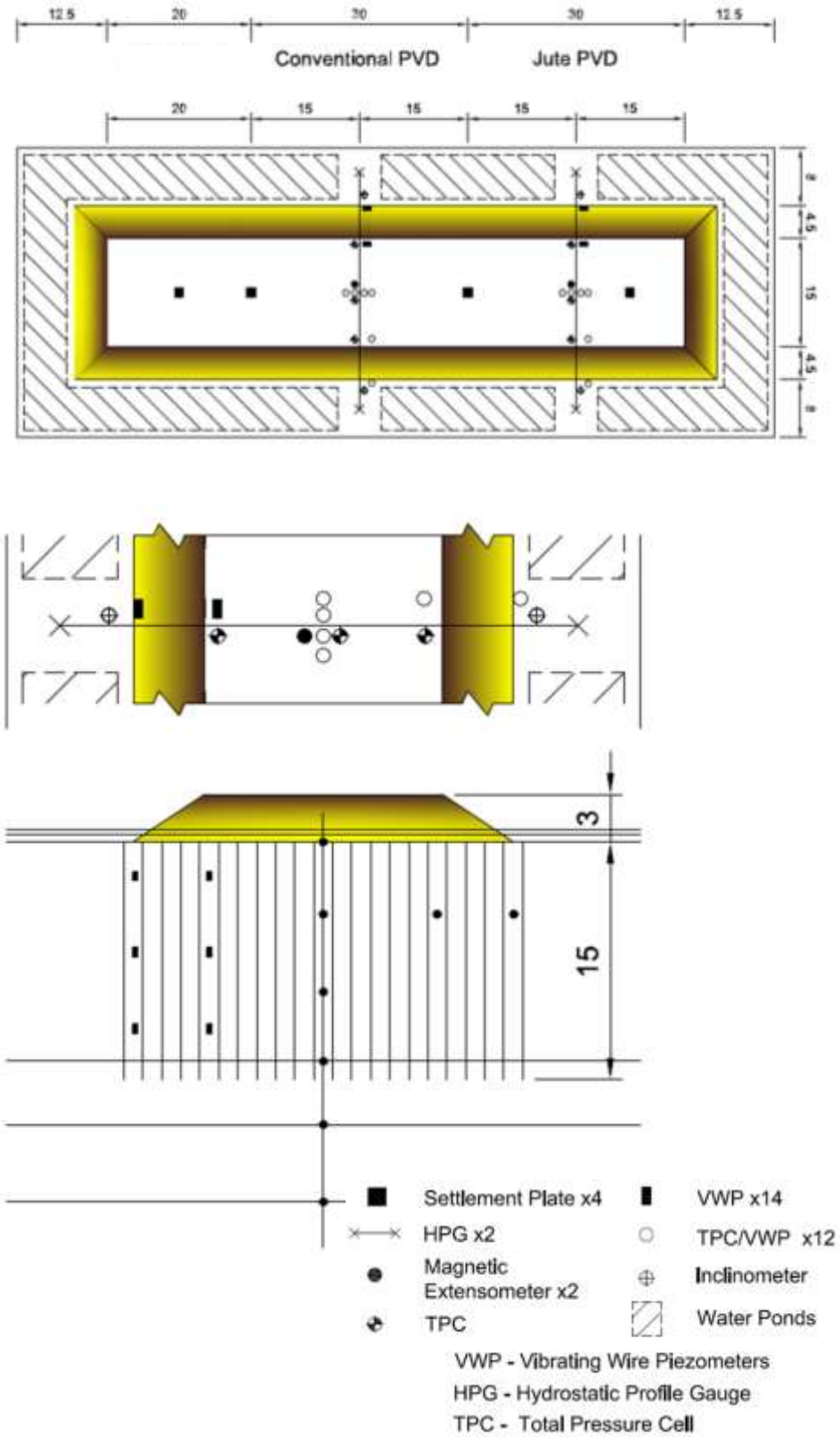

Figure 6.15 : Layout and Instrumentation plan of the embankment

6.3.2 Sub soil condition and drain installation parameters

Basic soil properties were obtained from Indraratna et. al. (2012) which presented the details of an embankment constructed in Ballina bypass project and some parameters were taken from the available bore hole logs and laboratory experiments conducted. Water table is taken as 0.3 m below the ground level. Bulk density of the soil was taken as 14.5 kN/m^3. Permeability of soil in the undisturbed zone was 1.2x10-9 m/s.

Extent of the smear zone was taken as 400mm and the permeability reduction in the smear zone and drain installation parameters are taken from Chpter 3. Lateral permeability of the soil next to the drain is reduced to 30% of the permeability of undisturbed zone while the average permeability of the smear zone is about 70% of the undisturbed zone permeability. The drain and subsoil parameters taken in the analysis are given in Tables 6.7 and 6.8 shown below

Table 6.7 : Soil parameters used in the analysis - Ballina test embankment (Indrartna et. al. (2012)

Depth (m)	c_c	c_s	γ (kN/m^3)	e_0	k_h (m/s)	*OCR*	c_k
0.0-2.7	1.404	0.156	14.5	2.90	1.2×10^{-9}	5.0	0.787
2.7-5.7	1.365	0.273	14.5	2.90	1.2×10^{-9}	1.2	0.787
5.7-8.7	1.677	0.429	14.5	2.90	1.2×10^{-9}	1.2	0.787
8.7-11.7	1.209	0.468	14.5	2.90	1.2×10^{-9}	1.0	0.787
11.7-15	1.521	0.195	14.5	2.90	1.2×10^{-9}	1.0	0.787

Table 6.8 : Drain parameters – Ballina test embankment (See Chapter 3)

Parameter	r_w *(mm)*	r_s *(mm)*	d_e *(mm)*	s	n	f_0	f_i	f_f
Value	51.5	400	1356	7.77	13.17	1.38	1.38	1.35

6.3.3 Embankment response prediction

The main aim of constructing this trail embankment is to use it for an Embankment prediction symposium scheduled to be held in 2016. Consolidation data recorded from the instruments inserted has not been available to author. However an attempt is made to predict the consolidation responses of the embankment stabilised with the conventional PVD using the analytical model presented in the Chapter 4 and the results were compared with the known radial consolidation models available. The analytical models considered are as follows;

Case A – Current Study: Even though the current model is developed for the radial consolidation with vacuum preloading, by selecting applied vacuum pressure to zero, an embankment stabilised with preloading and vertical drains can be simulated.

Case B - Walker & Indraratna, (2007): Radial consolidation model is capable of capturing linear variation of permeability within the smear zone. However the soil compressibility and permeability variation due to the soil structure effects caused by drain installation was not considered.

Case C – Kianfar et. al. (2013) : Non-Darcian flow relationship was considered in this solution. Applied vacuum pressure is taken as zero to simulate the embankment with preloading and vertical drains.

The ultimate settlement was calculated using the method described in Chapter 4. The predicted settlements and excess pore water pressure are plotted in Figures 6.16 and 6.17 respectively.

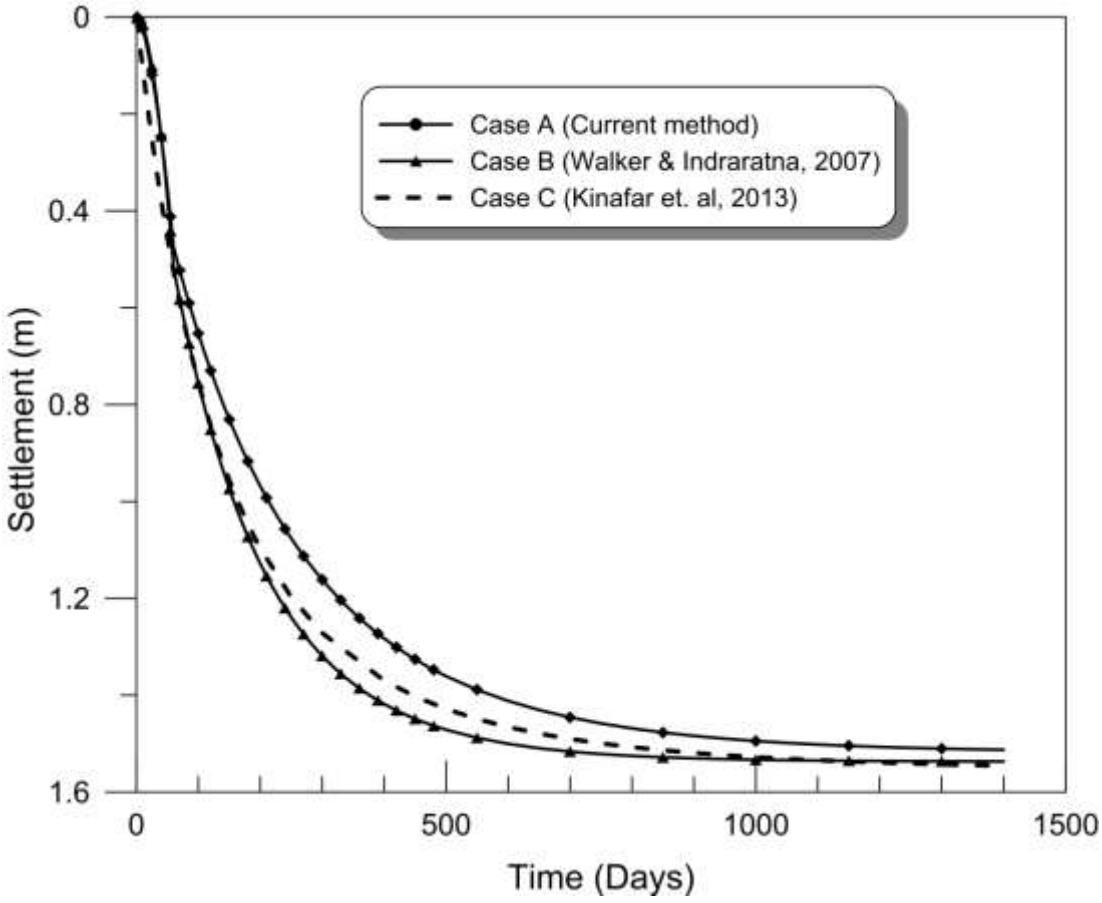

Figure 6.16 : Time settlement curve for the test embankment at Ballina

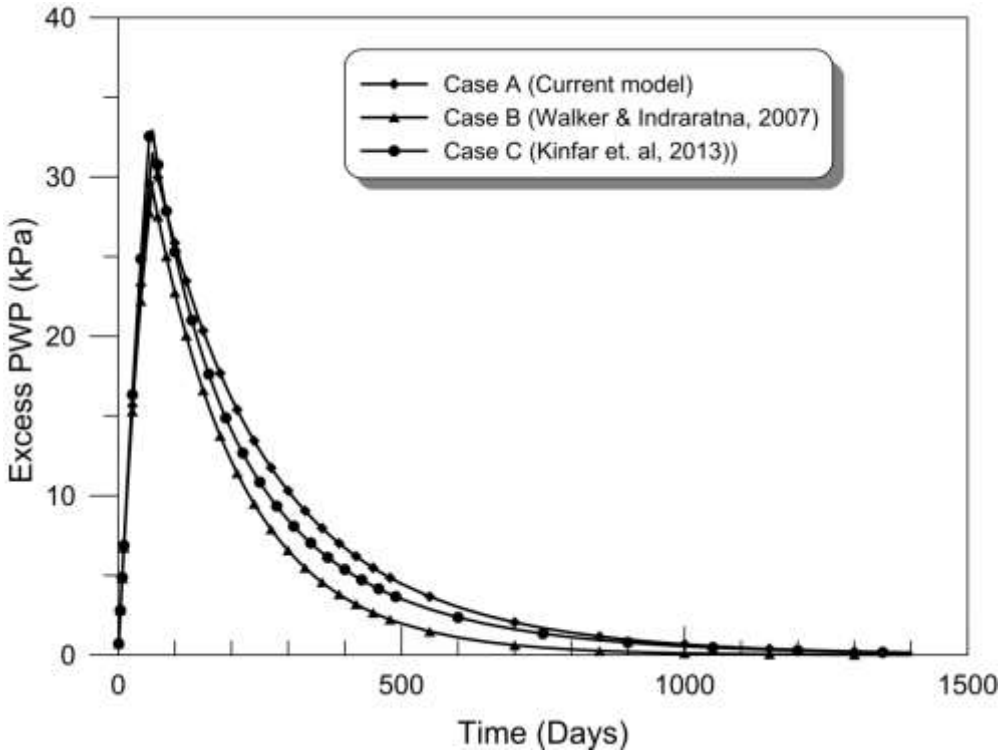

Figure 6.17 : Excess pore water pressure variation in the test embankment at Ballina

For the lateral displacement predictions, the ratio between lateral displacement and the settlement at that relevant depth reported in the previous literature was used. Indraratna et. al. (2012) reported this ratio to be about 0.2 after 200days for the Port of Brisbane project. However in this Ballina embankment an over-consolidated crust exists. For a 4.75m high embankment with 1.3m spacing triangular pattern vertical drains installed in Muar clay, Indrarathna et. al. (1997) reported the maximum lateral displacement at the toe to be 0.12 times the maximum settlement of the centreline of the embankment. For the current analysis ratio between lateral displacement and settlement was assumed to be 0.12 at the toe of the embankment and 0.19 in the subsequent layers below the over consolidated crust were assumed and the predicted lateral strain is shown in Figure 6.18.

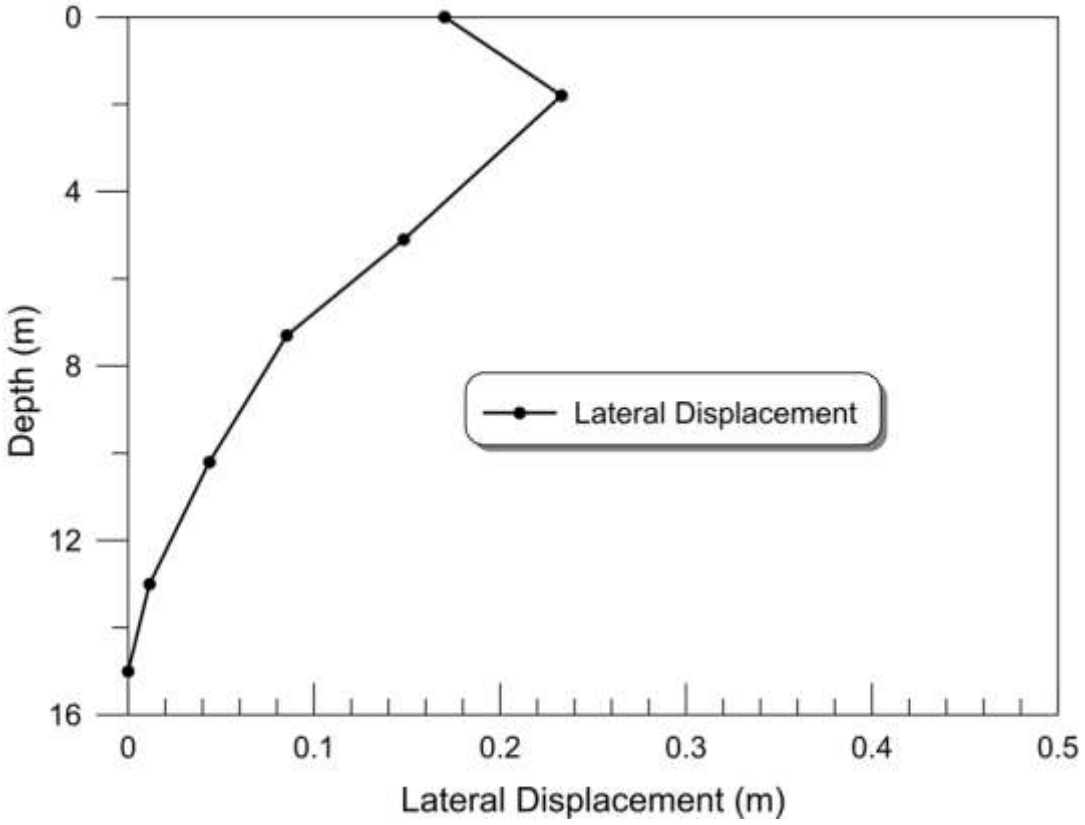

Figure 6.18 : Predicted Lateral displacements

6.3.4 Predictions based on the published fields data

The predictions presented in Section 6.3.3 is based on the soil properties extracted from Indraratna et. al. (2012) and from the laboratory experiments conducted. However some relevant soil properties obtained from laboratory testing conducted using Ballina clay samples at University of Newcastle are now available. Registered users can download these data from the prediction symposium website. Therefore the analysis of the embankment was carried out using the latest soil properties, and the consolidation response predictions are presented below. Comprehensive details of index properties of the soil are available, and a summary is presented in Table 6.9 below.

Table 6.9: Soil parameters extracted from prediction symposium website. (http://cgse.edu.au/eps2016)

Depth (m)	***w%***	***LL***	***PL***	e_0	G_s	γ (kN/m^3)
0.0-2.7	65	83	33	1.735	2.67	16.5
2.7-5.7	104	104	37	2.800	2.69	14.6
5.7-8.7	116	121	46	3.100	2.67	14.0
8.7-11.7	102	115	47	2.700	2.65	14.5
11.7-15	25	-	-	0.670	2.65	19.8

It can be observed from the data that the top 12m of the subsoil consists of high plastic clay with a larger void ratio, and the bottom 3m is predominantly a sandy soil. Ground investigations revealed that the sand content below 12m depth is more than 90%. Consolidation parameters were obtained from constant rate of strain (CRS) tests conducted on samples extracted at different locations and are presented in Table 6.10. The rate of constant strain is 0.004 mm/min and the sample diameter is 48mm and the sample height is 20mm.

Table 6.10: Consolidation parameters extracted from CRS tests

Depth (m)	σ_0 (kN/m^2)	C_r	C_c	e_0	OCR^1
2.27	18.90	0.168	1.19	1.735	3.20
5.49	35.35	0.275	3.00	2.800	2.06
9.76	53.90	0.162	2.39	3.100	1.95

Soil permeability was taken as $1.2x10^{-9}$ *m/s* and the soil disturbance parameters were observed to be similar to Section 6.3.3. Figures 6.16 and 6.17 give the predicted settlement and excess pore water pressure, respectively using the proposed analytical model (Chapter 4) and the Walker & Indraratna (2007) model. Along with these two curves (Case A and Case B), another settlement prediction curve was obtained using the soil parameters given in the prediction symposium website (Figure 6.19). Predictions were made based on both models mentioned earlier. Figure 6.20 shows the excess pore water pressure variation obtained using the new data along with the predictions discussed earlier in Section 6.3.3. Both the current model (Chapter 4) and Walker and Indraratna (2007) model were adopted to obtain the relevant excess pore water pressure plots.

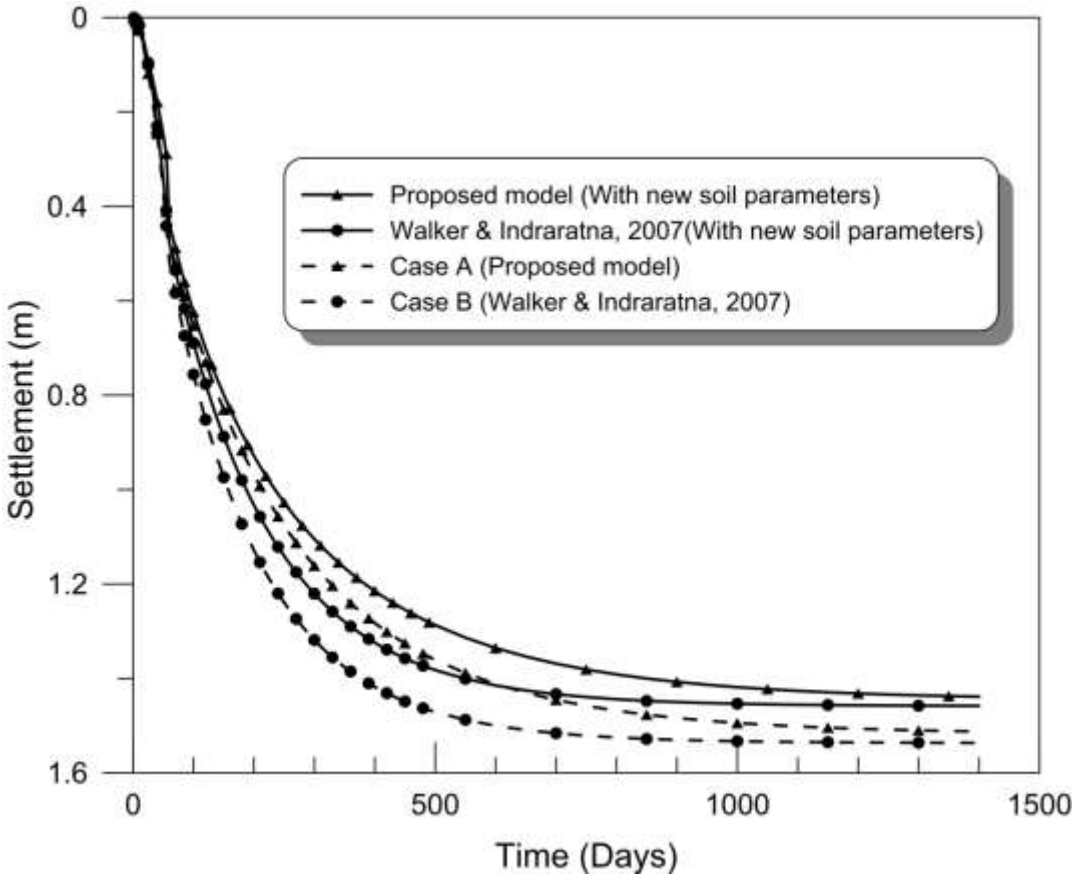

Figure 6.19 : Time settlement curve for the test embankment at Ballina with new data

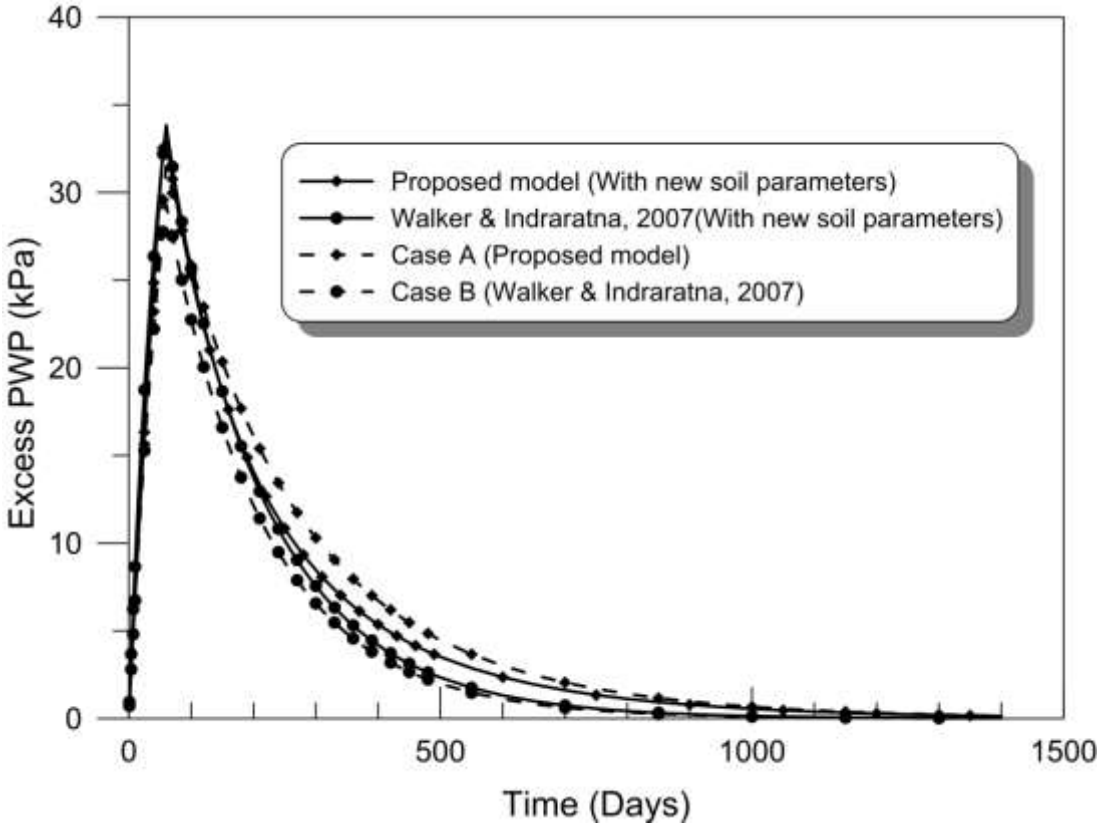

Figure 6.20: Excess pore water pressure variation in the test embankment at Ballina with new data

6.4 Summary

The consolidation of two completed embankments (Ballina bypass embankment and soil improvement work at Tianjin Port) stabilised with vertical drains and vacuum preloading was simulated using the proposed analytical solution. In addition to that, one embankment where field observation data was currently not available was also simulated.

The ground settlement and pore water pressure was estimated using the analytical model, whilst the lateral displacements were derived using the empirical relationship developed. The differences between the predictions of the current model

and those of previous analytical models were also presented, and it was concluded that the proposed method was more accurate at predicting the consolidation responses than the past methods. Finally a class A prediction was made for the Ballina trial embankment constructed for the prediction symposium to be held in 2016. Prediction was made based on the current model and the results were compared with two available mathematical models.

[1] The OCR values tend to be overly high compared to oedometer tests, and may have been increased by the speed of CRS tests.

Chapter 7 Numerical Analysis

7.1 Finite Element methods in Geomechanics

The Finite element method (FEM) has been used extensively to solve problems encountered in geotechnical engineering. With the correct material parameters, it can simulate the actual ground behaviour accurately. In general FEM provides an approximate solution to a governing mathematical equation by solving a series of algebraic equations, in order to obtain the responses of the individual parts created by dividing the area considered into finite elements; the accuracy of the approximated solution can then be controlled by the allowable error in iterations. To analyse embankments stabilised with vertical drains and vacuum preloading, the finite element software PLAXIS 2D was used. The latest model of PLAXIS released in 2015 can simulate vacuum preloading, but since the results of simulated embankments with vacuum pressure are not available in literature, this can be

considered as an early attempt at modelling an embankment stabilised with vertical drains and vacuum pressure.

7.1.1 Material models used in the analysis

The soft soil model based on the modified Cam-clay theory (Britto & Gunn, 1987) was used to simulate the soft compressible soil layers and the Mohr-Coulomb model was used to represent the underlying layers of sand and embankment fills. The modified compression parameters used in the soft soil model can be obtained using the following relationships,

$$\lambda^* = \frac{\lambda}{1+e}; \qquad \kappa^* = \frac{\kappa}{1+e} \tag{7.1}$$

The Modified Compression index (λ^*) and recompression index (κ^*) are defined using the original Cam-clay parameters and PLAXIS 2015 reference manual suggests using the initial void ratio (e_0) instead of the void ratio (e) for convenient.

7.1.2 Element types used in Plaxis 2D

To perform an analysis using the finite element method considered, the ground area must be divided into a finite number of elements. In PLAXIS 2D, triangular elements consisting of 15 nodes or 6 nodes are used and primary variables such as displacement values are calculated at these nodes. These primary values are continuous over the boundaries of the elements and a polynomial interpolation is used to obtain the values within the elements of the mesh created. The order of the polynomial equation depends on the number of nodes in the element considered and when elements with a higher number of nodes are used to create the finite element mesh, they produce more accurate results but the time taken for the analysis can increase significantly. In addition to the nodes, each element contains Gaussian

integration points that are useful when calculating secondary variables such as stress. 15 node elements have 12 Gaussian integration stress points and 6 node elements have 3 of them. The types of elements used in PLAXIS 2D are shown in Figure 7.1.

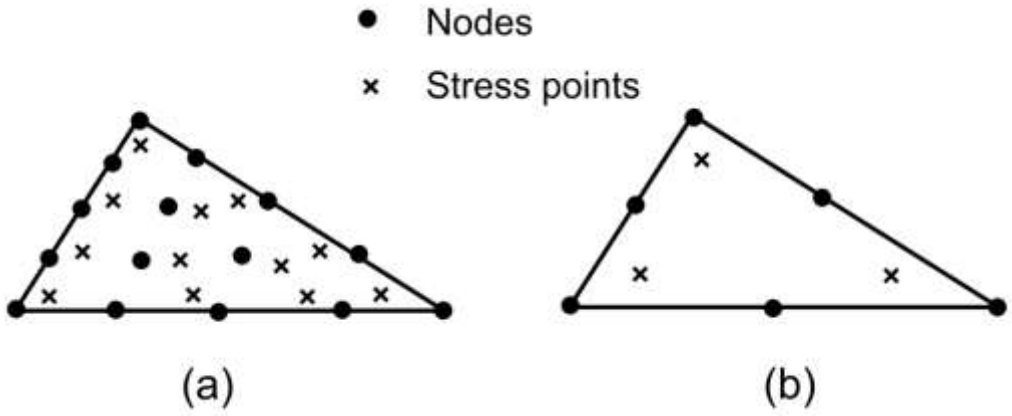

Figure 7.1 : a) 15-node element; b) 6-node element used in PLAXIS 2D

7.1.3 Plane strain modelling of vertical drains with vacuum pressure

When the behaviour of embankments stabilised with vertical drains are simulated using numerical methods, the use of 3D models can become cumbersome and might lead to complexities with the mesh and corresponding convergence (Indraratna & Redana, 2000). Converting the axisymmetric permeability to equivalent plane strain values to give the same degree of consolidation when considering smear effects and well resistance was extremely difficult until Indraratna & Redana (1997) proposed a rigorous analytical method. In Indraratna et al. (2005) this was further extended to cases where vacuum preloading was also applied along with vertical drains.

The ratio between permeability in the smear zone ($k_{s,ps}$) to the undisturbed zone ($k_{h,ps}$) in the plane strain model can be expressed as,

$$\frac{k_{s,ps}}{k_{h,ps}} = \frac{\beta}{\frac{k_{h,ps}}{k_{h,ax}}\left[\ln\left(\frac{n}{s}\right) + \left(\frac{k_{h,ax}}{k_{s,ax}}\right)\ln(s) - 0.75\right] - \alpha} \tag{7.2}$$

where $k_{h,ax}$ and $k_{s,ax}$ are the undisturbed and smear zone permeability of the axisymmetric model respectively; $n = d_e/d_w$; $s = d_s/d_w$; and,

$$\alpha = \frac{2}{3}\frac{(n-s)^3}{n^2(n-1)} \tag{7.3}$$

$$\beta = \frac{2(s-1)}{n^2(n-1)}\left[n(n-s-1) + \frac{1}{3}(s^2+s+1)\right] \tag{7.4}$$

When the smear and well resistance are ignored the ratio between the equivalent plane strain and axisymmetric permeability can be obtained as,

$$\frac{k_{h,ps}}{k_{h,ax}} = \frac{2\,(n-1)^2/n^2}{3[\ln(n) - 0.75]} \tag{7.5}$$

7.2 Simulation of Tianjin Port embankments using PLAXIS 2D 2015

7.2.1 Modelling vacuum pressure using PLAXIS

The latest version of PLAXIS can model vacuum pressure, however, since the new version was only released recently, case studies performed using PLAXIS with vacuum preloading do not exist in literature. Moreover, the tutorial manual provided by PLAXIS (2015) has no worked out examples using vacuum preloading, but it does present some useful guidelines to apply vacuum pressure with vertical drains. The salient aspects of the vacuum preloading module and the critical steps involved in modelling vacuum pressure in soft soil improvement using PLAXIS 2D 2015 are summarised as follows,

- Since PLAXIS does not take atmospheric pressure into consideration, and is assumed to be zero, the vacuum pressure was simulated as a reduction of the groundwater head. As a result, negative pore stresses (suction) were introduced, but this process is not the same as in reality.

- To model vacuum pressure, the groundwater head of the installed vertical drains should be lowered from the coordinates of the global phreatic level by the amount of vacuum pressure head that needs to be added, and then perform either a groundwater flow calculation or a fully-coupled flow-deformation analysis.

- Lowering the groundwater head would result in the soil becoming unsaturated, but in almost all instances, soil will mostly remain saturated beneath the static groundwater table. To make sure the soil is saturated, the unsaturated unit weight must be set as same as the saturated unit weight, and the hydraulic model must be selected as 'saturated' in the model group in the ground water tab sheet.

- While doing the consolidation analysis the pore pressure calculation must be changed to a steady- state groundwater flow, and then deselect the 'ignore suction' option in deformation control parameters section of the phases window.

- To enable the drains to propagate the vacuum pressure, the behaviour mode listed in the explorer section should be changed from a 'normal' state to a 'vacuum' state, because only vacuum drains will allow the pore pressure to be lower than the static pore water pressure.

- When vacuum pumps are switched 'off' after some time during consolidation, this condition can be simulated by changing the behaviour of the vertical drain to 'normal' and change the pore pressure calculation to 'Phreatic'.

- The distance between drains should be less than a quarter of the drain length.

7.2.2 Material parameters used for finite element model

The embankments built on sections 1 and 2 at the Tianjin port in China was simulated in this analysis; their construction details and basic material properties were given in Rujikiatkamjorn et al. (2007) and Yan & Chu (2005) and are summarised in Chapter 6. In this chapter, the variation in soil structure due to vertical drain installation was considered and therefore, the modified compressibility index and the void ratios were used and the modified parameters are given in Table 7.1. These values are obtained using Equation 4.19 and 4.21. However, PLAXIS will not allow the permeability within the smear zone to be varied, so a constant permeability ratio between the smear zone and the undisturbed zone was assumed. $k_{h,ps}$, $k_{v,ps}$ and $k_{s,ps}$ are the equivalent plane strain permeability in horizontal and vertical directions in the undisturbed region and horizontal direction in the smear zone, respectively. β and α values of 0.463 and 0.087 respectively were obtained using Equations 7.3 and 7.4 to convert axisymmetric permeability to equivalent plane stain values. The basic drain and soil parameters are presented in Table 6.5 and the permeability ratio between the undisturbed and smear zone was taken as a more realistic value of 2.0.

Table 7.1 : Parameters used in the PLAXIS model

Depth (m)	λ	κ	e_0	$k_{h,ps}$ *(m/day)*	$k_{v,ps}$ *(m/day)*	$k_{s,ps}$ *(m/day)*
0.0-3.5	0.113	0.03	1.03	5.76×10^{-5}	5.76×10^{-5}	2.57×10^{-5}
3.5-8.5	0.126	0.03	0.94	1.16×10^{-4}	1.15×10^{-4}	5.12×10^{-5}
8.5-16.0	0.178	0.04	1.26	5.76×10^{-5}	5.76×10^{-5}	2.57×10^{-5}
16.0-20.0	0.091	0.02	0.84	1.44×10^{-5}	1.44×10^{-5}	6.39×10^{-6}

15 node triangular elements were used for the finite element mesh and the constructed mesh for the section 1 embankment is shown in Figure 7.2a. A closer view around the toe of the embankment, with the vertical drain and smear zone, is shown in Figure 7.2b.

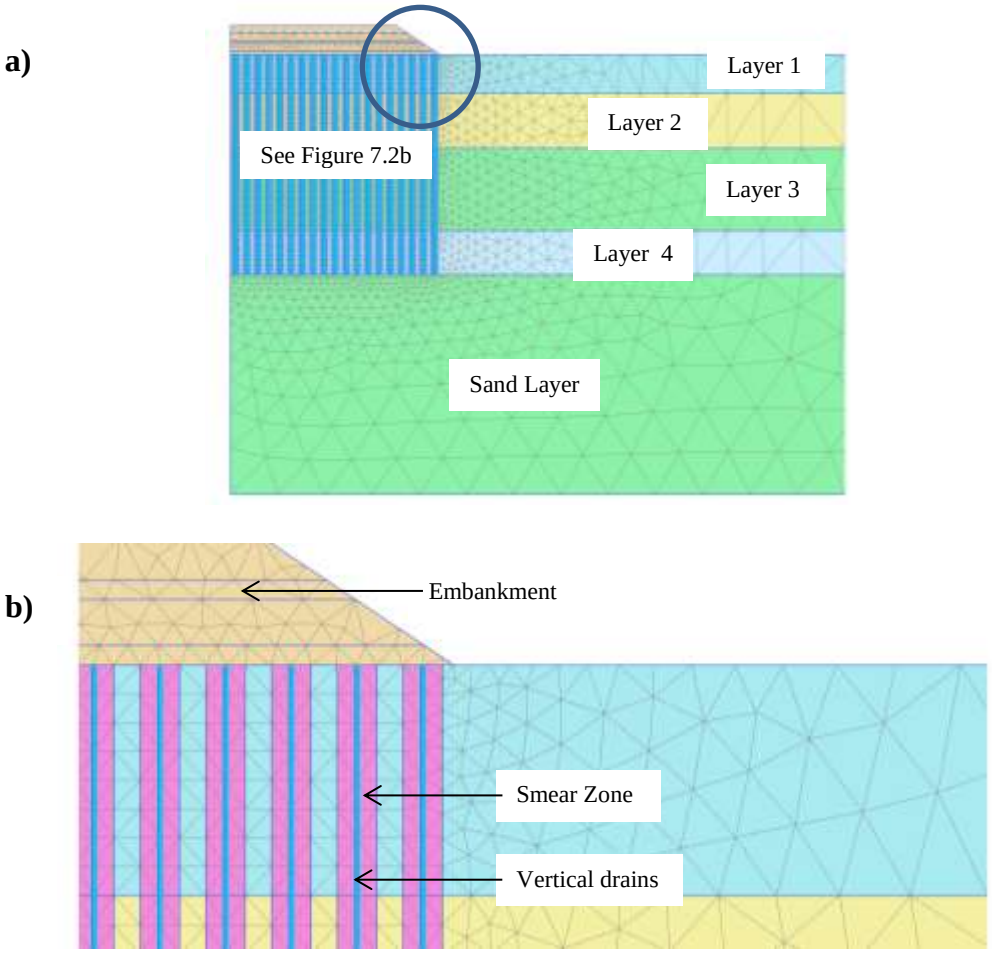

Figure 7.2 : Finite element mesh created for the embankment in section 1, Tianjin Port

7.2.3 Settlement predictions from the PLAXIS model

Vertical settlements obtained from the numerical analysis along with the field data is shown in Figure 7.3c for the Section 1 and Section 2 embankments (Section 1 and Section 2 are shown in Figure 6.10). Analytical model simulation results of case study analysis presented in chapter 6 for the section 1 embankment is also shown in

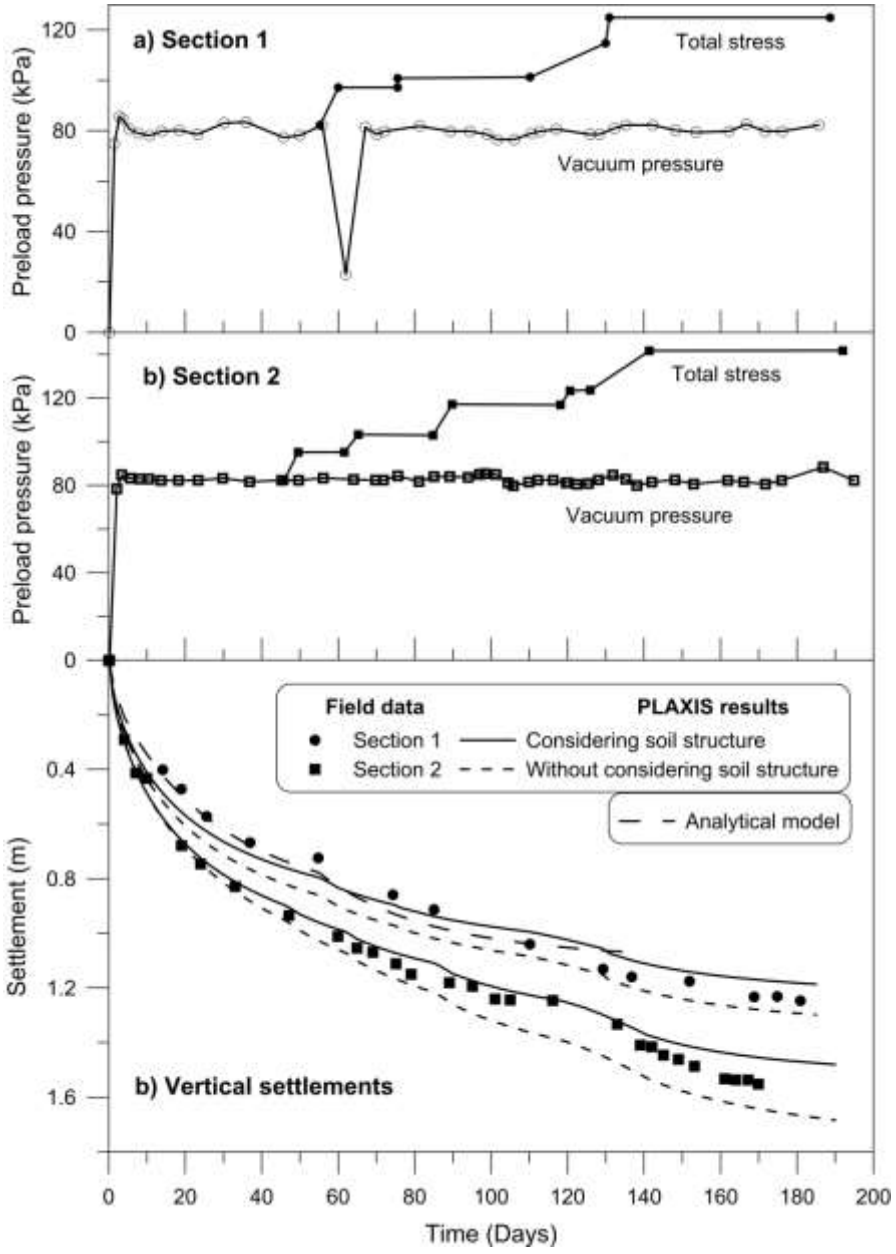

Figure 7.3 : loading sequence of a) Section 1; b) Section 2; and c) ground settlement

the same figure. Two separate numerical analyses were preformed considering the soil structure characteristics and without considering it. Figures 7.3a and 7.3b show the procedure for constructing the embankment and the vacuum pressure measured under the membrane and there was a sudden loss of vacuum from a temporary leak occurred after 60 days in the section 1. It can be observed that numerical model results are in good agreement with the field data and analytical model results when

soil structure characteristics were incorporated. An exact loading sequence was simulated in the PLAXIS numerical models and this led to very accurate trends of the settlement plots.

7.2.4 Excess pore water pressure predictions

Variations in the excess pore pressure obtained by the PLAXIS analysis for the Section 2 (Figure 6.10) embankments are shown in Figure 7.4. The pore pressure values were obtained midpoint of two rows of drains and at 6.0m, 9.0m, 12.0m, 15.0m and 18.0m below the ground surface. A vacuum pressure was applied to the soil within less than a day without affecting the stability of the embankment, and this is not possible with the same amount of the surcharge load. However, it appears that the program had calculated the change in pore pressure due to the vacuum pressure in a similar way it calculates the pressure increment due to the surcharge load. This behaviour must be considered when obtaining the pore pressure values and if a correction is needed it must be applied.

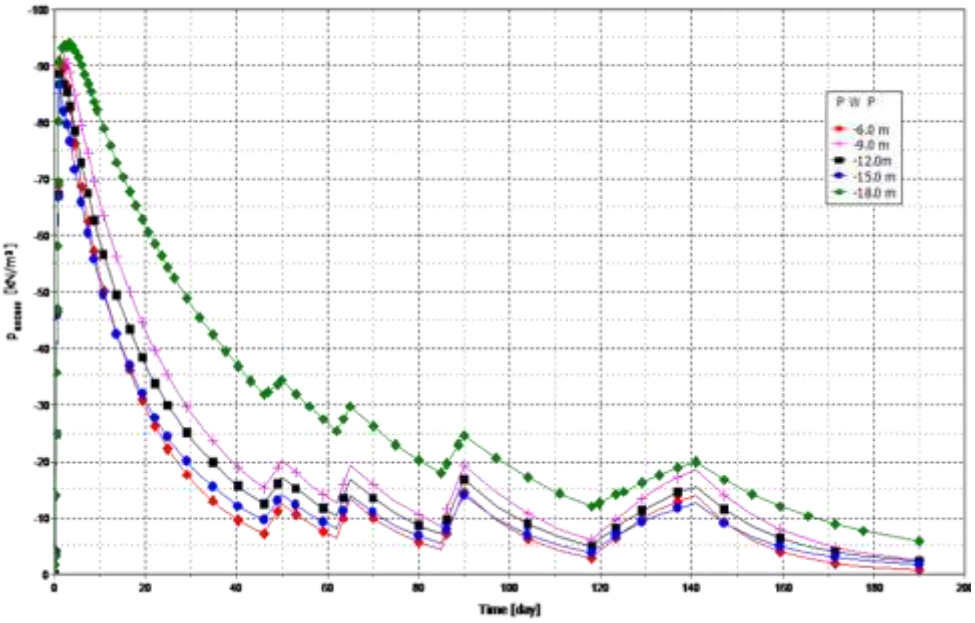

Figure 7.4: Excess pore water pressure values obtained by PLAXIS analysis.

The excess pore pressure obtained from the analysis was corrected accordingly and compared with the field data obtained from 9.0 m and 18.0 m below the ground water. The published data was extracted from Yan & Chu (2005) and the results are shown in Figure 7.5. There was a very good agreement between the field data and results obtained by the PLAXIS numerical model.

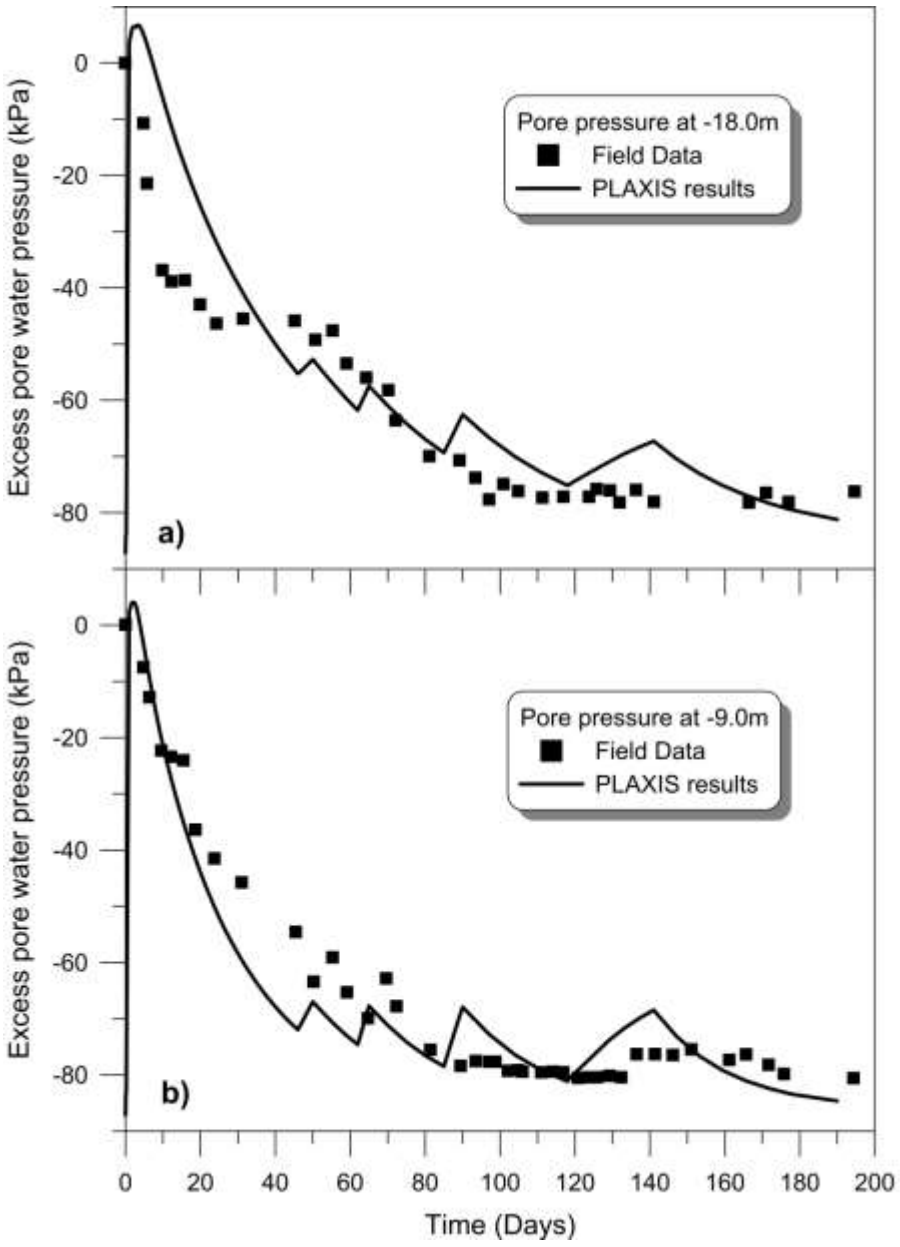

Figure 7.5 : Observed and predicted excess pore water pressure distributions for a) 18.0m and b) 9.0m; below the ground surface

7.2.5 Comparison of lateral displacements

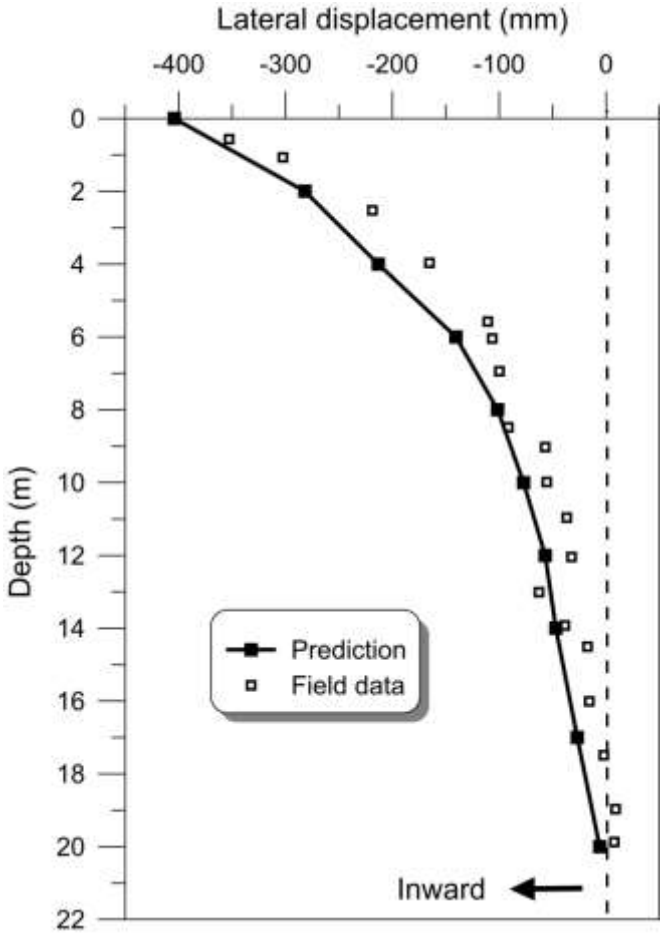

Figure 7.6 : Predicted and measured lateral displacements at the toe of the section 1 embankment after 168 days of consolidation.

Figure 7.6 compares the lateral displacements obtained using the numerical analysis and the field data presented in Rujikiatkamjorn et al. (2007) for the section 2 embankment (Figure 6.10) at Tianjin Port after 168 days of consolidation. There was an acceptable match between the predicted and actual values.

To accurately run a finite element numerical model, accurate shear strength parameters are required. Together with those parameters geotechnical characteristics

of the top crust layer and the details of outer berms constructed to stabilise the Ballina embankment was not available. Therefore it was not possible to conduct a finite element analysis with PLAXIS for Ballina road embankment.

7.3 Summary

The performance of two embankments built in Tianjin port China was simulated using the PLAXIS finite element package. The latest PLAXIS version could simulate a vacuum pressure with vertical drains. The effects of permeability and compressibility due to drain installation were also considered in the analysis. The conversion of axisymmetric permeability values to an equivalent plane strain values were extremely important in order to properly model the embankment stabilised with vertical drains and vacuum preloading. There was a very good agreement between the predicted and simulated values of settlement, pore water pressure and lateral displacements.

Chapter 8 Conclusions and recommendations

8.1 General Summary

The main aim of this work was to develop a mathematical model for radial consolidation with vertical drains and vacuum preloading that considers the characteristics of the soil structure. Following on from the Abstract, Chapter 1 introduced the problems encountered and outlined the content of the Thesis. Chapter 2 presented a comprehensive literature review of the use of vertical drains and vacuum preloading in ground improvement, as well as important concepts in soil mechanics. The analysis of soil disturbance conducted in a soft clay site near Ballina was described in Chapter 3. The development of the mathematical model and the parametric analysis used to compare the model's performance with previously developed models was described in Chapter 4. Experimental work was presented in Chapter 5, followed by a case study analysis in Chapter 6, and associated numerical modelling of selected embankments in Chapter 7.

8.2 Soil Disturbance observed in field conditions

An analysis of soil disturbance was performed using samples of undisturbed soil collected from around a vertical drain installed to stabilise a test embankment built over estuarine soil deposit in Ballina, Australia. The main conclusions from this study can be summarised as,

- The extent of the smear zone can be obtained using several methods. In this study the variation of moisture content, void ratio, horizontal permeability, normalised permeability, and degree of disturbance along the radius of the drain influenced area was successfully used to evaluate the extent of the smear zone.
- The radius of the smear zone was estimated to be 400 mm, using all the methods mentioned above, and a result that was 6.3 times larger than the equivalent mandrel dimension. This figure was comparatively larger than the smear zone observed (generally between 2-4) in the laboratory experiments conducted on large scale remoulded samples, where the model used scaled down mandrels and drain anchoring shoes.
- It was clear that methods used in field drain installations would create a larger disturbed zone due to the higher installation speeds and longer shearing time when vertical drains are installed in thick clay layers.
- Horizontal permeability within the smear zone increased from the lowest value next to the drain to a maximum value at the boundary between the smear zone and the undisturbed region. A linear variation of permeability could be assumed inside the smear zone.
- Previously developed analytical methods used the ratio between the permeability of the undisturbed zone to the average permeability inside the smear

zone as an input parameter, the laboratory tests conducted in this study revealed that this ratio for Ballina clay was 1.67.

- The compression curves obtained from the vertically and horizontally extracted samples indicated that soil was more disturbed towards the drain, while the soil next to the drain experienced severe remoulding. The pre-consolidation pressure (yield stress) inside the smear zone decreased towards the drain, which confirmed destructuring of the soil due to the installation of vertical drains.

- The volume compressibility anisotropy and the permeability anisotropy ratio decreased as they approached the drain, and became close to unity at the soil-drain interface.

- The water content beyond the smear zone was not affected in single drain case, but it decreased by about 4% with the multi-drain case. The samples were extracted within close proximity to each other and from the same depth, and therefore any spatial variation can be excluded. This behaviour supports the existence of an overlapping smear zone; similar trends were also observed in the variation of permeability and void ratios.

- The effects of variations in the compressibility of soil due to drain installation affected the rate of consolidation and dissipation of excess pore water pressure quite significantly, and therefore, they must be incorporated into the mathematical modelling of radial consolidation with vacuum preloading, as well as the variations of permeability within the smear zone, in order to accurately predict the consolidation responses.

8.3 Analytical model and its salient features

Vertical drains alter the characteristics of soil structure in underlying subsoil. In the proposed analytical model, variations of compressibility and permeability were incorporated, and they enhanced the accuracy of the predicted consolidation responses when vertical drains with vacuum preloading are used in soil improvement projects. The conclusions from this work can be presented as follows:

- The parameters obtained in the multi-drain analysis were used to simulate the proposed model, and then the results were compared with the predictions obtained from Indraratna et al. (2005). It was evident when both models were simulated with normally consolidated soil that Indraratna et al. (2005) model over-estimated the ultimate settlement, because, the variations in compressibility due to the altered soil structure during drain installation were not considered in that solution.

- The proposed model can also simulate over-consolidated soils, but when two models were simulated with lightly over-consolidated clay the results with different load increment ratios differed. Due to drain installation, the compressibility and pre-consolidation pressure of the soil decreased, therefore, the former will reduce settlement and the latter will increase it.

- When the load increment ratio increased, the ultimate settlement with proposed model was less than that predicted by Indraratna et al. (2005) model. This result confirmed that as the load increment ratio increased, the effect of pre-consolidation pressure to modify the settlement gradually decreased, while the effect of lowering compressibility had become more prominent.

- The proposed model seemed to dissipate the excess pore water pressure slower, and hence consolidation was slower than Indraratna et al. (2005) because the horizontal permeability within the smear zone had been assessed more accurately.

- Vacuum pressure can be lost along the length of the drain due to layers of sand and resistance created by high lateral strains in the deeper layers of clay. In the event of a complete loss of vacuum, ultimate settlement would be reduced and a different excess pore pressure distribution would occur. The proposed model can predict this behaviour accurately.

- When inevitable changes in compressibility and permeability due to drain installation are incorporated into the model, more realistic predictions of consolidation can be made, and this will improve the current design practises.

8.4 Laboratory experimental work

Vacuum preloading experiments were performed using a newly designed consolidometer. A sintered bronze drain was used to simulate the vertical drain and vacuum preloading tests were performed with remoulded and undisturbed samples, in addition to the oedometer tests.

- When testing undisturbed soils, care must be taken while obtaining, extracting, and trimming the undisturbed samples before beginning the experiment. Any disturbance that occurs as these procedures would alter the results of the consolidation test and ultimately lead to incorrect conclusions.

- When testing soft soils deposited in a marine environment, it is beneficial to perform a CT scan test on the steel sampling tube to identify the possible sections with the highest quality samples. This method will help to

identify any shells and any possible disturbance during sampling can also be inspected.

- The coefficient of secondary consolidation was almost identical on the undisturbed samples extracted from vertical and horizontal directions, although the Ballina soil exhibited some anisotropy in permeability and the coefficient of consolidation.

- In the over-consolidated region, the vertical sample showed more resistance to compression than the horizontal sample, possibly due to the arrangement of particles while the clay was being deposited, however, as the applied stress increased, both curves merged into one.

- Specially designed seals and a low friction cell ensured that the readings taken during vacuum preloading tests were reliable, while the sintered bronze porous drain maintained a constant drain diameter during consolidation.

- Vacuum preloading tests performed using remoulded Ballina clay indicated that when the vacuum surcharge ratio (VSR) increased, the soil would yield less settlement possibly due to an inward movement induced by isotropic consolidation with vacuum pressure. It was observed that sample had become detached from the sampling ring after the test, while the soil attained the same void ratio, even at different VSR values, thus confirming the same volumetric strain.

- This observation was less prominent in the experiments conducted with undisturbed samples because of the sample variations.

- Based on the laboratory experiments on vacuum preloading, an empirical relationship was presented to estimate lateral displacements when

different VSR levels were used. This can successfully be used as the design tool during the early stages of embankment analysis.

8.5 Case study analysis

The proposed model was simulated with two reported case histories namely the Ballina Bypass embankment built in NSW, Australia, and the Tianjin Port, (storage yard) China.

- The parameters of compressibility and permeability that were affected by variations in the soil structure due to drain installation were considered in the two case study analyses considered.
- There was good agreement between the field data and the proposed model predictions of surface settlements in the Ballina Bypass embankments, especially when deeper layers of clay were encountered. When simulating comparatively shallow layers of clay, the proposed model underestimated settlement because vertical drainage within the layers was ignored in the analysis. Omitting the vertical flow of water in the layers of soil was a reasonable assumption, because, vacuum preloading is only financially viable with very thick layers of clay where vertical drainage is insignificant.
- The predictions of ultimate settlement made for section SP12 shown in Figure 6.3using the proposed model, was comparatively better than the other two models analysed. Models of Indraratna et al. (2005) and Kianfar et al. (2013) overestimated final settlement because they did not consider the variations in compressibility due to drain installation. The dissipation of excess pore pressure predicted by the proposed model matched the observed values well compared to Indraratna et al. (2005) model.

- Similar trends were observed in the comparisons done at the Tianjin port soil improvement works where lateral settlement values were obtained using the empirical relationship proposed, and a reasonable agreement was observed.

8.6 Numerical modelling with PLAXIS

The latest version of the PLAXIS finite element package (PLAXIS 2D 2015) was used to simulate two sections of embankment at the Tianjin Port. This updated software now contains a vacuum pressure application model, so it can be considered to be among the first cases simulated with vacuum pressure.

- To simulate vertical drains in a plane strain condition the axisymmetric permeability values obtained using laboratory experiments must be converted into equivalent plane strain parameters to yield the same degree of consolidation. Indraratna & Redana (1997) method was used for this conversion.

- Vacuum pressure was applied to the soil by reducing the pore pressures at the vertical drains by an amount equal to the vacuum pressure applied, and then performed a consolidation analysis with steady- state ground water flow to calculate the pore water pressure and de-selecting the 'ignore suction' option. (According to the PLAXIS 2D 2015 Reference manual) Moreover, the soil must remain saturated below the pre-defined water table, otherwise permeability during consolidation would decrease drastically.

- There was a good match between the settlements and lateral strains in numerical model results, but there was a problem in excess pore water pressure calculations. The program does not distinguish between the pore pressure generated or dissipated by vacuum pressure and surcharge pressure; it treats them both in the same way. This will result in a pore pressure increment when vacuum

pressure is applied, but after the values were corrected manually there was good agreement with the field data.

8.7 Recommendations for future work

- In the field investigation of smear effects, samples were only obtained at one particular depth, but the smear effects would vary along the depth of the drain. Therefore it is suggested to extract samples from deeper layers and then to compare the results.

- The coefficient of secondary consolidation depends on the in-situ soil structure. Remoulded soils will yield less creep settlement than in-situ structured soil with same material but in a similar stress range. It is worthwhile studying how the coefficient of secondary consolidation would vary along the radius of the smear zone due to the influence of drain installation, and how it would change with the value in the undisturbed region. When drains were installed in square pattern with 1.2m spacing the area of disturbance observed is about one third of the total area and this is a considerable area. It was expected that smeared soil would have less secondary consolidation settlement and this might be useful as a controlling measure for post construction settlement, if more research is carried out in this area.

- The developed consolidometer could not measure the lateral strains with time, but if the cell was modified as suggested by the procedure given in Robinson et al. (2012), the lateral strains could be measured over time and the predictions would improve.

- Vacuum preloading tests using high quality undisturbed samples are needed to investigate the creep effects, on the basis that they would deliver better results. Use of thicker samples is also proposed.

- Most of the analytical models developed in vacuum consolidation assumed that strain only occurs in the vertical direction. This in generally not true, so the development of a radial consolidation model with lateral strains would be very helpful.

- It is important to vary the initial overburden pressure so that it would change the horizontal soil pressure in at-rest condition and then carry out vacuum consolidation experiments. This would simulate how horizontal strains would change along the depth of the underlying soil.

REFERENCES

Aboshi, H. (1973). An experimental investigation on the similitude in the consolidation of a soft clay, Including the secondary creep settlements. *Preceedings, 8th International conference on Soil Mechanics and Foundation Engineering, Moscow*, 4(3),pp. 88.

Akagi, T. (1977). Effect of mandrel-driven sand drains on strength *Proc. 9th Int. Conf. Soil Mech. and Found. Eng.* , 1, Tokyo,pp. 3-6.

Almeida, M. S. S. and C. A. M. Ferreira (1993). Field, in situ and laboratory consolidation parameters of a very soft clay. *Predictive soil mechanics. Proceedings of the Wroth memorial symposium*, Thomas Telford Limited, London,pp. 73-93.

AS (2011). AS 8700-2011: Execution of prefabricated vertical drains, Australian Standards.

Asaoka, A. (1978). Observation procedure of settlement prediction. *Soils and Foundations*, 18(4),pp. 87-101.

ASTM (2011). Standard Test Methods for One-Dimensional Consolidation Properties of Soils Using Incremental Loading. D2435/D2435M. Annual Book of ASTM Standards ASTM International, West Conshohocken, PA**:** Vol.04.08.

Atkinson, M. S. and P. J. L. Eldred (1981). Consolidation of soil using vertical drains. *Geotechnique*, 31(1),pp. 33-43.

Barron, R. A. (1948). Consolidation of fine-grained soils by drain wells. *Transactions ASCE*, 113(2346),pp. 718-724.

Basu, D. and M. Prezzi (2007). Effect of the Smear and Transition Zones around Prefabricated Vertical Drains Installed in a Triangular Pattern on the Rate of Soil Consolidation. *International Journal of Geomechanics*, 7(1),pp. 34-43.

Bergado, D. T., H. Asakami, M. C. Alfaro and A. S. Balasubramaniam (1991). Smear effects of vertical drains on soft Bangkok clay. *J. Geotech. Eng., ASCE*, 117(10),pp. 1509-1530.

Bergado, D. T., R. Manivannan and A. S. Balasubramaniam (1996). Proposed criteria for discharge capacity of prefabricated vertical drains. *Geotextiles and Geomembranes*, 14(9),pp. 481-505.

Bergado, D. T., J. C. Chai, N. Miura and A. S. Balasubramaniam (1998). PVD improvement of soft Bangkok clay with combined vacuum and reduced sand embankment preloading. *J. Geotech. Eng., Southeast Asian Geotch. Soc.*, 29(1),pp. 95-122.

Bjerrum, L. (1967). Engineering geology of Norwegian normally-consolidated marine clays as related to settlement of buildings. *Geotechnique*, 17(2),pp. 81-118.

Bo, M. W., J. Chu, B. K. Low and V. Choa (2003). Soil improvement; prefabricated vertical drain techniques, Thomson Learning, Singapore.

Boyd, J. P. (2001). Chebyshev and Fourier Spectral Methods: Second Revised Edition. New York, Dover Publications.

Britto, A. M. and M. J. Gunn, (1987). (1987). Critical State Soil Mechanics via Finite Elements. , Elis Horwood Limited, England.

Burland, J. B. (1990). On the compressibility and shear strength of natural clays. *Geotechnique*, 40,pp. 329-378.

Cao, L. F., C. I. Teh and M. F. Chang (2001). Undrained cavity expansion in modified Cam clay I: Theoretical analysis. *Geotechnique*, 51(4),pp. 323-334.

Carroll, R. G. (1983). Geotextile filter criteria. *Transportation research record*, 916,pp. 46-53.

Casagrande, A. and R. E. Fadum (1944). Reply to discussion on Application of Soil Mechanics in Designing Building Foundations. *Transactions, ASCE*, Vol. 109,pp. Paper No. 2213, pp 2383-2416.

Chai, J.-C. and N. Miura (1999). Investigation of factors affecting vertical drain behavior. *Journal of Geotechnical and Geoenvironmental Engineering*, 125(2-3),pp. 216-226.

Chai, J. C., N. Miura, H. H. Zhu and Yudhbir (2004). Compression and consolidation characteristics of structured natural clay. Canadian Geotechnical Journal, 41(6),pp. 1250-1258.

Chai, J. C., J. P. Carter and S. Hayashi (2005). Ground Deformation Induced by Vacuum Consolidation. *Journal of Geotechnical and Geoenvironmental Engineering*, 131(12),pp. 1552-1561.

Chai, J. C., J. P. Carter and S. Hayashi (2006). Vacuum consolidation and its combination with embankment loading. *Canadian Geotechnical Journal*, 43(10),pp. 985-985.

Christopher, B. R. and R. D. Holtz (1985). Geotextile Engineering Manual, U.S. Federal Highway Administration.

Chu, J., S. W. Yan and H. Yang (2000). Soil improvement by the vacuum preloading method for an oil storage station. *Geotechnique*, 50(6),pp. 625-632.

Chu, J., M. W. Bo and V. Choa (2004). Practical considerations for using vertical drains in soil improvement projects. *Geotextiles and Geomembranes*, 22(1-2),pp. 101-117.

Chu, J. and S. Yan (2005). Estimation of Degree of Consolidation for Vacuum Preloading Projects. *International Journal of Geomechanics*, 5(2),pp. 158-165.

Crawford, C. B. (1964). interpretation of the consolidation test. *Proc. Am. Soc.civ.Engrs.*, 90,SM5,pp. 349-362.

Degago, S. A., G. Grimstad, H. P. Jostad, S. Nordal and M. Olsson (2011). Use and misuse of the isotache concept with respect to creep hypotheses A and B. *Geotechnique*, 61(10),pp. 897-908.

Den Hoedt, G. (1981). Laboratory testing of vertical drains. *Eighth European Conference on Soil Mechanics and Foundation Engineering*, Vol.1, Helsinki,pp. 627-630.

Gavin, K., D. Gallagher, P. Doherty and B. McCabe (2010). Field investigation of the effect of installation method on the shaft resistance of piles in clay. *Canadian Geotechnical Journal*, 47(7),pp. 730-741.

Gens, A. and R. Nova (1993). Conceptual bases for a constitutive model for bonded soils and weak rocks. *In Geotechnical engineering of hard soils–soft rocks*

(eds A. Anagnostopoulos,F. Schlosser, N. Kalteziotis and R. Frank), Vol. 1, Rotterdam, the Netherlands: A. A. Balkema,pp. 485-494.

Ghandeharioon, A., B. Indraratna and C. Rujikiatkamjorn (2010). Analysis of Soil Disturbance Associated with Mandrel-Driven Prefabricated Vertical Drains Using an Elliptical Cavity Expansion Theory. *International Journal of Geomechanics*, 10(2),pp. 53-64.

Ghandeharioon, A., B. Indraratna and C. Rujikiatkamjorn (2012). Laboratory and Finite-Element Investigation of Soil Disturbance Associated with the Installation of Mandrel-Driven Prefabricated Vertical Drains. *Journal of Geotechnical and Geoenvironmental Engineering*, 138(3),pp. 295-308.

Gibson, R. E. and K. Y. Lo (1961). A Theory of consolidation for soils exhibiting secondary compression, NGI.

Hansbo, S. (1979). Conslidation of clay by band-shaped prefabricated drains. *Ground Engineering*, 12(5),pp. 16-25.

Hansbo, S. (1981). Consolidation of fine-grained soils by prefabricated drains. *Proc. 10th Int. Conf. SMFE.*, 3, Stokholm,pp. 677-682.

Hansbo, S. (1983). How to evaluate the properties of prefabricated drains. *Proceedings of Eighth European Conference on Soil Mechanics and Foundation Engineering*, Vol. 2, Helsinki,pp. 621-626.

Hansbo, S. (1987). Design aspects of vertical drains and lime column installation. *Proc. 9th Southeast Asian Geotechnical Conference*, 2,pp. 1-12.

Hird, C. C., I. C. Pyrah and D. Russell (1992). Finite element modelling of vertical drains beneath embankments on soft ground. *Geotechnique*, 42(3),pp. 499-511.

Hird, C. C. and V. J. Moseley (2000). Model study of seepage in smear zones around vertical drains in layered soil. *Geotechnique*, 50(1),pp. 89-97.

Holtz, R. D. and G. Holm (1973). Excavation and sampling around some sand drains at Ska-Edeby, Sweden. *Proc. Specialty Conference on Performance on Earth and Earth supported Structure*, Vol.1, Purdue University,pp. 435-464.

Holtz, R. D. (1975). Preloading by vacuum: current prospects. *Transportation research record*(548),pp. 26-29.

Holtz, R. D., M. Jamiolkowski, R. Lancellotta and S. Pedroni (1991). Prefabricated vertical drains: design and performance, CIRIA ground engineering report: ground improvement, Butterworth-Heinemann Ltd, UK.

Hvorslev, M. J. (1949). Subsurface exploration and sampling of soils for civil engineering purposes: report on a research project. Vicksburg, MS, USA, US Army Engineer Waterways Experiment Station.

Indraratna, B., A. S. Balasubramaniam and S. Balachandran (1992). Performance of test embankment constructed to failure on soft marine clay. *J. Geotech. Eng., ASCE*, 118,pp. 12-33.

Indraratna, B., A. S. Balasubramaniam and N. Sivaneswaran (1997). Analysis of settlement and lateral deformation of soft clay foundation beneath two full-scale embankments. *Int. J. for Numerical and Analytical Methods in Geomechanics*, 21,pp. 599-618.

Indraratna, B. and I. W. Redana (1997). Plane strain modeling of smear effects associated with vertical drains. *J. Geotech. Eng., ASCE*, 123(5),pp. 474-478.

Indraratna, B. and I. W. Redana (1998). Laboratory determination of smear zone due to vertical drain installation. *J. Geotech. Eng., ASCE*, 125(1),pp. 96-99.

Indraratna, B. and I. W. Redana (1999). Closure: Plane strain modeling of smear effects associated with vertical drains. *J. Geotech. Eng., ASCE*, 123(5),pp. 474-478.

Indraratna, B. and I. W. Redana (2000). Numerical modeling of vertical drains with smear and well resistance installed in soft clay, . *Canadian Geotechnical Journal*, 37,pp. 132-145.

Indraratna, B., I. Sathananthan, C. Rujikiatkamjorn and A. S. Balasubramaniam (2005). Analytical and numerical modeling of soft soil stabilized by prefabricated vertical drains incorporating vacuum preloading. *International Journal of Geomechanics*, 5(2),pp. 114-124.

Indraratna, B., C. Rujikiatkamjorn and I. Sathananthan (2005a). Analytical and numerical solutions for a single vertical drain including the effects of vacuum preloading. *Canadian Geotechnical Journal*, 42(4),pp. 994-1014.

Indraratna, B., C. Rujikiatkamjorn and I. Sathananthan (2005b). Radial consolidation of clay using compressibility indices and varying horizontal permeability. *Canadian Geotechnical Journal*, 42(5),pp. 1330-1341.

Indraratna, B., I. Sathananthan, C. Bamunawita and A. S. Balasubramaniam (2005c). Chapter 2 - Theoretical and numerical perspectives and field observations for the design and performance evaluation of embankments constructed on soft marine clay. Ground improvement case histories. B. Indraratna and J. Chu, *Elsevier Geo-Engineering Book Series.* 3**:** 51-117.

Indraratna, B., C. Rujikiatkamjorn, A. S. Balasubramaniam and V. Wijeyakulasuriya (2005d). Chapter 7 - Predictions and observations of soft clay foundations stabilized with geosynthetic drains and vacuum surcharge. Ground

improvement case histories. B. Indraratna and J. Chu, *Elsevier Geo-Engineering Book Series*. 3**:** 199-229.

Indraratna, B., C. Rujikiatkamjorn, R. Kelly and H. Buys (2009). Soft Soil Foundation Improved by Vacuum and Surcharge Preloading at Ballina Bypass, Australia *International Symposium on Ground Improvement Technologies and Case Histories*, Research Publishing, Singapore,pp. 95-105.

Indraratna, B. (2010). Recent advances in the application of vertical drains and vacuum preloading in soft soil stabilisation. *Australian Geomechanics Journal*, 45(2),pp. 1-44.

Indraratna, B., X. Geng and C. Rujikiatkamjorn (2010). Review of mehods of analysis for the use of vacuum preloading and vertical drains for soft clay improvement. *Geomechanics and Geoengineering*, 5(4),pp. 223-236.

Indraratna, B., C. Rujikiatkamjorn, J. Ameratunga and P. Boyle (2011). Performance and Prediction of Vacuum Combined Surcharge Consolidation at Port of Brisbane. *Journal of Geotechnical and Geoenvironmental Engineering*, 137(11),pp. 1009-1018.

Indraratna, B., C. Rujikiatkamjorn, R. Kelly and H. Buys (2012). Soft soil foundation improved by vacuum and surcharge loading. *Proceedings of the Institution of Civil Engineers: Ground Improvement*, 165(2),pp. 87-96.

Indraratna, B., K. Kianfar and C. Rujikiatkamjorn (2013). Laboratory Evaluation of Coefficient of Radial Consolidation Based on Pore-Water-Pressure Dissipation and Settlement. *Geotechnical Testing Journal*, 36(1),pp. 107-118.

Jamiolkowski, M., R. Lancellotta and W. Wolski (1983). Precompression and speeding up consolidation. *Proc. 8th ECSMFE*, 3,pp. 1201-1206.

Jamiolkowski, M., C. C. Ladd, J. T. Germaine and R. Lancellotta (1985). New Developments In Field And Laboratory Testing Of Soils. *Proceedings Of The*

Eleventh International Conference On Soil Mechanics And Foundation Engineering, San Francisco, 1,pp. 55-153

Jansen, H. L. and G. den Hoedt (1983). Vertical Drains: in-situ and laboratory performance and design conditions in fine soils. *Eighth European Conference on Soil Mechanics and Foundation Engineering*, Vol. 2, Helsinki,pp. 647-651.

Johnson, S. J. (1970a). Precompression for improving foundation soils. *J. Soil. Mech. Found. Div., ASCE*, 96(1),pp. 111-144.

Johnson, S. J. (1970b). Foundation Precompression with Vertical Sand Drains. *J. Soil. Mech. Found. Div., ASCE*, 96(1),pp. 145-175.

Kelly, R., J. Small and P. Wong (2008). Construction of an Embankment Using Vacuum Consolidation and Surcharge Fill. *GeoCongress 2008*,pp. 578-585.

Kelly, R. B. and P. K. Wong (2009). An embankment constructed using vacuum consolidation. *Australian Geomechanics*, 44(2),pp. 55-64.

Kianfar, K., B. Indraratna and C. Rujikiatkamjorn (2013). Radial consolidation model incorporating the effects of vacuum preloading and non-Darcian flow. *Geotechnique*, 63,pp. 1060-1073.

Kjellman, W. (1948). Accelerating consolidation of fine grain soils by means of cardboard wicks. *Proc. 2nd ICSMFE*, 2,pp. 302-305.

Kjellman, W. (1952). Consolidation of clayey soils by atmospheric pressure *Proceedings of a conference on soil stabilization*, Massachusetts Institute of Technology, Boston, ,pp. 258-263.

Kremer, R. (1981). Discussion to speciality session 6. *Eighth European Conference on Soil Mechanics and Foundation Engineering*, Vol. 3, Helsinki,pp. 1235-1237.

Ladd, C. C., R. Foott, K. Ishihara, F. Schlosser and H. G. Poulos (1977). Stress - deformation and strength characteristics: state of the art report.

Lambe, T. W. and R. V. Whitman (1979). Soil mechanics. New York U6, Wiley.

Larsson, R. (1981). Drained Behaviour of Swedish Clays. Report No. 12,pp. 157 p.

Lau, K. and J. Cowland (2000). Geosynthetically Enhanced Embankments for the Shenzhen River. *Advances in Transportation and Geoenvironmental Systems Using Geosynthetics*,pp. 140-161.

Le, T., B. Fatahi and H. Khabbaz (2012). Viscous Behaviour of Soft Clay and Inducing Factors. Geotechnical & Geological Engineering, 30(5),pp. 1069-1083.

Lekha, K. R., N. R. Krishnaswamy and P. Basak (2003). Consolidation of clays for variable permeability and compressibility. *Journal of Geotechnical and Geoenvironmental Engineering, ASCE*, 129(11),pp. 1001-1009.

Leroueil, S., M. Kabbaj, F. Tavenas and R. Bouchard (1985). Stress-strain-strain rate relation for the compressibility of sensitive natural clay. *Géotechnique* 35(2),pp. 159-180.

Leroueil, S. (1988). Tenth Canadian Geotechnical Colloquium: Recent developments in consolidation of natural clays. *Canadian Geotechnical Journal*, 25(1),pp. 85-107.

Leroueil, S. and P. R. Vaughan (1990). The general and congruent effects of structure in natural soils and weak rocks. *Geotechnique*, 40,pp. 467-488.

Liu, M. D. and J. P. Carter (1999). Virgin compression of structured soils. *Geotechnique*, 49,pp. 43-57.

Liu, M. D. and J. P. Carter (2000). Modelling the destructuring of soils during virgin compression. *Geotechnique*, 50,pp. 479-483.

Liu, M. D. and J. P. Carter (2002). A structured Cam Clay model. *Canadian Geotechnical Journal*, 39(6),pp. 1313-1332.

Long, R. and A. Covo (1994). Equivalent Diameter of Vertical Drains with an Oblong Cross Section. *Journal of Geotechnical Engineering*, 120(9),pp. 1625-1630.

Madhav, M. R., Y.-M. Park and N. Miura (1993). Modelling and study of smear zones around band shaped drains. *Soils and Foundations*, 33(4),pp. 135-147.

Mesri, G. and R. E. Olson (1971). Mechanisms controlling the permeability of clays. *Clays and Clay Minerals*, 19(3),pp. 151-158.

Mesri, G. and P. M. Godlewski (1977). Time and stress-compressibility interrelationship. *ASCE J Geotech Eng Div*, 103(5),pp. 417-430.

Mesri, G. and Y. K. Choi (1985). The uniqueness of end-of-primary (EOP) void ratio - effevtive stress relationship. *Proceedings Of The Eleventh International Conference On Soil Mechanics And Foundation Engineering, San Francisco* 2,pp. 587-590.

Mitchell, J. K. (1976). Fundamentals of Soil Behavior. New York, Wiley.

Miura, N. and J. C. Chai (2000). Discharge capacity of prefabricated vertical drains confined in clay. *Geosynthetics International*, 7(2),pp. 119-135.

Mohamedelhassan, E. and J. Q. Shang (2002). Vacuum and surcharge combined one-dimensional consolidation of clay soils. *Canadian Geotechnical Journal*, 39,pp. 1126-1138.

Moretto, O. (1946). An investigatiof the effect of certain factors on strength nd compressibility of clays. *PhD Thesis, University of Illinois*.

Nagaraj, T., Murthy, B., Vatsala, A., and Joshi, R (1990). Analysis of Compressibility of Sensitive Soils. *Journal of Geotechnical Engineering*, 116(1),pp. 105-118.

Onoue, A. (1988). Consolidation by vertical drains taking well resistance and smear into consideration. *J. Soils and Foundations*, 28(4),pp. 165-174.

Onoue, A., N. H. Ting, J. T. Germaine and R. V. Whitman (1991). Permeability of disturbed zone around vertical drains. *Proc. ASCE Geotech. Enggr. Congress,* Colorado,pp. 879-890.

Parry, R. H. G. and V. Nadarajah (1974) Observations on laboratory prepared, lightly overconsolidated specimens of kaolin. *Geotechnique* 24, 345-357.

Pelletier, J. H., R. E. Olson and J. J. Rixner (1979). Estimation of consolidation properties of clay from field observations. *Geotechnical Testing Journal*, 2,pp. 34-43.

PLAXIS (2015). PLAXIS 2D Reference Manual. R. B. J. Edited by Brinkgreve, *Delft University of Technology and PLAXIS b.v., The Netherlands.*

Porter, O. J. (1936). Studies of fill construction over mud flats including a description of experimental construction using vertical sand drains to hasten stabilization. *Proceedings, First International conference on Soil Mechanics and Foundation Engineering,* Volume 1, Cambridge, Massachusetts,pp. 229-235.

Pradhan, T. B. S., G. Imai, T. Murata, M. Kamon and S. Suwa (1993). Experiment study on the equivalent diameter of a prefabricated band-shaped drain. *Proc. 11th Southeast Asian Geotech. Conf.*, 1,pp. 391-396.

Qian, J. H., W. B. Zhao, Y. K. Cheung and P. K. K. Lee (1992). The theory and practice of vacuum preloading. *Computers and Geotechnics*, 13,pp. 103-118.

Randolph, M. F. and C. P. Wroth (1979). An analytical solution for the consolidation around a driven pile. *International Journal for Numerical and Analytical Methods in Geomechanics*, 3(3),pp. 217-229.

Richart, F. E., Jr. (1959). A review of the theories for sand drains. *J. Soil Mech. and Foundation Enggr. ASCE*, 83(SM3),pp. 1301(1301-1338).

Rixner, J. J., S. R. Kraemer and A. D. Smith (1986). Prefabricated Vertical Drains, Vol. I, II and III: Summary of Research Report-Final Report. Washington D.C**:** 433.

Robinson, R. G., B. Indraratna and C. Rujikiatkamjorn (2012). Final state of soils under vacuum preloading. *Canadian Geotechnical Journal*, 49(6),pp. 729-739.

Rouainia, M. and D. Muir Wood (2000). A kinematic hardening constitutive model for natural clays with loss of structure. *Geotechnique*, 50,pp. 153-164.

Rowe, P. W. and L. Barden (1966). A New Consolidation Cell. *Geotechnique*, 16,pp. 162-170.

Rowe, P. W. (1968). The influence of geological features of clay deposits on the design and performance of sand drains. *Proceedings ICE,* Paper 7058-S,pp. 1-72.

Rujikiatkamjorn, C. and B. Indraratna (2007). Analytical solutions and design curves for vacuum-assisted consolidation with both vertical and horizontal drainage. *Canadian Geotechnical Journal*, 44(2),pp. 188-200.

Rujikiatkamjorn, C., B. Indraratna and J. Chu (2007). Numerical modelling of soft soil stabilized by vertical drains, combining surcharge and vacuum preloading for a storage yard. *Canadian Geotechnical Journal*, 44(3),pp. 326-342.

Rujikiatkamjorn, C., B. Indraratna and J. Chu (2008). 2D and 3D Numerical Modeling of Combined Surcharge and Vacuum Preloading with Vertical Drains. *International Journal of Geomechanics*, 8(2),pp. 144-156.

Rujikiatkamjorn, C., M. D. W. Ardana, B. Indraratna and S. Leroueil (2013). Conceptual model describing smear zone caused by mandrel action. *Geotechnique,* 63(16),pp. 1377-1388.

Rujikiatkamjorn, C. and B. Indraratna (2014). Analytical solution for radial consolidation considering soil structure characteristics. *Canadian Geotechnical Journal*,pp. 1-14.

Samarasinghe, A. M., Y. H. Huang and V. P. Drnevich (1982). Permeability And Consolidation Of Normally Consolidated Soils. *Journal of the Geotechnical Engineering Division*, 108(6),pp. 835-850.

Sathananthan, I. and B. Indraratna (2006). Laboratory evaluation of smear zone and correlation between permeability and moisture content. *Journal of Geotechnical and Geoenvironmental Engineering*, 132(7),pp. 942-945.

Sathananthan, I., B. Indraratna and C. Rujikiatkamjorn (2008). Evaluation of Smear Zone Extent Surrounding Mandrel Driven Vertical Drains Using the Cavity Expansion Theory. *International Journal of Geomechanics*, 8(6),pp. 355-365.

Saye, S. R. (2003). Assessment of soil disturbance by the installation of displacement sand drains and prefabricated vertical drains. *Geotechnical Special Publication No. 119, ASCE*,pp. 325-362.

Shang, J. Q., M. Tang and Z. Miao (1998). Vacuum preloading consolidation of reclaimed land: a case study. *Canadian Geotechnical Journal*, 35,pp. 740-749.

Sharma, J. S. and D. Xiao (2000). Characteristics of a smear zone around vertical drains by large-scale laboratory tests. *Canadian Geotechnical Journal*, 37,pp. 1265-1271.

Sridharan, A. and A. Rao (1981). Rectangular Hyperbola Fitting Method for One Dimensional Consolidation. *Geotechnical Testing Journal* 4(4),pp. 161-168.

Suklje, L. (1957). The analysis of the consolidation process of the isotache method. *Preceedings, 4th International conference on Soil Mechanics and Foundation Engineering, London*, 1,pp. 200-206.

Tang, X.-W. and K. Onitsuka (2000). Consolidation by vertical drains under time-dependent loading. *International Journal for Numerical and Analytical Methods in Geomechanics*, 24(9),pp. 739-751.

Tavenas, F., P. Jean, P. Leblond and S. Leroueil (1983a). The permeability of natural soft clays. Part II: Permeability characteristics. *Canadian Geotechnical Journal*, 20(4),pp. 645-660.

Tavenas, F., P. Leblond, P. Jean and S. Leroueil (1983b). The permeability of natural soft clays, Part 2: Permeability characteristics. *Can. Geotech.J.*, 20,pp. 645-660.

Tavenas, F., P. Leblond, P. Jean and S. Leroueil (1983c). The permeability of natural soft clays, Part 1: Methods of laboratory measurement. *Canadian Geotechechnical Journal*, 20,pp. 629-644.

Taylor, D. W. (1948). Fundamentals of soil mechanics, John Wiley, New York.

Terzaghi, K. (1943). Theoretical Soil Mechanics, John Wiley and Sons, New York.

Vinod, J. S., A. Sridharan and B. Indraratna (2010). Determination of coefficient of radial consolidation using steepest tangent fitting method. *Geotechnical and Geological Engineering*, 28(4),pp. 533-536.

Vreeken, C., van der Berg, F., Loxham, M. (1983). The effect of clay-drain interface erosion on the performance of band-shaped vertical drains. *Eighth European Conference on Soil Mechanics and Foundation Engineering*, Vol. 2, Helsinki,pp. 713-716.

Walker, R. and B. Indraratna (2006). Vertical Drain Consolidation with Parabolic Distribution of Permeability in Smear Zone. *Journal of Geotechnical and Geoenvironmental Engineering*, 132(7),pp. 937-941.

Walker, R. and B. Indraratna (2007). Vertical drain consolidation with overlapping smear zones. *Geotechnique*, 57(5),pp. 463-467.

Walker, R. and B. Indraratna (2009) Consolidation analysis of a stratified soil with vertical and horizontal drainage using the spectral method. *Geotechnique* 59, 439-449.

Walker, R., B. Indraratna and N. Sivakugan (2009). Vertical and Radial Consolidation Analysis of Multilayered Soil Using the Spectral Method. *Journal of Geotechnical and Geoenvironmental Engineering*, 135(5),pp. 657-663.

Wang, X.-S. and J. J. Jiao (2004). Analysis of soil consolidation by vertical drains with double porosity model. *International Journal for Numerical and Analytical Methods in Geomechanics*, 28(14),pp. 1385-1400.

Wheeler, S. J. (1997). A rotational hardening elasto-plastic model for clays. *Proceedings of the 14th international conference on soil mechanics and foundation engineering*, Vol. 1, Hamburg,pp. 431-434.

Whittle, A. J. (1993). Evaluation of a constitutive model for overconsolidated clays. *Geotechnique*, 43,pp. 289-313.

Wong, R. C. K. and S. Varatharajan (2014). Viscous behaviour of clays in one-dimensional compression. Canadian Geotechnical Journal, 51(7),pp. 795-809.

Xiao, D. (2000). Consolidation of soft soil using vertical drains, PhD Thesis, *Nanyang Technological University, Singapore*.pp. 301.

Yan, S. W. and J. Chu (2003) Soil improvement for a road using the vacuum preloading method. *Proceedings of the ICE - Ground Improvement* 7, 165-172.

Yan, S. W. and J. Chu (2005). Soil improvement for a storage yard using the combined vacuum and fill preloading method. *Canadian Geotechnical Journal*, 42(4),pp. 1094-1104.

Yang, C., J. P. Carter and D. Sheng (2014). Description of compression behaviour of structured soils and its application. Canadian Geotechnical Journal, 51(8),pp. 921-933.

Yin, J.-H. and J. Graham (1994). Equivalent times and one-dimensional elastic viscoplastic modelling of time-dependent stress–strain behaviour of clays. *Canadian Geotechnical Journal*, 31(1),pp. 42-52.

Yin, J. H. and J. Graham (1989). Viscous–elastic–plastic modelling of one-dimensional time-dependent behaviour of clays. *Canadian Geotechnical Journal*, 26(2),pp. 199-209.

Yoshikuni, H. and H. Nakanodo (1974). Consolidation of Fine-Grained Soils by Drain Wells with Finite Permeability. *Japan Soc. Soil Mech. and Found. Eng*, 14(2),pp. 35-46.